

Regulation of chondroprogenitor cell gene expression and migration

A thesis submitted to the University of East Anglia
for the degree of Doctor of Philosophy

By
Matthew James Mayhew

School of Biological Sciences

Biomedical Research Centre
University of East Anglia
Norwich Research Park
Norwich
NR4 7TJ

September 2014

© This copy of the thesis has been supplied on condition that anyone who consults it is understood to recognise that its copyright rests with the author and that use of any information derived there from must be in accordance with current UK Copyright Law. In addition, any quotation or extract must include full attribution.

Abstract

Cartilage, which lines joint surfaces to allow near-frictionless movement, lacks the ability to adequately repair itself and there are currently no effective, disease-modifying drugs to halt or repair the damage. Development of powerful *in vitro* models to investigate gene expression changes during osteoarthritis and chondrogenesis is key in understanding how the disease develops and how cartilage might attempt to repair itself.

In this thesis, an enhanced model of chondrogenesis of the murine ATDC5 chondroprogenitor cell line was developed with cells cultured in micromass. Results revealed not only an increase in chondrogenesis markers, but markers of growth plate differentiation, including type X collagen, were either restricted or repressed, whilst expression of genes rich in articular cartilage were up-regulated. This suggests that the enhanced ATDC5 model is more reminiscent of articular cartilage, making this model suitable for investigations into osteoarthritis - a disease of articular cartilage.

The role of WNT5A signalling was then investigated (which is up-regulated in osteoarthritic cartilage) in a disease-like context by stimulating cultures with cytokines. Microarray analysis unearthed interesting and novel results, including a decrease in WNT5A signalling and in expression of members of the CCN family. Pathway analysis allowed further exploration of the interrelationship between cytokine and WNT signalling. Some changes in gene expression were reminiscent of those observed previously in *in vivo* models of early osteoarthritis.

Finally, migration studies revealed that non-induced, undifferentiated ATDC5 cells have a migratory phenotype reminiscent of chondroprogenitor cells, which have the capacity to migrate to sites of cartilage injury *in vivo*. A novel model of cartilage invasion was also developed, with results suggesting WNT5A may be a potential inducer of chondroprogenitor invasion.

Together, this thesis shows that the ATDC5 model is a good model for investigating articular cartilage both in a physiological and pathological setting.

Acknowledgements

There are many people who I'd like to show my appreciation to for their help in all aspects of this thesis. First and foremost, I'd like to thank my primary supervisor, Dr. Jelena Gavrilović for her invaluable thought, input and support throughout this project, as well as her sheer enthusiasm, which is much inspiring! I'd also like to thank our collaborators Lara Kevorkian, Adrian Moore and Colin Stubberfield, past and present at UCB Celltech, Slough, for their involvement and suggestions, and for providing me with the tools to conduct a large proportion of this work. Special thanks again to Adrian and also to Paul Hales for making me feel very welcome during my stay in Slough and for their help with the microarray analysis. I'd also like to extend my thanks to the rest of my supervisory team, Ian Clark and Ernst Pöschl for their helpful discussions, as well as Vera Knaüper for providing the vector which was used for a large proportion of this study. Special thanks must also go to Tracey Swingler who has been a fantastic source of information and who has helped me out so much with the molecular cloning.

I am also grateful to the rest of the Gavrilović group both past and present – Jonathan Howe for teaching me the ropes when I first started and Damon Bevan who has been a great source of knowledge throughout! To Matthew Fenech, who I can only admire for being able to manage both a PhD and working as a medical doctor at the hospital! Also to his primary supervisor, Jeremy Turner, for his helpful insights and questions. A special thanks must also go to my fellow lab mate, Matt Yates, who has been an amazing source of rivalry, friendship, support and entertainment for the past four years, and I wish him the absolute best of luck with his clinical career.

Thanks must also go to my various friends in the lab – Isabelle Piec, Audrey Dubourg, Jasmine Buck, Sandy Bednar, Deborah Goldspink. They've provided endless entertainment, support, ears for my endless rants, cakes and great friendship that I'm sure will last long outside the lab. Special thanks also to David Thurkettle and Steven Lewis for their amazing chippie dinners and seemingly endless supply of alcohol! Thanks must also go to the Clark group and to Ellie Jones, who I've distracted and bugged many times on my way to and from doing TaqMan for chats that lasted way longer than they probably should have done and for always letting me borrow stuff for the lab! Also to my best friend, Chris Woodward, for giving me some amazing holidays across the atlantic that helped keep me sane during the entire PhD! And also to my friends Hector and Mike for giving me a place to stay and taking me everywhere whilst over there!

Lastly, extra special thanks must go to my family – my dad, brother and sister for their support and playing taxi many times when I've wanted to come home over the past seven years that I've been at UEA (!), and especially to my mum for her undying support, love and encouragement. And finally to my beautiful partner, Jonas, who this past year has helped keep me sane writing this thesis, giving me all the love and encouragement I've needed.

Thank you.

Abbreviations

β -TrCP	β -transducin repeat-containing protein
Acan	Aggrecan
ACI	Autologous Chondrocyte Implantation
ADAM	A disintegrin and metalloproteinase
ADAMTS	ADAM with thrombospondin motifs
AER	Apical Ectodermal Ridge
ALPL	Alkaline Phosphatase (Liver/Bone/Kidney)
AMSC	Adipose-derived MSC
APC	Adenomatosis Polyposis Coli
BCA	Bicinchoninic acid
BMP	Bone Morphogenetic Protein
BMSC	Bone marrow-derived MSC
BSA	Bovine Serum Albumin
CAMKII	Ca ²⁺ /calmodulin-dependent kinase II
CCN	CYR61 CTGF NOV
cDNA	complementary DNA
CK1	Casein Kinase 1
COL10A1	Collagen, type 10, alpha 1
COL2A1	Collagen, type 2, alpha 1
CS	Chondrotin Sulphate
CT	C-terminal
C _T	Cycle Threshold
CTGF	Connective Tissue Growth Factor
CYR61	Cysteine Rich Protein 61
DAPI	4',6-diamidino-2-phenylindole
DKK	Dickkopf
DMM	Destabilisation of the medial meniscus
DVL	Dishevelled
ECM	Extracellular Matrix
FCS	Foetal Calf Serum
FRZB	Frizzled related protein B
FZD	Frizzled
GAG	Glycosaminoglycan
GSK3	Glycogen synthase kinase 3
GTP	Guanidine Triphosphate
HA	Hyaluronan
HIF	Hypoxia-inducible factor
ICAM	Intercellular Adhesion Molecule
IGD	Interglobular domain
IGF	Insulin-like growth factor
IGFBP	IGF binding protein
IL	Interleukin

ITS	Insulin, transferrin, sodium selenite
JNK	c-Jun-N-terminal kinase
KS	Keratan Sulphate
LRP	Low-density lipoprotein receptor-related protein
MAP	Mitogen Activated Protein
miRNA	microRNA
MMP	Matrix Metalloproteinase
mRNA	messenger RNA
MSC	Mesenchymal Stem Cell
NFAT	Nuclear factor of activated T-cells
NF- κ B	nuclear factor kappa-light-chain-enhancer of activated B cells
NOV	Nephroblastoma Overexpressed
OA	Osteoarthritis
OSM	Oncostatin M
PBS	Phosphate Buffered Saline
PCA	Principle Component Analysis
PCM	Pericellular Matrix
PCP	Planar Cell Polarity
PCR	Polymerase Chain Reaction
polyHEMA	poly-2-hydroxyethyl methacrylate
PPRD	Progressive Pseudorheumatoid Dysplasia
PTHrP	Parathyroid hormone-related protein
qRT-PCR	Quantitative RT-PCR
RA	Rheumatoid Arthritis
ROR2	Receptor Tyrosine Kinase-like Orphan Receptor 2
RT	Reverse Transcription
Runx2	Runt-related Transcription Factor 2
SDM	Site-directed Mutagenesis
SEM	Standard Error of the Mean
sFRP	secreted Frizzled related protein
siRNA	Short interfering RNA
SOX9	Sex-determining region Y box 9
SP	Signal Peptide
TCA	Trichloroacetic Acid
TCF/LEF	T cell-specific/lymphoid enhancer binding factor
TGF	Transforming Growth Factor
TIMP	Tissue Inhibitor of Metalloproteinases
TNF	Tumour Necrosis Factor
TSP1	Thrombospondin Type 1
VEGF	Vascular Endothelial Growth Factor
VWC	von Willebrand factor type C
WISP	WNT1-inducible secreted protein
WNT	Wingless (Wg)/Mouse mammary tumour virus integration site 1 (Int1)

Table of Contents

ABSTRACT	II
ACKNOWLEDGEMENTS	III
ABBREVIATIONS	IV
TABLE OF CONTENTS	VI
TABLE OF FIGURES	XII
TABLE OF TABLES	XV
CHAPTER 1 - INTRODUCTION	1
1.1 INTRODUCTION TO CARTILAGE	2
1.1.1 ARTICULAR CARTILAGE	2
1.1.2 TYPE II COLLAGEN	3
1.1.3 AGGRECAN	6
1.1.4 CHONDROCYTES AND CHONDROGENESIS	7
1.2 WNT SIGNALLING	10
1.2.1 CANONICAL WNT PATHWAY	10
1.2.2 NON-CANONICAL WNT PATHWAY	11
1.2.3 WNT5A/ROR2 SIGNALLING	12
1.2.4 WNT SIGNALLING AND CHONDROCYTES	13
1.2.5 WNT SIGNALLING IN OSTEOARTHRITIS	14
1.2.6 CCN FAMILY AND OSTEOARTHRITIS	15
1.2.6.1 <i>CYR61/CCN1</i>	16
1.2.6.2 <i>CTGF/CCN2</i>	17
1.2.6.3 <i>NOV/CCN3</i>	18
1.2.6.4 <i>WISP1/CCN4</i>	18
1.2.6.5 <i>WISP2/CCN5</i>	19
1.2.6.6 <i>WISP3/CCN6</i>	19
1.3 OSTEOARTHRITIS	22
1.3.1 CARTILAGE CHANGES IN OA	23
1.3.1.1 <i>Catabolic changes in OA</i>	23
1.3.1.2 <i>Anabolic changes in OA</i>	23
1.3.2 ENZYMES IN CARTILAGE DEGRADATION	24
1.3.2.1 <i>MMPs</i>	24
1.3.2.2 <i>ADAMTSs</i>	25
1.3.2.3 <i>Enzyme dysregulation</i>	25
1.3.2.4 <i>ADAMTS knockout studies</i>	26
1.3.3 STEM CELL REPAIR	27
1.4 MAINTAINING THE CHONDROCYTIC PHENOTYPE	29
1.4.1 SUSPENSION CULTURE	29
1.4.2 ENCAPSULATION	29
1.4.3 PELLET CULTURE	30

1.4.4 HIGH DENSITY MICROMASS CULTURE.....	31
1.4.5 MESENCHYMAL STEM CELL DIFFERENTIATION	32
1.4.6 HYPOXIA	33
1.5 SUMMARY.....	35
1.6 GENERAL HYPOTHESIS.....	35
1.7 AIMS	35
CHAPTER 2 – MATERIALS AND METHODS	36
2.1 ATDC5 CELL CULTURE	37
2.1.1 MAINTENANCE	37
2.1.2 EXPERIMENTAL CULTURE.....	37
2.1.2.1 <i>Monolayer Culture</i>	37
2.1.2.2 <i>High Density Micromass Culture</i>	37
2.1.2.3 <i>ATDC5 Chondrogenic Induction with Insulin</i>	37
2.1.2.4 <i>Stimulation with Ascorbic Acid</i>	38
2.1.2.5 <i>ECM Components</i>	38
2.2 GENE TRANSCRIPTION ANALYSIS BY QRT-PCR.....	38
2.2.1 RNA EXTRACTION USING RNEASY MINI/MICRO PLUS KITS FROM QIAGEN	38
2.2.2 RNA QUALITY/QUANTITY ANALYSIS WITH NANODROP	39
2.2.3 TWO-STEP REVERSE TRANSCRIPTION TO CDNA USING M-MLV.....	39
2.2.4 IDENTIFICATION OF SUITABLE HOUSEKEEPING GENE USING GENORM FROM PRIMERDESIGN	39
2.2.5 GENERATION OF CUSTOM ASSAYS USING THE UNIVERSAL PROBELIBRARY	40
2.2.6 GENERATION OF CUSTOM ASSAYS FROM PRIMERDESIGN.....	41
2.2.7 QRT-PCR ANALYSIS USING DOUBLE-DYE HYDROLYSIS PROBE TECHNOLOGY	47
2.3 HISTOLOGICAL STAINING.....	47
2.3.1 DETECTION OF PROTEOGLYCANS/GAGS WITH ALCIAN BLUE.....	47
2.3.2 IMMUNOFLUORESCENCE.....	48
2.3.3 PROTEIN DETECTION BY WESTERN BLOTTING	48
2.3.3.1 <i>Preparation of cell lysates</i>	49
2.3.3.2 <i>Protein quantification by Pierce BCA Protein Assay (RIPA-extracted samples)</i>	49
2.3.3.3 <i>Protein quantification by Pierce 660 nm assay (Urea/thiourea-extracted samples)</i>	49
2.3.3.4 <i>Preparation of conditioned media for Western Blotting</i>	50
2.3.3.5 <i>TCA precipitation of conditioned media</i>	50
2.3.3.6 <i>Protein resolution by SDS-PAGE</i>	50
2.3.3.7 <i>Semi-dry transfer of polyacrylamide gels to PVDF</i>	50
2.3.3.8 <i>Confirmation of transfer by Ponceau S staining</i>	50
2.3.3.9 <i>Immunodetection of proteins</i>	51
2.3.3.10 <i>Stripping membranes</i>	51
2.3.3.11 <i>Antibodies</i>	52
2.4 MOLECULAR CLONING.....	53
2.4.1 GENERATION OF COMPETENT DH5A CELLS.....	53
2.4.2 TRANSFORMATION OF DH5A CELLS	53
2.4.3 PLASMID ISOLATION FROM DH5A CELLS USING QIAGEN MINIPREP	53
2.4.4 WNT5A AMPLIFICATION AND END MODIFICATION VIA PCR	54
2.4.5 PLASMID RESTRICTION.....	55

2.4.6	FRAGMENT ISOLATION BY TRADITIONAL AGAROSE GEL ELECTROPHORESIS	56
2.4.7	RECOVERY OF FRAGMENTS FROM TRADITIONAL AGAROSE GEL	56
2.4.8	LIGATION OF INSERTS INTO pCDNA4:FLAG	56
2.4.9	SCREENING FOR SUCCESSFUL LIGATION	56
2.4.10	SITE-DIRECTED MUTAGENESIS (SDM) OF pCDNA4:WNT3A WITH QUIKCHANGE LIGHTNING	57
2.5	TRANSFECTION IN ATDC5 CELLS	58
2.5.1	HIGH QUALITY PLASMID PURIFICATION BY QIAGEN HiSPEED PLASMID MIDI KIT.....	58
2.5.2	PLASMID LINEARISATION AND PURIFICATION	58
2.5.3	DETERMINATION OF OPTIMUM SELECTIVE ANTIBIOTIC CONCENTRATION	59
2.5.4	TRANSFECTION WITH TURBOFECT	59
2.5.5	GENERATION OF CONDITIONED MEDIA FROM TRANSIENTLY TRANSFECTED CELLS	59
2.5.6	GENERATION OF STABLE CLONES.....	59
2.5.7	ANALYSING GENE EXPRESSION IN STABLE CLONES.....	60
2.6	CONDITIONED MEDIA STIMULATION	60
2.6.1	MICROARRAY ANALYSIS.....	60
2.7	CELL ADHESION ASSAY	61
2.8	RANDOM CELL MIGRATION ASSAY	61
2.9	MICROMASS INVERTED INVASION ASSAY	62
2.10	STATISTICAL ANALYSIS	64
CHAPTER 3 – ENHANCING AND MAINTAINING THE CHONDROCYTIC PHENOTYPE IN ATDC5 CELLS BY		
PHYSIOLOGICALLY-RELEVANT CULTURING		65
3.1	INTRODUCTION	66
3.1.1	MESENCHYMAL STEM CELLS AND THE ATDC5 CHONDROGENIC DIFFERENTIATION MODEL.....	66
3.1.2	CHONDROCYTES AND PHYSIOLOGICALLY RELEVANT CULTURING CONDITIONS	66
3.1.3	CHONDROCYTES AND ASCORBIC ACID	67
3.1.4	CARTILAGE PHENOTYPES	67
3.1.5	AIMS	67
3.2	RESULTS	68
3.2.1	SELECTION OF AN APPROPRIATE HOUSEKEEPING GENE FOR qRT-PCR ANALYSIS.....	68
3.2.2	TIME COURSE OF GENE EXPRESSION DURING ATDC5 DIFFERENTIATION.....	69
3.2.3	MORPHOLOGICAL DIFFERENCES AND VISUAL OBSERVATIONS BETWEEN DIFFERENT ATDC5 CULTURING CONDITIONS....	74
3.2.4	ASCORBIC ACID ENHANCES PROTEOGLYCAN DEPOSITION IN BOTH MONOLAYER AND MICROMASS CULTURES.....	77
3.2.5	THE EFFECT OF MICROMASS CULTURE AND ASCORBIC ACID STIMULATION ON GENE EXPRESSION OF ATDC5 CELLS FOR 14 DAYS	80
3.2.5.1	<i>Chondrogenesis/Articular Differentiation</i>	<i>80</i>
3.2.5.2	<i>Hypertrophic Differentiation/Mineralisation.....</i>	<i>82</i>
3.2.5.3	<i>CCN Growth Factors</i>	<i>84</i>
3.2.6	TYPE X COLLAGEN IS IMMUNOLocalISED TO A RESTRICTED REGION WITHIN THE CENTRE OF MICROMASSES.....	85
3.2.7	CONFIRMATION OF HYPERTROPHIC GENE EXPRESSION VIA WESTERN BLOT.....	88
3.3	DISCUSSION.....	91
3.3.1	CHONDROGENIC DIFFERENTIATION OF ATDC5 CELLS OVER TIME	91
3.3.2	MICROMASS CULTURE ENHANCES INSULIN-INDUCED ATDC5 CHONDROGENESIS	91
3.3.3	ASCORBIC ACID ENHANCES ATDC5 CHONDROGENESIS.....	91

3.3.4 MICROMASS CULTURE AND ASCORBIC ACID STIMULATION INHIBIT HYPERTROPHIC DIFFERENTIATION AND PROMOTE ARTICULAR DIFFERENTIATION	92
3.3.4.1 <i>Type II Collagen and Type X Collagen</i>	93
3.3.4.2 <i>Frzb and Grem1</i>	93
3.3.4.3 <i>CCN Growth Factors</i>	94
3.3.4.3.1 <i>Cyr61</i>	94
3.3.4.3.2 <i>Ctgf</i>	94
3.3.4.3.3 <i>Nov, Wisp1, Wisp2 and Wisp3</i>	95
3.3.4.4 <i>Mmp13</i>	95
3.3.4.5 <i>Alpl (Alkaline Phosphatase)</i>	96
3.3.4.6 <i>TGFβ</i>	96
3.3.4.6.1 <i>Tgfb3</i>	96
3.3.4.6.2 <i>Tgfb1</i>	96
3.3.4.7 <i>RUNX2</i>	97
3.3.4.8 <i>DDR2</i>	97
3.3.4.9 <i>WNT5A</i>	98
3.4 SUMMARY.....	98
CHAPTER 4 – INVESTIGATING WNT5A AND CYTOKINE SIGNALLING IN ATDC5 CELLS	100
4.1 INTRODUCTION	101
4.1.1 WNT SIGNALLING IN OSTEOARTHRITIS AND SKELETAL DISEASE.....	101
4.1.2 CYTOKINE SIGNALLING IN OSTEOARTHRITIS	101
4.1.3 AIMS	102
4.2 RESULTS	103
4.2.1 GENERATION OF STABLE CLONES OVEREXPRESSING WNT5A	103
4.2.2 GENE REGULATION IN NON-INDUCED OVEREXPRESSING WNT5A CLONES.....	104
4.2.3 STABLE CLONES FAILED TO UNDERGO CHONDROGENESIS	112
4.2.4 GENERATION OF WNT5A CONDITIONED MEDIUM FOR NAÏVE ATDC5 CELL STIMULATION.....	114
4.2.5 GENE REGULATION IN CONDITIONED MEDIA- AND CYTOKINE-STIMULATED NAÏVE ATDC5 CELLS	116
4.2.6 MICROARRAY ANALYSIS OF WNT5A AND CYTOKINE-STIMULATION IN DIFFERENTIATED ATDC5 CELLS	124
4.2.6.1 <i>Cytokine stimulation strongly regulated gene expression</i>	124
4.2.6.2 <i>Selecting genes for subsequent analysis</i>	126
4.2.6.3 <i>Comparison of candidate genes between qRT-PCR analysis and microarray analysis</i>	131
4.2.6.4 <i>Confirmation of gene regulation proposed by microarray analysis</i>	133
4.2.6.5 <i>Pathway Analysis</i>	135
4.3 DISCUSSION.....	140
4.3.1 GENE REGULATION IN NON-INDUCED WNT5A-OVEREXPRESSING CLONES	140
4.3.1.1 <i>Ror2</i>	140
4.3.1.2 <i>Adamts4 and Adamts5</i>	140
4.3.1.3 <i>Grem1</i>	140
4.3.1.4 <i>Alpl, Runx2 and Ddr2</i>	141
4.3.1.5 <i>CCN Growth Factor Family</i>	141
4.3.2 ATDC5 CLONES FAILED TO DIFFERENTIATE	142
4.3.3 WNT5A-MEDIATED GENE REGULATION USING CONDITIONED MEDIA ON DIFFERENTIATED ATDC5 MICROMASS CULTURES	142
4.3.3.1 <i>Cyr61</i>	143
4.3.3.2 <i>Col10a1</i>	143

4.3.3.3 <i>Anxa1 (Annexin A1)</i>	143
4.3.3.4 <i>Matn3 (Matrilin 3)</i>	144
4.3.3.5 <i>Variation in WNT5A-mediated gene regulation between experiments</i>	144
4.3.4 CYTOKINE-MEDIATED GENE REGULATION BY QRT-PCR IN DIFFERENTIATED ATDC5 MICROMASS CULTURES	145
4.3.4.1 <i>Ror2</i>	145
4.3.4.2 <i>Col2a1</i>	145
4.3.4.3 <i>Runx2 and Ddr2</i>	146
4.3.4.4 <i>CCN Growth Factor Family</i>	146
4.3.4.4.1 <i>Cyr61</i>	146
4.3.4.4.2 <i>Ctgf</i>	147
4.3.4.4.3 <i>Wisp1</i>	147
4.3.4.4.4 <i>Wisp2</i>	147
4.3.4.5 <i>Lcn2 (Lipocalin 2)</i>	148
4.3.4.6 <i>Prg4 (Proteoglycan 4/Lubricin)</i>	148
4.3.4.7 <i>WNT Pathway</i>	149
4.3.4.8 <i>Focal Adhesion Pathway</i>	149
4.3.5 SIMILARITIES WITH AN OA MODEL MICROARRAY	149
4.4 SUMMARY	150
CHAPTER 5 – INVESTIGATING ATDC5 MIGRATION AND INVASION AND THE POTENTIAL MODULATION BY CYTOKINE AND WNT SIGNALLING	151
5.1 INTRODUCTION	152
5.1.1 MIGRATION AND INVASION IN CARTILAGE AND CHONDROGENESIS.....	152
5.1.2 WNT5A AND MIGRATION/INVASION.....	152
5.1.3 AIMS	152
5.2 RESULTS	154
5.2.1 NON-INDUCED ATDC5 CELLS ADHERE BETTER TO FIBRONECTIN THAN TO TYPE II COLLAGEN.....	154
5.2.2 TYPE II COLLAGEN SUBSTRATE IMPEDES NON-INDUCED ATDC5 RANDOM MIGRATION	155
5.2.3 DIFFERENTIATED ATDC5 CELLS ARE LESS MIGRATORY THAN UNDIFFERENTIATED CELLS.....	156
5.2.4 EFFECT OF WNT STIMULATION ON NON-INDUCED ATDC5 MIGRATION	158
5.2.5 MODELLING CHONDROPROGENITOR CELL INVASION THROUGH CARTILAGE	162
5.3 DISCUSSION.....	166
5.3.1 NON-INDUCED ATDC5 CELLS ADHERE BETTER TO FIBRONECTIN THAN TO TYPE II COLLAGEN.....	166
5.3.2 TYPE II COLLAGEN IMPEDES THE SPEED OF MIGRATION	167
5.3.2.1 <i>DDR2</i>	167
5.3.3 THE DIFFERENTIATED STATE OF ATDC5 CELLS AFFECTS THE MIGRATORY POTENTIAL.....	167
5.3.3.1 <i>Aquaporin-1</i>	168
5.3.4 MODULATION OF MIGRATION AND INVASION BY WNT5A AND WNT3A	169
5.4 SUMMARY.....	171
CHAPTER 6 – GENERAL DISCUSSION	173
6.1 GENERAL DISCUSSION	174
6.1.1 AN ENHANCED ATDC5 CHONDROGENESIS MODEL.....	174
6.1.2 NOVEL CYTOKINE-MEDIATED REGULATION OF THE WNT AND CCN MOLECULAR SIGNALLING PATHWAYS.....	176
6.1.3 ATDC CELLS CAN BE USED TO MODEL CHONDROPROGENITOR MIGRATION AND INVASION	177
6.1.4 SUMMARY OF FINDINGS	178

6.2 FUTURE WORK	180
6.2.1 TRANSCRIPTOMIC ANALYSIS AND COMPARISON WITH ARTICULAR CARTILAGE	180
6.2.2 EPIGENETIC REGULATION OF WNT5A	180
6.3.3 OSTEOARTHRITIC CARTILAGE SECRETOME	181
6.3.4 HIGH-THROUGHPUT SCREENING	182
6.3 SUMMARY	183
APPENDIX	184
REFERENCES	212

Table of Figures

FIGURE 1.1 - ANATOMY OF AN ARTICULATED JOINT	3
FIGURE 1.2 - COLLAGEN FIBRIL SYNTHESIS	5
FIGURE 1.3 – STRUCTURE OF AGGREGAN	7
FIGURE 1.4 – CELLULAR ZONES OF ARTICULAR CARTILAGE.....	9
FIGURE 1.5 – CANONICAL WNT PATHWAY	11
FIGURE 1.6 – WNT5A SIGNALLING PATHWAYS.....	12
FIGURE 1.7 – THE MODULAR STRUCTURE OF THE CCN GROWTH FACTOR FAMILY	16
FIGURE 1.8 – SIMPLIFIED COMPARISON BETWEEN A HEALTHY JOINT AND AN OSTEOARTHRITIC JOINT ...	22
FIGURE 1.9 – SETTING UP A MICROMASS CULTURE.....	31
FIGURE 2.1 – PRIMERS TO AMPLIFY AND MODIFY THE ENDS OF WNT5A FROM PCMV5-XL4	54
FIGURE 2.2 – PCDNA4:FLAG MAMMALIAN EXPRESSION VECTOR MAP	55
FIGURE 2.3 – SDM OF WNT3A	57
FIGURE 2.4 – MICROMASS INVERTED INVASION ASSAY SCHEMATIC.....	63
FIGURE 3.1 – IDENTIFYING SUITABLE HOUSEKEEPING GENES THAT DO NOT SIGNIFICANTLY ALTER EXPRESSION DURING CHONDROGENIC CULTURE OF ATDC5 CELLS VIA GENORM ANALYSIS	68
FIGURE 3.2 – GENE EXPRESSION REGULATION OF ARTICULAR CARTILAGE MARKERS DURING ATDC5 DIFFERENTIATION	70
FIGURE 3.3 – GENE EXPRESSION REGULATION OF THE TGFB FAMILY DURING ATDC5 DIFFERENTIATION ..	71
FIGURE 3.4 – GENE EXPRESSION REGULATION OF HYPERTROPHIC MARKERS DURING ATDC5 DIFFERENTIATION	72
FIGURE 3.5 – GENE EXPRESSION REGULATION OF HYPERTROPHIC TRANSCRIPTION FACTOR RUNX2 DURING ATDC5 DIFFERENTIATION.....	73
FIGURE 3.6 – MORPHOLOGICAL CHANGES DURING ATDC5 DIFFERENTIATION	75
FIGURE 3.7 – CARTILAGE-LIKE NODULE OF ATDC5 CELLS	76
FIGURE 3.8 – ALCIAN BLUE STAINING COMPARISON DURING DIFFERENTIATION OF ATDC5 CELLS AFTER 14 DAYS IN MONOLAYER AND MICROMASS STIMULATED WITH OR WITHOUT INSULIN OR ASCORBIC ACID.....	78
FIGURE 3.9 – QUANTIFICATION OF ALCIAN BLUE STAINING	79
FIGURE 3.10 – CHANGES IN EXPRESSION OF VARIOUS CHONDROGENIC/ARTICULAR MARKERS DURING ATDC5 CHONDROGENESIS	81
FIGURE 3.11 – CHANGES IN GENE EXPRESSION RELATED TO HYPERTROPHIC DIFFERENTIATION DURING ATDC5 DIFFERENTIATION	83
FIGURE 3.12 – CHANGES IN CCN GENE EXPRESSION DURING ATDC5 DIFFERENTIATION.....	84
FIGURE 3.13 – OPTICAL SECTIONS OF DIFFERENTIATED MONOLAYER AND MICROMASS CULTURES IMMUNOSTAINED FOR TYPE II COLLAGEN AND TYPE X COLLAGEN.....	86
FIGURE 3.14 – NUMBER OF COMPLETE OR PARTIAL TYPE X COLLAGEN “RINGS”.	87

FIGURE 3.15 – AVERAGE TYPE II COLLAGEN FLUORESCENCE INTENSITY OF ATDC5 CELLS DIFFERENTIATED IN MONOLAYER AND MICROMASS	87
FIGURE 3.16 – DDR2 AND RUNX2 PROTEIN EXPRESSION DECREASE WITH INCREASING CHONDROGENESIS	89
FIGURE 3.17 – WNT5A EXPRESSION INCREASES DURING CHONDROGENESIS	90
FIGURE 4.1 – CONFIRMATION OF WNT5A OVEREXPRESSING CLONES	103
FIGURE 4.2 A-B – GENE REGULATION IN STABLE WNT5A-OVEREXPRESSING, NON-INDUCED ATDC5 CLONES	105
FIGURE 4.2 C-D – GENE REGULATION IN STABLE WNT5A-OVEREXPRESSING, NON-INDUCED ATDC5 CLONES	106
FIGURE 4.2 E-F – GENE REGULATION IN STABLE WNT5A-OVEREXPRESSING, NON-INDUCED ATDC5 CLONES	107
FIGURE 4.2 G-H – GENE REGULATION IN STABLE WNT5A-OVEREXPRESSING, NON-INDUCED ATDC5 CLONES	108
FIGURE 4.2 I-J – GENE REGULATION IN STABLE WNT5A-OVEREXPRESSING, NON-INDUCED ATDC5 CLONES	109
FIGURE 4.2 K-L – GENE REGULATION IN STABLE WNT5A-OVEREXPRESSING, NON-INDUCED ATDC5 CLONES	110
FIGURE 4.2 M – GENE REGULATION IN STABLE WNT5A-OVEREXPRESSING, NON-INDUCED ATDC5 CLONES	111
FIGURE 4.3 – <i>COL2A1</i> EXPRESSION IN INSULIN-INDUCED CLONES WITH CYTOKINE STIMULATION.....	113
FIGURE 4.4 – DETECTION OF WNT5A PROTEIN FROM TRANSIENT TRANSFECTION TIMECOURSE	115
FIGURE 4.5 A-C – GENE REGULATION IN WNT5A AND CYTOKINE STIMULATED DIFFERENTIATED ATDC5 MICROMASS CULTURES	118
FIGURE 4.5 D-E – GENE REGULATION IN WNT5A AND CYTOKINE STIMULATED DIFFERENTIATED ATDC5 MICROMASS CULTURES	119
FIGURE 4.5 F-G – GENE REGULATION IN WNT5A AND CYTOKINE STIMULATED DIFFERENTIATED ATDC5 MICROMASS CULTURES	120
FIGURE 4.5 H-I – GENE REGULATION IN WNT5A AND CYTOKINE STIMULATED DIFFERENTIATED ATDC5 MICROMASS CULTURES	121
FIGURE 4.5 J-K – GENE REGULATION IN WNT5A AND CYTOKINE STIMULATED DIFFERENTIATED ATDC5 MICROMASS CULTURES	122
FIGURE 4.5 L – GENE REGULATION IN WNT5A AND CYTOKINE STIMULATED DIFFERENTIATED ATDC5 MICROMASS CULTURES	123
FIGURE 4.6 – PRINCIPLE COMPONENT ANALYSIS (PCA) OF WNT5A AND CYTOKINE STIMULATED MICROMASS CULTURES FROM MICROARRAY ANALYSIS	124
FIGURE 4.7 – HIERARCHICAL CLUSTERING OF WNT5A AND CYTOKINE-TREATED MICROMASS CULTURES BY MICROARRAY ANALYSIS	87

FIGURE 4.8 – VOLCANO PLOT OF EFFECT OF WNT5A WITH AND WITHOUT CYTOKINE STIMULATION ON GENE REGULATION IN ATDC5 MICROMASS CULTURES	127
FIGURE 4.9 – VOLCANO PLOT OF EFFECT OF CYTOKINES WITH AND WITHOUT WNT5A STIMULATION ON GENE REGULATION IN ATDC5 MICROMASS CULTURES	128
FIGURE 4.10 – DISTRIBUTION OF CYTOKINE-REGULATED PROBE SETS WITH RESPECT TO PRESENCE OR ABSENCE OF WNT5A.....	130
FIGURE 4.11 – CONFIRMATION OF GENE REGULATION CHANGES SEEN BY MICROARRAY ANALYSIS BY QRT-PCR	134
FIGURE 4.12 – CYTOKINE STIMULATION WNT PATHWAYS	137
FIGURE 4.13 – CYTOKINE STIMULATION REGULATES THE FOCAL ADHESION PATHWAY	138
FIGURE 4.14 – CYTOKINE STIMULATION DOWN-REGULATES WNT5A.....	139
FIGURE 5.1 – ADHESION OF NON-INDUCED ATDC5 CELLS TO FIBRONECTIN AND TYPE II COLLAGEN AT DIFFERENT CONCENTRATIONS.....	154
FIGURE 5.2 – NON-INDUCED ATDC5 RANDOM MIGRATION	155
FIGURE 5.3 – COMPARISON OF SPEED IN RANDOMLY MIGRATING UNDIFFERENTIATED AND DIFFERENTIATED ATDC5 CELLS.....	157
FIGURE 5.4 – MORPHOLOGICAL DIFFERENCES ON PLASTIC OVER TIME AFTER ISOLATING CELLS FROM DIFFERENTIATED MICROMASS CULTURES	158
FIGURE 5.5 – MORPHOLOGICAL DIFFERENCES ON TYPE II COLLAGEN OVER TIME AFTER ISOLATING CELLS FROM DIFFERENTIATED MICROMASS CULTURES	159
FIGURE 5.6 – EFFECT OF WNT5A AND WNT3A STIMULATION ON NON-INDUCED ATDC5 MIGRATION	161
FIGURE 5.7 – EXTENDED FOCUS COMPARISON OF NON-INDUCED ATDC5 CELLS INVADING TOWARDS WNT5A	163
FIGURE 5.8 – IDENTIFYING THE POTENTIAL CHEMOATTRACTIVE ABILITY OF WNT5A ON NON-INDUCED ATDC5 CELLS INVADING THROUGH FIXED DIFFERENTIATED MICROMASS CULTURES	164
FIGURE 5.9 – CONFIRMING INVASION OF NON-INDUCED ATDC5 CELLS THROUGH FIXED MICROMASS CULTURES USING RHWNT5A	165
FIGURE 6.1 – SUMMARY OF FINDINGS	179
FIGURE S4.1 – DETECTION OF HUMAN WNT5A-FLAG WITH SPECIFIC WNT5A ANTIBODY.....	210
FIGURE S5.1 – WNT5A DECREASES SPEED OF MIGRATION IN CYTOKINE-STIMULATED ATDC5 CELLS ON TYPE II COLLAGEN COMPARED TO WNT3A	211

Table of Tables

TABLE 2.1 – PCR CYCLING CONDITIONS FOR GENORM ANALYSIS USING PERFECTPROBE TECHNOLOGY ...	39
TABLE 2.2 – GENES ANALYSED USING THE GENORM GENE SELECTION KIT	40
TABLE 2.3 – PRIMER/PROBE SEQUENCES FOR MURINE ASSAYS FOR USE WITH QRT-PCR	42
TABLE 2.4 – STANDARD TAQMAN CYCLING CONDITIONS FOR QRT-PCR USING DOUBLE-DYE HYDROLYSIS PROBES	47
TABLE 2.5 – DETAILS OF PRIMARY ANTIBODIES.....	52
TABLE 2.6 – DETAILS OF SECONDARY ANTIBODIES USED.....	53
TABLE 2.7 – CYCLING CONDITIONS FOR WNT5A AMPLIFICATION AND END-MODIFICATION WITH ACCUAQAQ	54
TABLE 2.8 – PCR CYCLING CONDITIONS FOR QUIKCHANGE LIGHTNING SDM OF PCDNA4:WNT3A	58
TABLE 3.1 – SUMMARY OF GENE REGULATORY CHANGES WITH INCREASING CHONDROGENESIS OF ATDC5 CELLS	99
TABLE 4.1 – EXPRESSION OF <i>COL2A1</i> IN INSULIN-INDUCED CLONES.....	112
TABLE 4.2 – NUMBER OF SIGNIFICANTLY REGULATED PROBE SETS ACCORDING TO P-VALUE BASED ON ABSOLUTE FOLD CHANGE GREATER THAN OR EQUAL TO 1.5 AND P-VALUE LESS THAN 0.05 BY MULTIPLE T-TESTS	129
TABLE 4.3 – NUMBER OF SIGNIFICANTLY REGULATED PROBE SETS ACCORDING TO Q-VALUE USING BENJAMINI-HOCHBERG PROCEDURE TO TAKE INTO ACCOUNT FALSE DISCOVERY RATE	129
TABLE 4.4 – COMPARISON BETWEEN MICROARRAY ANALYSIS AND QRT-PCR ANALYSIS	132
TABLE 4.5 – EFFECT OF CYTOKINES ON PATHWAY REGULATION	136
TABLE 4.6 – SUMMARY OF BASAL GENE REGULATION IN NON-INDUCED WNT5A CLONES.....	142
TABLE 5.1 – SUMMARY OF THE EFFECT OF VARIOUS COMPONENTS ON ADHESION, MIGRATION AND INVASION OF ATDC5 CELLS.....	172
TABLE S3.1 – TAQMAN C _T VALUES FOR FIGURE 3.2	185
TABLE S3.2 – TAQMAN C _T VALUES FOR FIGURE 3.3	186
TABLE S3.3 – TAQMAN C _T VALUES FOR FIGURE 3.4	187
TABLE S3.4 – TAQMAN C _T VALUES FOR FIGURE 3.5	188
TABLE S3.5 – TAQMAN C _T VALUES FOR FIGURE 3.7	189
TABLE S3.6 – TAQMAN C _T VALUES FOR FIGURE 3.8	190
TABLE S3.7 – TAQMAN C _T VALUES FOR FIGURE 3.9	192
TABLE S4.1 – TAQMAN C _T VALUES FOR FIGURE 4.1	193
TABLE S4.2 – TAQMAN C _T VALUES FOR FIGURE 4.4	200
TABLE S4.3 – EFFECT OF WNT5A IN THE ABSENCE OF CYTOKINES	204
TABLE S4.4 – EFFECT OF WNT5A IN THE PRESENCE OF CYTOKINES	205

TABLE S4.5 – EFFECT OF CYTOKINES IN THE ABSENCE OF WNT5A	206
TABLE S4.6 – EFFECT OF CYTOKINES IN THE PRESENCE OF WNT5A.....	207
TABLE S4.7 – TOP 50 GENES SIGNIFICANTLY REGULATED BY CYTOKINES ONLY IN PRESENCE OF WNT5A	208
TABLE S4.8 – TAQMAN C_T VALUES FOR FIGURE 4.11	209
TABLE S5.1 – TAQMAN C_T VALUES FOR FIGURE 5.4 B	211

Chapter 1

Introduction

1.1 Introduction to cartilage

Cartilage is a connective tissue found in various locations around the body, including the ear, nose, articulated joints and intervertebral discs, comprising primarily of collagens and proteoglycans. It is classified into three main types: hyaline cartilage, elastic cartilage and fibrocartilage, with each type exhibiting unique properties. Hyaline cartilage is the most prominent form of cartilage in the body, forming the framework of the embryonic skeleton to be largely replaced by bone in a process called endochondral ossification. As a result, hyaline cartilage is left lining the surfaces of bones in articulating joints, and thus is called articular cartilage. The main collagen in hyaline cartilage is type II collagen. This is also true for elastic cartilage, which is histologically similar to hyaline cartilage, but in addition, also contains elastin fibres, which can be seen by light microscopy (Horton, 1993; Worster, *et al.*, 2001). This is the most flexible type of cartilage and is found in areas such as the ears and nose. Finally fibrocartilage is the most rigid cartilage and is located in the intervertebral discs. Unlike hyaline cartilage and elastic cartilage, the main collagens in fibrocartilage are type I collagen with a small proportion of type III collagen (Eyre & Wu, 1983).

1.1.1 Articular Cartilage

Articular cartilage is hyaline cartilage that lines the surfaces of articulated joints (Figure 1.1) that resists deformation, aiding distribution of load and protecting the underlying bone (Buckwalter & Mankin, 1997; Hendren & Beeson, 2009). It is comprised primarily of an extracellular matrix (ECM) containing type II collagen; the large aggregating proteoglycan, aggrecan; and water. It is also sparsely populated by chondrocytes, which constitute less than 5% of the cartilage volume (Poole, *et al.*, 2002). The remainder of the cartilage is inhabited by the extensive ECM. It is the combined properties of the constituents of the matrix, as well as the synovial fluid that fills the joint cavity, that allow near-frictionless movement of articulated joints in healthy individuals (Wu, *et al.*, 2010).

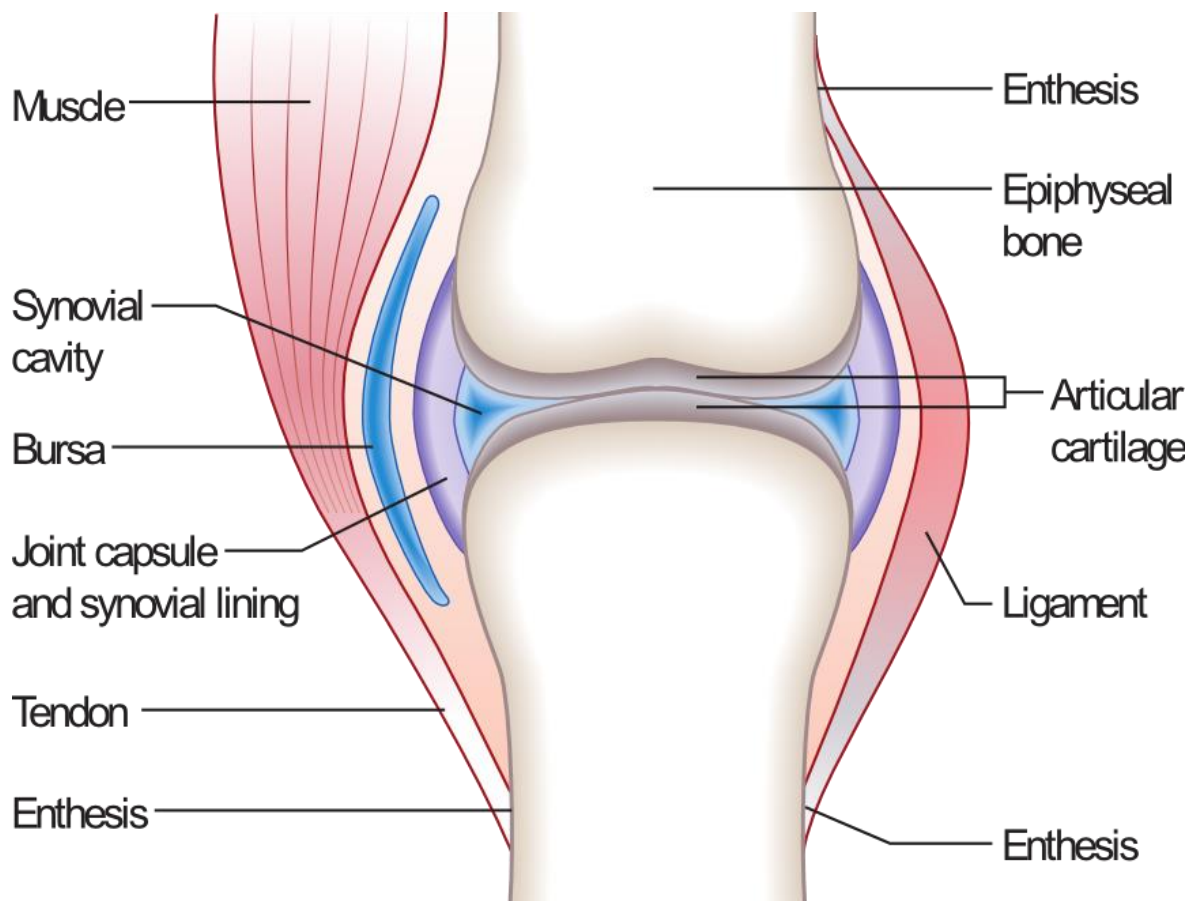


Figure 1.1 - Anatomy of an articulated joint. Simplified diagrammatic view of an articulated joint showing a layer of articular cartilage lining the surfaces of two meeting bones. Physical interaction between the bones is prevented by the lining cartilage and allows near-frictionless movement in healthy individuals, resisting deformation due to bearing load via the distribution of the load across the joint, protecting the underlying bone. Reproduced from (Maen, 2010)

1.1.2 Type II Collagen

Collagen is an abundant protein in the body, forming one third of the total protein in humans. Conservation of collagen proteins has been observed across phyla from simple organisms such as sponges, to complex animals such as vertebrates (Boot-Handford & Tuckwell, 2003) and has been reported to be discovered in a 65 million year old *Tyrannosaurus rex* fossil (Shoulders & Raines, 2009). This high conservation and abundance clearly demonstrates the importance of the collagen proteins.

Type II collagen is a classical fibrillar collagen, which consist of three helical polypeptide α chains that wrap around each other to form the characteristic triple helix. The various types of collagens contain either a mixture of different α chains (heterotrimer) or three of the same α chains (homotrimer), with type II collagen being a homotrimer consisting of three $\alpha 1(\text{II})$ chains (Shoulders & Raines, 2009). These chains contain the typical -Gly-X-Y- triple repeat domain, where X is typically proline and Y is typically hydroxyproline (Ramachandran, 1956). The repeat of glycine, due to its small size, at every third residue enables the α chains to twist around a central axis, wrapping round each other to form the triple helix. This structure is stabilised by hydroxyproline, forming hydrogen bonds along the helix (Cremer, *et al.*, 1998; Boot-Handford & Tuckwell, 2003).

Collagen is first synthesised as its separate α chains which undergo post-translational modification in the rough endoplasmic reticulum (RER). Once translocated into the endoplasmic reticulum lumen, the carboxy terminal non-collagenous (NC1) domain folds and selects other appropriate α chains with which to trimerise with, nucleating at the carboxy terminal and 'zipping up' the rest of the trimer in a C-N direction. For fibrillar collagens, this procollagen remains soluble due to the soluble C and N terminal domains. Once secreted and these prodomains cleaved, the insoluble collagenous domain containing the -Gly-X-Y- repeat aggregates and overlaps, with lysyl oxidase catalysing cross-links to stabilise the fibrils (Boot-Handford & Tuckwell, 2003)(Figure 1.2). Many of these collagen fibrils then associate to form a collagen fibre. This organised structure is what gives collagen its properties, providing strength and resistance to stretching forces.

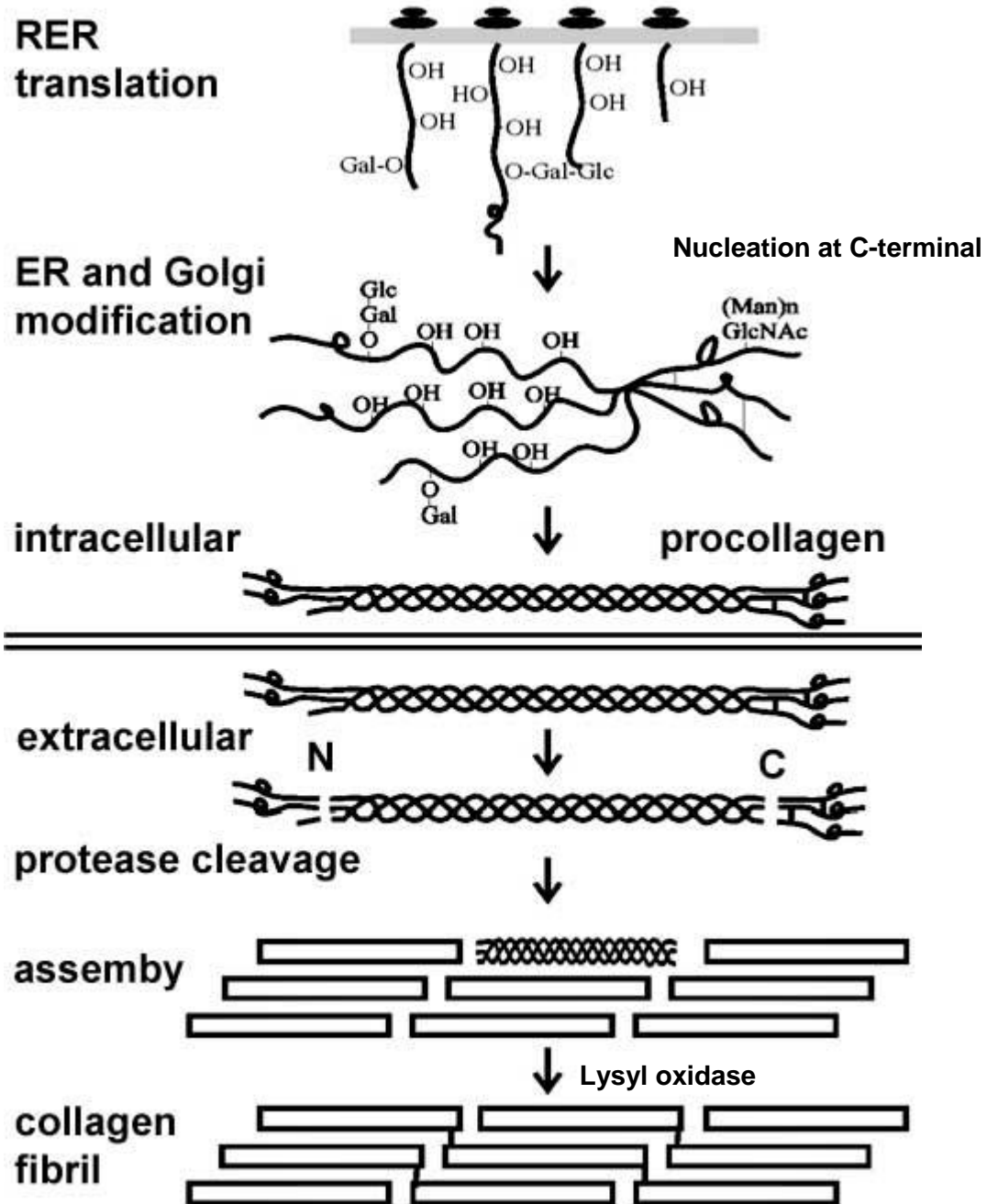


Figure 1.2 - Collagen fibril synthesis. Three translated α chains associate at their C-terminal and zip along the chains in a C-N direction, forming a triple helix. Once secreted from the cell, the C-terminal and N-terminal domains are cleaved and the individual collagen proteins associate together in a staggered formation. Cross-links are then catalysed by lysyl oxidase to form collagen fibrils. Figure adapted from Hill (2009).

1.1.3 Aggrecan

Aggrecan is a large proteoglycan and is another important constituent of cartilage, providing the cartilage with resistance to compressive forces (Haung & Wu, 2008). Its core protein contains three globular domains, termed G1, G2 and G3, rich in cysteine. The G1 and G2 domains are separated by an interglobular domain (IGD); and G2 and G3 are separated by a long glycosaminoglycan (GAG)-attachment region, consisting of three domains, one of which covalently links keratan sulphate (KS) and two (CS1 and CS2) that link chondroitin sulphate (CS) chains (Roughley, 2001, 2006) (Figure 1.3).

As its name suggests, aggrecan aggregates non-covalently onto a central filament of hyaluronan (HA) via a link protein in complex with G1, forming a ternary complex between the three components, with up to 100 aggrecan molecules radiating from the HA (Mörgelin, *et al.*, 1988; Dudhia, 2005; Roughley, 2006). The size of this complex traps aggrecan in the type II collagen framework in articular cartilage. However, aggrecan is rarely found in its whole form in cartilage, being subject to proteolytic processing of the core protein. This results in aggregation typically of G1-containing fragments within the collagen matrix (Roughley, 2006).

The essential function of aggrecan in cartilage comes from the attachment of GAGs - negatively-charged linear polysaccharides, KS and CS, forming a bottlebrush structure (Figure 1.3). In the presence of HA, many aggrecan monomers aggregate together along the HA core to form a bottlebrush superstructure. This creates a high charge density, resulting in a high degree of hydration and thus forming an osmotically active complex. This retention of water enables near-frictionless movement in an articulated joint, forming a hydrated gel-like structure. This osmotically active gel-like structure provides osmotic resistance to deswelling under compressive forces, and the collagen network provides resistance against swelling pressures. Aggrecan therefore allows reversible deformation of cartilage due to compressive forces, allowing the articulated joints to bear and distribute load, providing cartilage with one of its most important functions (Dudhia, 2005; Horkay, *et al.*, 2008).

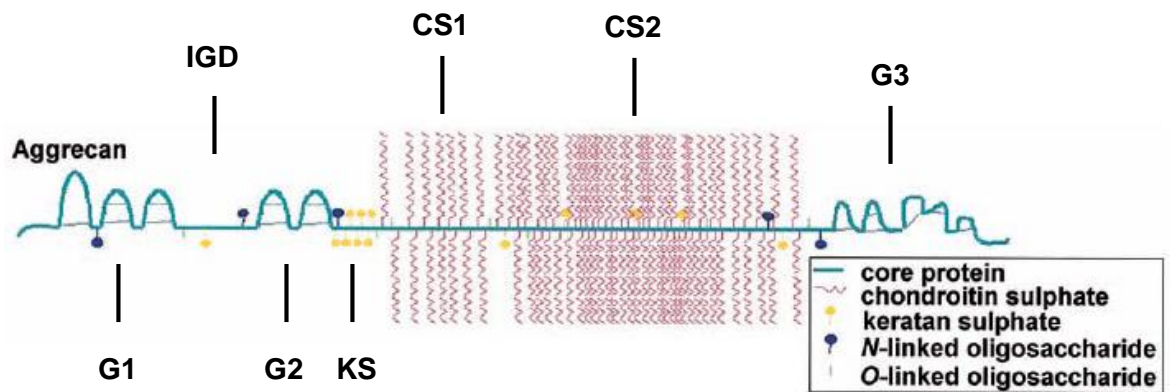


Figure 1.3 – Structure of Aggrecan. Aggrecan consists of a large core protein split into three main globular domains, G1, G2 and G3. Between G2 and G3 lies a keratan sulphate (KS) domain and two chondroitin sulphate domains (CS1 and CS2) which bind their respective glycosaminoglycans (GAGs). It is the binding of these GAGs which gives aggrecan its important property in cartilage to resist compressive forces. These negatively-charged side chains create a high charge density, resulting in the retention of water, creating a gel-like structure, enabling the joint to bear and distribute load. Figure reproduced and adapted from (Dudhia, 2005).

1.1.4 Chondrocytes and Chondrogenesis

Articular cartilage is an avascular, aneural and alymphatic connective tissue, and as such, was previously thought to be sparsely inhabited by just one cell type known as chondrocytes, which are responsible for the production, secretion and regulation of the cartilage matrix (Poole, 1997). It is now known that chondroprogenitor cells are also resident within cartilage (Dowthwaite, *et al.*, 2004), discussed later. This matrix also has an important role in regulating chondrocytic functions, with the function of the chondrocyte being dependent on its location (Archer & Francis-West, 2003).

Chondrocytes are derived from precursor cells known as mesenchymal stem cells (MSCs) in a process known as chondrogenesis, which, developmentally, occurs during endochondral ossification. This is the process of converting the hyaline collagen anlagen into the skeleton. During the first step, mesenchyme aggregates and condenses, regulated by bone morphogenetic proteins (BMPs). During this process, the MSCs express the master chondrogenesis transcription factor, sex-determining region Y box 9 (SOX9), a primary determinant of chondrogenesis. As these cells differentiate into chondrocytes, various components of the extensive cartilage ECM are laid down, such as type II collagen and aggrecan.

Most chondrocytes then undergo hypertrophy, withdraw from the cell cycle and subsequently commit themselves to apoptosis, allowing the space previously occupied by them to be replaced by bone and vascular architecture following the production of vascular endothelial growth factor (VEGF) by both hypertrophic chondrocytes and more terminal hypertrophic chondrocytes (Zuscik, *et al.*, 2008). However, chondrocytes at the distal ends of long bones proliferate and synthesize new cartilage which is substituted by bone by the approaching ossification front. Higher hydrostatic pressure at the joint surface slows the growth of cartilage and the ossification front stabilizes, defining the thickness of the articular cartilage that now lines the surface of the newly formed bone (Carter, *et al.*, 2004).

Chondrocytes in articular cartilage are maintained in four distinct areas: the superficial zone, the intermediate zone, the radial zone and the zone of calcified cartilage. As previously mentioned, the function of chondrocytes depends on its location. In the superficial zone, there are 1-2 layers of flattened chondrocytes expressing a variety of genes, including proteoglycan 4 (*PRG4*, also known as lubricin), *SOX9* and type II collagen (*COL2A1*). Chondrocytes in the intermediate zone are rounded and express many of the same genes as in the superficial zone with the exception of *PRG4*. In the radial zone, chondrocytes express markers of mature differentiation and hypertrophy, such as type X collagen (*COL10A1*) and alkaline phosphatase (*ALPL*) (Zuscik, *et al.*, 2008) (Figure 1.4).

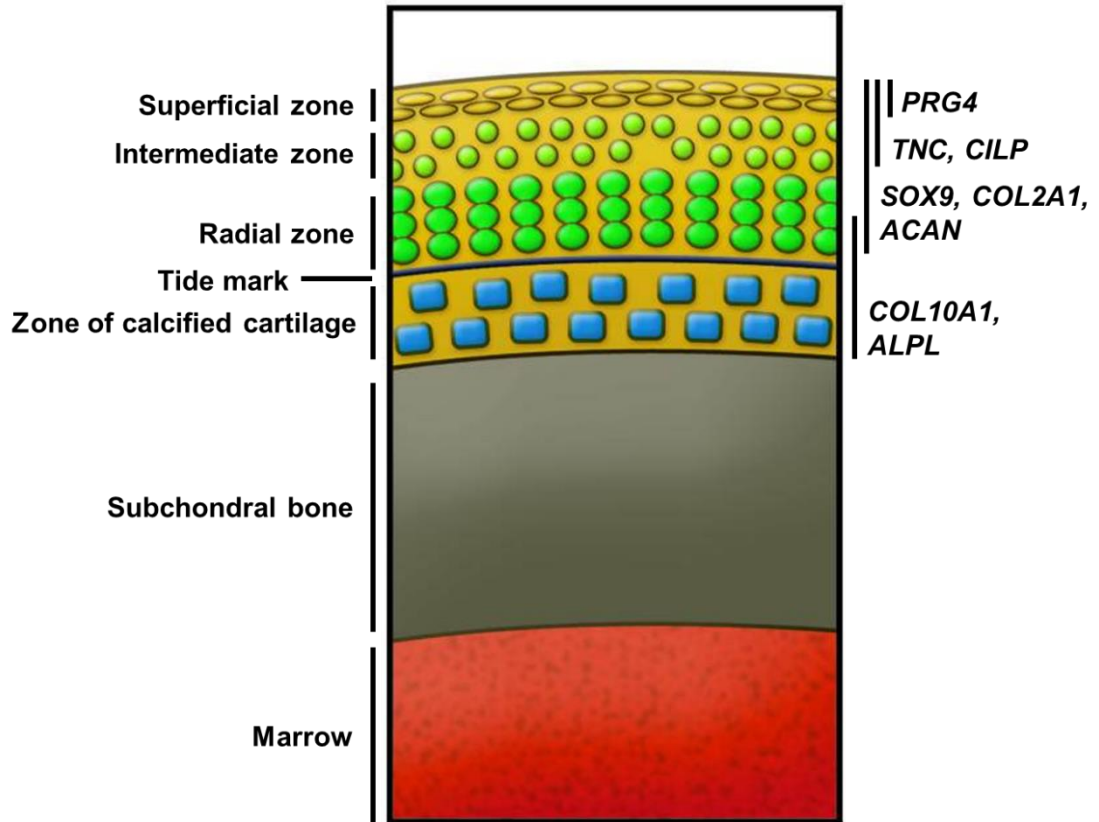


Figure 1.4 – Cellular zones of articular cartilage. Diagram showing the different zones within articular cartilage, highlighting the different gene expression of the chondrocytes shown in each zone. Figure modified from Zuscik, *et al.* (2008)

1.2 WNT Signalling

The WNT family of secreted glycoproteins, named after the discovery of the homologous *Drosophila wingless (Wg)* and murine *mouse mammary tumour virus integration site 1 (Int1)*, and its various pathways are well known for their role in developmental biology, with a variety of functions, including axis formation (Zeng, *et al.*, 1997; Liu, *et al.*, 1999) and cell fate determination (Dorsky, *et al.*, 1998). Dysregulation of WNT signalling can have a number of effects, ranging from formation of a secondary axis during development (Zeng, *et al.*, 1997), to tumourigenesis (Caldwell, *et al.*, 2004; Gatcliffe, *et al.*, 2008).

WNT signalling can be split into two broad pathways – the canonical signalling pathway (also known as β -catenin-dependent pathway) and the non-canonical pathway (also known as the β -catenin-independent pathway).

1.2.1 Canonical WNT Pathway

The canonical WNT pathway is transduced by the Frizzled (FZD) family of seven pass transmembrane receptors along with low-density lipoprotein receptor (LDRL)-related protein (LRP)5/6 (Tamai, *et al.*, 2000). In the absence of a WNT ligand binding to its receptors, β -catenin present in the cytoplasm is continually phosphorylated by glycogen synthase kinase 3 (GSK3) and casein kinase 1 (CK1) as a complex with axin and adenomatosis polyposis coli (APC), commonly collectively referred to as the destruction complex. Association with β -transducin repeat-containing protein (β -TrCP), an E3 ubiquitin ligase, marks it for ubiquitination and subsequent proteolysis by the proteasome.

A canonical WNT ligand binding to FZD and LRP5/6 results in phosphorylation of LRP5/6 by CK1 and GSK3. GSK3 is recruited by axin (MacDonald, *et al.*, 2009) and phosphorylates LRP5/6 at a PPP(S/T)P motif (Zeng, *et al.*, 2005), providing a docking site for axin, forming a positive feedback loop to enhance the signal. Axin and dishevelled (DVL) associate and DVL binds to the activated FZD. Activation of DVL inhibits GSK3 and thus inhibits the phosphorylation of β -catenin that marked it for degradation. β -catenin is then allowed to stabilise in the cytoplasm where it can translocate to the nucleus, associating with T cell-specific/lymphoid enhancer binding factor (TCF/LEF), activating gene transcription (Sethi & Videl-Puig, 2010; Clark, *et al.*, 2012; Staines, *et al.*, 2012; Kim, *et al.*, 2013c) (Figure 1.5)

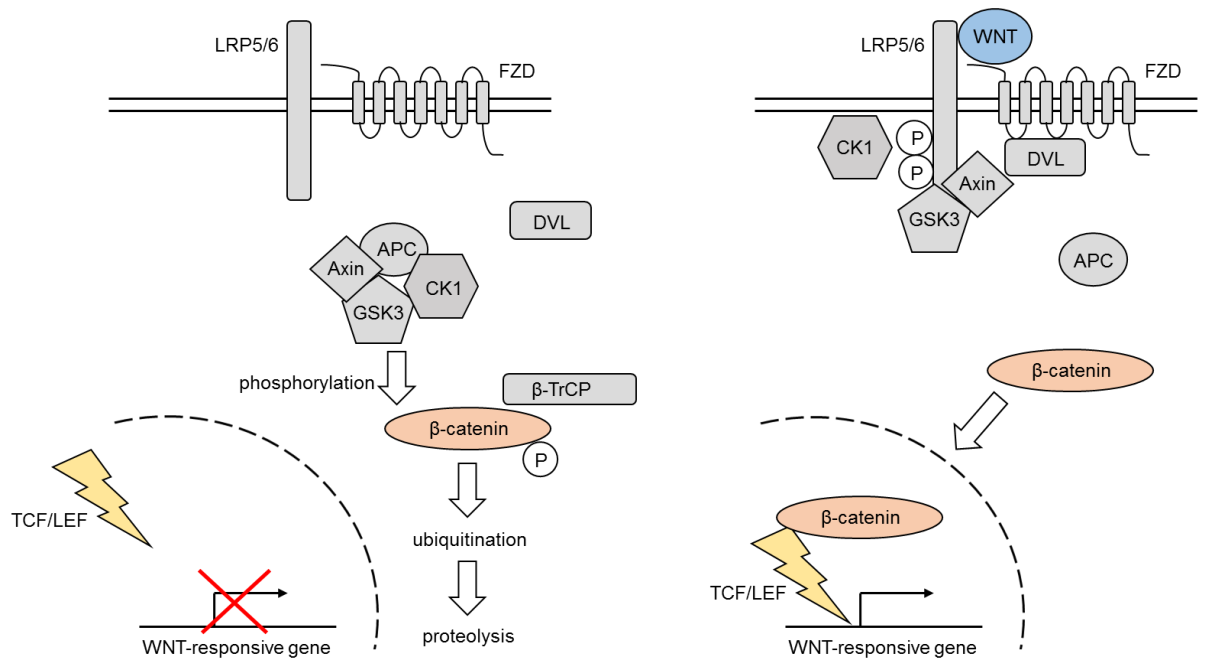


Figure 1.5 – Canonical WNT Pathway. Simplified cartoon showing that in the absence of WNT, β -catenin is phosphorylated by GSK3 and marked for degradation. In the presence of WNT, the GSK3 complex is dissociated and inhibited from marking β -catenin for degradation, which subsequently stabilises in the cytoplasm and translocates to the nucleus where it can activate transcription of WNT-responsive genes via TCF/LEF. Comprised using information from Nusse (2005), Sethi and Videl-Puig (2010), Clark, *et al.* (2012) and Kim, *et al.* (2013c).

1.2.2 Non-canonical WNT Pathway

The non-canonical WNT signalling pathway (β -catenin-independent pathway) has not been subject to as extensive study as the canonical pathway, and can be further subdivided into more specific pathways (Sethi & Videl-Puig, 2010). Broadly, this can be split into two main pathways, the calcium-dependent pathway (WNT/ Ca^{2+}) and the planar cell polarity pathway (PCP).

In the WNT/ Ca^{2+} pathway, WNT binding to FZD triggers an increase in cytoplasmic Ca^{2+} levels via phospholipase C (PLC), which in turn activates effectors such as Ca^{2+} /calmodulin-dependent kinase II (CAMKII), calcineurin and protein kinase C (PKC). Calcineurin activation may then also activate the transcription factor nuclear factor of activated T-cells (NFAT). PKC and CAMKII can also inhibit β -catenin signalling in the canonical WNT signalling pathway (Niehrs, 2012)(Figure 1.6).

In the PCP pathway, WNT binding to FZD activates small GTPases such as RhoA and RAC1, which in turn can activate RHO kinase (ROCK) and c-Jun-N-terminal kinase (JNK), leading to activation of JNK-dependent transcription factors such as activating transcription factor 2 (ATF2) (Niehrs, 2012)(Figure 1.6).

1.2.3 WNT5A/ROR2 Signalling

The WNT ligand WNT5A was traditionally thought to be a non-canonical WNT, although research has shown that WNT5A can activate the canonical WNT pathway via FZD4 (Mikels & Nusse, 2006) and therefore its effects may be dependent on the receptors present.

Primarily, WNT5A is known to activate the non-canonical WNT signalling pathway by binding to and activating receptor tyrosine kinase-like orphan receptor 2 (ROR2), a single-pass transmembrane receptor, which may work independently or in a complex with FZD to activate JNK-mediated signalling (Oishi, *et al.*, 2003; Clark, *et al.*, 2012; Niehrs, 2012) (Figure 1.6).

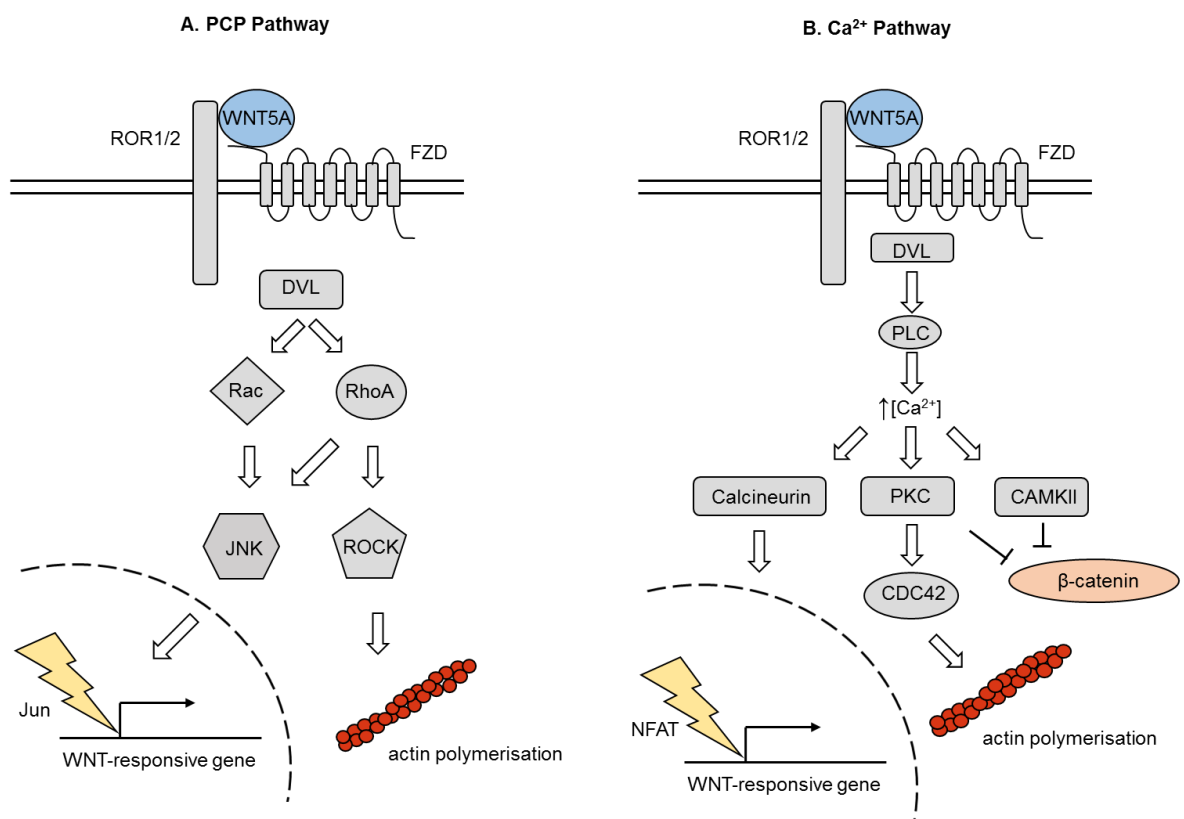


Figure 1.6 – WNT5A Signalling Pathways. Simplified cartoon of WNT5A signalling in the planar cell polarity (PCP) pathway (A) and calcium-dependent pathway (B) – two “non-canonical” WNT signalling pathways. A) In the PCP pathway, WNT5A acts via small GTPases to mediate changes in the cytoskeleton and activate JNK-mediated transcription factors. B) In the calcium-dependent pathway, WNT5A-mediated increases in intracellular Ca²⁺ concentrations may also result in changes in the cytoskeleton as well as inhibition of β-catenin signalling via PKC and CAMKII. Gene expression may also be modulated by NFAT transcription factor. Comprised using information from Niehrs (2012).

Knockout mice of WNT5A and ROR2 phenotypically mimic each other, suggesting an intricate relationship between ROR2 and WNT5A signalling. Both knockout mice die shortly after birth with respiratory dysfunction and also exhibit craniofacial defects such as cleft palate, limb shortening and tail shortening (Oishi, *et al.*, 2003; Schwabe, *et al.*, 2004; He, *et al.*, 2008). Both WNT5A and ROR2 have been implicated in Robinow syndrome, a disease that primarily results in a form of dwarfism, with limb shortening and craniofacial defects giving rise to a look described as 'foetal face' due to the similarities with the developing face of a foetus (Brunetti-Pierri, *et al.*, 2008; Beiraghi, *et al.*, 2011), due to loss-of-function mutations (Schwabe, *et al.*, 2004; Person, *et al.*, 2010; Roifman, *et al.*, 2014; Tamhankar, *et al.*, 2014). Due to the similarities and the known involvement of ROR2, *Ror2*^{-/-} mice have been used to model Robinow Syndrome (Schwabe, *et al.*, 2004).

Similar to *Wnt5a*^{-/-} mice, mice overexpressing *Wnt5a* specifically in cartilage (by driving expression from to the *Col2a1* promoter), resulted in severe skeletal defects, including shortening of the skeletal elements of the limb, despite an overall increase in cartilage thickness, and severe delay in hypertrophic differentiation of chondrocytes (Yang, *et al.*, 2003). Overexpression of *Wnt5a* resulted in an increase in p130 expression with a decrease in cyclin D1 expression, causing an expansion of zone I chondrocytes, which go on to form the articular cartilage, at the expense of zone II chondrocytes which undergo hypertrophy form the growth plate cartilage. In comparison, chondrocytes from *Wnt5a*^{-/-} mice enter zone II prematurely but are prevented from terminal differentiation (Yang, *et al.*, 2003).

Similarly, the effect of WNT5A and its inhibition of hypertrophy has also been seen *in vitro* in micromass cultures (three-dimensional culture, discussed in section 1.4.4) of immortalised mouse limb bud cells via nuclear factor kappa-light-chain-enhancer of activated B cells (NF-κB)-dependent inhibition of runt-related transcription factor 2 (*Runx2*), the major transcription factor driving hypertrophic differentiation. However, the effect of WNT5A on chondrocyte differentiation was shown to be stage dependent – whilst WNT5A inhibited hypertrophic differentiation at later stages of chondrogenesis, WNT5A enhanced chondrogenesis at earlier stages via NFAT-dependent induction of SOX9, the master transcription factor driving early chondrogenesis (Bradley & Drissi, 2010). This highlights the deep involvement of WNT5A in cartilage biology.

1.2.4 WNT signalling and chondrocytes

In addition to WNT5A, a number of other WNT family members are known for their role in the regulation of limb and skeletal development. Transfection with *WNT1* in the developing chick limb

bud resulted in a truncated radius and ulna. Abnormalities were also revealed by Alcian blue staining (which stains the sulphated GAGs attached to proteoglycans) of the cartilaginous elements in the beak when WNT1 was ectopically expressed in the craniofacial mesenchyme. Infection of micromass cultures with WNT1 virus, which ordinarily undergo chondrogenesis by the act of the high density culture alone, failed to undergo chondrogenesis. The same result was also observed with WNT7A (Rudnicki & Brown, 1997). These results suggest that WNT1 and WNT7A both have inhibitory effects on chondrogenesis.

Misexpression of WNT3A in the developing chick limb bud resulted in ectopic expression of apical ectodermal ridge (AER)-specific genes, a region that induces limb development, such as BMP-2, known to induce chondrogenesis (Kengaku, *et al.*, 1998). In a different micromass experiment in a murine multipotent cell line (C3H10T1/2), results showed that treatment with BMP-2 to induce chondrogenesis increased levels of *Wnt3a* mRNA during early stages of chondrogenesis and decreased levels of *Wnt7a* mRNA during late stages of chondrogenesis (Fischer, *et al.*, 2002a), in agreement with Rudnicki & Brown's report (2007) regarding the inhibitory effect of WNT7A. The same group later found that overexpression of *Wnt3a* was insufficient to induce chondrogenesis in the same cell line, requiring addition of BMP-2, although overexpression of *Wnt3a* made the cells more responsive to chondrogenesis induced by BMP-2 (Fischer, *et al.*, 2002b). Conversely, WNT3A has also been shown to inhibit chondrogenesis in micromass cultures of chick limb buds (Hwang, *et al.*, 2005), which can be restored by WNT inhibitory factor 1 (WIF1) (Surmann-Schmitt, *et al.*, 2009) and has been shown to induce de-differentiation of articular chondrocytes from New Zealand white rabbits (Hwang, *et al.*, 2005).

1.2.5 WNT Signalling in Osteoarthritis

In addition to their involvement in the cartilage development, various members of the WNT family have also been implicated in cartilage pathologies, such as osteoarthritis (OA), characterised by the degradation of articular cartilage (discussed in more detail in section 1.3), and matrix turnover.

WNT3A transfection in articular chondrocytes from rabbit knee and elbow decreased the levels of proteoglycans in the ECM. These cells also exhibited increased levels of matrix metalloproteinase (*MMP*)₃, *MMP*₁₃, A Disintegrin And Metalloproteinase with Thrombospondin Motif (*ADAMTS*)₄ and *ADAMTS*₅, known matrix-degrading enzymes. Additionally, in a Hartley guinea pig model of age-dependent OA, nuclear β -catenin staining was more prominent with worsening OA with severe cartilage degeneration and thinning, indicating canonical WNT signalling in the involvement of cartilage degeneration (Yuasa, *et al.*, 2008).

Mutations in Frizzled-related protein (*FRZB*, also known as “secreted Frizzled-related protein 3” [sFRP3]) have been associated with hip OA susceptibility in women (Loughlin, *et al.*, 2004; Lane, *et al.*, 2006). *FRZB* is a glycoprotein antagonist of WNT signalling that resembles the FZD transmembrane receptors but lacks the transmembrane domain, therefore competitively inhibiting WNT signalling (Jones & Jomary, 2002). Transfection studies in a human embryonic kidney cell line (HEK293) revealed that a single nucleotide polymorphism resulting in a R325G mutation in *FRZB*, associated with hip-OA in female patients, had a diminished ability to antagonise WNT signalling, as noted by nuclear levels of β -catenin, suggesting an importance of inhibiting WNT signalling to maintain the integrity of the cartilage (Loughlin, *et al.*, 2004).

Mouse models have also demonstrated the significance of WNT signalling in OA development via *FRZB*. *Frzb*^{-/-} mice, which were macroscopically and histomorphologically indistinguishable from wild-type littermates, were more susceptible to cartilage damage via various induced OA models with an increase in active WNT signalling. In arthritic *Frzb*^{-/-} mice, *Mmp3* mRNA expression was up-regulated, with no increase in *Mmp9*, *Mmp13*, *Adamts4* or *Adamts5* detected. Recombinant *FRZB* dose-dependently inhibited recombinant MMP3 activity in a colorimetric *in vitro* activity assay, indicating that inhibition of WNT signalling may impede cartilage damage by inhibiting matrix-degrading enzyme (Lories, *et al.*, 2007).

In addition to *FRZB*, Dickkopf-1 (*DKK1*), another WNT inhibitor, has also been implicated in osteoarthritis, with increased levels of *DKK1* protein and mRNA found in human knee OA cartilage (Weng, *et al.*, 2009; Oh, *et al.*, 2012) and in experimental mouse OA cartilage (Oh, *et al.*, 2012). Treatment of primary human chondrocytes with *DKK1* increased the number of observed apoptotic cells in a time-dependent manner. Antibody-mediated neutralisation of *DKK1* also abrogated interleukin (IL)-1 β -mediated induction of apoptosis (Weng, *et al.*, 2009). Conversely, cartilage-specific overexpression of *Dkk1* in mice significantly inhibited cartilage damage by destabilisation of the medial meniscus (DMM, a commonly used experimental OA model), and pre-exposure of primary mouse chondrocyte cultures with *DKK1* inhibited WNT3A-mediated up-regulation of *Mmp13* and *Adamts4*, two key enzymes in cartilage destruction (discussed in more detail in section 1.3.2) (Oh, *et al.*, 2012). Additionally, lower levels of circulating *DKK1* have been found in the plasma from OA patients, negatively correlating with worsening OA (Honsawek, *et al.*, 2010).

1.2.6 CCN family and osteoarthritis

The CCN proteins are a family of six cysteine-rich matricellular proteins of the ECM, named after the first three founding members: Cysteine-rich Protein 61 (CYR61), Connective Tissue Growth Factor (CTGF) and Nephroblastoma Overexpressed (NOV). Three further members were also

subsequently discovered – WNT-1-inducible Secreted Protein 1 (WISP1), WISP2 and WISP3 – and have since also been referred to as CCN1-6 respectively. These CCN proteins all contain a similar modular structure (Figure 1.7), containing four domains: insulin-like growth factor binding protein domain (IGFBP), von Williebrand factor type C (VWC) domain, thrombospondin type 1 repeat domain (TSP-1) and a c-terminal domain containing a cysteine knot (CT). However, NOV/CCN3 is unique in that it lacks the CT domain (Zuo, *et al.*, 2010).

These CCN proteins have been implicated in a number of biological processes, including cell adhesion, migration, differentiation, survival and mitogenesis (Dhar & Ray, 2010). They have also been implicated in a number of chondrocytic processes.



Figure 1.7 – The modular structure of the CCN Growth Factor family. Each member of the CCN family contain a similar modular structure consisting of a signal peptide (SP) necessary for secretion from the cell, an insulin-like growth factor binding protein domain (IGFBP), a von Williebrand factor type C domain (VWC), a thrombospondin type 1 repeat domain (TSP1) separated from the VWC domain via a linker bridge, and a c-terminal domain containing a cysteine knot (CT), which is absent in CCN5. Figure comprised using information from Brigstock, *et al.* (2003) and Chen and Lau (2009)

1.2.6.1 CYR61/CCN1

CYR61/CCN1, the first founding member of the CCN family, has been shown to be involved in mammalian chondrogenesis. Immunohistochemistry of mouse embryos revealed staining for CYR61/CCN1 in the maturing cartilage and perichondrium of the forelimb digits; in the skeletal anlagen of the forelimb; and in the less mature, condensing mesenchyme of posterior somites, indicating a role in chondrogenesis. Antibody neutralisation of CYR61/CCN1 in single-cell suspended isolated limb bud mesenchymal cells significantly inhibited the cells' ability to aggregate, an important step in chondrocyte differentiation. Treatment of a micromass culture with CYR61/CCN1 also significantly increased levels of *Col2a1* (Wong, *et al.*, 1997). These results indicate that CYR61/CCN1 induce differentiation of MSCs into chondrocytes during chondrogenesis in the mouse. On the contrary in human bone marrow-derived mesenchymal stem cells (hBMSCs), mRNA levels

of *CYR61* decreased from high expression prior to differentiation to undetectable levels one week after initiation of differentiation (Schütze, *et al.*, 2005).

CYR61/CCN1 has also been implicated in fracture healing of rat femur, an environment that reportedly recapitulates embryonic development, displaying significantly elevated mRNA expression and protein levels in proliferating chondrocytes, but not hypertrophic chondrocytes (Hadjjargyrou, *et al.*, 2000). Furthermore, CYR61/CCN1 has been shown to be up-regulated in response to WNT3A in a mouse pluripotent progenitor cell line (C3H10T1/2). siRNA knockdown of *Cyr61* also inhibited osteogenic differentiation in WNT3A-overexpressing cells, demonstrating the importance of *Cyr61* in WNT3A-induced osteogenic differentiation of MSCs (Si, *et al.*, 2006).

1.2.6.2 CTGF/CCN2

CTGF/CCN2, the second founding member of the CCN family, has been well documented to be involved in chondrocyte hypertrophy, with immunohistochemical analysis showing localisation of CTGF/CCN2 expression in the most hypertrophic cells (Huang, *et al.*, 2010). Immortalised chondrocytes isolated from a chondrosarcoma from a 72 year Japanese male (Takigawa, *et al.*, 1989), HCS-2/8 cells, transfected with *CTGF* resulted in earlier and increased expression of aggrecan core protein, a marker of chondrocyte maturation, and earlier and increased expression of type X collagen, a marker of chondrocyte hypertrophy (Nakanishi, *et al.*, 2000). These results have also been mimicked in rabbit auricular chondrocytes (Fujisawa, *et al.*, 2008), demonstrating the importance of CTGF/CCN2 in chondrocyte differentiation and hypertrophy.

It has been shown that SOX9 represses *Ctgf* expression in chondroprogenitor cells by binding to a TCF/LEF-SOX9 consensus site in the *Ctgf* promoter. In hypertrophic cells where SOX9 levels are decreased, the TCF/LEF consensus site is occupied by β -catenin, leading to increased levels of *Ctgf*. WNT3A stimulation of chondroprogenitor cells also lead to an increase in *Ctgf* expression, further implicating the involvement of WNT signalling in the various stages of chondrogenesis (Huang, *et al.*, 2010).

The importance of CTGF/CCN2 was established in 2003 upon the discovery that *Ctgf*^{-/-} mice die within minutes after birth due to respiratory failure caused by skeletal defects (Ivkovic, *et al.*, 2003). These mice exhibited shortened sterna which were bent inwards and had kinked ribs. Mineralised cartilage zones were expanded whilst ossification was reduced, suggesting a defective replacement of cartilage with bone. The hypertrophic zone in the cartilage of long bones was also disorganised. Although growth plate cartilage had normal expression and distribution of type II collagen and type

X collagen, expression of aggrecan and link protein were decreased (Ivkovic, *et al.*, 2003). Together, this highlights the importance of CTGF/CCN2 in cartilage.

1.2.6.3 NOV/CCN3

NOV/CCN3, the third founding member of the CCN family, has also been implicated in chondrocyte hypertrophy. Immunohistochemistry and semi-quantitative RT-PCR revealed NOV/CCN3 expression in the pre-hypertrophic and hypertrophic zones of the embryonic murine growth plate. Treatment with parathyroid hormone-related protein (PTHrP), known to delay terminal differentiation, resulted in a decrease of type X collagen in murine explant cultures and decrease of NOV/CCN3 mRNA and protein, indicating NOV/CCN3's involvement in chondrocyte hypertrophy (Yu, *et al.*, 2003). This has also been shown by siRNA knockdown (Lafont, *et al.*, 2005a). Furthermore, the same group also demonstrated that NOV/CCN3 up-regulates transforming growth factor (TGF)- β 2, implicating NOV/CCN3 in two stages of chondrogenesis: condensation (TGF β 2 increase) and hypertrophy (type X collagen increase). Additionally, deletion of *Ctgf* in mouse chondrocytes has been shown to increase levels of *Nov*, and stimulation of wild-type chondrocytes with recombinant NOV/CCN3 decreased expression of *Ctgf*, suggesting regulation of the CCN family by itself (Kawaki, *et al.*, 2008).

1.2.6.4 WISP1/CCN4

WISP1/CCN4 is the first member of the WNT1-inducible secreted proteins and the fourth member of the CCN family, and has been implicated in OA directly. WISP1/CCN4 protein has been shown to be increased in murine OA knee joints up to day 21 after OA induction by collagenase, after which WISP1/CCN4 levels decreased with decreasing chondrocytes in the cartilage. Additionally, immunohistochemistry revealed strong WISP1/CCN4 staining at the cell surface and ECM in human knee and hip OA cartilage, especially in the midzone and chondrocyte clusters (Blom, *et al.*, 2009). WISP1/CCN4 expression has also been shown in hypertrophic zone of the developing tibia in murine embryos in a non-OA model (Yanagita, *et al.*, 2007).

Dose-dependent induction of *Adamts4*, *Mmp3*, *Mmp9* and *Mmp13* was observed by WISP1/CCN4 treatment in the murine RAW 264.7 macrophage cell line, and *MMP3* and *MMP9* in both primary human synovial cells and primary human chondrocytes (Blom, *et al.*, 2009), all known matrix-degrading enzymes, further implicating the involvement of WISP1/CCN4 in the progression of OA.

Furthermore, overexpression of WISP1/CCN4 in HCS-2/8 cells did not regulate expression of *Col2a1* and aggrecan (*Acan*), but did significantly increase expression of *ALPL*, and may therefore be important in chondrocyte differentiation in endochondral ossification (Yanagita, *et al.*, 2007).

1.2.6.5 WISP2/CCN5

WISP2/CCN5 is unique amongst the CCN family as it lacks the CT domain that is present in the remaining five members (Wei, *et al.*, 2009). *In situ* hybridisation revealed localised strong expression of *Wisp2* mRNA in osteoblasts of calcified cartilage in human foetal femur with weaker expression in chondrocytes and osteoclasts (Kumar, *et al.*, 1999). RT-PCR has also shown *WISP2* to be expressed in BMSCs from human femoral heads and is expressed prior to initiation, and in the initial stages, of adipogenesis. However no differences were found during chondrogenic differentiation of MSCs (Schütze, *et al.*, 2005). *WISP2* has also been detected by RT-PCR preferentially in the synovium of rheumatoid arthritis (RA) patients compared to that of OA patients, and shown via immunohistochemistry to be restricted to fibroblast cells in extensive fibrotic tissue in RA patients (Tanaka, *et al.*, 2005). These findings suggest that WISP2/CCN5 may therefore be preferentially implicated in RA and pathologies involving the bone rather than OA.

1.2.6.6 WISP3/CCN6

WISP3/CCN6 is the final member of the WISP and CCN families and has been implicated in a number of diseases, such as breast cancer (Marrakchi, *et al.*, 2010) and is mutated in progressive pseudorheumatoid dysplasia (PPRD) (Hurvitz, *et al.*, 1999; Zhou, *et al.*, 2007; Ye, *et al.*, 2010). PPRD is a disease affecting articular cartilage of multiple joints, most commonly the interphalangeal joints of the hands and then hips and elbows, leading to restricted mobility, osseous swelling and progressive reduction of cartilage starting from the age of about 3-4, resulting in severe joint degeneration as the patient ages (Wynne-Davies, *et al.*, 1982; Mampaey, *et al.*, 2000).

Wisp3 mRNA has been observed via RT-PCR in human synoviocytes, articular cartilage chondrocytes and BMSCs induced to undergo chondrogenesis *in vitro* (Hurvitz, *et al.*, 1999). It has been suggested that WISP3/CCN6 has a role in post-natal skeletal and cartilage homeostasis, due to the lack of extraskeletal abnormalities and prominence of degenerated cartilage in patients with PPRD (Hurvitz, *et al.*, 1999; Sen, *et al.*, 2004). This role in cartilage homeostasis is further backed by the localisation of WISP3/CCN6 in clusters of proliferating chondrocytes in human OA cartilage, in midzone chondrocytes in normal cartilage and in areas of chondrocyte proliferation in foetal cartilage growth plates with reduced expression in the hypertrophic zone (Sen, *et al.*, 2004). Furthermore, studies have shown down-regulation of *MMP1*, *MMP3* and *MMP13* in PPRD articular chondrocytes (Zhou, *et al.*, 2007) and up-regulation of *COL2A1*, *ACAN* (aggrecan) and *SOX9* in *WISP3*-transfected immortalised chondrocyte cell line (C-28/I2) (Sen, *et al.*, 2004) implicating a chondroprotective role of WISP3/CCN6.

It has been proposed that WISP3/CCN6 inhibits the action of insulin-like growth factor (IGF)-1, which has been shown to enhance chondrocyte hypertrophy, by its IGFBP domain, and thus stabilises the chondrocyte phenotype. Loss of WISP3/CCN6 function, via mutations, may therefore promote chondrocyte hypertrophy by increasing sensitivity to IGF1 (Yang & Liao, 2007). Consequently, mutations have been found in WISP3/CCN6 in PPRD families (Hurvitz, *et al.*, 1999; Zhou, *et al.*, 2007). To further back this, a C78R mutation of a conserved cysteine residue in the IGFBP motif of *WISP3* failed to up-regulate *COL2A1* and *ACAN* (aggrecan) mRNA or type II collagen protein when transfected in an immortalised human chondrocyte cell line (C28/I2) cells unlike transfection with wild-type *WISP3* (Sen, *et al.*, 2004).

Previous work in the Gavrilović group has demonstrated the ability of WISP-3/CCN6 to also regulate metalloproteinase expression (Baker, *et al.*, 2012). In WISP3/CCN6 overexpressing C28/I2 cells, *MMP10* was upregulated 14-fold at the message level, whilst *ADAMTS5* was down-regulated five-fold. Pharmacological inhibition of MEK1/2, p38 MAPK and IKK each partially suppressed *MMP10* up-regulation, whereas only IKK inhibition further reduced *ADAMTS5* expression. Stimulation of β -catenin also partially reversed the suppression of *ADAMTS5* and further enhanced *MMP10* expression in these WISP3/CCN6 overexpressing cells, implicating a number of potential signalling pathways involved in WISP3/CCN6-mediated metalloproteinase regulation (Baker, *et al.*, 2012).

Baker, *et al.* showed that *WISP3* was up-regulated at the mRNA level of cartilage. By immunohistochemistry, it was demonstrated that WISP3/CCN6 was detected in osteoarthritic cartilage samples, mainly localised to the pericellular regions, in sites of cartilage damage. Similarly, WISP3/CCN6 was also detected in patients with no clinical history of osteoarthritis, but exhibited cartilage damage, localised to these damaged regions.

In addition to its role in cartilage homeostasis, WISP3/CCN6 has also been implicated in the regulation of BMSCs. RT-PCR revealed high expression of *WISP3* in undifferentiated primary human chondrocytes from the femoral head of patients undergoing total hip replacement arthroplasty. During high-density pellet chondrogenic differentiation, mRNA levels decreased 5.5-fold (Schütze, *et al.*, 2005). The same group then later showed that WISP3/CCN6 and CYR61/CCN1 can stimulate migration of hBMSCs dose-dependently across gelatin-coated chemotaxis filters and that WISP3/CCN6-mediated migration, and not CYR61/CCN1, was mediated by integrin $\alpha\beta 5$, shown by antibody-blocking (Schütze, *et al.*, 2007). Furthermore, WISP3/CCN6 has also been shown to increase migration across a matrigel-coated porous transwell in the chondrosarcoma cell line JJ012, through up-regulation of intercellular adhesion molecule (ICAM)-1 (Fong, *et al.*, 2011).

Taking these findings together, it is possible to envisage that WISP3/CCN6 has a protective/reparative role in cartilage, up-regulating expression of cartilaginous genes and remodelling the matrix which could theoretically allow for the chemoattractive invasion of progenitor cells to help repair cartilage damage by undergoing chondrogenesis.

1.3 Osteoarthritis

Osteoarthritis is the most common form of arthritis (CDC, 2010), affecting up to 8 million people in the UK alone (Arthritis Research UK, 2011). It is a painful disease characterised by the degradation of articular cartilage, with changes in the underlying subchondral bone, along with limited intra-articular inflammation (Poole, 1999), outlined in Figure 1.8. Rheumatoid arthritis (RA), on the other hand, involves persistent synovitis, systemic inflammation and generation of auto-antibodies (Scott, *et al.*, 2010). Current treatment for OA primarily focuses on temporary pain relief and anti-inflammatories, with no effective drugs on the market to combat the underlying causes (Poole, *et al.*, 2002; Seed, *et al.*, 2009; Arthritis Research UK, 2011). Joint replacement surgery is the only effective option, although these need to be replaced after a certain number of years. Research into OA, its biological causes and the molecular pathways involved is therefore of big interest in order to develop potential effective future therapies.

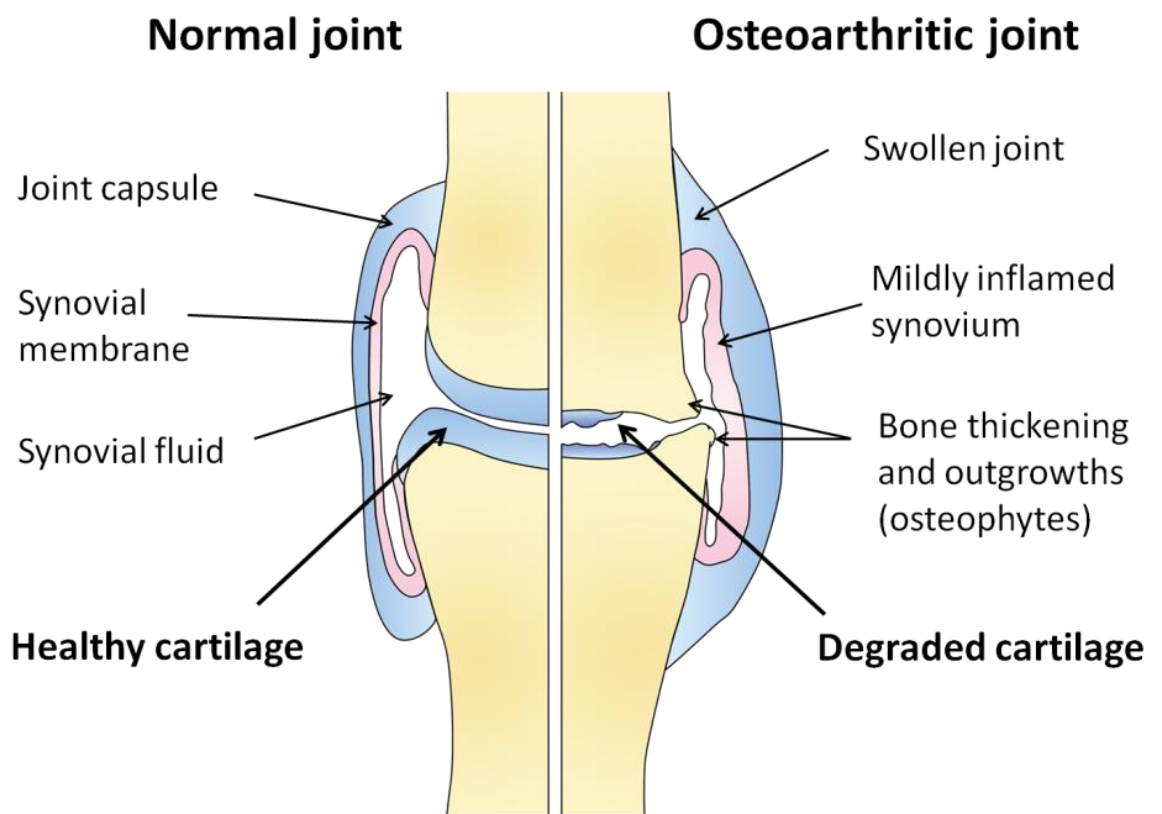


Figure 1.8 – Simplified comparison between a healthy joint and an osteoarthritic joint. In osteoarthritis, cartilage is degraded. This increases the friction when moving the joint, leading to pain and stiffness. Wearing away of this cartilage may therefore lead to the two bones of the joint rubbing against each other, causing further pain and stiffness. Other symptoms of OA include joint swelling and changes in the subchondral bone, such as bone thickening and outgrowths (osteophytes).

1.3.1 Cartilage changes in OA

OA is commonly described as the result of one of two routes: abnormal loading on normal cartilage, or normal loading on abnormal cartilage, with the former normally resulting from some sort of mechanical stress possibly due to injury and the latter normally being an idiopathic form of OA that develops over long periods of time (Sandell & Aigner, 2001; Poole, *et al.*, 2002; Horton Jr, *et al.*, 2006).

At the macroscopic level, the first indicators of OA are fibrillation at the surface of articular cartilage as the collagen fibrils are damaged, softening of the cartilage (chondromalacia) and ulceration of the cartilage (Poole, *et al.*, 2002; Horton Jr, *et al.*, 2006).

1.3.1.1 Catabolic changes in OA

Osteoarthritis results in a number of catabolic changes leading to the destruction of cartilage. In addition to the enzymatic destruction of cartilage matrix components, discussed in section 1.3.2, osteoarthritis also results in the activation of other functional catabolic pathways, including chondrocyte apoptosis and changes in the retention of water due to the loss of aggregating aggrecan attached to hyaluronan. Despite an overall increase in water content in OA joints resulting in swelling, hydrostatic pressure of the joint is decreased as the water is not fixed to the GAG side chains of the aggrecan (Horton Jr, *et al.*, 2006), thereby diminished the resistance to compressive forces that aggrecan normally protects against.

Studies have investigated apoptosis of chondrocytes both *in vivo* and *in vitro*. *In vitro* studies have shown that primary human articular chondrocytes from non-OA donors, treated with IL-1 β , an inflammatory cytokine up-regulated in OA tissue, in the presence of oxygen radical scavengers, can induce cell death by the interaction of oxygen radicals with nitric oxide (Blanco, *et al.*, 1995). An association has also been reported between low production of endogenous IL-1 β with higher frequencies of absence of hip-OA in volunteers aged over 85 (Goekoop, *et al.*, 2010). Furthermore, it has been shown by immunohistochemistry of mice and rat knee cartilage that chondrocyte apoptosis increases with age (Adams & Horton Jr, 1998). However, the impact of chondrocyte apoptosis in the development of OA has been under scrutiny (Sandell & Aigner, 2001).

1.3.1.2 Anabolic changes in OA

In addition to the catabolic changes found during the progression of OA, it is known that OA cartilage also induces anabolic activity, eliciting a repair response to repair the damaged cartilage. Therefore degeneration of cartilage is as a result of increased net catabolic activity and not due to the lack of synthesis, since chondrocytes in OA cartilage are anabolically hyperactive.

To observe the synthesis of new type II collagen, studies have observed the release of CPII, the C-propeptide of type II procollagen, from both human articular cartilage explants (Nelson, *et al.*, 1998; Hermansson, *et al.*, 2004) and porcine articular cartilage explants (Hermansson, *et al.*, 2004). Additionally, it has been reported that OA cartilage samples revealed increased expression of two prolyl-4-hydroxylase subunits (*P4HA2* and *P4HB*), a key enzyme in type II collagen synthesis, along with increases in *COL2A1* itself (Grimmer, *et al.*, 2006).

Aggrecan synthesis has also been shown to be increased in OA cartilage compared to non-OA cartilage. This has been achieved in one study by observing the presence of epitope 846, an epitope present on large aggrecan that has been newly synthesised, analogous to the use of observing CPII for type II collagen synthesis. The study showed an increase in the presence of epitope 846 in OA human knee cartilage compared to non-OA knee cartilage. This increase in presence was also more profound in late-stage OA compared to early-stage OA (Lohmander, *et al.*, 1999).

However, studies on the increase of cartilage matrix components have tended to examine the cartilage as a whole, disregarding the different zones present in cartilage. Immunostaining against CPII showed that type II collagen synthesis was restricted to the mid and deep zones of the cartilage and was absent from natural and new articular surface (Nelson, *et al.*, 1998). This has also been shown in a separate experiment for proteoglycans, with hyper-anabolic activity of chondrocytes being restricted to the middle and deeper zones of OA cartilage. Chondrocytes in the upper zone, which does not relate to the superficial zone due to erosion, showed no expression of type II collagen or aggrecan (Aigner & Dudhia, 1997).

1.3.2 Enzymes in cartilage degradation

The catabolic activities involved during osteoarthritis are primarily mediated by a family of enzymes known as the metalloproteinases, which encompasses the matrix metalloproteinases (MMPs), a disintegrin and metalloproteinases (ADAMs) and ADAM with thrombospondin motifs (ADAMTSs), all part of the metzincin superfamily of zinc-based enzymes.

1.3.2.1 MMPs

The MMP family, which together can degrade all components of the ECM, can be further subdivided into different groups, based upon their substrate specificity, primary structure or cellular location. Of note in cartilage remodelling and degradation are the collagenases (MMP1, MMP8 and MMP13) that are able to cleave triple-helical, fibrillar collagens into the characteristic three-quarter and one-quarter fragments; and the gelatinases (MMP2 and MMP9) (Murphy, *et al.*, 2002), which are then able to degrade the collagen fragments further (Burrage, *et al.*, 2006). While all three collagenases

have been shown to degrade type II collagen *in vitro*, MMP13 has the most catalytic activity, with MMP8 having the least (Billinghurst, *et al.*, 1997).

1.3.2.2 ADAMTSs

Although various MMPs can also degrade aggrecan *in vitro* (Fosang, *et al.*, 1993; Murphy, *et al.*, 2002), it is now known that the principle enzymes involved in aggrecan degradation are the aggrecanases, ADAMTS4 and ADAMTS5 (Huang & Wu, 2008). Other members of the ADAMTS family have also been shown to have aggrecanase activity (ADAMTS1, -8, -9, -15, -16 and -18), with ADAMTS5 being the most active, with aggrecanase activity 1000-fold greater than ADAMTS4 (Gendron, *et al.*, 2007). Despite both MMPs and ADAMTSs degrading aggrecan, it has been shown that they exert their activity at different preferential sites, with MMPs primarily cleaving aggrecan at Asn³⁴¹–Phe³⁴², while the ADAMTSs preferentially cleave at Glu³⁷³–Ala³⁷⁴ (Porter, *et al.*, 2005). These cleavage sites occur within the IGD of aggrecan, thereby releasing the GAG-rich portion of aggrecan, which provides aggrecan with its vital function of retaining water, which is then free to leave the ECM, devoiding the cartilage of its resistance to compressive forces (Huang & Wu, 2008).

1.3.2.3 Enzyme dysregulation

While metalloproteinases are required by the body for remodelling of the ECM, dysregulation of their activities can lead to a net increase of cartilage degradation, potentially aiding the onset of idiopathic OA. This dysregulation has been shown in early work on tissue inhibitors of metalloproteinases (TIMPs), which as the name suggests, inhibit MMPs. It was shown that in non-arthritis human cartilage, there is a small excess of TIMP over MMPs present. In OA cartilage, levels of both TIMP and MMPs were increased, however, the increase of MMPs were proportionally higher than that of TIMP, suggesting a net increase of MMP activity and decrease in TIMP activity, implicating the role of dysregulation of MMPs in OA (Dean, *et al.*, 1989).

MMP13, which has the highest catalytic activity against type II collagen, has been shown to be dysregulated in OA, such that inhibition of MMP13 abrogates the release of a collagenase-derived neo-epitope in human OA articular cartilage explants (Billinghurst, *et al.*, 1997); knockout of *Mmp13* in mice provides resistance to structural cartilage damage in an induced-OA model compared to wild-type mice (Little, *et al.*, 2009); and RT-PCR has shown *MMP13* to be significantly up-regulated in late-stage OA (Bau, *et al.*, 2002; Davidson, *et al.*, 2006). This expression of *MMP13* has been shown to be mediated by the inflammatory cytokines IL-1 β and tumour necrosis factor (TNF)- α , regulated via activation of various mitogen-activated protein (MAP) kinases (Bau, *et al.*, 2002; Liacini, *et al.*, 2003; Burrage, *et al.*, 2006).

In addition to MMPs, the dysregulation of the ADAMTSs have also been implicated in OA. While many ADAMTSs are able to cleave aggrecan, specifically ADAMTS4 and ADAMTS5, with their higher aggrecanase activity, are the likeliest candidates for involvement in OA pathology (Huang & Wu, 2008). The involvement of ADAMTSs and not MMPs in aggrecan degradation in OA cartilage has been shown by dose-dependent inhibition of GAG release into culture media, which correlated with the ³⁷⁴ARGS neo-epitope produced by ADAMTS cleavage of aggrecan and not MMP cleavage (Malfait, *et al.*, 2002). Both ADAMTS4 and ADAMTS5 were detected at the mRNA and protein levels in OA cartilage, however, only ADAMTS5 was detected in healthy cartilage (Malfait, *et al.*, 2002). However, by qRT-PCR, another report has detected both *ADAMTS4* and *ADAMTS5* expression in healthy human cartilage, with up-regulation of both in OA cartilage, with ADAMTS4 levels elevated to a higher fold compared to ADAMTS5 (Song, *et al.*, 2007b).

The contribution of both ADAMTS4 and ADAMTS5 have been affirmed by further inhibition studies using siRNA knockdown of both genes, which significantly reduced the amount of GAGs released into the culture medium from OA cartilage explants and normal cartilage with cytokine-induced catabolic activity, representing a reduction in the cleavage of aggrecan (Song, *et al.*, 2007b). These results suggest that both ADAMTS4 and ADAMTS5 are involved in the pathology of OA.

1.3.2.4 ADAMTS knockout studies

However, perhaps the biggest discovery regarding ADAMTS4 and ADAMTS5 came in 2005 when two groups, Glasson *et al.*, and Stanton *et al.*, published their findings concurrently in Nature. Both teams used cre-loxP transgenics to excise the catalytic domains in the ADAMTS genes (exon 4 in *Adamts4* and exon 3 in *Adamts5*) to create functional knockout mice. Antibodies raised against the aggrecan neo-epitope TEGE³⁷³, a new epitope present in tissue extracts as a result of ADAMTS-cleavage of aggrecan, were used in both studies and demonstrated a substantial reduction of the neo-epitope in *Adamts4* knockout cartilage compared to wild-type and *Adamts5* knockout cartilage, with Glasson, *et al.*, reporting negligible staining of the proximal tibial growth plate in *Adamts4* knockout mice, implicating ADAMTS4 as the enzyme responsible for normal aggrecanase-mediated aggrecan turnover of the murine growth plate. In a surgically-induced model of cartilage degradation, Glasson, *et al.*, reported markedly reduced staining for the TEGE³⁷³ neo-epitope in the *Adamts5* knockout cartilage, implicating ADAMTS5 in the early phase of degradation. *Adamts4* knockout mice showed no protection of cartilage.

Inflammatory modulators (IL-1 α in Stanton, *et al.*, and IL-1 α in combination with retinoic acid in Glasson, *et al.*) to induce 'degradative enzyme activity' resulted in no proteoglycan release in *Adamts5* knockout cartilage compared to a significant increase in wild-type (Glasson, *et al.*, 2005)

and *Adamts4* knockout cartilage (Glasson, *et al.*, 2005; Stanton, *et al.*, 2005), suggesting ADAMTS5 is responsible for the proteoglycan release. IL-1 α was also seen to increase *Adamts5* mRNA expression 18-fold compared to *Adamts4* by 3-fold (Stanton, *et al.*, 2005). Stanton, *et al.*, also investigated the ALGSV neo-epitope, the other neo-epitope formed from the Glu³⁷³/Ala³⁷⁴ cleavage, which is released into the medium, as well as investigating the AGE₂ C-terminal neo-epitope formed from ADAMTS cleavage of Glu¹⁵⁷²/Ala¹⁵⁷³. The report found all three neo-epitopes (TEGE, ALGSV and AGE₂) were absent from the cartilage or media of *Adamts5* knockout samples in response to IL-1 α stimulation, similar to unstimulated controls, compared to stimulation of *Adamts4* knockout and wild-type samples. Toluidine blue staining of the tibiofemoral joint after injection with methylated bovine serum albumin (BSA), to induce monoarticular arthritis, revealed significantly less aggrecan loss in *Adamts5* knockout mice compared to controls. Furthermore, only 7% of *Adamts5* knockout joints showed cartilage erosion compared to 36% of joints from control mice (Stanton, *et al.*, 2005), suggesting that loss of ADAMTS5 activity in mice is sufficient to protect against aggrecan loss and cartilage erosion in a model of inflammatory arthritis. Put together, these results from the Glasson and Stanton studies show that ADAMTS5, and not ADAMTS4, is the key aggrecanase in mice involved in cartilage degradation.

1.3.3 Stem cell repair

Currently, the only effective treatment for patients with osteoarthritis is joint replacement surgery for end-stage cases in load-bearing joints, with no effective drugs on the market to reverse the damage caused by the disease. This therefore does not benefit patients with osteoarthritis in non-load-bearing joints such as the joints in the hands, or those with early-stage disease who must first endure the painful progression through the disease to be eligible for surgery. This makes investigation into the disease to find therapeutic targets a huge area of scientific and pharmaceutical interest.

One area of interest lies in a treatment known as *autologous chondrocyte implantation* (ACI). This is the process of taking a cartilage biopsy, extracting the chondrocytes, expanding them in culture and implanting them into the site of cartilage damage in the osteoarthritic joint (Giannini, *et al.*, 2010; Akgun, *et al.*, 2015; Buda, *et al.*, 2015). However, obvious complications arise; in order to obtain the chondrocytes, damage has to be inflicted to another area of (non-load-bearing) cartilage. Furthermore, due to the small proportion of chondrocytes in cartilage, expansion in culture is a necessary step in order to generate enough cartilage for implantation, which risks dedifferentiation of the cells, as discussed in section 1.4.

Stem cells, derived from the bone marrow, are therefore an attractive alternative to overcome these problems, eliminating the need for further cartilage damage and cell culture. Furthermore, use of BMSCs has the potential to reduce the number of hospitalisations from two visits with ACI down to one visit (Giannini, *et al.*, 2010; Buda, *et al.*, 2015). Both techniques have resulted in improved patient outcome with the use of BMSCs sometimes achieving slightly better results based on various clinical scores of cartilage damage and osteoarthritis stage (Akgun, *et al.*, 2015; Buda, *et al.*, 2015) as well as rate of return to sporting activity (Buda, *et al.*, 2015).

Nevertheless, both techniques require surgery and a more favourable approach would be to avoid the complications of surgery all together by having the body repair the cartilage itself. Therefore work continues to identify a suitable therapeutic target to pursue via drugs to prevent the need for surgery and benefit patients of all stages and forms of OA.

1.4 Maintaining the chondrocytic phenotype

Isolated primary chondrocytes are typically expanded in two-dimensional monolayer culture to increase their number, since chondrocytes present in cartilage are limited in number. However, chondrocytes grown in 2D are known to rapidly de-differentiate, reducing expression of chondrocytic genes, such as *COL2A1*, losing their chondrocytic phenotype and gaining a more fibroblast-like phenotype with the up-regulation of fibroblastic genes, such as for type I collagen (*COL1A1*, *COL1A2*) (Stokes, *et al.*, 2001; Francioli, *et al.*, 2010). Three-dimensional culture is therefore preferred to maintain the chondrocytic phenotype, mimicking the *in vivo* microenvironment in a number of ways.

1.4.1 Suspension culture

One way of culturing chondrocytes in suspension is via the use of poly-2-hydroxyethyl methacrylate (polyHEMA), coated onto culture surfaces to prevent cell adhesion to the substratum. Cells plated onto polyHEMA therefore remain in suspension, allowing chondrocytes to regain their spherical shape and re-establish their cell-cell and cell-matrix contacts in all three dimensions (Stokes, *et al.*, 2001).

Stokes, *et al.* (2001) demonstrated the recovery of the chondrocytic phenotype. By RT-PCR, they reported that isolated primary chondrocytes lost expression of *COL11A2* (encoding the $\alpha 2$ chain of type XI collagen) by passage (P)3, lost expression of *ACAN* (aggrecan) by P2 and diminished expression of *COL2A1* by P1 compared to P0. Transfer to polyHEMA returned expression of *COL11A2* and *ACAN* back to P0 levels. De-differentiation was attributed to diminished binding of SOX9 to the promoter region of *COL2A1* (Stokes, *et al.*, 2001).

1.4.2 Encapsulation

An alternative method of culturing chondrocytes in 3D involves encapsulation, for example, by using alginate beads, a linear co-polymer of D-mannuronic acid and L-guluronic acid (Bonaventure, *et al.*, 1994). Previous studies have directly compared culture in alginate beads compared to 2D monolayer. It was found that in 2D, $\alpha 1(I)$, $\alpha 2(I)$ and $\alpha 1(III)$ chains, abundantly present in de-differentiated chondrocytes, represented 90% of the total collagen, indicating a high amount of type I collagen and type III collagen. These chains were almost undetectable in the alginate culture system (Bonaventure, *et al.*, 1994). Seeding at high density is also known to preserve the chondrocytic phenotype with up-regulation of *COL2A1* mRNA, however, chondrocytes isolated from cartilage biopsies do not allow this due to the limited amount present in cartilage. However, alginate culture was able to re-differentiate chondrocytes that had been isolated and expanded in

monolayer culture to overcome this problem, with a high detection of *COL2A1* and no detection of *COL1A1* (type I collagen)(Bonaventure, *et al.*, 1994).

However, seeding at a high density into alginate may not be necessary. It has been shown that seeding at a low density (1×10^4 cells/ml alginate) resulted in higher expression of *COL2A1* (up to 26-fold higher) and sulphated GAG deposition compared to high density cultures (1×10^6 cells/ml alginate). The rate of proliferation was also observed to be higher in the low density culture than the high density culture. Thin fibrils, similar in size to type II collagen, were also observed throughout the matrix in low density cultures via scanning electron microscopy, but not in high density cultures. This ability of increased proliferation and re-differentiation of chondrocytes in a low density culture was seen to be dependent on the formation of clonal populations not observed in the high density cultures (Gagne, *et al.*, 2000).

1.4.3 Pellet Culture

An alternative method of three-dimensional culture is pellet culture. Essentially, cells are pelleted by centrifugation and the pellet incubated. In time, the chondrocytes lay down an ECM typical of a cartilage biopsy, displaying typical physal patterning with the hypertrophic zone at the top, proliferative zone in the middle and the resting zone at the bottom (Cheung, *et al.*, 2008).

One report has suggested that pellet culture “elicits superior chondrogenic re-differentiation” compared to culturing in alginate beads (Bernstein, *et al.*, 2009). Immunohistological staining showed high accumulation of type II collagen in the pellet cultures with very little in the alginate beads. qRT-PCR showed consistently high levels of *SOX9* expression, similar to native cartilage, compared to low levels in monolayer and variable expression in alginate-based encapsulated chondrocytes. Type II collagen levels were also significantly increased in pellet cultures compared to alginate. Type I collagen levels on the other hand were decreased in both pellet culture and alginate-based cultures compared to monolayer (Bernstein, *et al.*, 2009).

Another paper compared pellet culture directly to hyaline cartilage explants from chicks, with results revealing that after 1-2 weeks, neo-cartilage from the pellet cultures shared many similarities with cartilage explants. For example, immunohistochemical staining showed similar staining patterns for aggrecan and type IX collagen; type I collagen was only seen at the edge of some of the pellet and explant; no type X collagen was observed in either; chondrocytes were spherical in both pellet and explant, and were observed to look healthy and active; and collagen fibrils were observed in both. However, these collagen fibrils appeared to be disorganised in the pellet compared to the explant. Staining of type II collagen was also different, with staining in the

pericellular matrix (PCM) of the chondrocytes in the explant compared to more ECM-located staining in the pellet culture (Zhang, *et al.*, 2004).

1.4.4 High density micromass culture

High density micromass culture (not to be confused with the pellet culture system described in 1.4.3 which is also sometimes referred to as a micromass) was established by Ahrens, *et al.* (1977) for the *in vitro* chondrogenic differentiation of cells isolated from the chick wing bud. It is a culture system whereby a high density of cells that is spotted onto a plate and is allowed to adhere to the plate before flooding with media (Figure 1.9). This ensures that cells grow as a central spot growing in three dimensions, increasing their cell-cell contacts, and secreting their own extensive matrix and thus increases their cell-matrix contacts in all three dimensions.

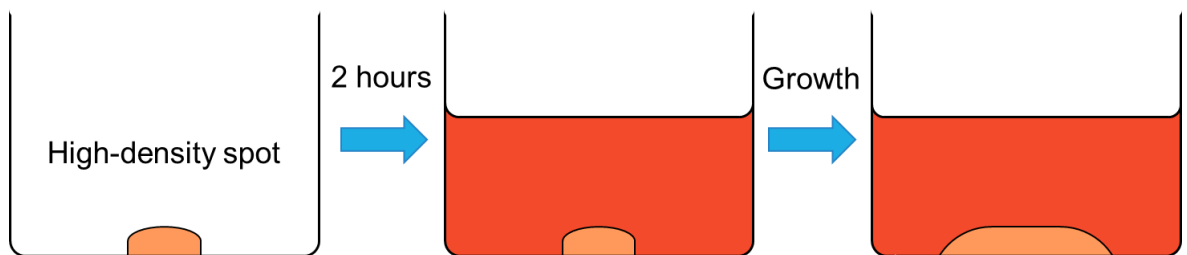


Figure 1.9 – Setting up a micromass culture. Cells are plated in a high-density, low volume (typically around 10 μ l) spot into a culture well and allowed to adhere in the incubator for two hours. The wells are then flooded with the desired media, with the cells remaining as a spot. The micromass is then allowed to differentiate and/or grow for the desired period of time.

This system has been shown to give increased expression of chondrocytic genes, such as *COL2A1*, compared to other three-dimensional culture systems, such as growth in alginate (Tanaka, *et al.*, 2004). Compared to pellet culture, micromass culture has been shown by immunohistochemistry to increase deposition of type II collagen and decrease deposition of fibroblastic type I collagen and hypertrophic type X collagen (Zhang, *et al.*, 2010).

There are many variations of micromass culture to enhance the culture of chondrocytes. One such example is to enhance chondrogenesis from chondrocyte precursors, MSCs. It has become a widely established culture system for inducing chondrogenesis, utilising many types of cells to undergo chondrogenesis, such as primary BMSCs (Tropel, *et al.*, 2004; Taipaleenmaki, *et al.*, 2008; Markway,

et al., 2010; Zhang, *et al.*, 2010), primary adipose-derived mesenchymal stem cells (AMCs) (Malladi, *et al.*, 2006; Xu, *et al.*, 2007b), primary embryonic limb bud mesenchyme (Yoon, *et al.*, 2000; Matta, *et al.*, 2011), and various cell lines (Denker, *et al.*, 1999; Kipnes, *et al.*, 2003; Seriwatanachai, *et al.*, 2012).

Additionally, micromass culture has also been used in conjunction with hypoxia culture (Egli, *et al.*, 2008; Ströbel, *et al.*, 2010), discussed in section 1.4.6, to further enhance differentiation and re-differentiation. The smaller culturing vessels needed for micromass culture (e.g. 24-well plate) makes this an attractive culturing model to use compared to other cultures such as pellet cultures, which are normally cultured in 15 ml tubes, making micromass cultures more practical than pellet cultures, which may need larger hypoxia chambers or require a larger incubator space for the same number of samples.

1.4.5 Mesenchymal Stem Cell Differentiation

'Healthy', non-OA primary chondrocytes are normally obtained post mortem. Although these donors may not have had a clinical history of OA, it cannot be ruled out that there may be some degree of the disease that has gone unnoticed. Furthermore, obtaining these 'healthy' primary chondrocytes is infrequent, dependent on consenting patients undergoing joint replacement surgery locally and only a limited number of chondrocytes are present within cartilage explants. Since the initial steps of chondrogenesis involve condensation of MSCs and their subsequent differentiation into chondrocytes, MSCs are therefore an attractive, alternative and plentiful source of chondrocytes, overcoming the difficulty of obtaining 'healthy', non-OA primary chondrocytes, and eliminating the need to use 2D monolayer expansion of primary chondrocytes which would otherwise result in de-differentiation prior to re-differentiation.

It has been suggested that 3D culture of MSCs enables cell-cell contact, reminiscent of the *in vivo* situation when MSCs condense as one of the initial steps of chondrogenesis (Wang, *et al.*, 2005). It has previously been reported that N-cadherin is required for *in vitro* chondrogenesis whereby antibody blocking of the adhesion molecule inhibited chondrogenesis in micromass cultures of embryonic chick limb MSCs (Oberlender & Tuan, 1994). However, chondrogenesis has also been observed in 3D scaffold cultures (Nam, *et al.*, 2010), which limits cell-cell contact. Furthermore, paraformaldehyde inactivation of MSCs, which keeps transmembrane signalling molecules intact on the cell surface, has been shown to inhibit chondrogenesis, indicating that cell-cell contact alone is not enough to initiate chondrogenesis and that various signalling is required (Liu, *et al.*, 2010).

In addition to differentiating MSCs into chondrocytes in the various three-dimensional culture systems outlined previously, some studies have demonstrated the additional benefits of co-culturing MSCs with mature articular chondrocytes. Equine MSCs isolated from the marrow of the sternbra, when co-cultured with equine articular chondrocytes isolated from the femoropatellar joint, produced higher levels of *COL2A1* and *SOX9* mRNA, and stronger, more homogeneous Alcian blue staining (indicating proteoglycan deposition) compared to separate MSC and chondrocyte cultures with and without stimulation via TGF β 1 (Lettry, *et al.*, 2010).

It has also been shown that co-culture of MSCs with articular chondrocytes reduces markers of chondrocyte hypertrophy, a fate spared from articular cartilage and reportedly to occur prematurely in differentiating MSC micromass cultures (Pelttari, *et al.*, 2006). A report by Fischer, *et al.*, (2010) revealed a decrease in mRNA levels of ALPL, which encodes the enzyme alkaline phosphatase produced by hypertrophic chondrocytes responsible for matrix mineralisation during endochondral ossification, in human articular chondrocyte-conditioned MSC pellets. Supplementation of unconditioned media with PTHrP (parathyroid hormone-related protein), previously detected in culture supernatants, strongly reduced alkaline phosphatase activity in MSC pellets and significantly decreased *COL10A1* and Indian hedgehog (*IHH*) mRNA levels (Fischer, *et al.*, 2010) suggesting PTHrP may be one soluble factor secreted by chondrocytes to repress hypertrophy and may therefore be added to MSC-derived chondrocytes to prevent them from going down the hypertrophic pathway to maintain the articular chondrocyte phenotype.

1.4.6 Hypoxia

Articular cartilage is an avascular, aneural, alymphatic connective tissue. As such, cartilage is subject to a low oxygen tension and therefore the chondrocytes live in a hypoxic environment with oxygen tension varying from 1 - 7 % O₂ in humans, depending on how deep the cartilage zone is from the articular surface, in comparison to arterial blood ranging from 11 - 14 % O₂ (Grimshaw & Mason, 2000; Murphy & Polak, 2004). Culturing cells under normoxic conditions (20 % O₂) is therefore unphysiological and not suitable for the *in vitro* culture of chondrocytes. Many studies have shown the benefits of culturing chondrocytes under hypoxic conditions, in conjunction with a three-dimensional environment, to closely mimic more realistic *in vivo* conditions.

One study observed the effects of encapsulation of human hip articular chondrocytes in alginate beads at 20 % O₂ and 5 % O₂, in comparison to P0 isolated chondrocytes. qRT-PCR revealed strong decreases in *COL2A1*, *ACAN* (aggrecan) and *SOX9* expression following monolayer subculture of chondrocytes (P3). Encapsulation of P3 chondrocytes slowly increased expression, but after 28 days at 20 % O₂, expression was still lower than that of encapsulated P0 chondrocytes. In comparison,

encapsulated P3 chondrocytes restored expression of *COL2A1*, *ACAN* and *SOX9* by 28, 14 and 7 days respectively when cultured at 5 % O₂ (Murphy & Polak, 2004). These results show that although 3D culture up-regulates chondrocytic genes, the effects can be significantly enhanced by reducing the oxygen tension to a more physiologically-relevant level.

Another study also observed the effects of hypoxic culture using pellet culture on the anabolic and catabolic activities of non-OA human knee articular chondrocytes. Results showed that, in addition to increases in type II collagen and aggrecan, culture of chondrocytes at 5 % O₂ also decreased expression of MMP1 and MMP13. Switching to 19 % O₂ after this initial 5 % O₂ phase resulted in increased release of MMP1 and MMP13 as well as collagen fibrils with a decrease in persistence length and bending ratio seen by scanning electron microscopy, similar to OA cartilage, indicative of softening of the cartilage (Ströbel, *et al.*, 2010). Decreasing oxygen tension therefore improves the structure, reduces catabolic activities and enhances anabolic activities.

However, hypoxia also has been reported to exert catabolic effects. The murine chondroprogenitor cell line, ATDC5 (described in more detail in Chapter 3), readily undergoes chondrogenesis with insulin stimulation at normal oxygen levels. However, upon hypoxic stimulation at 1 % O₂, insulin-induced chondrogenesis was inhibited, resulting in decreased expression of *Col2a1*, *Acan* (aggrecan), *Col10a1*, as well as decreased proteoglycan deposition as seen by Alcian blue staining (Chen, *et al.*, 2006). Similar results were also seen in chondrogenically differentiating murine AMCs in micromass, with decreased expression of type II collagen protein and sulphated GAG content (Malladi, *et al.*, 2006). Additionally, hypoxia inducible factor (HIF)-2 α , a member of the HIF transcription factor family responsible for the regulation of genes under hypoxia, has been shown to increase expression of MMP3 and MMP13 in mice via the inflammatory cytokine, IL-6, in mouse cartilage (Ryu, *et al.*, 2011). Conversely, HIF-2 α has been reported to be responsible for the hypoxic induction of *COL2A1* and *SOX9* in human articular chondrocytes (Lafont, *et al.*, 2007). This highlights the complexity of hypoxia and its importance in cartilage, and additionally, consideration may need to be taken regarding cell source as mice have thinner cartilage than larger mammals and as a result may be subject to different oxygen tensions *in vivo* (Murphy, *et al.*, 2009).

1.5 Summary

Osteoarthritis is a painful and debilitating disease with no disease-modifying drugs available on the market. A number of signalling pathways have been implicated in the progression of osteoarthritis, including the WNT signalling pathway and the CCN growth factor family. Although these two families are known to be tightly linked, the extent of their relationship and the mechanisms behind their involvement in the progression of osteoarthritis are not fully understood.

Additionally, cartilage is now known to be a complex tissue consisting of many layers which all regulate different sets of genes, and different cartilages in the body have unique functions depending on its location. Previously, little regard has been taken as to the phenotype of cartilage-like tissue produced from the culture of chondrocytes and chondrogenically differentiating MSCs.

1.6 General Hypothesis

It was therefore hypothesised that WNT and CCN signalling may be implicated in the destruction of cartilage and may therefore be implicated directly or indirectly in inflammatory cytokine and metalloproteinase signalling in chondrocytes and chondroprogenitor cells.

As mentioned before, chondrocytes and their progenitors are the only cells present in cartilage. Given that WNT signalling has been implicated in both the differentiation of chondrocytes and the migration of other cells in both a positive and negative manner, it was also therefore hypothesised that WNT signalling may be involved in the modulation of the migration of the cells in response to cartilage damage to either promote or impede repair.

1.7 Aims

To investigate these hypotheses with physiological relevance, this thesis therefore aimed to:

1. Establish a culturing model of physiological relevance to model articular cartilage and the changes that occur during osteoarthritis
 - a. Identify the phenotype of the cartilage model to ascertain its biological relevance by examining regulation of known cartilage phenotypic genes
 - b. Investigate the gene expression changes of the WNT and CCN signalling families during chondrogenesis using the above model
2. Investigate the impact of WNT signalling in an osteoarthritic-like setting via examining gene and protein regulation
3. Investigate the functional outcomes of WNT signalling via migration and invasion studies

Chapter 2

Materials and Methods

2.1 ATDC5 Cell Culture

2.1.1 Maintenance

ATDC5 cells, originally cloned from the AT805 mouse embryonic teratocarcinoma cell line (Atsumi, *et al.*, 1990), were obtained from Dr. Tracey Swingler (University of East Anglia). Undifferentiated ATDC5 cells were maintained in a culture medium consisting of DMEM:F12 (Invitrogen) containing 5% (v/v) foetal calf serum (FCS), 1% (v/v) L-glutamine and 1% (v/v) penicillin/streptomycin (Invitrogen) supplemented with 10 µg/ml transferrin (Sigma-Aldrich) and 30 nM sodium selenite (Sigma-Aldrich), referred to as maintenance medium. Medium not supplemented with transferrin or sodium selenite was referred to as basal medium. Cells were maintained in a humidified incubator at 37 °C with 5% CO₂. Undifferentiated cells doubled every day and were passaged using 0.05% Trypsin/EDTA (Invitrogen) roughly twice weekly at 1:8 or 1:16 in maintenance medium in filter-capped tissue culture flasks (Nunc).

2.1.2 Experimental Culture

For experiments, ATDC5 cells were grown in several different culture models.

2.1.2.1 Monolayer Culture

Monolayer cultures of ATDC5 cells were plated at a density of 6×10^3 cells/cm² into a 24-well tissue culture plate (Nunc) in 500 µl maintenance medium, and allowed to grow for 2 days until just sub-confluent, unless stated otherwise. After two days, medium was refreshed or switched to the stated condition and this time point is referred to as Day 0.

2.1.2.2 High Density Micromass Culture

High density micromass cultures of ATDC5 cells were established essentially as described previously (Ahrens, *et al.*, 1977). Briefly, ATDC5 cells were plated in 10 µl droplets in maintenance medium at a density of 2×10^7 cells/ml into a 24-well tissue culture plate, unless stated otherwise, and allowed to adhere for 2 h in a humidified incubator at 37 °C, 5% CO₂ before flooding wells with 500 µl of the appropriate medium according to the experiment. This time point was referred to as Day 0.

2.1.2.3 ATDC5 Chondrogenic Induction with Insulin

Insulin was used to induce differentiation of ATDC5 cells essentially as described previously (Atsumi, *et al.*, 1990), by supplementing basal medium with an insulin, transferrin and sodium selenite (ITS) premix (Invitrogen), giving final concentrations of 10 µg/ml insulin, 5.5 µg/ml transferrin and 38.73 nM sodium selenite. Differentiating medium was added at Day 0 and refreshed every 2-3 days for 14 days. For the time course analysis, cells were differentiated for 7, 14 and 21 days.

Undifferentiated (non-induced) ATDC5 cells in maintenance medium were used as controls for differentiated ATDC5 cells and maintained for the same time period.

2.1.2.4 Stimulation with Ascorbic Acid

In some experiments, maintenance or differentiation media were also supplemented with 50 µg/ml L-ascorbic acid sodium salt (hereafter “ascorbic acid”) (Sigma-Aldrich), as previously established in chondrogenic culture (Spagnoli, *et al.*, 2005; Taipaleenmaki, *et al.*, 2008; Temu, *et al.*, 2010). Media were then refreshed every 2-3 days.

2.1.2.5 ECM Components

Where indicated, culture wells or 13 mm sterilised glass coverslips (VWR International) were coated with either Type II Collagen (from chick sternal cartilage, Sigma-Aldrich), or Fibronectin (from human plasma, Sigma-Aldrich) at the desired concentration and incubated overnight at 4 °C. Excess liquid was removed, the plates and coverslips washed with PBS and allowed to air dry under sterile conditions.

2.2 Gene Transcription Analysis by qRT-PCR

2.2.1 RNA Extraction using RNEasy Mini/Micro Plus kits from QIAGEN

Total RNA was extracted using RNEasy Mini Plus or RNEasy Micro Plus kits from QIAGEN, according to the manufacturer’s instructions. Briefly, cells were washed with PBS and lysed in RLT+ lysis buffer containing guanidine thiocyanate, supplemented with β-mecaptoethanol (to a final concentration of 143 mM). Cell lysates were homogenised by repeatedly pipetting up and down before being transferred to gDNA eliminator columns. Micromass cultures that had been induced with insulin were further homogenised using a TissueLyser (QIAGEN) by vigorous shaking with a sterile ball-bearing in a 2 ml safety-lock tube (Eppendorf) at 30 Hz for 30 s before being transferred to a gDNA eliminator column due to the ECM produced in micromass cultures that may otherwise prevent complete homogenisation. After centrifugation, flow-through was precipitated with equal volumes of 70 % ethanol before being transferred to the RNA spin columns and centrifuged again. RNA was trapped on the silicone membrane and a series of washes with high-salt buffers further purified the RNA before elution in RNase-free water. Eluted RNA was stored at -20 °C.

2.2.2 RNA quality/quantity analysis with NanoDrop

RNA quality and quantity was analysed using the NanoDrop 2000 spectrophotometer (Thermo Scientific) at wavelengths of 230, 260 and 280 nm. RNA concentration was measured at 260 nm. Ratios of 260/280 and 260/230 were used to analyse the quality of the RNA for protein contamination and guanidine contamination respectively. Samples with ratios above 1.8 were deemed as high quality with respect to contaminants.

2.2.3 Two-step reverse transcription to cDNA using M-MLV

RNA was reverse transcribed to cDNA in a two-step process. Random primers (0.5 µg/µg RNA) (Invitrogen) were annealed to RNA by heating to 70 °C for 10 min then immediately plunged into ice to prevent restoration of secondary structures. Primed RNA was reverse transcribed using M-MLV (200 u/µg RNA) (Promega) with 0.2 mM dNTP mix (Bioline) by heating to 42 °C for 60 min to allow primer extension. Enzyme activity was destroyed by heating to 70 °C for 10 min, and samples stored at -20 °C until use.

2.2.4 Identification of suitable housekeeping gene using geNorm from PrimerDesign

To identify a suitable housekeeping gene for experimental analysis, a geNorm reference analysis was carried out using a 12 gene geNorm gene selection kit (PrimerDesign) using PerfectProbe technology with a 6-carboxyfluorescein (FAM) reporter, according to manufacturer's instructions. Briefly, 5 ng cDNA from different conditions were loaded onto a qPCR plate (Applied Biosystems) along with a mixture containing 2x qPCR MasterMix (Applied Biosystems) and selected primer/probe mixes at 300 nM. The loaded plate was sealed and loaded into a 7500/7500 Fast Real-Time PCR System (Applied Biosystems) and subjected to the following cycling conditions detailed in Table 2.1.

Table 2.1 – PCR cycling conditions for geNorm analysis using PerfectProbe Technology

	Step	Time (min:sec)	Temperature (°C)
	Enzyme Activation	10:00	95
Cycling x50	Denaturation	00:15	95
	Data Collection	00:30	50
	Extension	00:15	72

C_T s were analysed using qbase^{PLUS} (Biogazelle) and subjected to geNorm analysis (Vandesompele, *et al.*, 2002). Reference genes were ranked using a geNorm *M* value from worst (higher value) to

best (lower value). A geNorm *M* value below 0.5 was considered acceptable for use as a reference gene. A list of genes used in the geNorm analysis can be found in Table 2.2.

Table 2.2 – Genes analysed using the geNorm gene selection kit. Full gene names taken from National Centre for Biotechnology Information (NCBI).

Symbol	Name
<i>18s</i>	18S ribosomal RNA
<i>Actb</i>	Actin, beta
<i>Atp5b</i>	ATP synthase, H+ transporting mitochondrial F1 complex, beta subunit
<i>B2m</i>	Beta-2 microglobulin
<i>Canx</i>	Calnexin
<i>Cyc1</i>	Cytochrome c-1
<i>Eif4a2</i>	eukaryotic translation initiation factor 4A2
<i>Gapdh</i>	Glyceraldehyde-3-phosphate dehydrogenase
<i>Rpl13a</i>	Ribosomal protein L13A
<i>Sdha</i>	Succinate dehydrogenase complex, subunit A, flavoprotein (Fp)
<i>Ubc</i>	Ubiquitin C
<i>Ywhaz</i>	Tyrosine 3-monooxygenase/tryptophan 5-monooxygenase activation protein, zeta polypeptide

2.2.5 Generation of custom assays using the Universal ProbeLibrary

Custom-made primer/prone sets (hereafter referred to as assays) for use with the Universal ProbeLibrary (UPL)(Roche) for use in qRT-PCR were designed using the UPL assay design centre using the ProbeFinder database. Assays were designed to be intron-spanning to eliminate PCR amplification of any potential, residual, contaminating gDNA. Designed DNA primers were synthesised and purchased from Sigma-Aldrich and used in combination with the relevant LNA UPL probe (8-9 mers), purchased from Roche, labelled with FAM (5') and a dark quencher dye (3'). The use of LNA, DNA analogues which incorporate a methylene bridge between the 2'-O atom and 4'-C atom to "lock" the ribose ring, in the UPL probes gives increased thermal stability with a greater ΔT_m between perfectly matched and mismatched pairing, and thus allows for more sensitive discrimination of mismatches in base-pairing (Roche Applied Science, 2009). In qRT-PCR reactions using the UPL, primers and probes were used at 250 nM and 125 nM respectively and used under

standard TaqMan cycling conditions (Table 2.4). Primer sequences and UPL probe numbers can be found in Table 2.3

2.2.6 Generation of custom assays from PrimerDesign

For assays that were not able to be designed through the UPL, either due to a lack of intron-spanning assays available or lack of specificity, custom assays, using primer and double-dye (TaqMan-style) technology, were designed by PrimerDesign (Southampton, UK). Custom assays were designed and checked for efficiency and specificity by PrimerDesign, and supplied as a primer/probe mix used at a final concentration of 300 nM per reaction. PrimerDesign assays were used under standard TaqMan cycling conditions (Table 2.4) with sequences detailed in Table 2.3.

Table 2.3 – Primer/Probe sequences for murine assays for use with qRT-PCR. Where more than one accession number is given, the primer/probes are designed as a common assay that detects all variants listed. Exact probe sequences for assays designed by the UPL and primer/probe sequences for housekeeping genes designed by PrimerDesign are property of, and withheld by, the respective companies. All given probes are labelled with FAM (5') and tetramethylrhodamine (TAMRA) (3').

	Official Gene Symbol	Other Names	Accession Number(s)	Design Source	Sequence (5'-3')
Housekeeping Genes	<i>18S</i>	18S rRNA	M10098	Corps, et al., (2006)	Forward Primer: GCCGCTAGAGGTGAAATTCCTG Reverse Primer: CATCTTTGGCAAATGCTTTCG Probe: ACCGGCGCAAGACGGACCAG
	<i>Ywhaz</i>	Tyrosine 3-monooxygenase/tryptophan 5-monooxygenase activation protein, zeta polypeptide	NM_001253805.1 NM_001253806.1 NM_001253807.1 NM_011740.3	PrimerDesign	Forward Primer: Property of PrimerDesign Reverse Primer: Property of PrimerDesign Probe: Property of PrimerDesign
Metalloproteinases	<i>Adamts4</i>	Aggrecanase 1	NM_172845.2	Folgueras, et al., (2008)	Forward Primer: TCAACACCCCTAACGACTCAGA Reverse Primer: CAGCTCCTAGCTGGATCACACA Probe: CTGACCACTTTGACACAGCCATTCTGTTCA
	<i>Adamts5</i>	Aggrecanase 2	NM_011782.2	UPL	Forward Primer: CCTGGATGATGGTCATGGTA Reverse Primer: AGTTCCTCGGGACCCAAA Probe: UPL Probe #38
	<i>Mmp13</i>	Collagenase 3	NM_008607.2	UPL	Forward Primer: CTTTTCCTCCTGGACCAAACT Reverse Primer: TCATGGGCAGCAACAATAAA Probe: UPL Probe #105

CCN Growth Factors	<i>Cyr61</i>	CCN1; Cysteine rich protein 61	NM_010516.2	UPL	Forward Primer: Reverse Primer: Probe:	GGATCTGTGAAGTGCCTCCT CTGCATTTCTTGCCCTTTT UPL Probe #66
	<i>Ctgf</i>	CCN2; Connective tissue growth factor	NM_010217.2	UPL	Forward Primer: Reverse Primer: Probe:	TGACCTGGAGGAAAACATTAAGA AGCCCTGTATGTCTTCACACTG UPL Probe #71
	<i>Nov</i>	CCN3; Nephroblastoma overexpressed	NM_010930.4	UPL	Forward Primer: Reverse Primer: Probe:	AGTGGACCTGTGGCTCAGA TCAACTCCTACGGTGGCTTC UPL Probe #11
	<i>Wisp1</i>	CCN4; WNT1 inducible signaling pathway protein 1	NM_018865	PrimerDesign	Forward Primer: Reverse Primer: Probe:	TTATCCCCTGTGGCTCCTC CCATTTATGAGTGTGTATAGTTCT ATGATGATTCAGTTTGCCCCACACCATACA
	<i>Wisp2</i>	CCN5; WNT1 inducible signaling pathway protein 2	NM_016873.2	UPL	Forward Primer: Reverse Primer: Probe:	TCCTCTGCATTCTCTCAATGG GTGTCCAAGGACAGGCACA UPL Probe #104
	<i>Wisp3</i>	CCN6; WNT1 inducible signaling pathway protein 3	NM_001127376	PrimerDesign	Forward Primer: Reverse Primer: Probe:	GCAAGCAACCAAGTGGACTC CAGCCTCCTCTCCTTTCTCAT CGGGTAACCAACGATAACGCCAACTGTGA

Collagens	Col1a1	Collagen, type I, alpha 1	NM_007742.3	UPL	Forward Primer: Reverse Primer: Probe:	CATGTTTCAGCTTTGTGGACCT GCAGCTGACTTCAGGGATGT UPL Probe #15
	Col1a2	Collagen, type I, alpha 2	NM_007743.2	UPL	Forward Primer: Reverse Primer: Probe:	GCAGGTTACCTACTCTGTCTCT CTTGCCCCATTCATTGTCT UPL Probe #46
	Col2a1	Collagen, type 2, alpha 1	NM_001113515.2 NM_031163.3	UPL	Forward Primer: Reverse Primer: Probe:	ACCCCCAGGTGCTAATGG AACACCTTTGGGACCATCTTT UPL Probe #18
	Col9a1	Collagen, type 9, alpha 1	NM_007740.3	UPL	Forward Primer: Reverse Primer: Probe:	CCTGGGTATCCGCAACTCT CCTGATCTTGGGACACAGTTC UPL Probe #31
	Col10a1	Collagen, type 10, alpha 1	NM_009925.4	UPL	Forward Primer: Reverse Primer: Probe:	GCATCTCCCAGCACCAGA CCATGAACCAGGGTCAAGAA UPL Probe #84
Non-collagenous ECM Components	Acan	Aggrecan	NM_007424.2	UPL	Forward Primer: Reverse Primer: Probe:	CCAGCCTACACCCAGTG GAGGGTGGGAAGCCATGT UPL Probe #76
	Matn3	Matrilin 3	NM_010770.4	UPL	Forward Primer: Reverse Primer: Probe:	GCTATGGAGGTTACGCCTTG GTACCAGAGCGCATTTGTC UPL Probe #2
	Prg4	Proteoglycan 4 (Lubricin)	NM_021400.3	UPL	Forward Primer: Reverse Primer: Probe:	GGCAAGTGCTGTGCAGATTA AGGCGGAGGTGCAGTCTT UPL Probe #9

WNT Signalling	<i>Dkk1</i>	Dickkopf homolog 1	NM_010051.3	UPL	Forward Primer: Reverse Primer: Probe:	CCGGGAAGTACTGCAAAAAT CCAAGGTTTTCAATGATGCTT UPL Probe #76
	<i>Dkk3</i>	Dickkopf homolog 3	NM_015814.2	UPL	Forward Primer: Reverse Primer: Probe:	TCGTGACCAGATCCAGCTT AGCCGCTGCATGTTTGTT UPL Probe #70
	<i>Frzb</i>	Frizzled-related protein; Secreted frizzled-related protein 3 (Sfrp3)	NM_011356.4	UPL	Forward Primer: Reverse Primer: Probe:	CACCGTCAATCTTTATACCACCT GAGCCTTCTACCAAGAGTAACCTG UPL Probe #34
	<i>Grem1</i>	Gremlin 1	NM_011824.4	UPL	Forward Primer: Reverse Primer: Probe:	GACCCACGGAAGTGACAGA CCCTCAGCTGTTGGCAGTAG UPL Probe #63
	<i>Ror2</i>	Receptor tyrosine kinase-like orphan receptor 2	NM_013846.3	UPL	Forward Primer: Reverse Primer: Probe:	TCATCAGCCAGCACAAAACA GTGGCCTTTGTAGACCTTGC UPL Probe #25
	<i>Wnt3a</i>	Wingless-related MMTV integration site 3A	NM_009522.2	UPL	Forward Primer: Reverse Primer: Probe:	CTTAGTGCTCTGCAGCCTGA GAGTGCTCAGAGAGGAGTACTGG UPL Probe #76
	<i>Wnt5a</i>	Wingless-related MMTV integration site 5A	NM_009524.2	UPL	Forward Primer: Reverse Primer: Probe:	ACGCTTCGCTTGAATTCCT CCCGGGCTTAATATTCCAA UPL Probe #55
Phosphatases	<i>Alpl</i>	Alkaline phosphatase, liver/bone/kidney	NM_007431.2	UPL	Forward Primer: Reverse Primer: Probe:	CGGATCCTGACCAAAAACC TCATGATGTCCGTGGTCAAT UPL Probe #12

ECM Receptors	<i>Ddr1</i>	Discoidin domain receptor 1	NM_007584.2 NM_172962.1	UPL	Forward Primer: Reverse Primer: Probe:	TGTGCCCTAGGGAGACTGAAAC TCCCTCTGGTCTATGGAGGA UPL Probe #56
	<i>Ddr2</i>	Discoidin domain receptor 1	NM_022563.2	UPL	Forward Primer: Reverse Primer: Probe:	CGAAAGCTTCCAGAGTTTGC GCTTCACAACACCACTGCAC UPL Probe #55
TGFβ Family	<i>Tgfb1</i>	Transforming growth factor, beta 1	NM_011577.1	UPL	Forward Primer: Reverse Primer: Probe:	TGGAGCAACATGTGGAAC TC CAGCAGCCGGTTACCAAG UPL Probe #72
	<i>Tgfb2</i>	Transforming growth factor, beta 2	NM_009367.3	UPL	Forward Primer: Reverse Primer: Probe:	TGGAGTTCAGACACTCAACACA AAGCTTCGGGATTATGGTGT UPL Probe #73
	<i>Tgfb3</i>	Transforming growth factor, beta 3	NM_009368.3	UPL	Forward Primer: Reverse Primer: Probe:	TGGCTGTCTTTCGATGTCAC GCTGATTTCCAGACCCAAGT UPL Probe #91
Transcription Factors	<i>Runx2</i>	Runt related transcription factor 2	NM_001146038.1 NM_009820.4 NM_001145920.1	UPL	Forward Primer: Reverse Primer: Probe:	GATGATGACACTGCCACCTCT AAAAGGGCCCAGTTCTGAAG UPL Probe #34
	<i>Sox9</i>	SRY-box containing gene 9	NM_011448.4	UPL	Forward Primer: Reverse Primer: Probe:	CAGCAAGACTCTGGGCAAG TCCACGAAGGGTCTCTTCTC UPL Probe #66
Others	<i>Anxa1</i>	Annexin A1	NM_010730.2	UPL	Forward Primer: Reverse Primer: Probe:	CTTTGCCAAGCCATCCTG TGGGATGTCTAGTTTCCACCA UPL Probe #66

2.2.7 qRT-PCR analysis using double-dye hydrolysis probe technology

Five nanograms of cDNA were used for gene expression analysis using the 7500/7500 Fast Real-Time PCR System (Applied Biosystems) with 2x qPCR MasterMix (Applied Biosystems) and selected primer/probe combinations at the relevant concentrations described above. For qRT-PCR analysis using double-dye hydrolysis probes, standard TaqMan cycling conditions were used (Table 2.4). Gene expression was normalised using the relative standard curve method against expression of the housekeeping genes, *18S* or *Ywhaz*.

Table 2.4 – Standard TaqMan cycling conditions for qRT-PCR using double-dye hydrolysis probes. Data collection was under the FAM channel.

	Step	Time (min:sec)	Temperature (°C)
	Enzyme Activation	10:00	95
Cycling x40	Denaturation	00:15	95
	Data Collection	01:00	60

2.3 Histological Staining

2.3.1 Detection of proteoglycans/GAGs with Alcian Blue

Proteoglycans/GAGs were detected by Alcian blue staining using a modified protocol from Kawai, *et al.*, (2012) and Cha, *et al.*, (2013). Briefly, cells cultured directly on 24-well plates were washed twice with PBS and fixed with ice-cold methanol at -20 °C for 5 min. Methanol was then immediately replaced with an equal amount of Alcian Blue 8GX (0.1 % w/v in 0.1 M HCl) (Sigma-Aldrich Aldrich) and left at room temperature overnight. Cells were repeatedly washed with water until the water pipetted off was clear, then cells were left in fresh water for imaging. Cells were imaged using a Zeiss SV11 stereo widefield microscope (Zeiss) with a colour AxioCam HRc camera (Zeiss) using AxioVision software (Zeiss).

The amount of Alcian blue staining was quantified using a modified protocol based on Frazier, *et al.*, (2008). Briefly, Alcian blue staining was removed from cultures and solubilised with 8 M guanidine hydrochloride for 6 h with gentle shaking at room temperature. One hundred microlitres was then removed and placed into a 96-well plate (Nunc) and absorbance read at 630 nm. The absorbance of unused 8 M guanidine hydrochloride was subtracted from all absorbance readings before data analysis.

2.3.2 Immunofluorescence

To ensure adequate antibody penetration in cultures which have been induced to differentiate, due to the thickness of the developed micromass and the three-dimensional cartilaginous nodules in monolayer cultures, immunofluorescence was carried out using a modified protocol based on Bader, et al., (1998).

Cells were seeded, according to the experiment, onto sterile 13 mm glass coverslips (VWR International) in a 24-well plate. For immunofluorescent detection of ECM components, cells were washed in PBS and fixed in ice cold acetone for 5 min at -20 °C. Cells were rehydrated to PBS in stepwise 10 min incubations from 80, 50 and 20 % acetone/PBS to 100 % PBS at room temperature. Non-specific sites in the ECM were then blocked in either 10 % normal goat serum + 5 % BSA in PBS or 10% normal donkey serum (Sigma-Aldrich) + 5% BSA in PBS, depending on the antibody for 2 x 60 min incubations at room temperature. Coverslips were then inverted onto a 50 µl droplet containing the primary antibody diluted in the blocking buffer on parafilm (Bemis Company, Inc) overnight at 4 °C in a humidified chamber. Cells were then placed cell-side up back into the 24-well plate and washed seven times for 60 min each in TBS. The same process was then used to incubate with the secondary antibody overnight before seven more washes in TBS to remove residual unbound antibody. The fifth wash also contained 1 µg/ml 4',6-diamidino-2-phenylindole (DAPI) to stain for nuclear content. Coverslips were then mounted onto a glass slide using Hydromount (National Diagnostics) and kept in the dark at 4 °C until imaging.

Cells were imaged using either a Zeiss LSM510 META confocal microscope with an inverted Axiovert 200M stand or a Leica TCS SP2 UV confocal microscope with an inverted Leica DM IRE2 stand. Z stacks were taken at 2 µm steps through and beyond positively DAPI-stained areas at a resolution of 2048 x 2048 pixels per slice. Images were then processed using Volocity software (PerkinElmer, Waltham, MA). Fluorescence intensity was calculated using ImageJ per slice and the results per slice added together and divided by the number of slices. Total intensity was then normalised to the no primary controls by subtracting the total intensity for the no primary conditions.

A full list of primary and secondary antibodies can be found in Table 2.5 and Table 2.6 respectively.

2.3.3 Protein Detection by Western Blotting

Western blotting was performed essentially as described in Baker, *et al.*, (2012), detailed below.

2.3.3.1 Preparation of cell lysates

Cell cultures were washed twice in ice cold PBS and lysed in either RIPA buffer (50 mM Tris HCl pH 8, 150 mM NaCl, 1 % Triton X100, 0.5 % Sodium Deoxycholate, 0.1 % SDS) (recipe from Abcam, Cambridge, UK) or Urea/Thiourea buffer (7 M urea, 2 M thiourea, 4 % CHAPS, 30 mM Tris HCl pH 8.5, 1 mM DTT) (recipe based on Ngoka (2008) and Peach, *et al.* (2012)) containing Halt™ Protease and Phosphatase Inhibitor Cocktail (Pierce). RIPA extraction was carried out on ice for at least 30 min with occasional scraping. Urea/thiourea extraction was carried out at room temperature for 15 min. For further homogenisation, if needed, lysate was transferred to a 2 ml safety-lock tube (Eppendorf) with a sterile ball bearing, and homogenised using a pre-cooled TissueLyser (QIAGEN) machine by vigorous shaking at 30 Hz for 30 s. Some RIPA samples were cleared of insoluble material by centrifugation at 4 °C at 13 000 RPM for 10 min and any insoluble material discarded by placing supernatant in a fresh tube, stored at -20 °C until use.

For SDS-PAGE, prepared protein lysates at the desired concentration were mixed with either 5x reducing or non-reducing sample buffer (625 mM Tris pH 6.8, 2 % SDS, 10 % glycerol, bromophenol blue ± 12.5 % β-mercaptoethanol). RIPA-extracted samples were denatured by incubating at 95 °C for 5 min. Urea/thiourea-extracted samples were not boiled to prevent carbamylation of samples.

2.3.3.2 Protein quantification by Pierce BCA Protein Assay (RIPA-extracted samples)

Protein concentration of RIPA-extracted samples was quantified using a Pierce Bicinchoninic Acid (BCA) Protein Assay kit, following manufacturer's instructions.

Briefly, protein standards of known concentrations of BSA were prepared and 25 µl plated in duplicate, ranging from 0 – 2000 µg/ml. The same volume of unknown protein samples were also plated in duplicate. Two hundred microlitres of working reagent at 50:1 Reagent A:Reagent B were added to each standard/unknown sample and incubated at 37 °C for 30 min. Absorbance was then read at 562 nm in a spectrophotometer plate reader.

For calculation of protein concentration in unknown samples, the absorbance reading from the control (0 µg/ml BSA) was subtracted from all standards/samples. A standard curve was prepared from the average values of the known BSA standards and the equation of the trendline used to calculate the concentration of the unknown samples via interpolation.

2.3.3.3 Protein quantification by Pierce 660 nm assay (Urea/thiourea-extracted samples)

Due to incompatibility of thiourea with the BCA protein assay, protein concentration of urea/thiourea-extracted samples was determined using the Pierce 660 nm assay following

manufacturer's instructions. Briefly, 10 µl protein standards of known concentrations of BSA were plated in duplicate from 50 – 2000 µg/ml in a 96-well plate. The same volume of unknown protein samples were also plated in duplicate before adding 150 µl of protein assay reagent to each well containing either known or unknown samples. Samples were incubated for 5 min before reading absorbance at 660 nm in a spectrophotometer plate reader. Calculation of protein concentration in unknown samples were then carried out as in the BCA protein assay.

2.3.3.4 Preparation of conditioned media for Western Blotting

Cell cultures were washed twice with PBS and media replaced with serum-free medium or medium containing 0.2 % FCS. Media samples were collected after 24 h, unless otherwise stated, and were centrifuged to remove cell debris and stored at -20 °C until required.

2.3.3.5 TCA precipitation of conditioned media

To concentrate protein content of conditioned media samples, trichloroacetic acid (TCA) was added to collected samples to 5 % and left to incubate overnight at 4 °C. Samples were centrifuged at 6000 g for 10 min at 4 °C. Supernatant was discarded and pellets transferred to microcentrifuge tubes and were washed twice in ice cold acetone with centrifugation at 13 000 g. Acetone was removed and pellets allowed to air dry before reconstituting in 1 x reducing sample buffer, followed by denaturation at 95 °C for 5 min.

2.3.3.6 Protein resolution by SDS-PAGE

Proteins were resolved using SDS-PAGE. Typically, 15-30 µg of protein, or total TCA-precipitates of conditioned media, were loaded onto polyacrylamide gels, with 8 or 10 % resolving gels and 5 % stacking gel. Samples were run alongside a well containing Spectra Multicolor Broad Range Protein Ladder (Pierce), a pre-stained molecular weight marker (10 kDa to 260 kDa). Gels were run at a constant 30 mA per gel until proteins were adequately resolved based on the protein ladder.

2.3.3.7 Semi-dry transfer of polyacrylamide gels to PVDF

Polyvinylidene fluoride (PVDF) membranes (Immun-blot, BIO-RAD) were activated by incubation in methanol for 5 min. Activated PVDF, thick filter paper (BIO-RAD) and resolving polyacrylamide gels were then equilibrated in semi-dry transfer buffer for 5 min before protein transfer at 15 V for 35 min using a Transblot SD Semi-Dry Transfer Cell (BIO-RAD).

2.3.3.8 Confirmation of transfer by Ponceau S staining

Transfer of proteins to the PVDF membrane was confirmed by immediately incubating the PVDF membranes in 0.2 % Ponceau S in 5 % TCA for 10 min with rocking. Membranes were repeatedly

washed in ddH₂O with rocking until excess Ponceau S had been removed, allowing visualisation of protein bands. Ponceau S was then removed by repeated washes in TBS-T until clear and then proceeded to blocking step.

2.3.3.9 Immunodetection of proteins

Depending on the antibody and samples used, membranes were blocked overnight at 4 °C or for two hours at room temperature in TBS-T (0.1 % Tween-20) containing either 5 % (dried, skimmed) milk, 5 % milk with 3 % bovine serum albumin (BSA) or 5 % BSA. Membranes were incubated with primary antibody diluted in blocking buffer for 2 hours at room temperature or overnight at 4 °C before being washed for 5 times over 60 min. Membranes were then incubated with the secondary antibody conjugated with horse radish peroxidase (HRP) diluted in the blocking buffer for 60 min at room temperature and then washed again in TBS-T four times over 30 min. Probed membranes were incubated in in-house ECL (0.24 % luminol, 0.0045 % coumaric acid, 0.03 % H₂O₂, 100 mM Tris HCl pH 8.5) for 1 min, which reacts with the HRP enzyme to give chemiluminescence specifically where the primary/secondary antibody complex is bound, and exposed to photosensitive film (Amersham Hyperfilm ECL, GE Healthcare) before being developed using an autoradiograph film processor (Xograph Healthcare).

A full list of primary and secondary antibodies can be found in Table 2.5 and Table 2.6 respectively.

2.3.3.10 Stripping membranes

To re-probe membranes for different proteins, membranes were stripped using ReBlot Plus Strong stripping buffer (Millipore) for 15 min before blocking for 2 x 5 min in the desired blocking buffer and proceeding to primary antibody incubation.

2.3.3.11 Antibodies

Table 2.5 – Details of primary antibodies; WB = Western Blotting; IF = Immunofluorescence

Target	Supplier	Product Code	Host Species Clonality Isotype	Application	Concentration /Dilution
β-Actin	Abcam	ab8227	Rabbit Polyclonal IgG	WB	1:20000
β-catenin	Abcam	ab32572	Rabbit Monoclonal IgG	WB	0.2 µg/ml
DDR2	Abcam	ab126773	Rabbit Monoclonal IgG	WB	1:500
FLAG (DYKDDDDK)	Sigma-Aldrich	F7425	Rabbit Polyclonal IgG	WB	5 µg/ml
FRZB	Abcam	ab102811	Rabbit Polyclonal IgG	WB	5 µg/ml
phospho-β- catenin (T41+S45)	Abcam	ab38511	Rabbit Polyclonal IgG	WB	2 µg/ml
RUNX2	Santa Cruz	sc-10758	Rabbit Polyclonal IgG	WB	2 µg/ml
Type II Collagen	Millipore	AB2031	Rabbit Polyclonal IgG	IF	12.5 µg/ml
Type X Collagen	Santa Cruz	sc-323750	Goat Polyclonal IgG	IF	4 µg/ml
WNT5A	Abcam	ab174100	Rabbit Polyclonal IgG	WB	1 µg/ml

Table 2.6 – Details of secondary antibodies used. Antibody names are designated as host species, reactive species, conjugation. The numbers in the antibody name represent the conjugated Alexa-Fluor® dyes, used in IF. HRP = horse radish peroxidase, used in WB.

Antibody	Supplier	Product Code	Concentration
Donkey anti-goat-488	Molecular Probes	A-11055	4 µg/ml
Donkey anti-rabbit-488	Molecular Probes	A-21206	4 µg/ml
Goat anti-rabbit-488	Molecular Probes	A-11008	2 µg/ml
Goat anti-rabbit-HRP	Dako	P0448	1:2000 – 1:10000

2.4 Molecular Cloning

Molecular cloning was conducted with the kind help of Dr. Tracey Swingler (UEA).

2.4.1 Generation of competent DH5α cells

One colony of DH5α *Escherichia coli* cells (kindly provided by Dr. Tracey Swingler, UEA) was inoculated into LB broth grown at 37 °C until an optical density of 0.6 at 600 nm. Cells were chilled and pelleted at 4000 rpm at 4 °C and washed and resuspended twice in 0.1 M CaCl₂. Resuspended cells were left to incubate at 4 °C for 60 min before 400 µl sterile glycerol was added per 1 ml aliquotted cells. Aliquots were kept at -80 °C.

2.4.2 Transformation of DH5α cells

One hundred nanograms of plasmid was used to transform 70 µl of competent DH5α cells. Plasmid/cell mixtures were incubated on ice for 20 min, heat shocked at 42 °C for 1 min, then immediately placed back onto ice for 2 min. Transformed DH5α were allowed to recover in 500 µl antibiotic-free LB for 1 h at 37 °C before streaking onto selective LB agar plates containing 50 µg/ml kanamycin (Sigma-Aldrich) (for pJ201 plasmids) or 100 µg/ml ampicillin (Sigma-Aldrich) (for pcDNA3.1⁺ and pcDNA4 plasmids) and grown overnight at 37 °C. Single colonies were inoculated into 5 ml selective LB and grown overnight at 37 °C with shaking.

2.4.3 Plasmid isolation from DH5α cells using QIAGEN Miniprep

Plasmid DNA was isolated from transformed DH5α cells by using the QIAGEN QIAprep Spin Miniprep Kit according to manufacturer's instructions. Briefly, pelleted cells were lysed in an alkaline buffer, neutralised and adjusted to a high salt concentration to aid plasmid binding to the silica spin column. LyseBlue was added to the lysis buffer as a colour indicator to ensure complete buffer mixing. The silica membrane of the spin columns traps the plasmid DNA during centrifugation and a series of washes removes endonucleases and reduces the salt concentration, allowing elution

in nuclease-free H₂O. Plasmid concentration was determined as previously described using the NanoDrop system.

2.4.4 WNT5A amplification and end modification via PCR

WNT5A was amplified from its supplied pCMV6-XL4 vector (Origene) using primers designed to add HindIII and XhoI restriction sites at the 5' and 3' ends, insert a Kozak consensus sequence and remove the endogenous WNT5A stop codon (Figure 2.1).

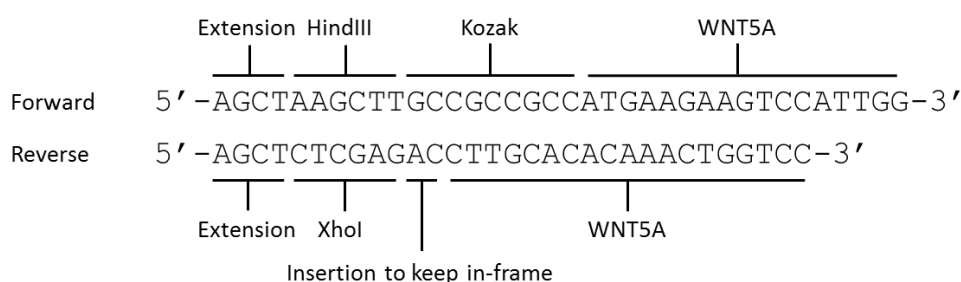


Figure 2.1 – Primers to amplify and modify the ends of WNT5A from pCMV5-XL4 highlighting the extra sequences upstream and downstream of the *WNT5A* gene to allow insertion into pcDNA4:FLAG, allowing expression of the c-terminal tags.

PCR was carried out using AccuTaq™ LA DNA Polymerase (Sigma-Aldrich) according to manufacturer's instructions, designed with proof-reading activity, on 100 ng plasmid with PCR cycling conditions described in Table 2.7. Various annealing temperatures were initially tested for efficiency in PCR amplification, confirmed by gel electrophoresis (data not shown). The PCR product was cleaned up using QIAGEN MinElute PCR Purification kit, according to manufacturer's instructions, and then restricted with HindIII and XhoI to reveal sticky ends to enable insertion into pcDNA4:FLAG, as described below, after gel purification.

Table 2.7 – Cycling conditions for WNT5A amplification and end-modification with AccuTaq.

	Step	Temperature (°C)	Time (min:sec)
	Initial Denaturation	95	01:00
Cycling x35	Denaturation	95	00:15
	Annealing	60	00:15
	Extension	72	01:00
	Final Extension	72	07:00
	Hold	4	

2.4.5 Plasmid restriction

Human *WNT3A* was isolated from its supplied pcDNA3.1⁺ plasmid (gifted from UCB, Slough) using HindIII + XhoI (New England Biolabs) at 37 °C for 15 min follow by 75 °C to inactivate the enzymes. The pcDNA4:FLAG expression vector set to receive the inserts was also restricted using the same enzymes. pcDNA4:FLAG was kindly provided by Dr. Vera Knäuper (Cardiff University) and is a modified version of pcDNA™4 (Invitrogen), replacing the V5 tag with an in-frame FLAG tag. Expressed proteins are therefore tagged with both FLAG and 6xHis at the c-terminus (Figure 2.2)

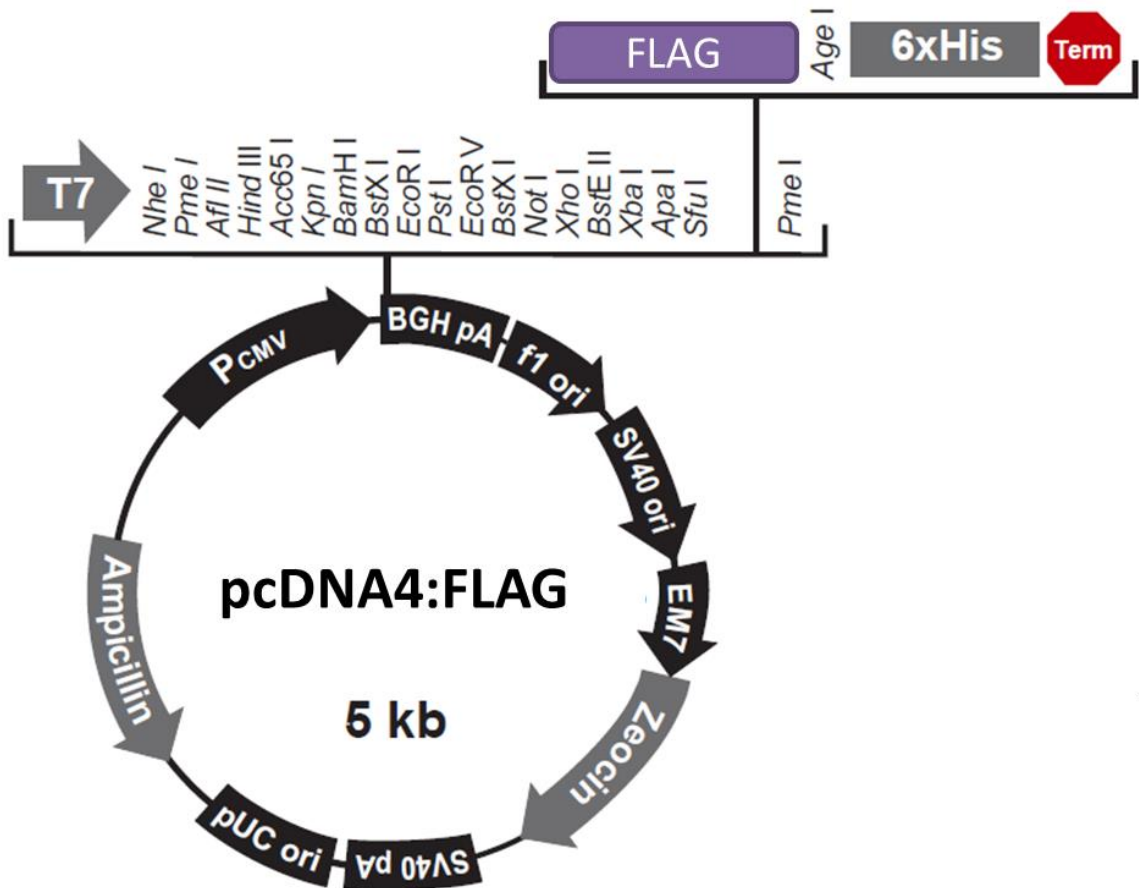


Figure 2.2 – pcDNA4:FLAG mammalian expression vector map – a modified version of pcDNA™4/V5-His A (Invitrogen) replacing the V5 epitope with an in-frame FLAG (DYKDDDDK) tag by Dr. Vera Knäuper (Cardiff University). Inserted genes are expressed under the P_{CMV} promoter (Cytomegalovirus promoter) for constitutive expression. Transfected cells can be selected for using the Zeocin™ selective antibiotic. Modified from Invitrogen.

2.4.6 Fragment isolation by traditional agarose gel electrophoresis

Restricted samples containing loading buffer were separated using agarose gel electrophoresis on a 1% agarose gel (Lonza SeaKem GTG Agarose) in TBE buffer containing ethidium bromide alongside a DNA ladder (1 kb plus, Invitrogen) running at 120 V.

2.4.7 Recovery of fragments from traditional agarose gel

Bands were quickly visualised in gels using UV light and excised from the gel. DNA was recovered from the gel using the QIAquick Gel Extraction Kit (QIAGEN) according to manufacturer's instructions. Briefly, gel pieces are solubilised in a high salt buffer that allows DNA binding to the silica membrane of the spin columns. A series of washes by centrifugation removes impurities such as agarose and small DNA fragments. A reduction in salt concentration allows elution of the DNA in nuclease-free H₂O. DNA recovery was assessed by NanoDrop.

2.4.8 Ligation of inserts into pcDNA4:FLAG

Isolated inserts were ligated into the pcDNA4:FLAG mammalian expression vector using T4 DNA ligase (Roche), incubating at 14 °C overnight at a molar ratio of 3:1, 1:1 and 1:3 of insert:vector, using 50 ng vector, using the Promega BioMath equation:

$$\text{mass of insert (ng)} = \frac{\text{length of insert (kb)}}{\text{length of vector (kb)}} \times \text{mass of vector (ng)}$$

2.4.9 Screening for successful ligation

Ligation mixtures were then transformed and cells grown as described previously. Plasmids were extracted and tested for the correct insert by observing the correct bands from a restriction digest on an agarose gel, as previously described. Plasmid samples from cultures containing the correct banding patterns were sequenced at Source Bioscience (Cambridge, UK) using T7 forward and bGH reverse primers. Received sequence information was checked by aligning with the predicted sequence using the BLASTN sequence alignment tool (NCBI).

Table 2.8 – PCR Cycling conditions for QuikChange Lightning SDM of pcDNA4:WNT3A

Cycles	Temperature (°C)	Time (min:sec)
1	95	02:00
18	95	00:20
	60	00:10
	68	06:00 (00:30/kb)
1	68	05:00

Parental/Non-mutated DNA was removed by restriction with DpnI to target methylated or hemi-methylated DNA for 5 min at 37 °C. DpnI-treated plasmid was transformed into X40-Gold ultracompetent *E. coli* supplemented with β -mercaptoethanol by incubation on ice for 30 min, followed by heatshock at 42 °C for 30 sec before immediately plunging back into ice for 2 min. Transformed cells were allowed to recover for 60 min in 500 μ l LB at 37 °C before spreading onto selective (ampicillin) LB agar plates, incubating overnight at 37 °C. Colonies were picked, grown and screened by sequencing as previously described to ensure successful mutation.

2.5 Transfection in ATDC5 cells

2.5.1 High quality plasmid purification by QIAGEN HiSpeed Plasmid Midi Kit

Transfection-quality plasmid was extracted from transformed DH5 α cells grown in 50 ml LB using the QIAGEN HiSpeed Plasmid Midi Kit per manufacturer's instructions. Briefly, pelleted cells were lysed in an alkaline lysis buffer and neutralised. Complete homogenisation was observed by the addition of LyseBlue. Lysed cells are cleared of SDS precipitates by syringe filtration. Plasmid DNA was then precipitated by the addition of isopropanol, which allows the plasmid DNA to become trapped in the precipitator module and finally eluted in TE buffer. Plasmid quality and quantity was assessed by NanoDrop, as previously described.

2.5.2 Plasmid linearisation and purification

For stable transfections, plasmids were linearised at a known position to aid stable integration into the genome, using BglII (New England Biolabs) for 2 h at 37 °C. Successful linearisation was confirmed by agarose gel electrophoresis. Linearised plasmid was then purified by combining with equal amounts of phenol chloroform, mixed by vortex and spun down at max speed for 10 min. The aqueous phase containing the DNA was then transferred to a new tube before adding 3M sodium acetate to 10% v/v. DNA was precipitated via addition of 100% ethanol (2.5x volume), mixed by vortex and spun down at max speed for 10 min. Supernatant was discarded, the pellet washed in

70% ethanol, before spinning at max speed again for 10 min. Ethanol was then removed and the pellet allowed to air dry before reconstitution in nuclease-free water.

2.5.3 Determination of optimum selective antibiotic concentration

To determine the optimum concentration of selective antibiotic (Zeocin™, Invivogen), a kill curve was performed using 0, 200, 400, 600, 800 and 1000 µg/ml Zeocin. ATDC5 cells were plated at 2×10^4 cells/well in a 24-well plate with zeocin-containing medium added the following day. Cells were then observed via phase-contrast microscopy over the following 14 days for death. The concentration giving complete death after 14 days was then selected for use with stable transfections (1000 µg/ml).

2.5.4 Transfection with TurboFect

Plasmid DNA was transfected into ATDC5 cells grown in monolayer until ~70 % confluent using TurboFect (Thermo Scientific), a cationic reagent that forms positively-charged complexes with DNA that allows passage through the lipid membrane, according to manufacturer's instructions. Briefly, 1 µg plasmid per 100 µl serum-free DMEM:F12 was used per millilitre of final culture medium volume. Plasmid diluted in serum-free medium was incubated with 2 µl TurboFect per 100 µl DNA for 15 min at room temperature to allow positively-charged complexes to form. DNA/Turbofect mixture was then pipetted drop-wise onto the cells and incubated at 37 °C and left for up to 3 days, depending on type of transfection, described below. In all cases, transfection with pcDNA4:FLAG with no insert (termed "Vector Only") was used as a control.

2.5.5 Generation of conditioned media from transiently transfected cells

For transiently transfected cells, DNA/Turbofect-containing media were removed after five hours, cells washed with PBS and replaced with fresh maintenance media containing 0.2 % FCS and conditioned for 24 h. Collected media were centrifuged for 5 min at 800 g and filter sterilised with 0.2 µm pore-sized Minisart filters (Sartorius). Conditioned media were kept at -20 °C until needed. Presence or absence of overexpressing protein was confirmed by western blotting for each batch of medium.

2.5.6 Generation of Stable Clones

For stable transfections, DNA/Turbofect-containing medium was removed after 3 days. Cells were washed in PBS, trypsinised, and placed into T75 culture flasks with maintenance medium supplemented with 1000 µg/ml Zeocin. Medium was replaced every 2-3 days, killing cells that did not take up the plasmid.

To obtain a monoclonal population, cells were seeded at 0.5 - 1 cells/well in a 96-well plate format and subsequently gradually passaged, with kind help from Mr. Promise Ogor (UEA), into larger culture dishes from 24-well plate, to 6-well plate, to T25 and finally T75 culture flasks (Nunc). Cells were checked periodically for expression of the transfected gene (or lack thereof in vector only clones) via qRT-PCR and western blotting from cell lysates and/or conditioned medium.

2.5.7 Analysing gene expression in stable clones

Non-induced stable clones were plated in both monolayer and micromass culture for 4 days before RNA extraction to examine gene expression.

For differentiation, stable clones were plated in monolayer and micromass culture as described for naïve ATDC5 cells in the presence or absence of both insulin and ascorbic acid for 14 days. After 14 days, cells were stimulated with or without 10 ng/ml OSM (R&D) and 5 ng/ml IL-1 α (R&D) in maintenance media (no insulin or ascorbic acid).

Due to the length of time needed in some experiments to allow differentiation to occur, all experiments using stable clones were conducted in the presence of 1000 μ g/ml Zeocin.

2.6 Conditioned Media Stimulation

Naïve ATDC5 cells were cultured in monolayer or micromass in the presence or absence of insulin and ascorbic acid as before. At day 14, cells were washed and media replaced with neat conditioned media generated from transiently transfected cells for 24 h before RNA or protein extraction. In some experiments, 10 ng/ml OSM and 5 ng/ml IL-1 α were added to the conditioned media, stimulating the cells at the exact same time.

2.6.1 Microarray Analysis

RNA was extracted from stimulated cells as previously described and checked for quality (OD 260/280 ratio between 1.68 - 2.08) by Nanodrop before sending 15 μ l RNA above a minimum concentration of 50 ng/ μ l to Almac Diagnostics (Craigavon, Northern Ireland) for microarray analysis using the Mouse Genome 430 2.0 Affymetrix GeneChip. Each condition consisted of three biological replicates. All samples were confirmed to pass QC.

Microarray results were analysed with Paul Hales at UCB Pharma LTD (Slough, UK). Results were normalised using GeneChip Robust Multiarray Averaging (GC-RMA) normalisation and analysed using Genedata's Analyst software. Probes with an expression value of 10 or below were below the minimum threshold of background noise and considered to not be expressed and therefore not

used for subsequent analysis unless regulated to appreciable levels. Expression levels from probes were compared across the conditions and expressed as a fold change. Probes above an arbitrary cut off of 1.5 fold change with $P < 0.05$ by *t*-test and Q-Value < 0.05 by Benjamini-Hochberg analysis were considered significant and used for subsequent analysis. Pathway analysis was carried out with the significantly regulated genes using the freely available DAVID Bioinformatics Resources 6.7 (National Institute of Allergy and Infectious Diseases).

2.7 Cell Adhesion Assay

Cell adhesion assays were performed using a modified protocol from Messent, et al., (1998). Wells of a 96-well plate (Nunc) were coated with 100 μ l of the desired matrix component as above, then washed with PBS and blocked with 1% heat-denatured BSA (Sigma-Aldrich) in PBS for 1 h at 4 °C. The wells were again washed with PBS and ATDC5 cells plated at 6×10^4 cells/well in 100 μ l serum-free maintenance medium. Cells were allowed to adhere for 60 min at 37 °C, then unattached cells were flicked off and wells washed with warmed serum-free maintenance medium. Adhered cells were fixed in 70% ethanol at room temperature for 10 min and stained with 100 μ l 1% methylene blue in 0.01M borate buffer (pH 8.5) for 30 min. Excess dye was washed off and adhered cells were lysed with EtOH/0.1M HCl (1:1) for 10 min with shaking and absorbance read at 630 nm with a multiwell plate-reader. The average absorbance for adhesion to BSA was subtracted from each value of adhesion to the matrix components, and these new values were expressed as an average per condition, with the amount of absorbance from the released methylene blue being proportional to the number of cells that adhered to the matrix substrate.

2.8 Random Cell Migration Assay

Random cell migration assays were performed essentially as described in (Murray, *et al.*, 2013). In brief, undifferentiated ATDC5 cells were plated at the desired concentration on matrix-coated plates in maintenance medium containing 0.2 % FCS and allowed to adhere for three hours in a humidified incubator at 37 °C with 5% CO₂. Cell stimulated with either neat WNT3A, WNT5A or Vector Only conditioned media from transiently-transfected cells, and/or stimulated with cytokines (10 ng/ml OSM and 5 ng/ml IL-1 α) were done so after these three hours. Plated cells were transferred to a motorised stage within a controlled, humidified environment at 37 °C with 5 % CO₂. Images were taken every 10 min for 17 h with AxioVision software (Zeiss) using a monochrome AxioCam MRm camera (Zeiss) attached to a widefield, Axiovert 200M inverted light microscope (Zeiss). Cell migration was manually tracked using the 'Manual Tracking' plugin (F. Cordelières,

Institute Curie, France) for ImageJ (National Institutes of Health), and expressed as the average cell speed in $\mu\text{m}/\text{h}$.

2.9 Micromass Inverted Invasion Assay

Micromass inverted invasion assays were carried out using a modified protocol from Hennigan, *et al.* (1994). ATDC5 micromass cultures were plated in the standard 10 μl droplets at 2×10^7 cells/ml but onto the top of 6.5 mm 8 μm pore transwells placed into 24 well plates (Corning Life Sciences) and allowed to adhere for two hours before flooding with 1 ml insulin- and ascorbic acid-containing differentiation medium, allowing the differentiation medium to flood both the top chamber and the bottom chamber, covering both sides of the transwell membrane. Micromass cultures were differentiated for 14 days, carefully replacing the medium every 2-3 days, as before.

After 14 days, micromass cultures were washed in PBS and stimulated in maintenance medium containing 0.2 % FCS with or without the addition of 10 ng/ml OSM and 5 ng/ml IL-1 α for 48 h. After 48 h, micromass cultures were washed in PBS and fixed in ice cold methanol at -20 $^{\circ}\text{C}$ for 5 min. Micromass cultures were then washed in PBS and warm 0.2 % FCS-containing maintenance medium before inverting the transwells and plating 100 μl non-induced (undifferentiated) ATDC5 cells at 1×10^6 cells/ml on the underside of the transwell membrane in standard 5 % FCS-containing maintenance medium. Cells were allowed to adhere for 3 hours before inverting again to place the transwells the right way up and washing the base containing the freshly-adhered live ATDC5 chondroprogenitor cells in 0.2 % FCS-containing maintenance medium. Transwells were then placed into wells containing 1 ml Vector Only conditioned medium and 200 μl chemoattractant (WNT5A conditioned medium) was placed in the top chamber, or control medium (Vector Only conditioned medium). In one experiment, 0.2 $\mu\text{g}/\text{ml}$ commercial WNT5A (R&D Systems, kind gift from Dr. Victoria Sherwood, UEA) was used or carrier control (from 0.1 % BSA stock). Concentration of commercial WNT5A used was based on Ekstrom, *et al.* (2011) which inhibited WNT3A-mediated canonical WNT signalling. Cells were allowed to invade for 48 h before culture media were replaced with 1 ml 4 μM calcein-AM and 4 μM ethidium homodomer-1 to stain live or dead cells respectively. A diagram of this set-up can be found in Figure 2.4.

Transwells were then imaged using a Leica TCS SP2 UV confocal microscope with an inverted Leica DM IRE2 stand taking images every 2 μm to form a Z-stack. The bottom of the transwells were wiped after confirming the presence of adhered cells before imaging the Z-stack. The first image was taken from the wiped underside and analysis was carried out using images 10 μm from the starting position, which equated to the thickness of the membrane. Images were analysed using

Volocity (PerkinElmer) and expressed as the average number of invading cells per field of view from three fields of view per transwell across two transwells (n=6).

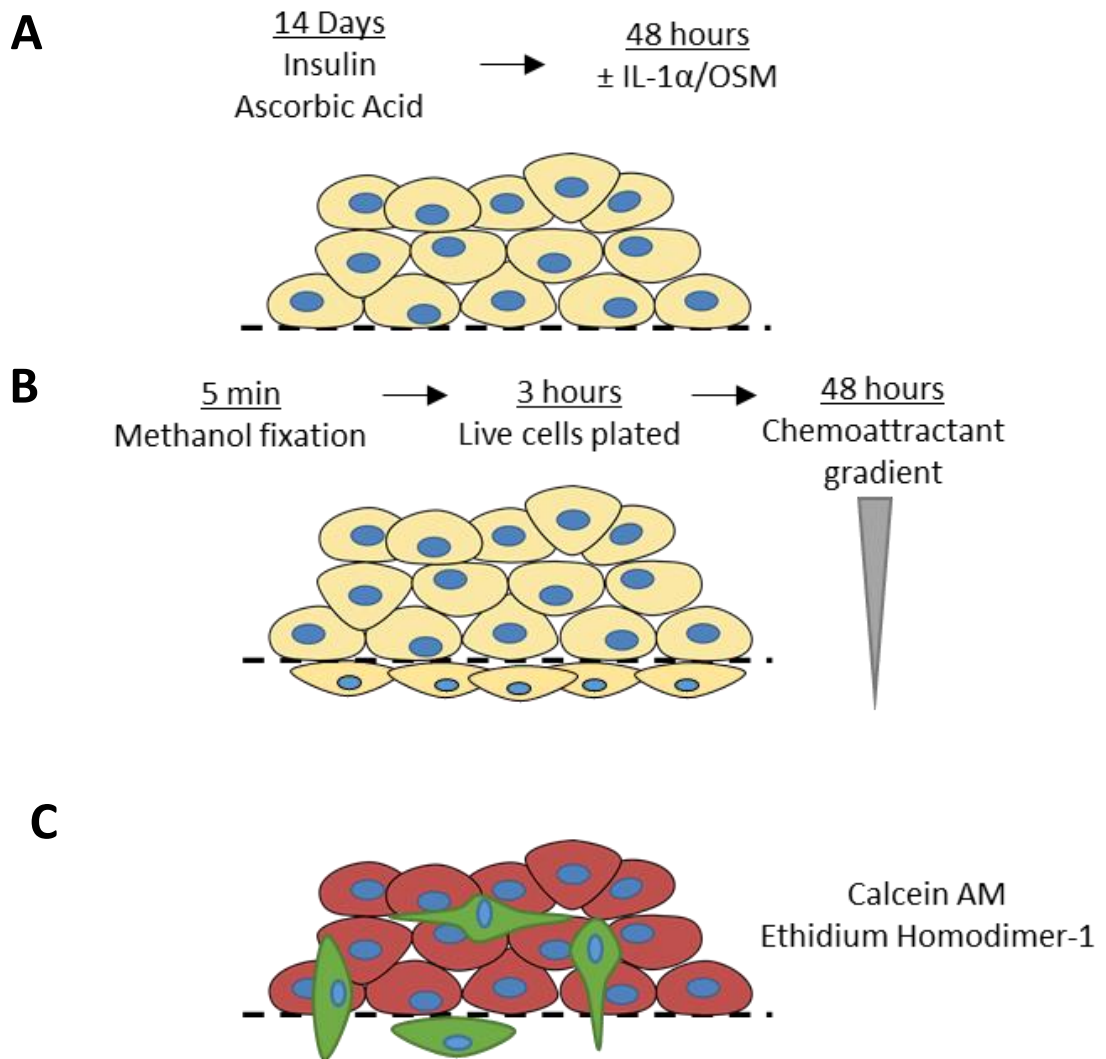


Figure 2.4 – Micromass inverted invasion assay schematic. A) ATDC5 micromass cultures are plated onto transwell inserts and stimulated with insulin and ascorbic acid to induce differentiation for 14 days before media removed and replaced with maintenance media supplemented with or without 5 ng/ml IL-1 α and 10 ng/ml OSM for 48 hours. B) Micromasses are fixed in methanol and live undifferentiated ATDC5 cells plated underneath the transwell. A chemoattractive gradient is established by adding the chemoattractant (WNT5A) to the top well and the control condition in the bottom well for 48 hours. C) Wells are flooded with calcein AM (green) and ethidium homodimer-1 (red) to stain for live and dead cells respectively before imaging with a confocal microscope.

2.10 Statistical Analysis

Statistical analysis was performed using either Student's independent sample *t*-test, or one-way ANOVA with Tukey post-hoc test, unless otherwise stated, using SPSS software (IBM). Unless otherwise stated, statistical analyses are only shown between conditions where only one factor has changed. All error bars represent standard error of the mean (SEM). The traditional 'star' system was used to represent statistical significance, depending on *P* value as shown below:

* $0.01 < P \leq 0.05$

** $0.001 < P \leq 0.01$

*** $0.0001 < P \leq 0.001$

**** $P \leq 0.0001$

Chapter 3

Enhancing and Maintaining the Chondrocytic Phenotype in ATDC5 cells by Physiologically-Relevant Culturing

3.1 Introduction

3.1.1 Mesenchymal Stem Cells and the ATDC5 chondrogenic differentiation model

Cartilage is a notable tissue for its extensive extracellular matrix. Chondrocytes and their precursors, the only cell types resident within cartilage, comprise < 5 % of the total cartilage volume (Poole, *et al.*, 2002). Therefore due to the limited number obtainable from cartilage samples, and with difficulty in maintaining a differentiated phenotype, MSCs (which have the ability to differentiate into chondrocytes as well as other lineages), along with chondrogenic cell lines, are widely used as an attractive alternative (Demoor, *et al.*, 2014).

The ATDC5 chondrogenic cell line, originally described by Atsumi, *et al.*, (1990), is a murine chondrogenic precursor derived from the AT805 embryonic teratocarcinoma. ATDC5 cells plated in monolayer can readily and reproducibly undergo chondrogenesis with insulin stimulation, producing aggregates rich in cartilage-associated matrix proteins, and can be maintained and subcultured in its undifferentiated state in the absence of insulin (Atsumi, *et al.*, 1990). ATDC5 cells may also be stimulated to undergo hypertrophic differentiation and mineralisation, enabling observations over the full spectrum of chondrogenesis from the initial condensation stages and chondrocyte maturation, to processes associated with endochondral ossification (Shukunami, *et al.*, 1997). They have also been shown to be transfectable (Morimoto & Obinata, 2011; Kawai, *et al.*, 2012; Caron, *et al.*, 2013; Kobayashi, *et al.*, 2013). Taken together, these traits made the ATDC5 cell line an attractive cell line to study chondrogenesis, which can be genetically manipulated, and to provide a ready source of chondrocytes that can produce extensive extracellular matrix.

3.1.2 Chondrocytes and physiologically relevant culturing conditions

It has been long established that primary chondrocytes rapidly de-differentiate upon isolation and expansion using traditional *in vitro* culturing methods, down-regulating chondrocytic genes, such as *COL2A1* (which encodes type II collagen), and up-regulating more fibroblastic genes, such as *COL1A1* (which encodes the α 1 chain of type I collagen) (Stokes, *et al.*, 2001). Re-differentiation of chondrocytes can occur when isolated chondrocytes are grown using physiologically-relevant culturing systems that, for example, allow them to regain their spherical shape that occurs naturally *in vivo* and to regain their cell-cell and cell-matrix interactions in all three dimensions. One such system is the high-density micromass culture, originally established to induce the chondrogenic differentiation of isolated chick limb bud cells (Ahrens, *et al.*, 1977), which has subsequently been used extensively and routinely for the chondrogenic differentiation of MSCs (Bobick & Cobb, 2012;

Diaz-Mendoza, *et al.*, 2014; Juhasz, *et al.*, 2014) and the re-differentiation of primary chondrocytes and chondrocyte cell lines (Schulze-Tanzil, *et al.*, 2002; Banu & Tsuchiya, 2007; Greco, *et al.*, 2011).

3.1.3 Chondrocytes and Ascorbic Acid

Ascorbic acid is an essential co-factor in collagen biosynthesis for the prolyl- and lysyl- hydroxylase enzymes to produce hydroxyproline and hydroxylysine, stabilising the triple helical collagen structure and forming intermolecular cross-links respectively (Murad, *et al.*, 1981; Pinnell, 1985). The use of ascorbic acid in the chondrogenic differentiating medium of mesenchymal stem cells is well-established (Tropel, *et al.*, 2004; Spagnoli, *et al.*, 2005; Taipaleenmaki, *et al.*, 2008; Markway, *et al.*, 2010), and the ability for ascorbic acid to induce chondrogenic differentiation of ATDC5 cells in monolayer in the absence of insulin has previously been shown (Temu, *et al.*, 2010). However, it remains unknown whether ATDC5 differentiation may be enhanced by the combination of ascorbic acid with micromass culture, and this is investigated in this study.

3.1.4 Cartilage Phenotypes

Several different types of cartilage exist within the body, with hyaline cartilage produced in developing joints. Hyaline cartilage may also be further subdivided depending on its characteristics and location with the body, providing different functions depending on the type. At the ends of articulating joints, articular cartilage provides joints with near-frictionless movement and cushions the joints from impact. Loss of articular cartilage during osteoarthritis increases friction and joint stiffness, resulting in pain. Growth plate cartilage on the other hand, undergoes hypertrophic differentiation in a process called endochondral ossification, which becomes mineralised and replaced with bone to form and elongate the bone. Articular cartilage and growth plate cartilage are therefore two different types of hyaline cartilage which serve different functions within the joint, whereby different genes are regulated to provide the two different phenotypes. It is therefore important to ascertain the type of cartilage produced by *in vitro* culture.

3.1.5 Aims

It was hypothesised that the combined use of ascorbic acid and micromass culture would enhance insulin-induced chondrogenic differentiation in ATDC5 cells. Whilst ATDC5 cells have been cultured in micromass before, the beneficial effects over monolayer culture were not investigated and so comparisons were also made with the use of micromass culture compared to monolayer, as well as the addition of ascorbic acid. Further to this, the resulting cartilage phenotypes of differentiated ATDC5 cells under these conditions were also investigated to ascertain the biological relevance for future studies.

3.2 Results

3.2.1 Selection of an appropriate housekeeping gene for qRT-PCR analysis

To investigate changes in gene expression during the course of chondrogenesis, qRT-PCR analysis was used. To achieve this, a geNorm analysis was first used to identify a suitable housekeeping gene from a selection of 12 genes that would not alter expression across the various chondrogenic conditions being investigated, which has not been reported for this experimental set up previously. More specifically, geNorm analysis was performed on ATDC5 cells grown in both monolayer and micromass cultures and stimulated with or without insulin to induce chondrogenesis for 14 days, before RNA extraction. For more detail, please see section 2.1.2 and 2.2.4. Results showed that *Actb*, *Ywhaz*, *Atp5b*, *Cyc1*, *Rpl13a*, *18S* and *Gapdh* were all suitable housekeeping genes for non-induced or insulin-induced ATDC5 cells in either monolayer or micromass cultures (Figure 3.1), with *Ywhaz* and *18S* being used in future experiments to normalise gene expression, and β -actin (encoded by *Actb*) being used as a loading control in subsequent western blot experiments.

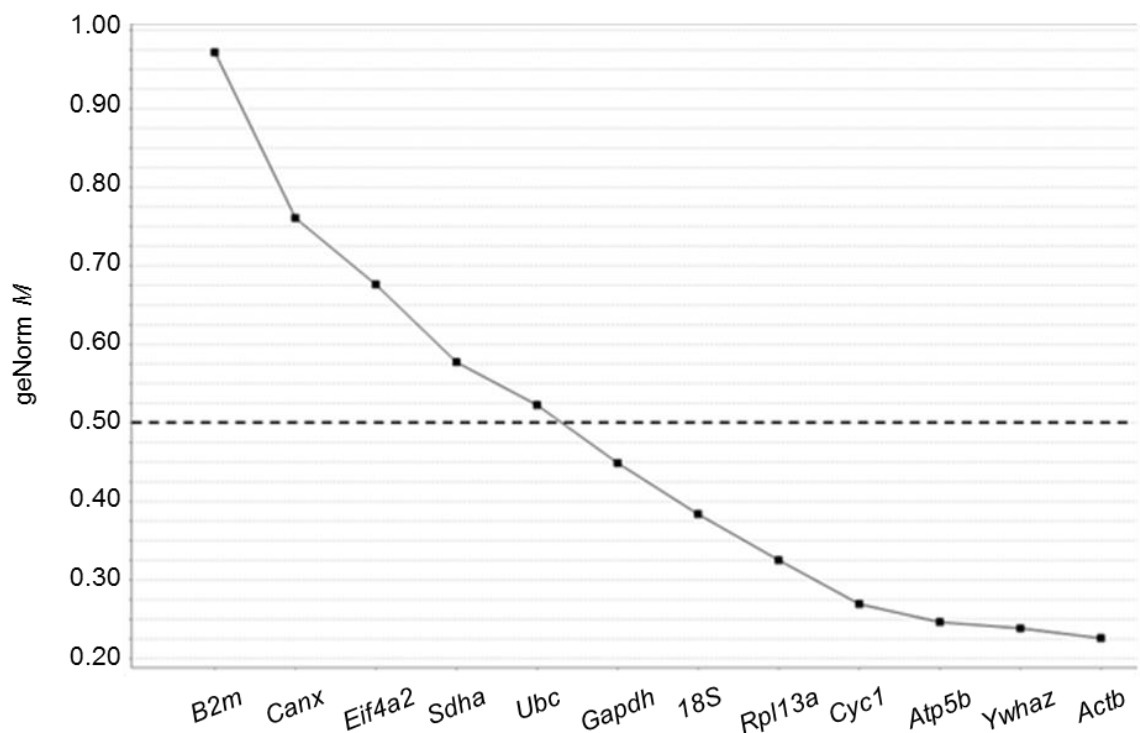


Figure 3.1 – Identifying suitable housekeeping genes that do not significantly alter expression during chondrogenic culture of ATDC5 cells via geNorm analysis. geNorm analysis performed on ATDC5 cells grown in monolayer or micromass in duplicate stimulated with or without insulin for 14 days. Genes with an *M* value below 0.5 were deemed acceptable for use as housekeeping genes. Line graph produced from geNorm *M* analysis using qbase^{PLUS} software. Experiment performed once.

3.2.2 Time course of gene expression during ATDC5 differentiation

To investigate gene expression changes over the course of differentiation, ATDC5 cells were cultured in micromasses induced to differentiate with insulin, stimulated with and without ascorbic acid for 7, 14 or 21 days, and compared with culture in monolayer or undifferentiated controls. Steady-state mRNA levels were examined by qRT-PCR analysis and preliminary results from one experiment are shown (Figure 3.2-3.5). *Col2a1*, *Frzb*, *Tgfb1*, *Tgfb3*, *Col10a1*, *Alpl* and *Runx2* mRNA expression were analysed due to their roles in chondrogenesis, as well as articular and hypertrophic differentiation. Only significant statistical differences relating to time in culture are shown. No RNA (NR) was recoverable from the insulin-induced, ascorbic acid-stimulated, 21 day time-point monolayer condition as this condition peeled off and died before the end of the experiment.

Expression of *Col2a1*, the major marker of chondrocytes which encodes type II collagen, was increased with increasing time in micromasses induced to differentiate with insulin (hereafter referred to as insulin-induced) (Figure 3.2 A). *Frzb* expression, a secreted wnt antagonist and a marker of articular differentiation, was also increased in a similar fashion in insulin-induced micromasses (Figure 3.2 B). Expression of *Tgfb1* was largely up-regulated in insulin-induced micromasses (Figure 3.3 A), whilst *Tgfb3* was largely unchanged with regards to time in culture (Figure 3.3 B). *Col10a1*, which encodes the hypertrophy-associated type X collagen, displayed increased expression with respect to time in insulin-induced micromasses (Figure 3.4 A). Similarly, levels of *Alpl*, which encodes the mineralising enzyme, alkaline phosphatase (Liver/Bone/Kidney), also increased with respect to time in differentiating micromass cultures. However, it was increased in other conditions stimulated with ascorbic acid in both monolayer and micromass cultures (Figure 3.4 B). Interestingly, *Runx2* expression, the major transcription factor driving hypertrophy, remained unchanged with respect to time in insulin-induced cultures, but was significantly up-regulated after 21 days in culture in micromasses that had not been induced to undergo chondrogenesis with insulin (hereafter referred to as non-induced) (Figure 3.5).

Based on these results, further experiments were performed at the 14 day culture time point, minimising any potential hypertrophy whilst still providing adequate chondrogenic differentiation. This also allowed analysis across all culturing conditions as monolayer cultures induced with insulin and stimulated with ascorbic acid die before day 21 from overgrowth.

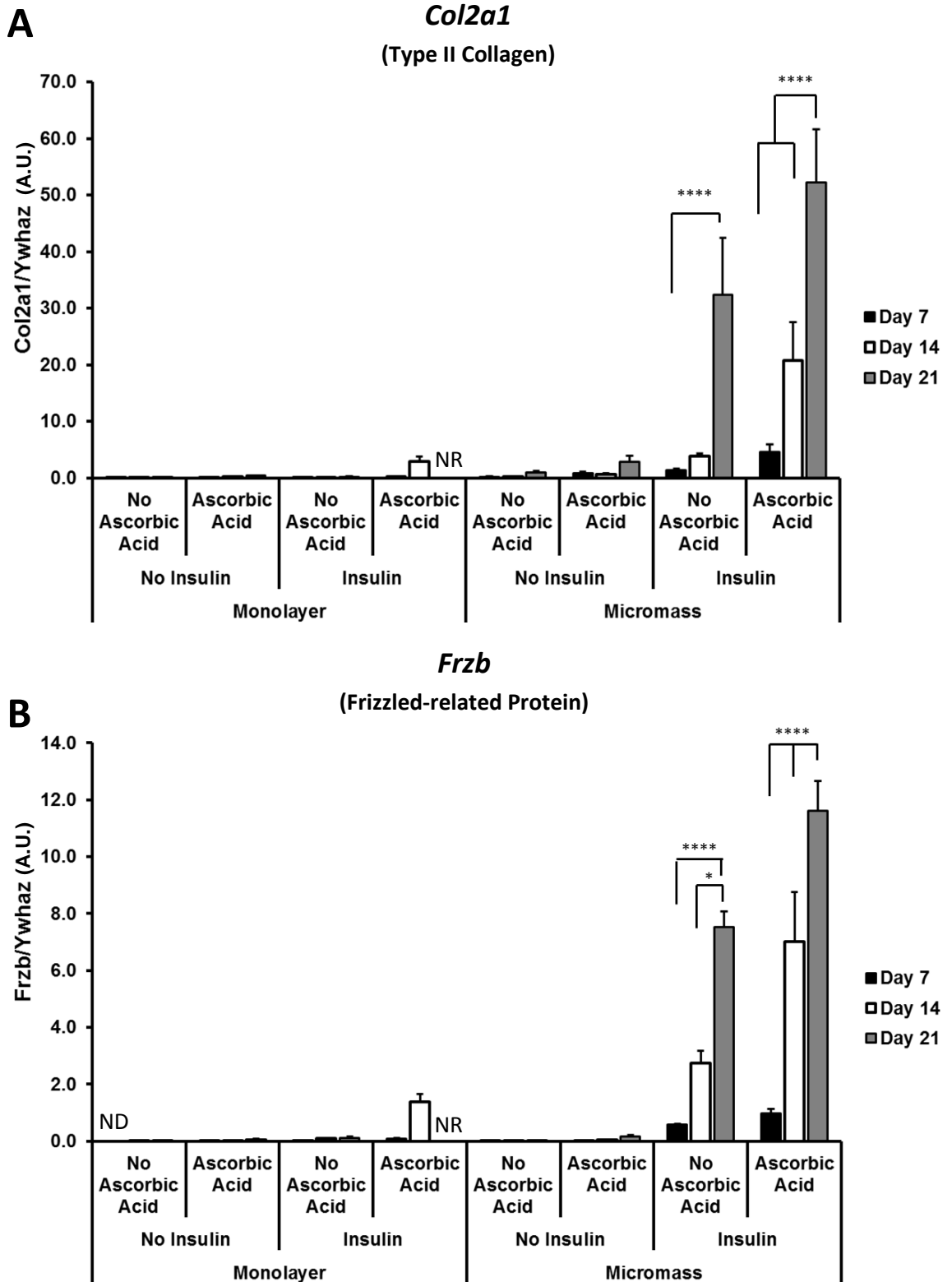


Figure 3.2 – Gene expression regulation of articular cartilage markers during ATDC5 differentiation. Steady-state mRNA levels of *Col2a1* (A) and *Frzb* (B) were analysed after 7, 14 and 21 days of culture in monolayer or micromass, stimulated with or without insulin or ascorbic acid, normalised to *Ywhaz* housekeeping gene. Preliminary experiment performed once – time course data not repeated. Statistical analyses performed and shown in relation to time only. NR = No RNA obtained from samples because of cell death. ND = Not detected. C_T values can be found in Appendix Table S3.1

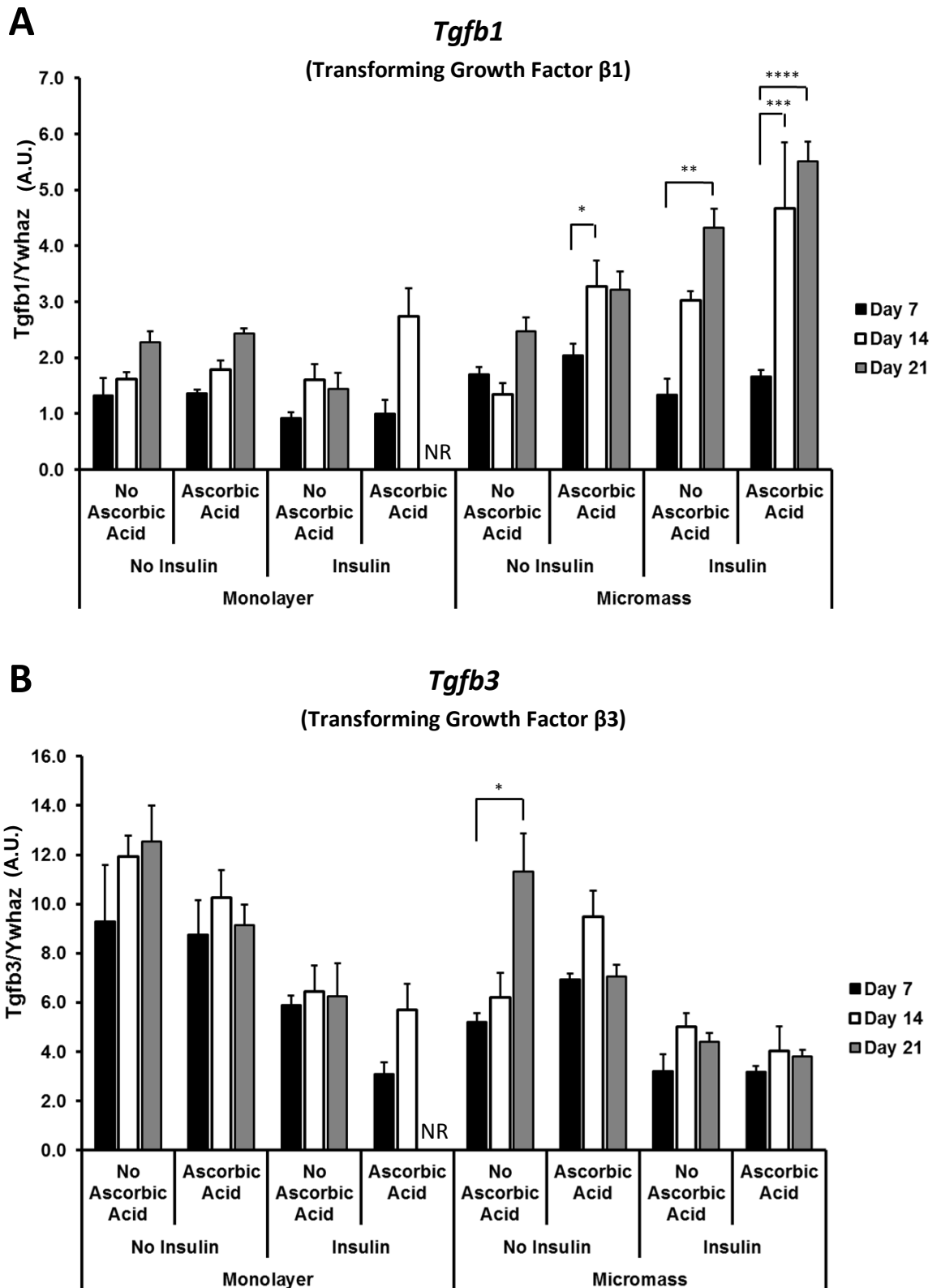


Figure 3.3 – Gene expression regulation of the TGF β family during ATDC5 differentiation. Steady-state mRNA levels of *Tgfb1* (A) and *Tgfb3* (B) were analysed after 7, 14 and 21 days of culture in monolayer or micromass, stimulated with or without insulin or ascorbic acid,, normalised to *Ywhaz* housekeeping gene. Preliminary experiment performed once – time course data not repeated. Statistical analyses performed and shown in relation to time only. NR = No RNA obtained from samples because of cell death. C_T values can be found in Appendix Table S3.2

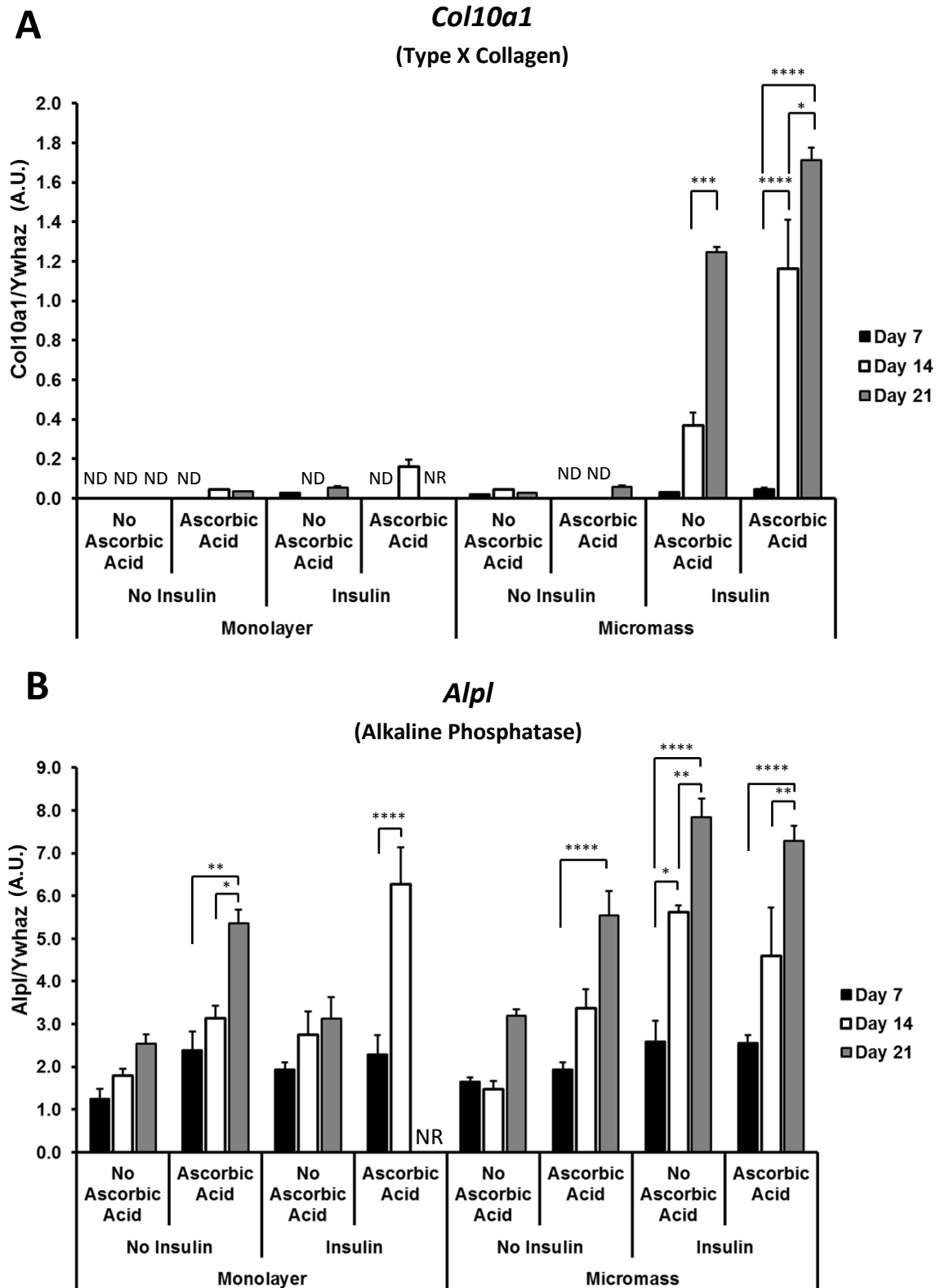


Figure 3.4 – Gene expression regulation of hypertrophic markers during ATDC5 differentiation. Steady-state mRNA levels of *Col10a1* (A) and *Alpl* (B) were analysed after 7, 14 and 21 days of culture in monolayer or micromass, stimulated with or without insulin or ascorbic acid, normalised to *Ywhaz* housekeeping gene. Preliminary experiment performed once – time course data not repeated. Statistical analyses performed and shown in relation to time only. NR = No RNA obtained from samples because of cell death. ND = not detected. C_T values can be found in Appendix Table S3.3

Runx2
(Runt-related Transcription Factor 2)

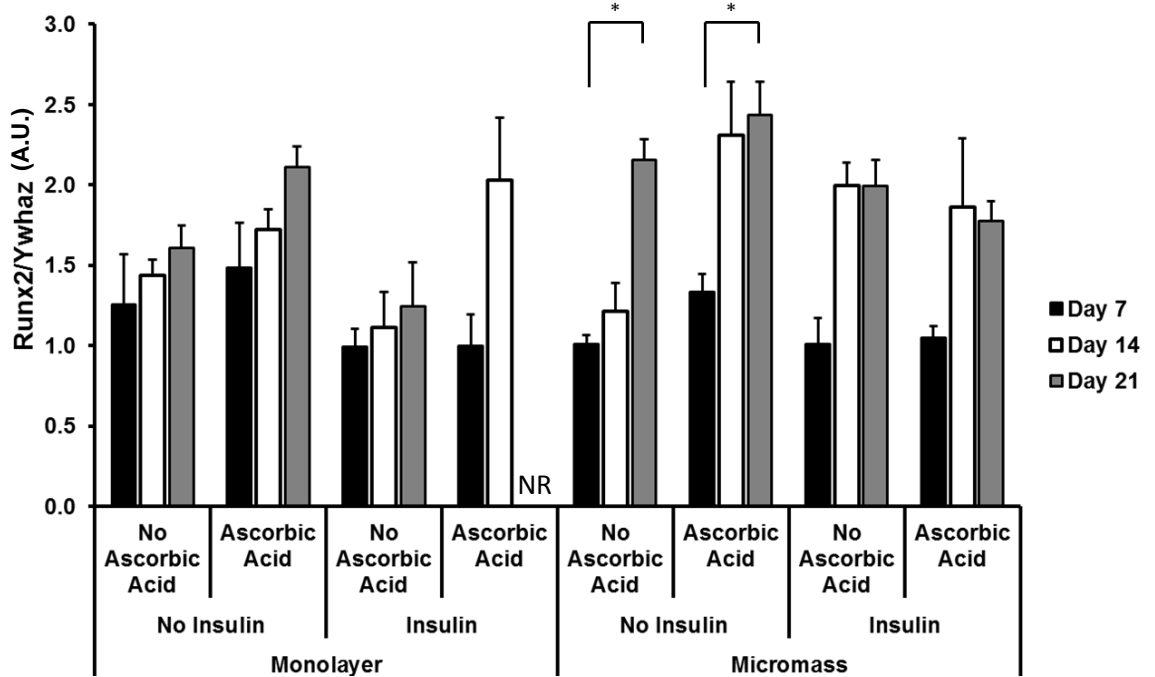


Figure 3.5 – Gene expression regulation of hypertrophic transcription factor Runx2 during ATDC5 differentiation. Steady-state mRNA levels of *Runx2* were analysed after 7, 14 and 21 days of culture, in monolayer or micromass, stimulated with or without insulin or ascorbic acid, normalised to *Ywhaz* housekeeping gene. Preliminary experiment performed once – time course data not repeated. Statistical analyses performed and shown in relation to time only. NR = No RNA obtained from samples because of cell death. C_T values can be found in Appendix Table S3.4

3.2.3 Morphological differences and visual observations between different ATDC5 culturing conditions

Changes in cell morphology were observed during the 14 day culture period of non-induced ATDC5 cells cultured in monolayer or micromass compared to chondrogenic induction with insulin (insulin-induced) and stimulated with or without ascorbic acid for the same time period (see section 2.1.2).

In monolayer cultures, non-induced cells were flat and in a confluent sheet, which did not seem to change upon addition of ascorbic acid (Figure 3.6 A-B). Upon insulin induction, cells became smaller, rounder and more condensed, forming aggregates termed cartilage-like nodules (Figure 3.7), which were surrounded by larger, non-aggregating cells, suggesting a mixed population of cell morphologies. This was regardless of the stimulation with or without ascorbic acid as seen by the lack of differences seen between Figures 3.6 C and D which display regions absent of these aggregates. However, these aggregates were numerous when stimulated with ascorbic acid when observed at lower magnifications or with the naked eye.

In non-induced micromass cultures, after 14 days, cells were flat and resembled monolayer cultures in appearance under the microscope (Figure 3.6 E-F). The central micromass in non-induced cultures became hard to see with naked eye with time, but was slightly more evident with addition of ascorbic acid. In contrast, insulin-induced micromass cultures were very evident by the naked eye. Cells were very condensed across the entirety of the central micromass (Figure 3.6 G-H) indicating a more uniform population of differentiated cells compared to insulin-induced monolayer cultures. Finally, addition of ascorbic acid had no discernable effect on cell morphology in insulin-induced micromasses, although the vast majority of cells are largely obscured by the sheer density of the produced matrix when cultures had been treated with insulin (Figure 3.6 G-H).

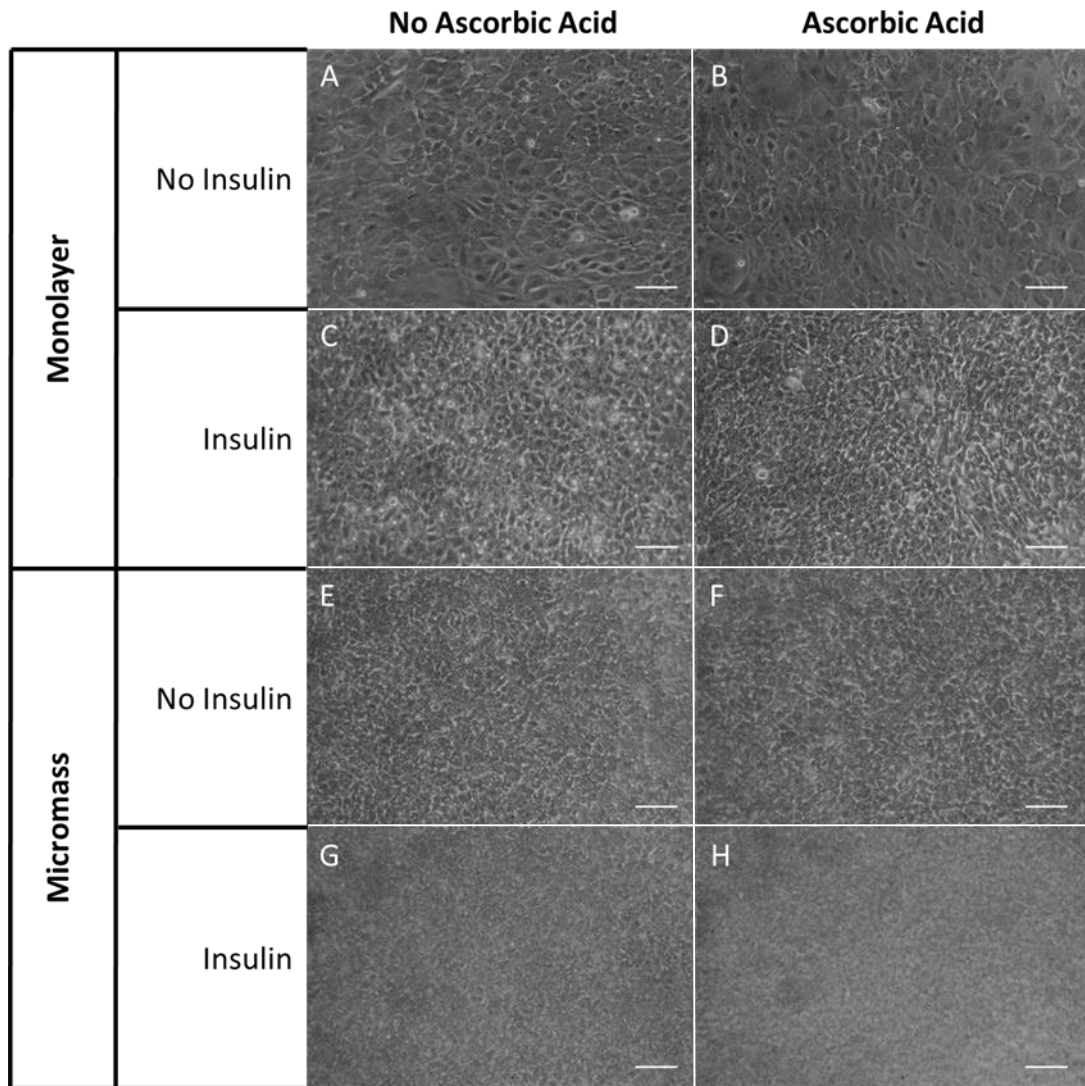


Figure 3.6 – Morphological changes during ATDC5 differentiation. ATDC5 cells were grown for 14 days in monolayer or micromass culture, stimulated with or without insulin (to induce differentiation) and stimulated with or without ascorbic acid. Images were taken at random locations within the wells using a phase contrast microscope at 10x mag. No differences are observed at this magnification between stimulation with or without ascorbic acid. Cartilage-like nodules are not visible in the monolayer images (please see Figure 3.7 for an example at the same magnification to highlight the feature). Images of experiment taken once but observations made >5 times. Scale bar = 100 μ m



Figure 3.7 – Cartilage-like nodule of ATDC5 cells. Aggregates formed in insulin-induced ATDC5 cells culture in monolayer, surrounded by non-aggregating cells. Image taken after 14 days induction by phase contrast microscopy at 10x magnification. Image taken from same experiment as in Figure 3.6 at the same magnification and resolution, but focussing directly on a cartilage-like nodule not visible in Figure 3.6. Scale bar = 100 μ m

3.2.4 Ascorbic Acid enhances proteoglycan deposition in both monolayer and micromass cultures

Fixed cultures of ATDC5 cells grown for 14 days with and without insulin induction and ascorbic acid stimulation were stained with Alcian Blue to visualise proteoglycan deposition (see 2.3.1). Little staining was observed in monolayer cultures which were not induced to differentiate with insulin or stimulated with ascorbic acid (Figure 3.8 A). Little staining was also observed in non-induced micromass cultures (Figure 3.8 E), consistent with the morphological changes seen by phase contrast microscopy (Figure 3.6 E). This result suggests that micromass culture alone is not enough to stimulate chondrogenesis of ATDC5 cells.

Addition of ascorbic acid to both non-induced monolayer and micromass cultures resulted in slight staining with Alcian Blue (Figure 3.8 B+F), but this was not deemed significant upon release of the dye (Figure 3.9), indicating that ascorbic acid stimulation alone was unable to significantly induce proteoglycan deposition, and thus chondrogenesis.

Induction of chondrogenesis with insulin in monolayer cultures resulted in cartilage-like nodules that stained deeply with Alcian Blue (Figure 3.8 C), consistent with the original ATDC5 report (Atsumi, *et al.*, 1990). Large areas in these cultures which did not stain with Alcian Blue indicate areas of cells which presumably did not deposit proteoglycan, suggesting a mixed population was observed of differentiated and undifferentiated cells, consistent with the mixed cellular morphologies observed by phase contrast microscopy. Quantification of Alcian Blue staining by measuring the absorbance of the Alcian Blue, released from the cultures by guanidine hydrochloride, revealed a significant increase in staining with the addition of ascorbic acid to monolayer cultures (Figure 3.9), however, the heterogeneity of the cell population remained (Figure 3.8 D). In contrast, insulin-induced micromass cultures were homogeneously stained with Alcian Blue, suggesting a more uniform population of cells within it (Figure 3.8 G+H). Culture in micromass, regardless of the presence or absence of ascorbic acid, significantly increased Alcian Blue staining compared to their monolayer counterparts. Addition of ascorbic acid further increased the amount of Alcian Blue staining compared to insulin-induced micromass cultures (Figure 3.9) resulting in deeper staining of the central micromass, surrounded by a greater halo of stained matrix produced by migrated, differentiated cells (Figure 3.8 H).

These findings indicate that both culture in three-dimensional micromasses and stimulation of ascorbic acid can enhance insulin-induced differentiation of ATDC5 cells, but cannot significantly induce chondrogenesis without the addition of insulin after 14 days of culture.

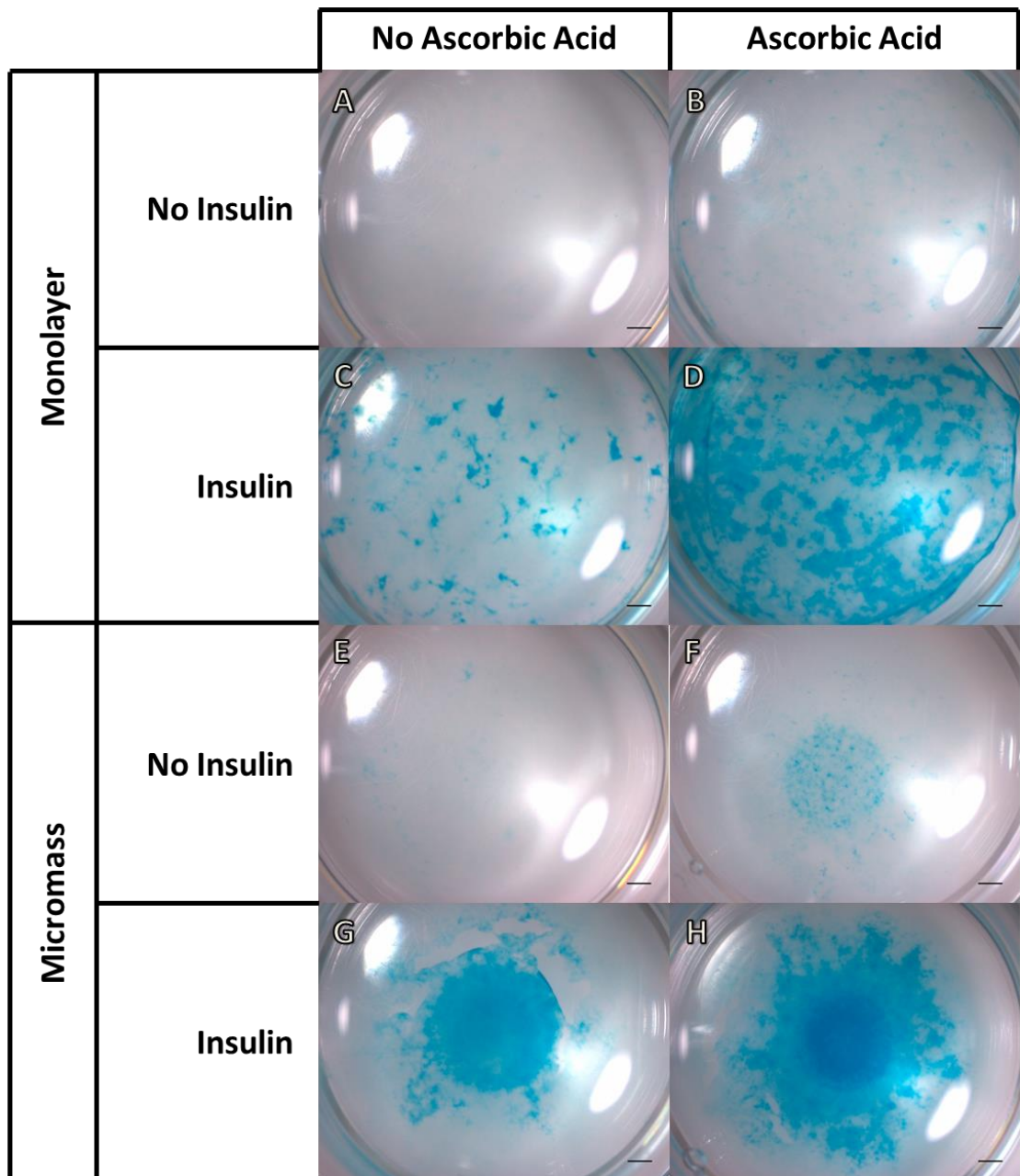


Figure 3.8 – Alcian Blue staining comparison during differentiation of ATDC5 cells after 14 days in monolayer and micromass stimulated with or without insulin or ascorbic acid. Samples were fixed in ice cold methanol before staining with Alcian Blue. Alcian Blue staining represents proteoglycan deposition, an indicator of chondrogenesis. Representative experiment from four repeats shown. Scale bar = 1 mm.

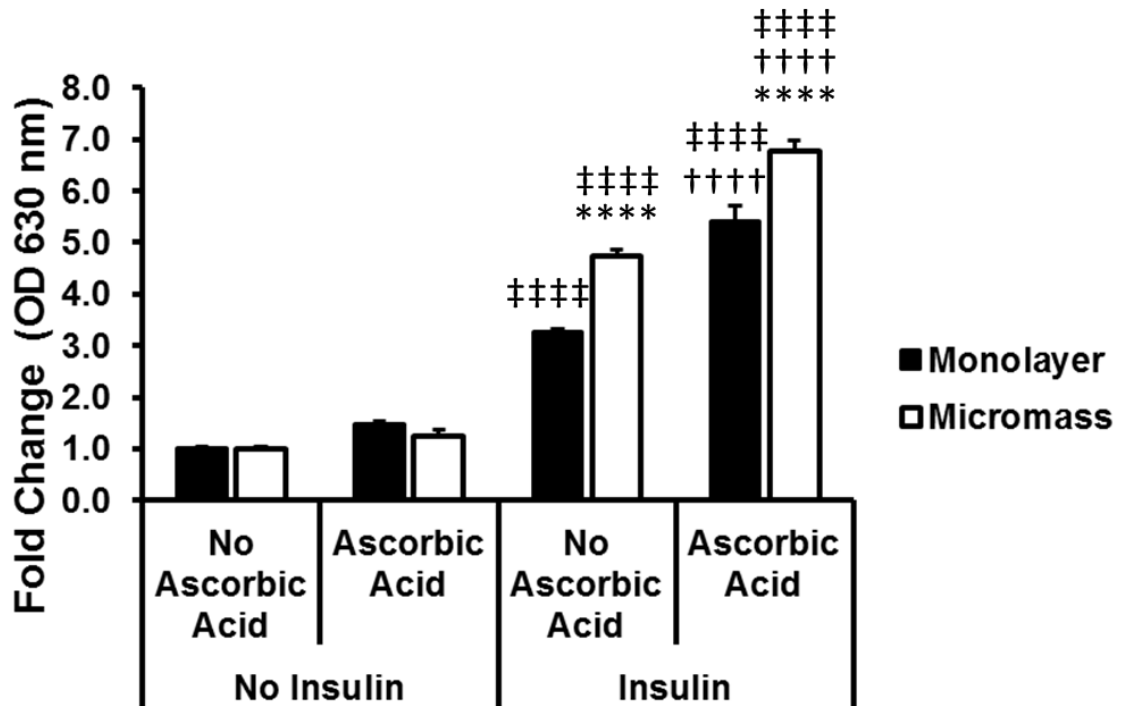


Figure 3.9 – Quantification of Alcian Blue staining. Alcian Blue staining (seen in Figure 3.8) was released by 8 M Guanidine Hydrochloride and read at 630 nm in a spectrophotometer. Due to different number of cells input at the start of the culture between monolayer and micromass conditions, results are shown as a fold change relative to either monolayers or micromasses not induced to differentiate with insulin or stimulated with ascorbic acid. Experiment performed four times showing highly consistent results among 3 experiments, with representative data shown.

- * = significant compared to Monolayer.
- † = significant compared to No Ascorbic Acid.
- ‡ = significant compared to No Insulin

3.2.5 The effect of micromass culture and ascorbic acid stimulation on gene expression of ATDC5 cells for 14 days

To identify the individual and synergistic effects of ATDC5 culture in micromass and stimulated with ascorbic acid, gene expression analysis was carried out after the chosen 14 day culture period on genes known to be related to chondrogenesis and cartilage phenotype. This experiment was repeated 3 times and the most representative example of each gene shown.

3.2.5.1 Chondrogenesis/Articular Differentiation

Col2a1 expression was significantly increased after 14 days of culture using the traditional culturing method, as expected. This was significantly increased upon induction with insulin when put into micromass culture, and even further increased when combined with ascorbic acid stimulation (Figure 3.10 A). Without chondrogenic induction with insulin, *Frzb* was not expressed to appreciable levels consistently ($C_T \geq 35$). Upon insulin induction, *Frzb* was expressed, which was significantly increased in micromass culture when compared to monolayer culture, regardless of ascorbic acid stimulation (Figure 3.10 B). Conversely, an overall trend towards a reduction of *Grem1* (gremlin-1) expression was observed with increasing chondrogenesis with an additional decrease in expression due to micromass culture in non-induced cells (Figure 3.10 C). A significant increase in *Tgfb1* expression was seen upon the induction of chondrogenesis with insulin in micromass cultures in the presence of ascorbic acid compared to non-induced micromass cultures in the presence of ascorbic acid. In two of three experiments, addition of ascorbic acid also trended towards an increase in *Tgfb1* expression in insulin-induced micromass cultures compared to insulin-induced micromass cultures without ascorbic acid (Figure 3.10 D). *Tgfb1* expression in monolayer cultures was not consistent between three experiments and so not shown.

Levels of *Acan* mRNA, which encodes the core protein of aggrecan, could not be detected to any appreciable level ($C_T \geq 35$), along with *Wnt3a*, *Wnt5a*, *Dkk3* and *Col9a1* (type IX collagen), although known positive controls were not tested for these assays (data not shown).

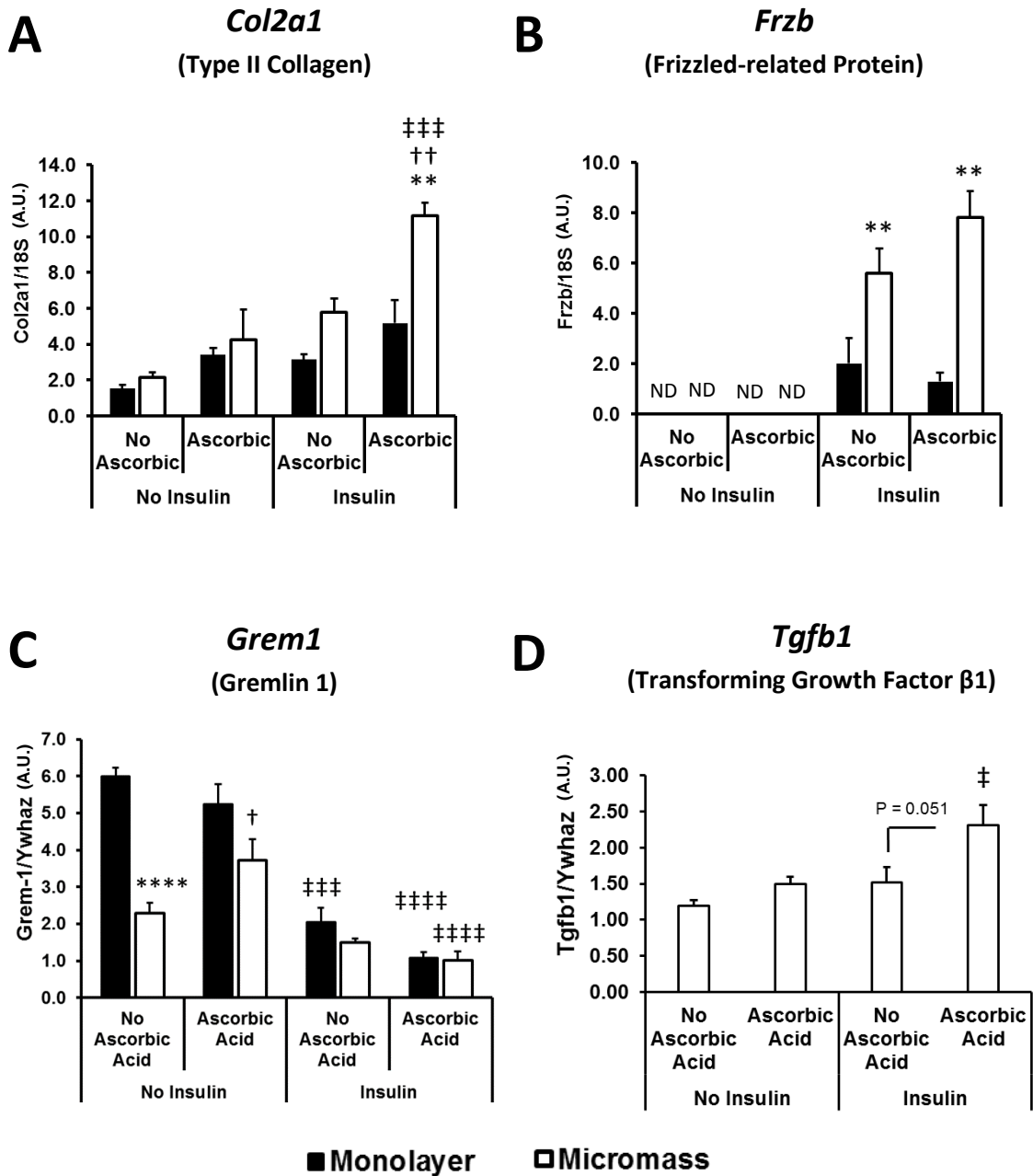


Figure 3.10 – Changes in expression of various chondrogenic/articular markers during ATDC5 chondrogenesis. Normalised steady-state mRNA expression levels of *Col2a1* (A), *Frzb* (B), *Grem1* (C) and *Tgfb1* (D) were measured after 14 days of culture in monolayer or micromass, stimulated with or without insulin or ascorbic acid. Experiment performed three times and representative experiments are shown. Only data for micromass cultures shown for *Tgfb1* due to inconsistent regulation in monolayer cultures. ND = not detected. C_T values may be found in Appendix Table S3.5

* = significant compared to Monolayer.
 † = significant compared to No Ascorbic Acid.
 ‡ = significant compared to No Insulin

3.2.5.2 Hypertrophic Differentiation/Mineralisation

In two out of three experiments, *Col10a1* expression was barely detected in non-induced cells, becoming expressed with insulin induction when combined with culture in micromass and/or stimulation with ascorbic acid, with a significant increase with the combination of micromass culture and ascorbic acid stimulation when compared to either micromass culture or ascorbic acid stimulation alone in insulin-induced cells (Figure 3.11 A). However, in one out of the three experiments, no *Col10a1* expression could be detected (data not shown).

Ddr2 expression was seen to be decreased upon insulin-induction of ascorbic acid-stimulated cells and was down-regulated in non-induced micromass cultures compared to non-induced monolayer cultures. Expression did not change in micromass cultures upon insulin induction or ascorbic acid stimulation (Figure 3.11 B).

Runx2, the major transcription factor driving hypertrophic differentiation, was not significantly regulated by any condition (Figure 3.11 C).

In two out of three experiments, *Alpl*, which encodes the liver/bone/kidney form of alkaline phosphatase, was significantly up-regulated upon insulin-induction of ascorbic acid-stimulated monolayer cells and micromass cultures in the absence of ascorbic acid. *Alpl* was also up-regulated in insulin-induced micromass cultures in the absence of ascorbic acid compared to monolayer and up-regulated in the presence of ascorbic acid in insulin-induced monolayer cells (Figure 3.11 D).

Tgfb3 was down-regulated upon insulin induction of both monolayer and micromass cultures. Micromass culture also significantly down-regulated *Tgfb3* expression in non-induced cells. Ascorbic acid stimulation did not significantly alter *Tgfb3* expression, although a clear trend towards down-regulation is seen with increasing differentiation (Figure 3.11 E).

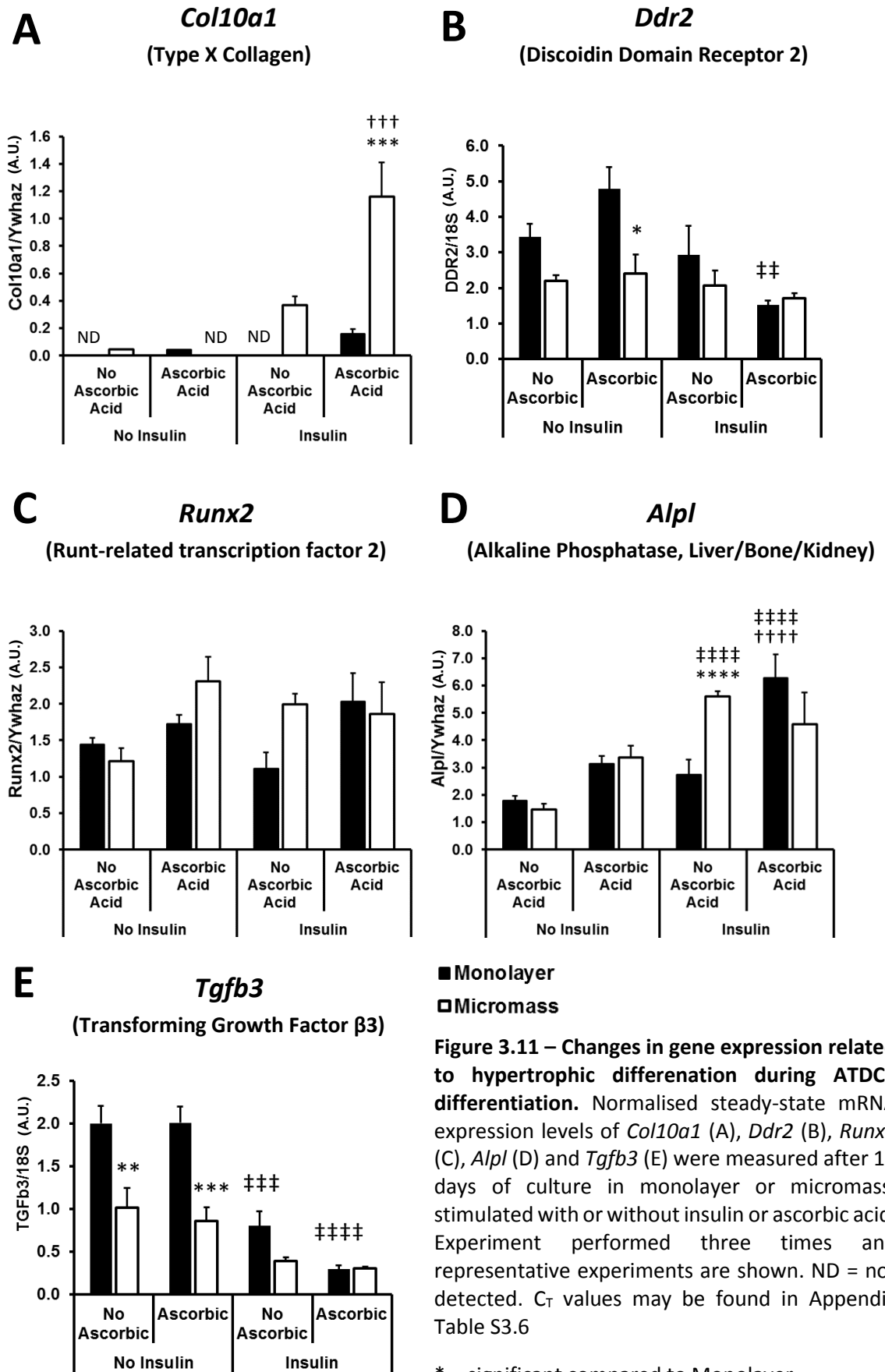


Figure 3.11 – Changes in gene expression related to hypertrophic differentiation during ATDC5 differentiation. Normalised steady-state mRNA expression levels of *Col10a1* (A), *Ddr2* (B), *Runx2* (C), *Alpl* (D) and *Tgfb3* (E) were measured after 14 days of culture in monolayer or micromass, stimulated with or without insulin or ascorbic acid. Experiment performed three times and representative experiments are shown. ND = not detected. C_T values may be found in Appendix Table S3.6

* = significant compared to Monolayer.
 † = significant compared to No Ascorbic Acid.
 ‡ = significant compared to No Insulin

3.2.5.3 CCN Growth Factors

Of the CCN family of growth factors, expression of *Cyr61* and *Ctgf* were readily detected. Expression of *Cyr61* was significantly decreased upon chondrogenic induction with insulin in monolayer cultures in the presence of ascorbic acid. A similar trend was seen in micromass cultures, although this did not reach significance. Culture in micromass had no effect on the regulation of *Cyr61* in comparison to monolayer (Figure 3.12 A).

In contrast, micromass culture significantly down-regulated *Ctgf* expression in non-induced cells (Figure 3.12 B). *Ctgf* expression was also down-regulated upon insulin induction of monolayer cultures. The reduced levels of *Ctgf* expression in micromass cultures were not modulated by insulin induction or ascorbic acid stimulation. Interestingly, ascorbic acid stimulation significantly up-regulated *Ctgf* expression in non-induced monolayer cells (Figure 3.12 B). Expression of *Nov*, *Wisp1* and *Wisp2* were not consistent across experiments. *Wisp3* was not detected in any experiment (data not shown).

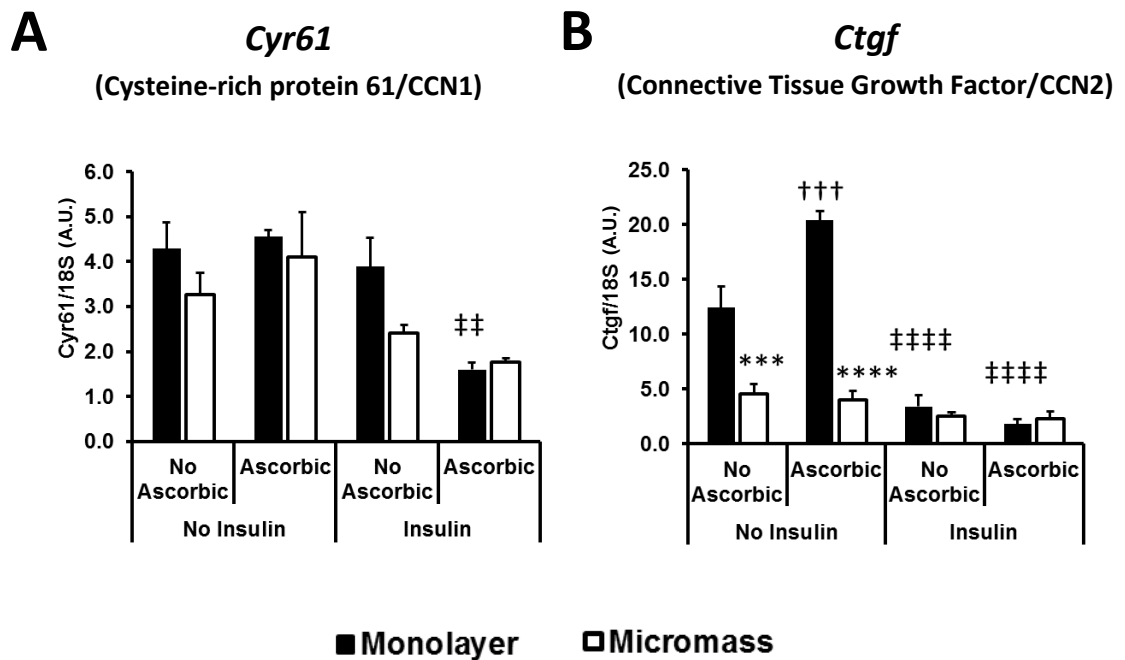


Figure 3.12 – Changes in CCN gene expression during ATDC5 differentiation. Normalised steady-state mRNA expression levels of *Cyr61* (A) and *Ctgf* (B) were measured after 14 days of culture in monolayer or micromass, stimulated with or without insulin or ascorbic acid. Experiment performed three times and representative experiments are shown. C_T values may be found in Appendix Table S3.7

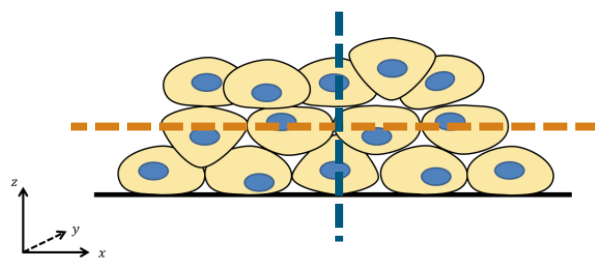
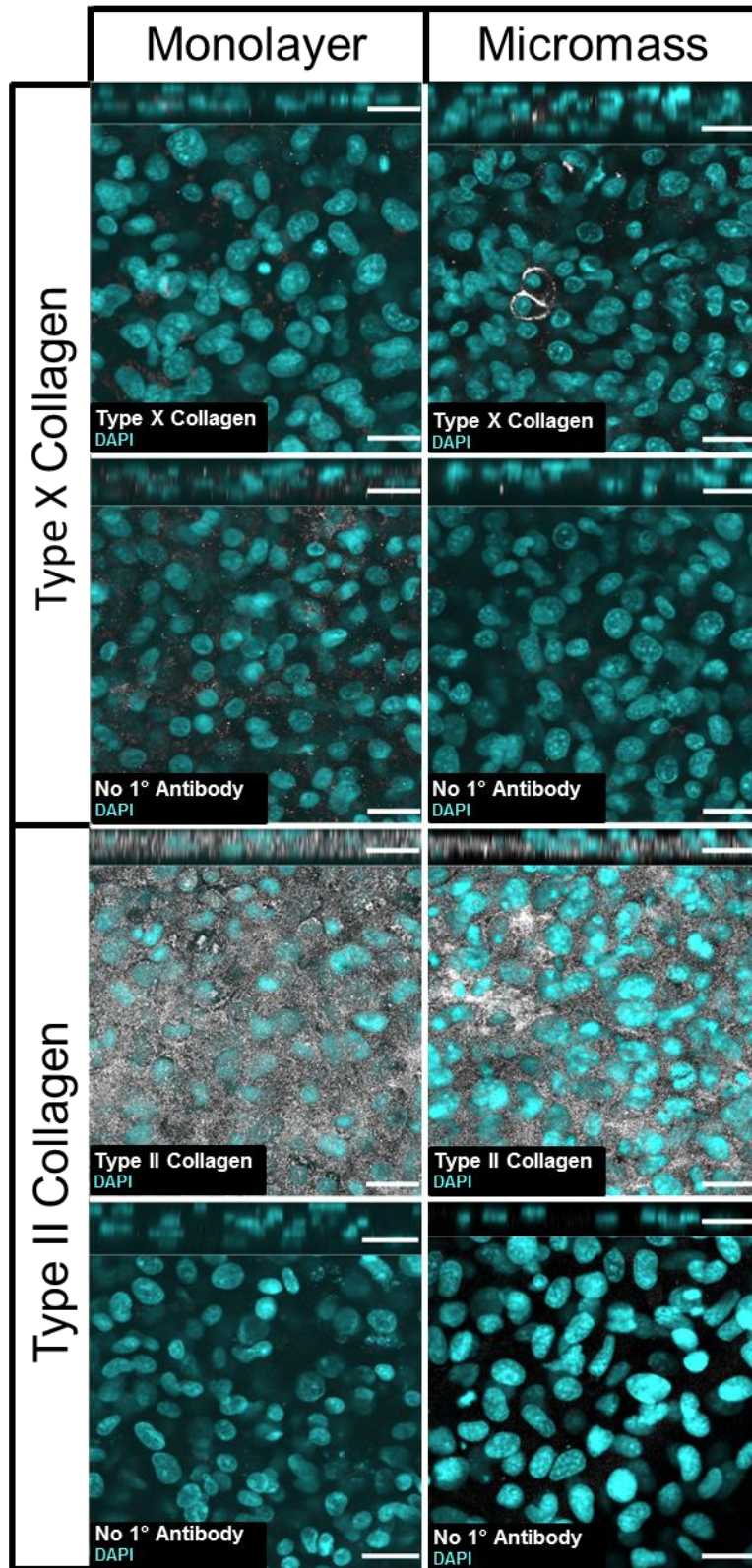
* = significant compared to Monolayer.
 † = significant compared to No Ascorbic Acid.
 ‡ = significant compared to No Insulin

3.2.6 Type X Collagen is immunolocalised to a restricted region within the centre of micromasses

Despite an increase in the articular marker *Frzb*, *Col10a1* mRNA expression, a hypertrophic marker, was also increased with increasing chondrogenesis. To elucidate whether the majority of the culture was undergoing hypertrophic differentiation or whether this was restricted to particular cells/regions, type X collagen protein expression was explored by immunocytochemistry alongside type II collagen expression on fixed cells that had been cultured using the same conditions described above. In insulin-induced monolayer and micromass cultures stimulated with ascorbic acid, very little type X collagen protein was detected, and only in one of two experiments. Detected type X collagen protein was largely found to be restricted to within the centre of the micromass, which mainly appeared to be localised close to possibly the cell surface, although no cell surface or PCM marker was used to confirm this (Figure 3.13). Intriguingly, no type X collagen positive “rings” were found in monolayer cultures (Figure 3.14). Although *Col10a1* mRNA levels increased with increasing chondrogenesis, these results suggest little hypertrophic differentiation.

In contrast to type X collagen, type II collagen protein was highly expressed in the interstitial matrix throughout the entirety of the cartilage-like nodules in monolayer culture and the micromass (Figure 3.13). Interestingly, culture in monolayer gave rise to a higher average fluorescence intensity of type II collagen compared to micromass culture (Figure 3.15). However, this is based from one experiment with only two fields of view from one culture per condition. Although a second experiment was performed, quantifiable analysis cannot be carried as some samples cannot be normalised due to a lack of no primary control as they were destroyed accidentally during handling during the staining process due to their delicate nature. As such, further repeats with additional fields of view per well and additional wells per condition are necessary to confirm this finding statistically.

Figure 3.13 – Optical sections of differentiated monolayer and micromass cultures immunostained for Type II Collagen and Type X Collagen. Cells were differentiated with insulin in the presence of ascorbic acid for 14 days in monolayer or micromass culture. Optical sections were taken using laser confocal microscopy for either Type II Collagen or Type X Collagen (both white). Nuclei were stained using DAPI (cyan). Monolayer images shown represent cartilage-like nodule. Cartoon representation of micromass highlights the location of the sections shown. Orange = cross section. Blue = sagittal section derived computationally from multiple images in the xy plane along the z -axis. N=2. Type X Collagen detected in only one experiment. Scale = 30 μm .



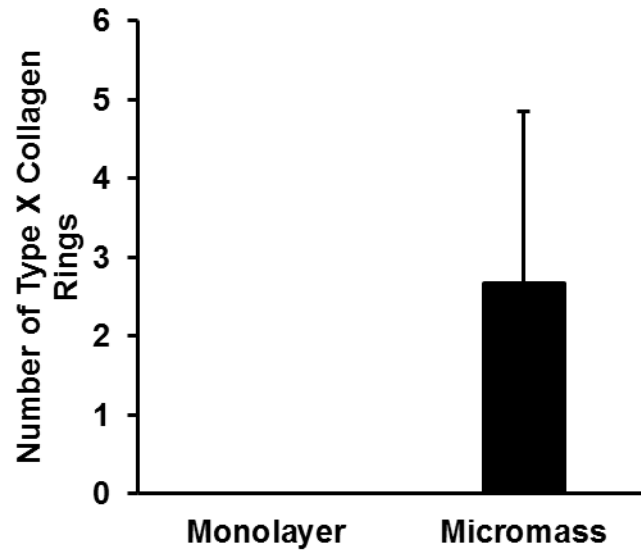


Figure 3.14 – Number of complete or partial Type X Collagen “rings”. ATDC5 cells were differentiated with insulin and stimulated with ascorbic acid for 14 days in monolayer or micromass culture and immunostained for Type X Collagen. Positive staining was detected throughout the culture by confocal microscopy, creating z-stacks with images 2 μm apart. Experiment performed twice with Type X Collagen detected in only experiment. Results shown are the average number of Type X Collagen-positive rings in one experiment for one well with two or three fields of view for monolayer and micromass respectively.

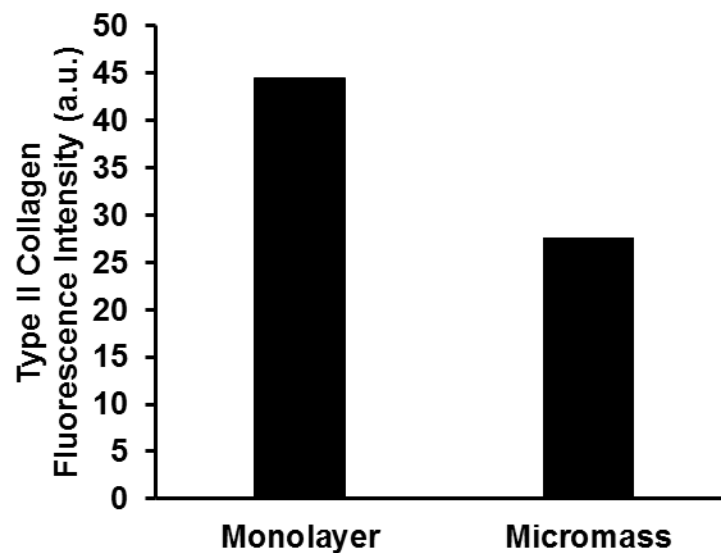


Figure 3.15 – Average type II collagen fluorescence intensity of ATDC5 cells differentiated in monolayer and micromass. Fluorescence intensity was calculated using ImageJ per slice of each z-stack. Due to the different number of slices between images, the fluorescence intensity of each slice were added together and divided by the number of slices, normalised to the intensities of the no-primary controls. Results are derived from two fields of view from one culture per condition. Two experiments performed with results from one shown coinciding with the experiment analysed in Figures 3.13 and 3.14.

3.2.7 Confirmation of hypertrophic gene expression via western blot

Western blot analysis was used to confirm whether patterns of gene expression of hypertrophy-related genes were also true at the protein level to identify the state of hypertrophic differentiation in this ATDC5 model.

DDR2 protein was found to be consistently decreased with increasing chondrogenesis (Figure 3.16), in contrast to the mRNA level which remained unchanged in micromass cultures (Figure 3.11 B). Expression of RUNX2 protein remained largely unchanged (Figure 3.16), although in one of three experiments, a clear decrease was seen in a similar fashion to DDR2 expression. On the other hand, WNT5A, known to inhibit hypertrophic differentiation (Bradley & Drissi, 2010), was increased upon chondrogenic induction with insulin (Figure 3.17), although this was only tested once.

Together, this suggests that with increasing chondrogenesis, hypertrophic differentiation is inhibited or limited.

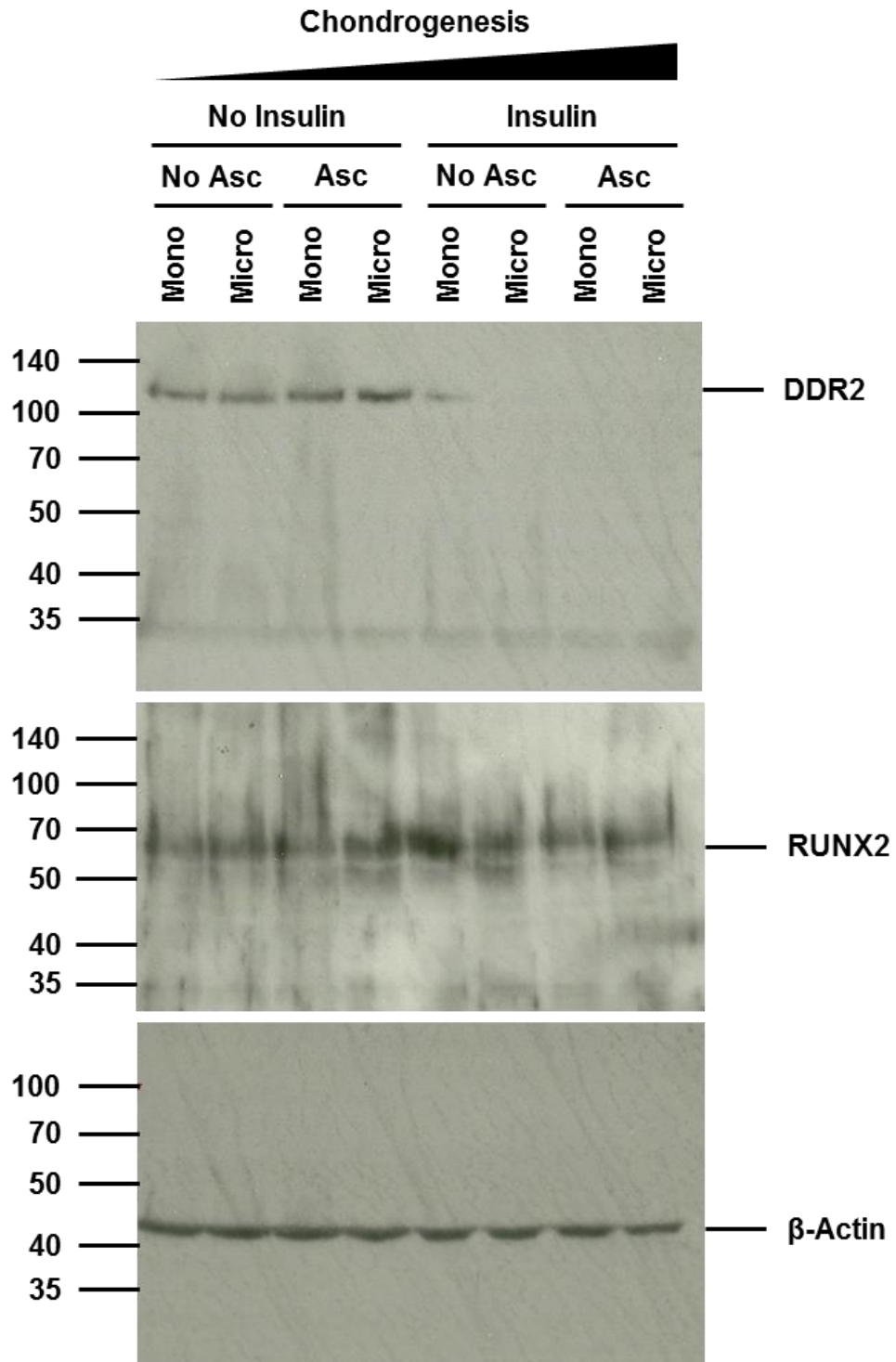


Figure 3.16 – DDR2 and Runx2 protein expression decrease with increasing chondrogenesis after 14 days of culture in monolayer or micromass, stimulated with or without insulin or ascorbic acid. Equal loading of protein for western blot was confirmed by probing for β -Actin, shown to be stably expressed in this culture system at the mRNA level. Predicted M_r DDR2 96.5 kDa; Runx2 57.43 kDa (isoform 1), 55.9 kDa (isoform 2), 49.47 kDa (isoform 3), 45.59 kDa (isoform 4); β -Actin 41.74 kDa, based on amino acid sequence, not including any post-translational modifications. Western blot performed three times using three different samples obtained from two experimental repeats. Mono = monolayer. Micro = micromass. Asc = ascorbic acid.

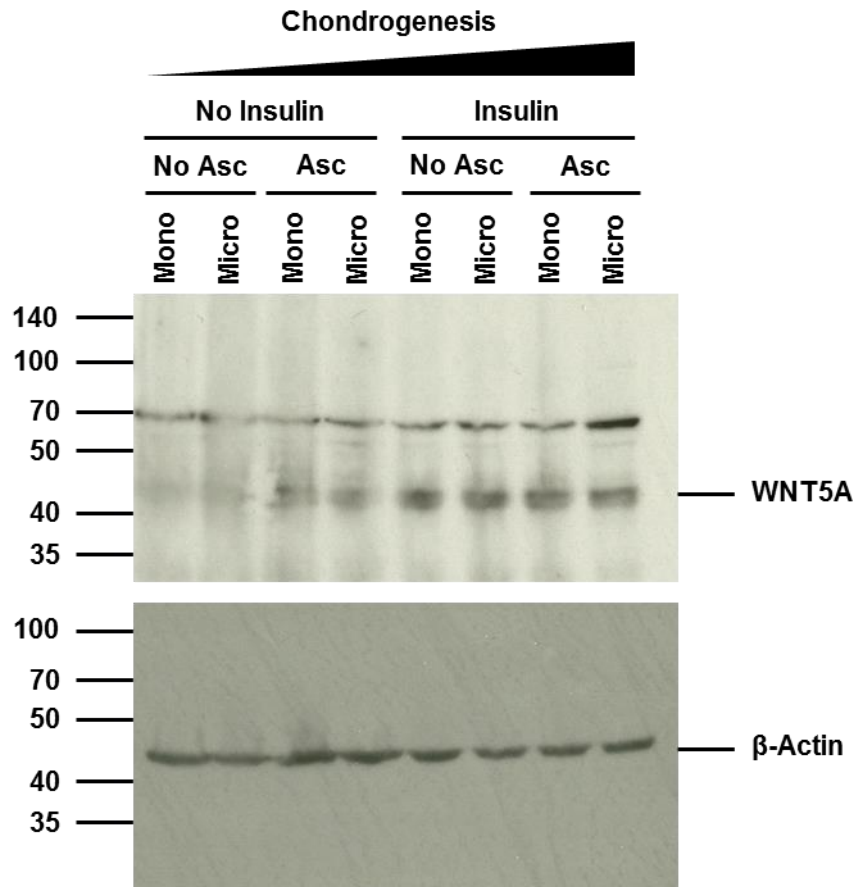


Figure 3.17 – WNT5A expression increases during chondrogenesis after 14 days of culture in monolayer or micromass, stimulated with or without insulin or ascorbic acid. Equal loading of protein for western blot was confirmed by probing for β -Actin, shown to be stably expressed in this culture system at the mRNA level. Predicted M_r endogenous mouse WNT5A = 42.35 kDa (isoform 1) or 40.89 kDa (isoform 2); β -Actin 41.74 kDa, based on amino acid sequence, not including any post-translational modifications. Experiment performed once. Mono = monolayer. Micro = micromass. Asc = ascorbic acid.

3.3 Discussion

3.3.1 Chondrogenic differentiation of ATDC5 cells over time

Expression levels of *Col10a1* and *Alpl* (alkaline phosphatase), two genes well characterised to be involved in the hypertrophic stages of chondrogenesis and endochondral ossification, were increased with respect to time in micromass cultures (Figure 3.4). Conversely, expression of *Col2a1*, *Tgfb1* and *Frzb* were significantly up-regulated over time (Figure 3.2 and 3.3 A), three genes known to be involved in chondrogenesis and the articular phenotype. Therefore based on these data, the 14 day timepoint was chosen to conduct further experiments investigating ATDC5 differentiation, since hypertrophic differentiation was less advanced at this stage compared to the 21 day point, whilst still increasing chondrogenesis over the 7 day time point. Furthermore, since a goal was to investigate the impact of each factor in the different models (three-dimensional culture, insulin and ascorbic acid), not all comparisons would be able to be made at the 21 day timepoint as insulin-induced ATDC5 cells stimulated with ascorbic acid die from overgrowth and detach from the culture vessel.

3.3.2 Micromass culture enhances insulin-induced ATDC5 chondrogenesis

This study has shown enhanced chondrogenesis in ATDC5 cells cultured in micromass by the increase in *Col2a1* expression (Figure 3.10 A) and proteoglycan deposition (Figure 3.9), which was more homogenous compared to monolayer cultures (Figure 3.8), suggesting a more uniform population of differentiated cells compared to large areas of undifferentiated cells in monolayer cultures. Although ATDC5 cells have been cultured in micromass previously (Lodewyckx, *et al.*, 2012; Sun & Beier, 2014), this appears to be the first time the beneficial effects of micromass differentiation have been directly compared to monolayer differentiation. Micromass culture alone appears to be insufficient to induce maximal chondrogenesis in ATDC5 cells (Figure 3.5 E; 3.6; 3.7) unlike in chick limb bud cells which were used in the original micromass experiment (Ahrens, *et al.*, 1977).

3.3.3 Ascorbic Acid enhances ATDC5 chondrogenesis

The use of ascorbic acid in the culture of primary chondrocytes is well established to promote stable collagen structures. Ascorbic acid has also previously been used in the culture of ATDC5 cells, primarily in the induction of hypertrophic differentiation and mineralisation, whereby after 21 days, CO₂ is dropped from 5% to 3% and DMEM/F12 culture medium is replaced by α -MEM (Shukunami, *et al.*, 1997; Shukunami, *et al.*, 1998; Swingle, *et al.*, 2012), which contains ascorbic acid (Altaf, *et al.*, 2006). One study identified that ascorbic acid was capable of shortening the prechondrogenic

proliferation stage of ATDC5 cells from 21 days to 7 days when cells had been pre-stimulated with ascorbic acid (in the form of ascorbate 2-phosphate) for 7 days before chondrogenic induction with insulin for 21 days (Altaf, *et al.*, 2006). The effect of ascorbic acid on proliferation has also been seen in primary bovine chondrocytes, causing an increase in cell density and cell number (Hering, *et al.*, 1994). Although this was not directly tested in this thesis, ascorbic acid did increase cellular aggregation in the form of nodules, which appeared apparently larger and more numerous (Figure 3.8), which was also described by Altaf, *et al.* in pre-stimulated ATDC5 cells.

In addition, several studies have shown in chondrocytes that ascorbic acid can enhance levels of type II collagen mRNA and/or protein (Hajek & Solursh, 1977; Dozin, *et al.*, 1992; Altaf, *et al.*, 2006; Cigan, *et al.*, 2013) and proteoglycan expression/GAG content (Hering, *et al.*, 1994; Priddy, *et al.*, 2001; Altaf, *et al.*, 2006; Cigan, *et al.*, 2013), which was also seen in this thesis (Figures 3.6, 3.7 A), and could further enhance the already increased chondrogenic effect of micromass culture.

However, Ronzière, *et al.*, (2003) reported that whilst ascorbic acid increased *COL2A1* expression in bovine chondrocytes cultured on collagen sponge scaffolds, there was no change in matrix deposition of collagen or GAG content. On the other hand, Priddy, *et al.*, (2001) noted that whilst ascorbic acid increased GAG content in canine chondrocytes cultured in agarose gels, the effect on type II collagen as measured by immunohistochemistry, was minimal. However, this may be due to the hydroxyproline already present in the RPMI-1640 medium used, since hydroxyproline, which stabilises the collagen structure, is the product of the enzyme prolyl-hydroxylase, of which ascorbic acid is the co-factor. Therefore the addition of exogenous ascorbic acid may not have an additional effect over the hydroxyproline already present in the medium, suggesting the beneficial effect of ascorbic acid may be dependent on the culturing conditions.

Together, this indicates ascorbic acid is an important factor in enhancing chondrogenesis, and in particular in ATDC5 cells cultured in micromass.

3.3.4 Micromass culture and ascorbic acid stimulation inhibit hypertrophic differentiation and promote articular differentiation

Articular cartilage and growth plate cartilage (which undergoes hypertrophic differentiation) have different functions within the body and thus have two different phenotypes. Articular cartilage escapes the hypertrophic process in order to provide its protective effects on the joint from various forces, whereas growth plate cartilage undergoes hypertrophy during endochondral ossification in order to produce and elongate the bone. These phenotypic differences are therefore important to distinguish when studying cartilage to identify the biological relevance of the model.

qRT-PCR and protein analysis revealed that hypertrophic differentiation, which can be problematic in chondrogenesis cultures *in vitro*, whilst expression of chondrogenic or articular factors increased.

3.3.4.1 Type II Collagen and Type X Collagen

Expression of *Col10a1* was seen to be increased with increasing chondrogenesis in ATDC5 cells (Figure 3.11 A), which has previously been reported in ATDC5 cells induced to differentiate with both insulin and BMP-2 (Shibuya, *et al.*, 2013), and in ATDC5 micromass culture (Sun & Beier, 2014). However, little type X collagen protein was detected after 14 days of induction, and was primarily immunolocalised to the centre of the micromass, possibly in the pericellular region with some faint staining in the interstitial region (Figure 3.13). Co-localisation with other PCM components, such as type VI collagen or perlecan, would be needed to confirm type X collagen in the PCM of this culture, although type X collagen has been previously found to be localised to the pericellular region of chondrocytes (Morrison, *et al.*, 1996; Boos, *et al.*, 1997).

In comparison, type II collagen, which is characteristically decreased during hypertrophic differentiation (Weiss, *et al.*, 2010) was widespread throughout the micromass and cartilage-like nodules in monolayer culture in the interstitial ECM (Figure 3.13), and was significantly up-regulated by both micromass culture and ascorbic acid, which was further increased when combined together at the mRNA level (Figure 3.10 A).

3.3.4.2 *Frzb* and *Grem1*

Upon ATDC5 cell differentiation, *Frzb* expression was induced and was significantly up-regulated by micromass culture (Figure 3.10 B). *Frzb* has been previously identified as a marker of articular cartilage, which is highly expressed in articular cartilage, along with *Grem1* (gremlin 1), compared to growth plate cartilage (Leijten, *et al.*, 2012) and osteophytic cartilage (Gelse, *et al.*, 2012), suggesting results presented in this thesis may show articular differentiation in ATDC5 cells, which have commonly been used instead to model endochondral ossification when inducing hypertrophy.

Attempts at confirming FRZB expression at the protein level were made, however, reliable detection and its effects of the phosphorylated state of β -catenin (which would indicate either activation or inhibition of the canonical β -catenin-dependent WNT signalling pathway) using antibodies bought from Abcam could not be achieved by western blotting (data not shown).

Overexpression of *Frzb* in ATDC5 micromasses has been shown to significantly enhance the levels of the chondrogenic markers *Col2a1* and *Acan* (aggrecan), whilst silencing of *Frzb* inhibited chondrogenesis (Lodewyckx, *et al.*, 2012). Furthermore, stimulation of differentiating hBMSCs with FRZB down-regulated the hypertrophic markers *ALPL* and *COL10A1* and decreased mineralisation,

with the authors suggesting that FRZB acts as a natural brake on hypertrophic differentiation (Leijten, *et al.*, 2012).

Interestingly, this thesis showed that *Grem1* expression decreased with increasing chondrogenesis (Figure 3.10 C). However, although *Grem1* has been found to be highly expressed in articular cartilage, recombinant human Gremlin-1 has been found to inhibit chondrogenesis in chick embryos (Merino, *et al.*, 1999). It may therefore be interesting to examine how *Grem1* expression changes throughout the course of chondrogenesis.

3.3.4.3 CCN Growth Factors

3.3.4.3.1 *Cyr61*

With increasing chondrogenesis, a trend to a reduction in *Cyr61* expression was seen (Figure 3.12 A), in agreement with previous findings in hBMSCs, in which it was highly expressed prior to differentiation (Schütze, *et al.*, 2005). Treatment of mouse limb bud cells with CYR61/CCN1 has been shown to increase cell aggregation in suspension culture and micromasses (Wong, *et al.*, 1997), indicating a role in the early stages of chondrogenesis, which may explain the down-regulation in the most differentiated cultures (with ascorbic acid stimulation in insulin-induced cells), and not in less differentiated cells in monolayer without ascorbic acid stimulation (Figure 3.12 A). Additionally, *Cyr61*^{-/-} mice die early in development, making detailed skeletal analysis difficult, although no obvious skeletal phenotype was observed by the time of death (Mo, *et al.*, 2002).

3.3.4.3.2 *Ctgf*

Ctgf expression was found to be significantly decreased in differentiating monolayer cultures of ATDC5 cells (Figure 3.12 B). No effect was observed in differentiating micromass cultures, likely due to the already decreased expression of *Ctgf* as a result of micromass culture compared to undifferentiated monolayer cultures. This reduction in *Ctgf* expression with three-dimensional culture has previously been described in breast cancer cells irrespective of the nature of the three-dimensional culture (Barbolina, *et al.*, 2009). Interestingly, *Ctgf* expression has previously been reported to be increased in ATDC5 monolayer cultures that have been induced to differentiate with insulin for 14 days compared to earlier timepoints (Lafont, *et al.*, 2005b), although this was not compared to undifferentiated cells that had been grown for the same timeframe, as in this thesis.

CTGF/CCN2 involvement in hypertrophy has been well established and is strongly expressed in hypertrophic chondrocytes (Moritani, *et al.*, 2003; Huang, *et al.*, 2010), correlating with *Col10a1* expression over the timecourse of differentiation (Huang, *et al.*, 2010). CTGF/CCN2, via stimulation and overexpression, has been shown to increase type X collagen mRNA/protein expression in a

human chondrosarcoma cell line (Nakanishi, *et al.*, 2000), rabbit growth plate chondrocytes (Nishida, *et al.*, 2002) and rabbit auricular chondrocytes (Fujisawa, *et al.*, 2008), although interestingly not in rabbit articular chondrocytes (Nishida, *et al.*, 2002). Global knockout of *Ctgf* in mice results in perinatal lethality minutes after birth from respiratory troubles brought upon by severe skeletal abnormalities. In these mice, an enlarged and disorganised hypertrophic zone is observed, with a decrease in aggrecan and link protein. Despite an enlarged hypertrophic zone, *Ctgf*^{f/l} mice also have decreased amounts of VEGF in hypertrophic chondrocytes, another marker of hypertrophy that is important in growth plate angiogenesis (Ivkovic, *et al.*, 2003). Down-regulation of *Ctgf* with increasing chondrogenesis in ATDC5 cells may therefore suggest inhibition of hypertrophic differentiation in this system.

Additionally, CTGF/CCN2 has also been implicated in the initial condensation stages of chondrogenesis (Song, *et al.*, 2007a), perhaps explaining the significant increase in expression in cells which had been stimulated with ascorbic acid in the absence of insulin (Figure 3.12 B) which have shown signs of early chondrogenesis from increased *Col2a1* expression (Figure 3.10 A).

3.3.4.3.3 *Nov*, *Wisp1*, *Wisp2* and *Wisp3*

Expression patterns of *Nov*, *Wisp1* and *Wisp2* were not consistent across experiments, and *Wisp3* was not detected in any experiment. However, previous reports have shown *Nov* to be increased over time during insulin-induced chondrogenesis in ATDC5 cells, peaking at day 8 (Lafont, *et al.*, 2005b), and has been shown to be expressed in the prehypertrophic and hypertrophic zones of the murine embryonic growth plate (Yu, *et al.*, 2003). Gelse, *et al.*, (2012) found *Wisp3* to be highly expressed in articular cartilage compared to osteophytic cartilage, however, *Wisp3* could not be detected in this present system using two different sets of primer/probes, one designed using the Universal ProbeLibrary (Roche) and one designed by PrimerDesign LTD (Southampton, UK).

3.3.4.4 *Mmp13*

In addition to increasing type X collagen and decreasing Type II Collagen, hypertrophic differentiation is also defined (amongst other factors) by an increase in alkaline phosphatase activity, which produces PO₄³⁻ leading to mineralisation; MMP13 expression, involved in the remodelling of the matrix; and RUNX2 expression, which is the major transcription factor driving hypertrophic differentiation (Weiss, *et al.*, 2010; Studer, *et al.*, 2012). In this system, no *Mmp13* was detected across any condition, although it has been detected by others in ATDC5 cells at similar time points in differentiating monolayer cultures (Wang, *et al.*, 2004), and has been shown to be enhanced by ascorbate stimulation in ATDC5 cells which were pre-stimulated for 7 days with ascorbate 2-phosphate before induction with insulin (Altaf, *et al.*, 2006). As confirmation of a

working primer/probe set used in this study, the primer/probe sequences used for *Mmp13* have previously been used successfully by another group in this department (personal communication).

3.3.4.5 *Alpl* (Alkaline Phosphatase)

On the otherhand, *Alpl*, which encodes the liver/bone/kidney isoform of alkaline phosphatase, was significantly increased by ascorbic acid in differentiating monolayer cultures, but was not regulated by ascorbic acid in differentiating micromass cultures, likely due to the significant increase by insulin in micromass cultures (Figure 3.11 D). However, further analysis would be needed to identify the effect of increased *Alpl* expression on mineralisation of ATDC5 ECM by measuring alkaline phosphatase activity, which has previously been detected in differentiating ATDC5 cells in monolayer (Mushtaq, *et al.*, 2002; Nakatani, *et al.*, 2007; Mitani, *et al.*, 2013).

3.3.4.6 TGF β

3.3.4.6.1 *Tgfb3*

With increasing chondrogenesis, a decreasing trend in the level of *Tgfb3* was observed, which was also significantly down-regulated by micromass culture in undifferentiated cells (Figure 3.11 E). The use of adding various isoforms of TGF β exogenously to stimulate chondrogenesis is widely reported, particularly with the use of TGF β 3 (Chowdhury, *et al.*, 2013; Song, *et al.*, 2013; Tay, *et al.*, 2014), including in ATDC5 cells (Tare, 2005; Zhai, *et al.*, 2013). *Tgfb3* has been shown to be down-regulated at the same timepoint (day 14) in ATDC5 cells by microarray analysis (Chen, *et al.*, 2005), becoming up-regulated in ATDC5 cells when induced to undergo hypertrophic differentiation (Han, *et al.*, 2008). Further to this, TGF β 3-mediated induction of hBMSCs, in addition with BMP6, has been shown to promote a more growth plate phenotype, with down-regulation of the articular markers *DKK1* (dickkopf 1), *FRZB* and *GREM1* (gremlin 1), and up-regulation of *LEF1* and *PANX3* (pannexin 3), which are up-regulated in growth plate cartilage compared to articular cartilage (Leijten, *et al.*, 2012).

3.3.4.6.2 *Tgfb1*

Tgfb1 expression was significantly increased by insulin induction in micromass cultures in the presence of ascorbic acid and trended towards increased expression by the addition of ascorbic acid in insulin-induced micromass cultures (Figure 3.10 D). TGF β 1-mediated induction of chondrogenesis has been reported to result in significantly less matrix mineralisation compared to TGF β 3-mediated chondrogenic induction of hBMSCs (Cals, *et al.*, 2012) and has been shown to inhibit hypertrophic differentiation in rat epiphyseal chondrocytes (Ballock, *et al.*, 1993).

The findings in this thesis correlate with these previous reports suggesting an inhibition of hypertrophy with decreasing *Tgfb3* and increase in *Tgfb1* expression.

3.3.4.7 RUNX2

No changes in *Runx2* expression were observed between 7, 14 and 21 days of culture in monolayer or micromass in insulin-induced cells (Figure 3.5). At day 14, *Runx2* expression was not regulated by any culturing condition, which was also confirmed at the protein level in two of three experiments (Figure 3.11 C), suggesting hypertrophic differentiation was not induced. Reports have previously shown *Runx2* expression increases with time in differentiating ATDC5 cells in monolayer culture by day 14 (Wigner, *et al.*, 2013), however, this study supplemented chondrogenic medium with β -glycerophosphate, a known inducer of matrix mineralisation (Farrell, *et al.*, 2011), which is typically added in media to induce osteogenesis of MSCs (Cho, *et al.*, 2014; Gawronska-Kozak, 2014; Peng, *et al.*, 2014).

RUNX2 is a transcription factor, strongly expressed in hypertrophic cartilage (Higashikawa, *et al.*, 2009) that regulates transcription of various hypertrophy-related genes, including *Mmp13* (Boumah, *et al.*, 2009; Shimizu, *et al.*, 2010) and *Col10a1* (Takeda, *et al.*, 2001; Higashikawa, *et al.*, 2009). As such, it would be interesting to immunolocalise its expression to see whether RUNX2 translocates to the nuclei of the few type X collagen-positive cells or in any other cells in the differentiated conditions. This would indicate activation of RUNX2 which may promote expression of various hypertrophy-related genes and may give a clearer indication of any potential further (pre)hypertrophic regions within the three-dimensional cultures, which appeared to be minimal and restricted according to the type X collagen staining.

3.3.4.8 DDR2

DDR2 is a receptor tyrosine kinase that preferentially binds type II collagen which can stimulate hypertrophic differentiation in response to DDR2 ligation (Pulsatelli, *et al.*, 2013). Such an interaction is normally prevented by an intact PCM (Xu, *et al.*, 2011). This thesis has shown that at the mRNA level, *Ddr2* expression is down-regulated in monolayer cultures when induced with insulin in the presence of ascorbic acid. No changes were observed due to insulin or ascorbic acid due to the already decreased levels in micromass culture (Figure 3.11 B). At the protein level, DDR2 was down-regulated with increasing chondrogenesis (Figure 3.16). *Ddr2* mRNA expression has previously been shown to be very slightly up-regulated at day 14 in ATDC5 monolayer cultures compared to earlier timepoints (Zhang, *et al.*, 2011). However, this was not compared to ATDC5 cells that had been maintained undifferentiated for the same time period, as in this thesis.

Knockdown of *Ddr2* in ATDC5 cells has been shown to decrease mRNA expression of *Runx2* (Kawai, *et al.*, 2012) and inhibit RUNX2 protein activation and binding to DNA, leading to a decrease *Col10a1* expression (Zhang, *et al.*, 2011). Additionally, overexpression of *DDR2* has been shown to increase *MMP13* expression in human OA chondrocytes (Xu, *et al.*, 2005), which was not detected in this study, further suggesting inhibition of hypertrophy in micromass and ascorbic acid-stimulated ATDC5 cultures.

3.3.4.9 WNT5A

At the protein level, WNT5A was observed to be increased upon insulin induction of ATDC5 cells (Figure 3.17). Studies have shown that stimulation of micromass cultures with exogenous WNT5A, or overexpression of WNT5A, can increase chondrogenesis in both chick and mouse limb cells (Church, *et al.*, 2002; Bradley & Drissi, 2010). Additionally, WNT5A has been shown to inhibit hypertrophic differentiation via NF- κ B-mediated inhibition of RUNX2 (Hartmann & Tabin, 2000; Bradley & Drissi, 2010). This increase in WNT5A upon insulin induction further suggests inhibition of hypertrophy. More detailed discussions on WNT5A can be found in Chapters 1, 4 and 5.

3.4 Summary

Many genes were regulated during the chondrogenesis of ATDC5 cells, briefly summarised in Table 3.1. Taken together, despite the increases in *Col10a1* and *Alpl* (alkaline phosphatase), the down-regulation of several hypertrophy-associated genes and proteins and the limited type X collagen that was detected suggest that hypertrophy was inhibited in this system by differentiating ATDC5 cells for 14 days with insulin with the combination of micromass culture and stimulation with ascorbic acid. High expression of *Frzb* and widespread type II collagen staining may suggest that this culture system instead generates a more articular cartilage-like phenotype. This is in contrast to many reports that use ATDC5 cells to model changes that occur during endochondral ossification and the use of ascorbic acid in ATDC5 mineralisation (Shukunami, *et al.*, 1997; Faith, *et al.*, 2012; Swingler, *et al.*, 2012; Miron, *et al.*, 2013) highlighting the diverse nature of ATDC5 cells and their usefulness in their adaptability to study different cartilage phenotypes.

Table 3.1 – Summary of gene regulatory changes with increasing chondrogenesis of ATDC5 cells cultured for 14 days in monolayer or micromass and stimulated with/without insulin and ascorbic acid using information from Figures 3.10-12. For more specific changes per condition tested, please see original individual figures given above.

Gene Association/Family	Up-regulated	Down-regulated	No Regulation
Chondrogenesis	<i>Col2a1</i> <i>Frzb</i> <i>Tgfb1</i>	<i>Grem1</i>	
Hypertrophy	<i>Col10a1</i> <i>Alpl</i>	<i>Ddr2</i> (monolayer) <i>Tgfb3</i>	<i>Ddr2</i> (micromass) <i>Runx2</i>
CCNs		<i>Cyr61</i> <i>Ctgf</i> (monolayer)	<i>Ctgf</i> (micromass)

Investigating WNT5A and cytokine signalling in ATDC5 cells

4.1 Introduction

4.1.1 WNT signalling in osteoarthritis and skeletal disease

WNT signalling is tightly implicated with the progression of osteoarthritis (see Chapter 1). As such, many members of the WNT signalling family, as well as known modulators of the WNT signalling pathway, are aberrantly expressed in osteoarthritic joints, including WNT3A (Nakamura, *et al.*, 2005), FRZB (Nakamura, *et al.*, 2005; Velasco, *et al.*, 2010) and WISP3 (Sen, *et al.*, 2004; Baker, *et al.*, 2012), reviewed in (Staines, *et al.*, 2012). Expression of WNT5A is also highly up-regulated in osteoarthritic cartilage compared to normal cartilage as seen by microarray (Karlsson, *et al.*, 2010; Thorfve, *et al.*, 2011), qRT-PCR and immunofluorescence (Thorfve, *et al.*, 2011). *WNT5A* expression has also been shown to be increased in knee OA osteoblasts but decreased in hip OA osteoblasts compared to hip fracture osteoblasts (Velasco, *et al.*, 2010). Furthermore, *Wnt5a*^{-/-} mice have a strong skeletal phenotype, exhibiting truncated limbs (Yamaguchi, *et al.*, 1999). Missense mutations in *WNT5A* have also been associated with Robinow syndrome, a form of dwarfism (Person, *et al.*, 2010).

Many studies have investigated WNT5A in a developmental context, identifying the role of WNT5A in promoting early stage chondrogenesis and inhibiting hypertrophic differentiation (Hartmann & Tabin, 2000; Church, *et al.*, 2002; Bradley & Drissi, 2010). However, little work has been reported on the mechanisms and potential role of WNT5A induction in cartilage pathophysiology. It has been reported that WNT5A is up-regulated in chondrocytes by IL-1 β stimulation via the NF- κ B pathway (Ge, *et al.*, 2011). Furthermore, WNT5A has been shown to be a potent inducer of matrix degradation in chick beak cartilage via up-regulation of various metalloproteinases, including *ADAMTS5* (Hosseini-Farahabadi, *et al.*, 2013), a major enzyme involved in the destruction of cartilage in osteoarthritis, discussed previously. However, the exact mechanisms and the impact on other signalling pathways in osteoarthritis remain to be elucidated.

4.1.2 Cytokine signalling in osteoarthritis

The involvement of inflammatory cytokines in the development of osteoarthritis is well documented. Interleukin (IL)-1 β , one of the key inflammatory cytokines in osteoarthritis, is elevated in osteoarthritic chondrocytes (Melchiorri, *et al.*, 1998) and is commonly used to model osteoarthritic-like changes *in vitro* (Clutterbuck, *et al.*, 2013; Yang, *et al.*, 2014; Zhang, *et al.*, 2014). The combination of IL-1 α and oncostatin M (OSM) is also used to the same effect to induce expression of a number of metalloproteinases, including *ADAMTS4* and *ADAMTS5* (Hui, *et al.*, 2001; Koshy, *et al.*, 2002; Milner, *et al.*, 2003; Baker, *et al.*, 2012). In 2012, Baker, *et al.*, reported IL-1 α

and OSM-induced expression of *ADAMTS5* was repressed by overexpression of *WISP3* (WNT1-inducible secreted protein 3) via the beta-catenin-dependent pathway. As previously mentioned, IL-1 β has also been shown to induce expression of *WNT5A* in rabbit chondrocytes (Ge, *et al.*, 2011) and increase *WNT5A* and its receptor *ROR2* expression during osteogenesis (Sonomoto, *et al.*, 2012). Together, this highlights growing evidence for the interplay between the cytokine and WNT signalling pathways, however, this interplay and its involvement in osteoarthritis is not fully understood.

4.1.3 Aims

It was hypothesised that *WNT5A* may regulate gene expression during osteoarthritis and that cytokine signalling may also regulate the WNT signalling pathway in ATDC5 cells.

To test this, a number of approaches were taken:

1. Stable clones of ATDC5 overexpressing *WNT5A* were generated and gene expression changes investigated.
2. Naïve, differentiated ATDC5 cells were stimulated with neat *WNT5A*-conditioned medium generated by transiently transfecting separate ATDC5 cells, and stimulated in combination with IL-1 α and OSM cytokines to induce osteoarthritic-like changes.
3. A mixture of candidate and unbiased studies were carried out via qRT-PCR and microarray analysis respectively to investigate gene regulation as a result of *WNT5A* and/or cytokine signalling.

4.2 Results

4.2.1 Generation of stable clones overexpressing WNT5A

Non-induced ATDC5 cells were transfected with human *WNT5A* tagged at the C-terminus with an in-frame FLAG tag for ease of detection and selected for based on resistance to Zeocin™. Several clones were eventually generated after two separate attempts at cloning from single cells, and were expanded in culture before confirming *WNT5A* protein expression, and the lack of *WNT5A* in cells transfected with the empty pcDNA4-FLAG vector only (hereafter referred to as Vector Only). Six clones were chosen for further analysis; three Vector Only clones and three *WNT5A* clones (Figure 4.1). For more information on the generation of the plasmids and the transfection/cloning process, please see sections 2.4 and 2.5.

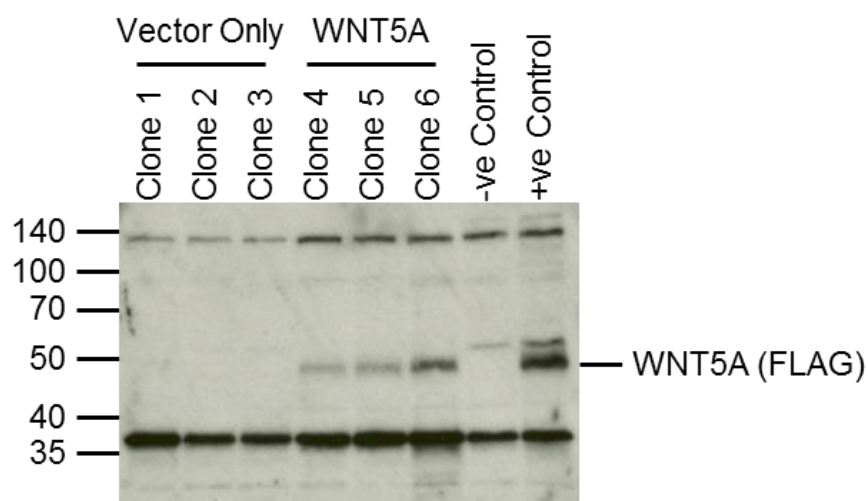


Figure 4.1 – Confirmation of WNT5A overexpressing clones. Cell lysates from stable ATDC5 clones overexpressing WNT5A or Vector Only control were examined for WNT5A expression using the anti-FLAG antibody. Protein lysates were taken from clones expanded in monolayer from single cells. Transiently transfected cells transfected were used as positive and negative controls. Predicted M_r WNT5A-FLAG = 44.99 kDa based on amino-acid sequence. N=2

4.2.2 Gene regulation in non-induced overexpressing WNT5A clones

Expression of candidate genes associated with WNT5A signalling and the chondrocytic phenotype were explored by qRT-PCR in non-induced clones plated in monolayer or micromass for four days. Three Vector Only clones and three WNT5A clones were used for the analysis and the experiment was performed once as a preliminary experiment. Results are expressed as the average of three separate WNT5A clones and three separate Vector Only clones, with results from individual clones displayed on the right-hand side.

Overexpression of WNT5A did not result in any regulation of its receptor, *Ror2* (Figure 4.2 A). Although clones were not induced to differentiate with insulin, low *Col2a1* expression was detected with C_T values averaging around 33 (Appendix Table S4.1). C_T values of *Col2a1* in WNT5A clones was detected largely above C_T 35, which is deemed not to be expressed, suggesting WNT5A overexpression may inhibit *Col2a1* expression (Figure 4.2 B). Expression of *Adamts4* and *Adamts5* were low, with C_T values close to 35 or above. No regulation of *Adamts4* was seen by WNT5A, although interestingly, *Adamts5* may be down-regulated by WNT5A which was not detected in most WNT5A clones (Figure 4.2 C-D). Neither *Runx2* nor *Ddr2*, two genes involved in hypertrophic differentiation, were regulated by WNT5A overexpression (Figure 4.2 E-F). *Grem1*, which is enriched in articular cartilage, was up-regulated by WNT5A, whilst *Alpl* (alkaline phosphatase), an enzyme involved in matrix mineralisation, was down-regulated by WNT5A (Figure 4.2 G-H). Of the CCN growth factor family, *Cyr61*, which encodes CYR61/CCN1, was up-regulated by WNT5A in both monolayer and micromass culture, whereas *Ctgf* (CTGF/CCN2) and *Nov* (NOV/CCN3) were not (Figure 4.2 I-K). A slight down-regulation of *Wisp1* (WISP1/CCN4) was seen in monolayer culture and of *Wisp2* (WISP2/CCN5) in micromass culture in WNT5A overexpressing clones compared to Vector Only (Figure 4.2 L-M). The final member of the CCN family, *Wisp3* (WISP3/CCN6) could not be detected (data not shown).

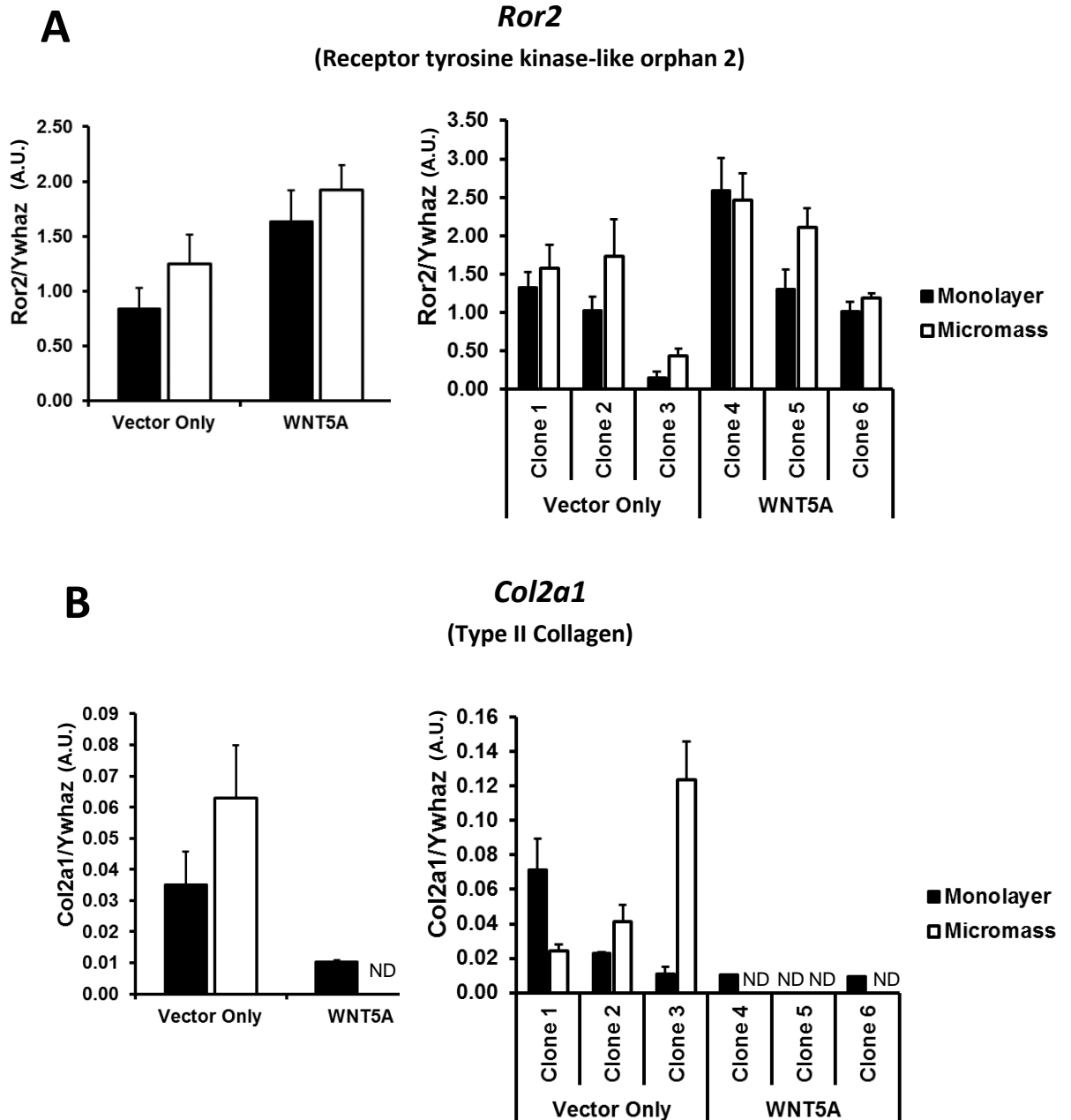


Figure 4.2 A-B – Gene regulation in stable WNT5A-overexpressing, non-induced ATDC5 clones. Steady-state mRNA expression levels of *Ror2* (A) and *Col2a1* (B) in WNT5A-overexpressing, non-induced ATDC5 clones cultured in monolayer or micromass for four days compared to Vector Only clones as measured by qRT-PCR. Left hand figure composed from averaging all three clones per condition shown in right-hand figure. C_T values can be found in Appendix, Table S4.1. Experiment performed once. ND = Not Detected

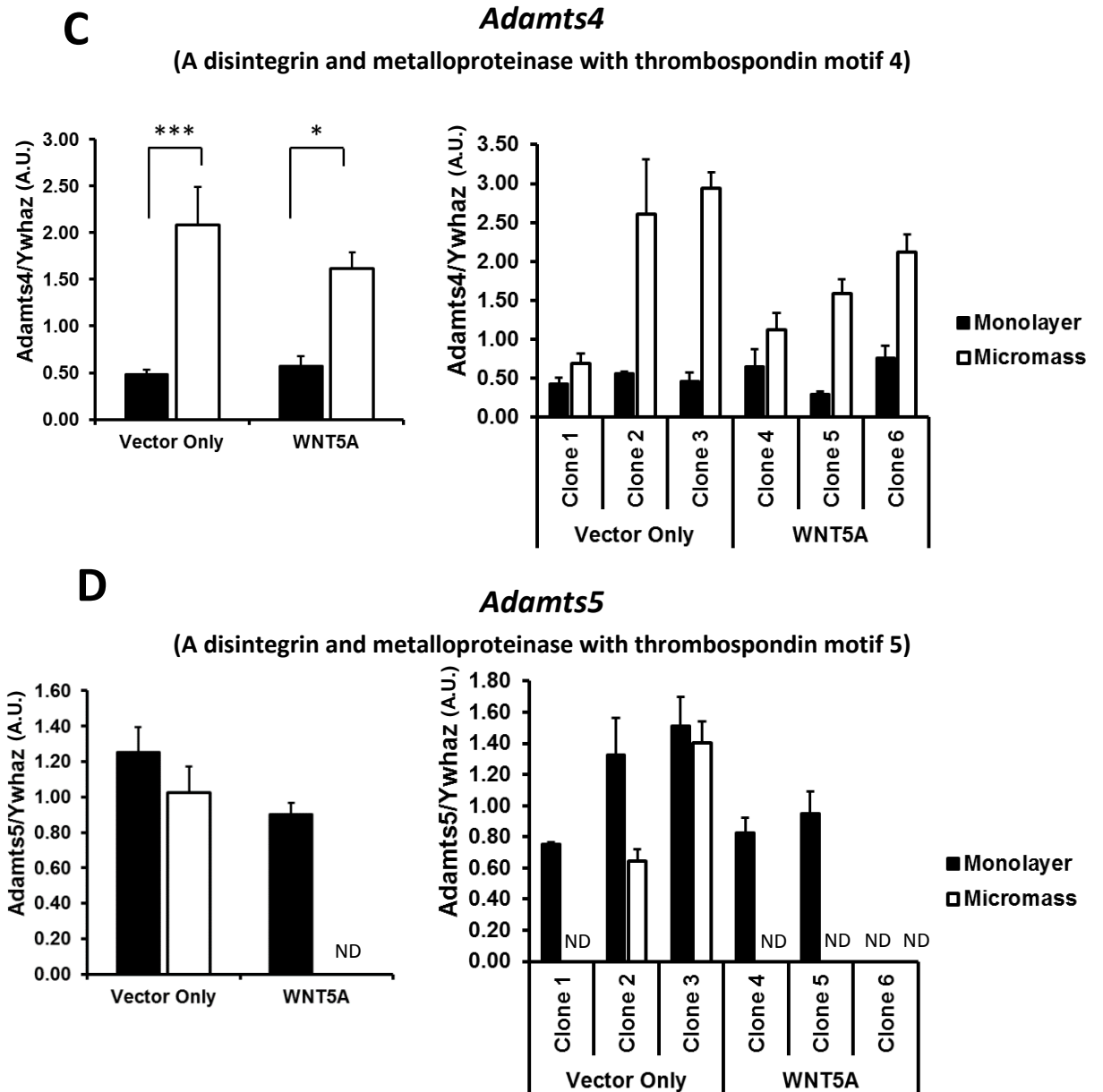


Figure 4.2 C-D – Gene regulation in stable WNT5A-overexpressing, non-induced ATDC5 clones. Steady-state mRNA expression levels of *Adamts4* (C) and *Adamts5* (D) in WNT5A-overexpressing, non-induced ATDC5 clones cultured in monolayer or micromass for four days compared to Vector Only clones as measured by qRT-PCR. Left hand figure composed from averaging all three clones per condition shown in right-hand figure. ND = Not detected. C_T values can be found in Appendix, Table S4.1. Experiment performed once.

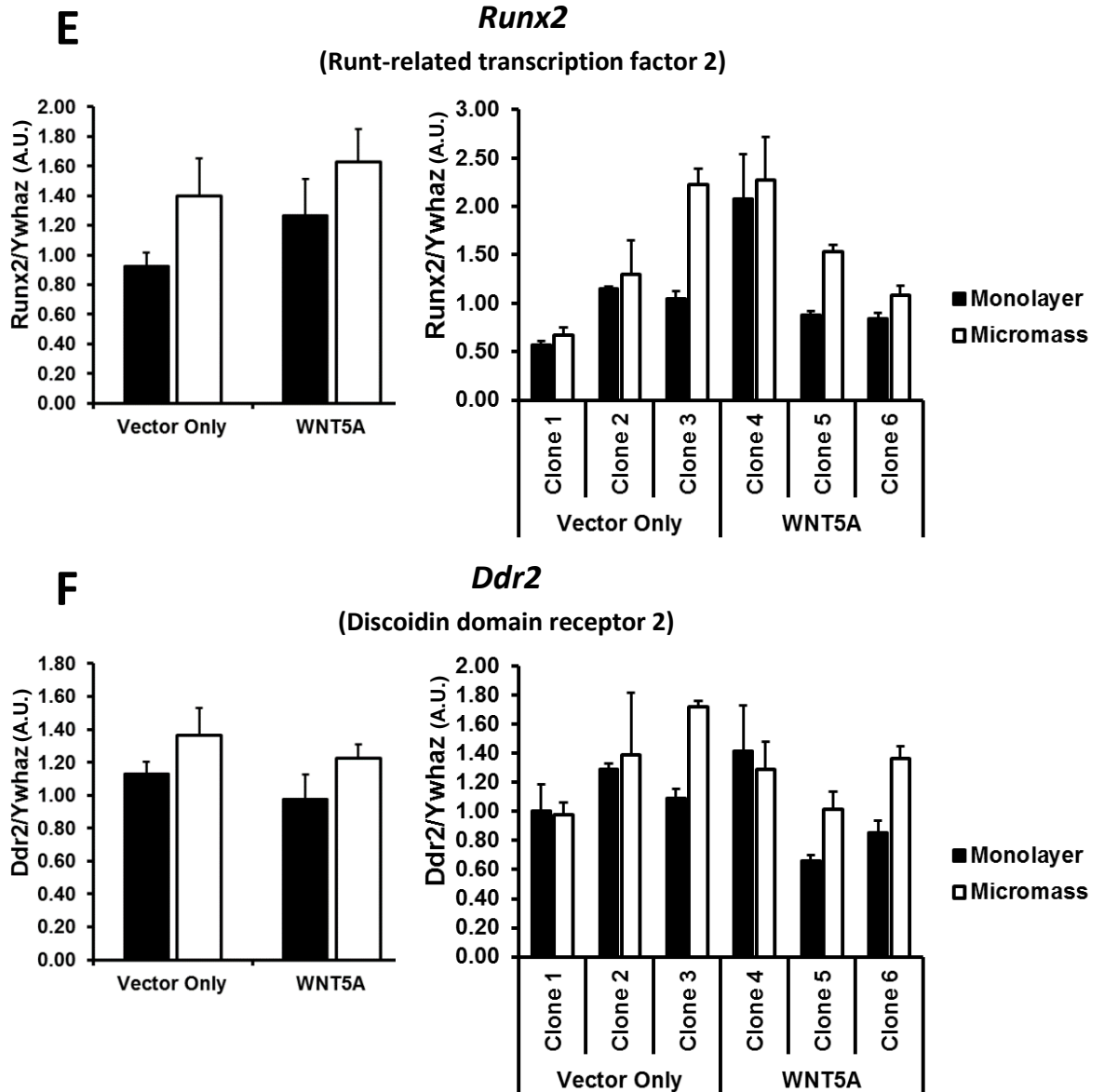


Figure 4.2 E-F – Gene regulation in stable WNT5A-overexpressing, non-induced ATDC5 clones. Steady-state mRNA expression levels of *Runx2* (E) and *Ddr2* (F) in WNT5A-overexpressing, non-induced ATDC5 clones cultured in monolayer or micromass for four days compared to Vector Only clones as measured by qRT-PCR. Left hand figure composed from averaging all three clones per condition shown in right-hand figure. C_T values can be found in Appendix, Table S4.1. Experiment performed once.

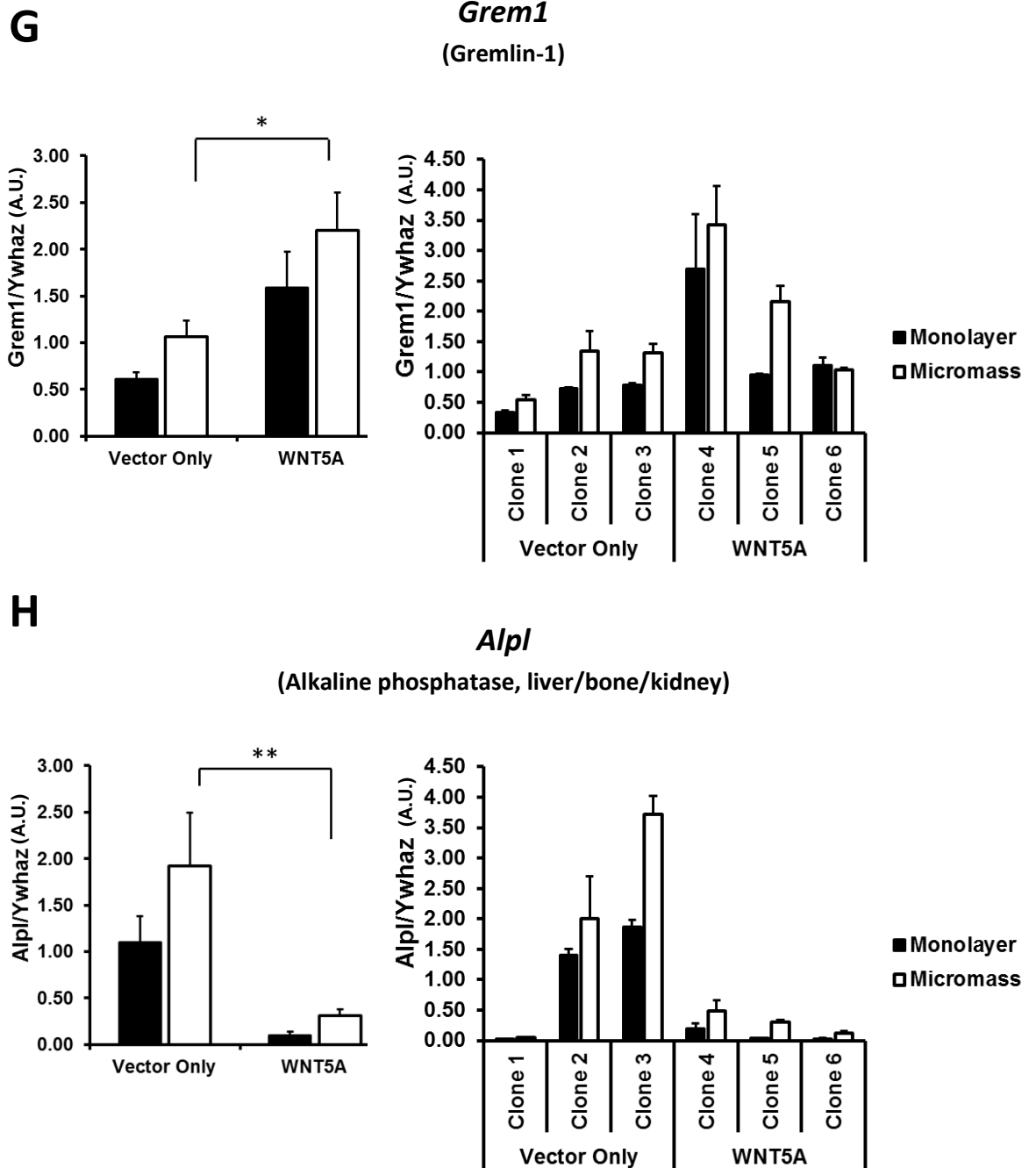


Figure 4.2 G-H – Gene regulation in stable WNT5A-overexpressing, non-induced ATDC5 clones. Steady-state mRNA expression levels of *Grem1* (G) and *Alpl* (H) in WNT5A-overexpressing, non-induced ATDC5 clones cultured in monolayer or micromass for four days compared to Vector Only clones as measured by qRT-PCR. Left hand figure composed from averaging all three clones per condition shown in right-hand figure. C_T values can be found in Appendix, Table S4.1. Experiment performed once.

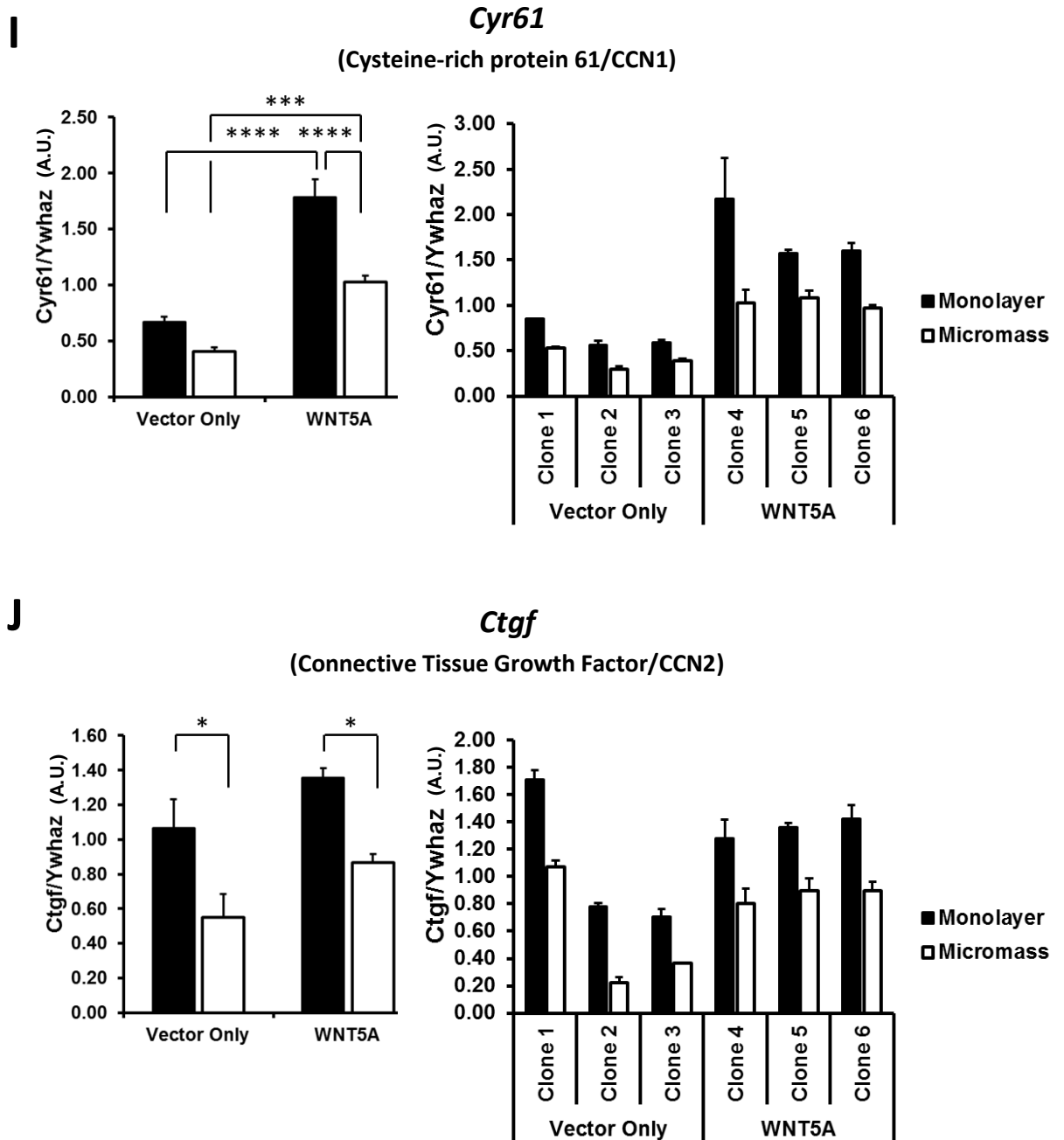


Figure 4.2 I-J – Gene regulation in stable WNT5A-overexpressing, non-induced ATDC5 clones. Steady-state mRNA expression levels of *Cyr61* (I) and *Ctgf* (J) in WNT5A-overexpressing, non-induced ATDC5 clones cultured in monolayer or micromass for four days compared to Vector Only clones as measured by qRT-PCR. Left hand figure composed from averaging all three clones per condition shown in right-hand figure. C_T values can be found in Appendix, Table S4.1. Experiment performed once.

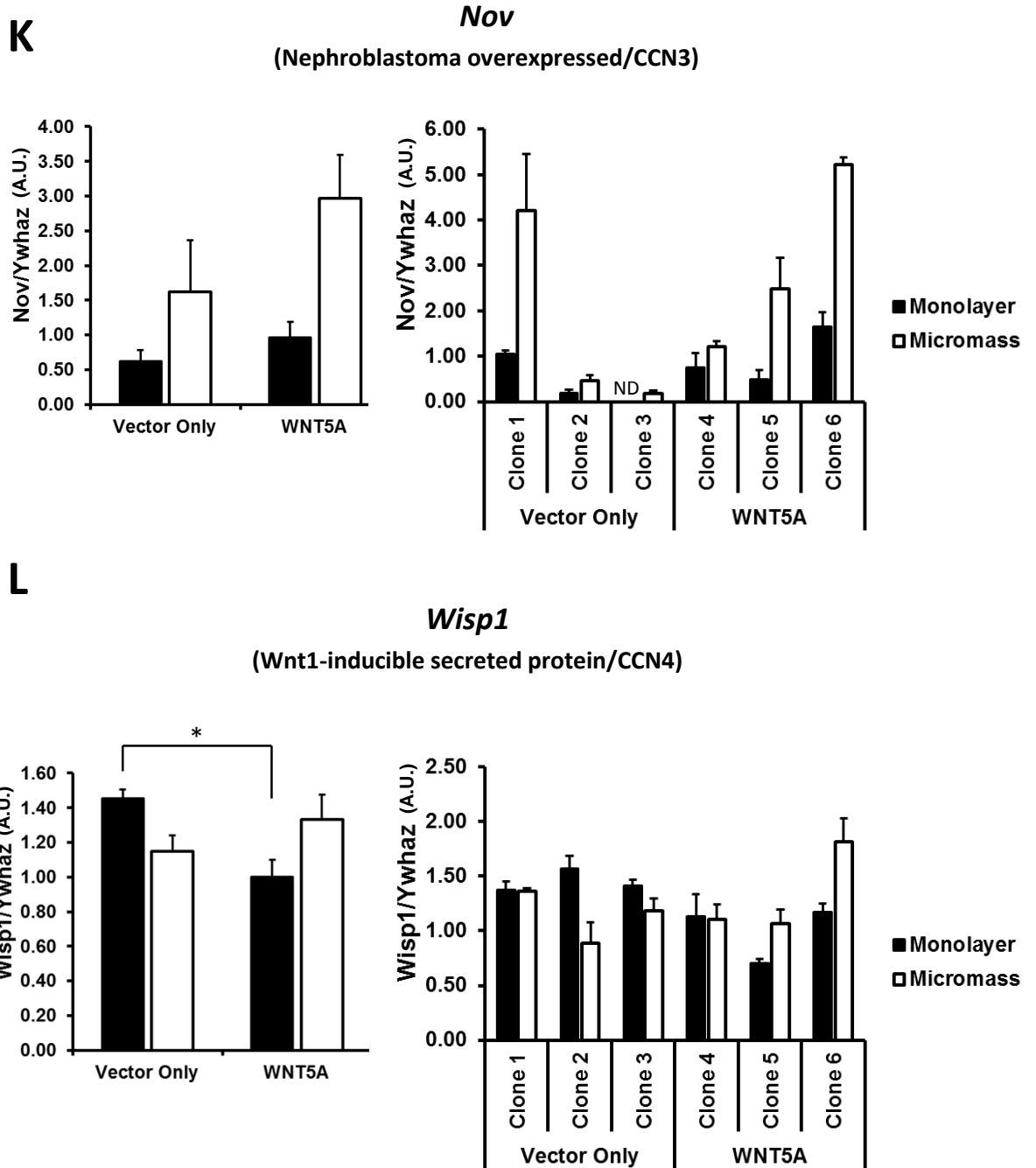


Figure 4.2 K-L – Gene regulation in stable WNT5A-overexpressing, non-induced ATDC5 clones. Steady-state mRNA expression levels of *Nov* (K) and *Wisp1* (L) in WNT5A-overexpressing, non-induced ATDC5 clones cultured in monolayer or micromass for four days compared to Vector Only clones as measured by qRT-PCR. Left hand figure composed from averaging all three clones per condition shown in right-hand figure. ND = not detected. C_T values can be found in Appendix, Table S4.1. Experiment performed once.

M

Wisp2
(Wnt1-inducible secreted protein 2/CCN5)

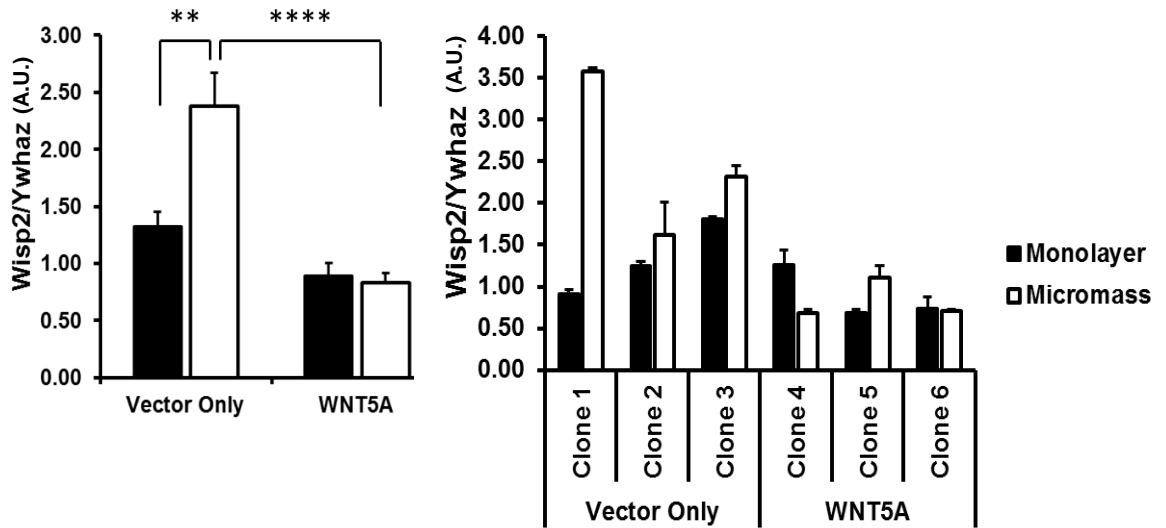


Figure 4.2 M – Gene regulation in stable WNT5A-overexpressing, non-induced ATDC5 clones. Steady-state mRNA expression levels of *Wisp2* in WNT5A-overexpressing, non-induced ATDC5 clones cultured in monolayer or micromass for four days compared to Vector Only clones as measured by qRT-PCR. Left hand figure composed from averaging all three clones per condition shown in right-hand figure. C_T values can be found in Appendix, Table S4.1. Experiment performed once.

4.2.3 Stable clones failed to undergo chondrogenesis

The effect of WNT5A overexpression on gene regulation was examined in clones induced to undergo chondrogenesis with insulin and stimulated with ascorbic acid for 14 days. Twenty four hour stimulation with IL-1 α and OSM (hereafter referred to as “cytokines” in experiments) was also used after differentiation had occurred to investigate gene regulation in osteoarthritic-like conditions and whether this affected WNT5A-mediated gene regulation. For more information, please see section 2.5.7.

Despite not directly comparing insulin-induced clones to non-induced clones, it was apparent that both WNT5A and Vector Only clones failed to differentiate. This was evident by visual observations, whereby cells had a larger, flatter appearance with a lack of aggregation in monolayer cultures (data not shown). Expression of *Col2a1* was also low with C_T values above 30 (Table 4.1), with many samples over the detection limit (C_T \geq 35). Non-induced clones investigated previously also had a similar C_T range (Appendix Table S4.1). One WNT5A clone (Clone 6) partially differentiated, but despite the slight increase in *Col2a1* compared to the rest of the clones (Figure 4.3), still did not visually appear to differentiate fully, with flat cells and a lack of aggregation (data not shown). Since adequate chondrogenesis did not occur even in Vector Only clones, further investigations in insulin-induced clones were not conducted.

Table 4.1 – Expression of *Col2a1* in insulin-induced clones cultured for 14 days in monolayer or micromass then stimulated with or without IL-1 α and OSM cytokines for 24 h without insulin. Steady-state expression levels of *Col2a1*, highlighting the C_T range for three individual clones, combined, and their normalised values. Expression of individual clones can be found in Figure 4.3. Experiment performed once

<i>Col2a1</i>			Min C _T	Max C _T	Normalised	SEM
Monolayer	Vector Only	No Cytokines	30.16	38.58	0.30	0.09
		Cytokines	33.11	39.67	0.04	0.01
	WNT5A	No Cytokines	28.20	36.59	1.33	0.97
		Cytokines	28.75	39.02	1.33	0.44
Micromass	Vector Only	No Cytokines	30.89	39.90	0.38	0.16
		Cytokines	31.59	35.61	0.16	0.08
	WNT5A	No Cytokines	26.64	38.43	2.95	2.43
		Cytokines	27.20	39.07	3.82	2.47

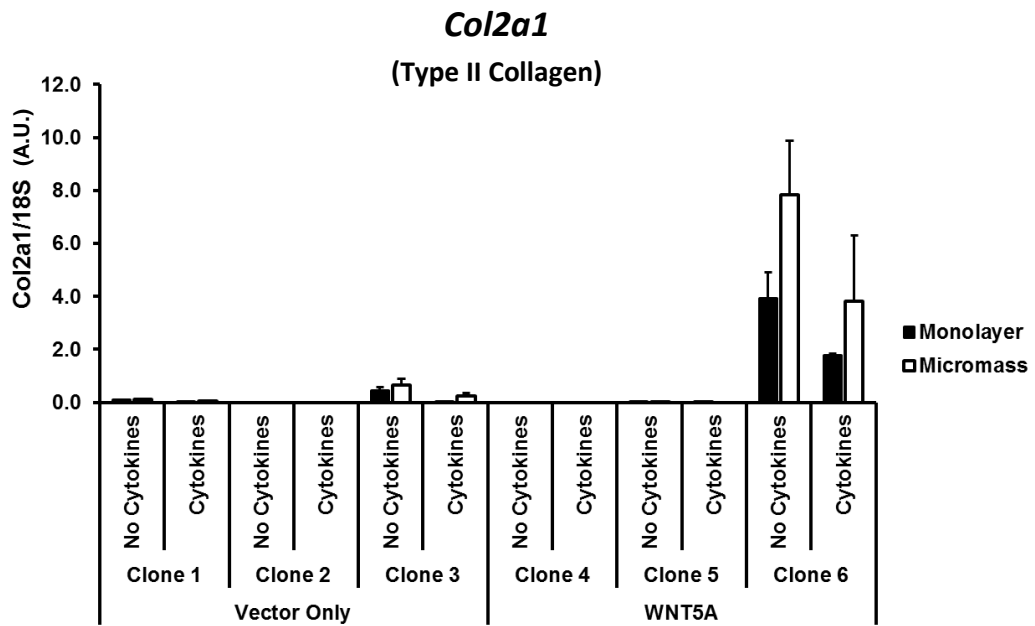


Figure 4.3 – *Col2a1* expression in insulin-induced clones with cytokine stimulation. Normalised steady-state expression levels of *Col2a1* are shown for individual insulin-induced clones grown for 14 days then stimulated with and without IL-1 α and OSM cytokines without insulin for 24 h. C_T values for combined clones can be found in Table 4.1. Experiment performed once.

4.2.4 Generation of WNT5A conditioned medium for naïve ATDC5 cell stimulation

Since chondrogenesis failed to occur in both Vector Only and WNT5A-overexpressing ATDC5 clones, investigations were then carried out using naïve ATDC5 cells instead, stimulating 14-day old insulin-induced, ascorbic acid-stimulated ATDC5 micromass cultures with conditioned media for 24 hours generated from transiently transfecting separate ATDC5 cells, with and without cytokines for the same 24 hour period (see section 2.6)

Prior confirmation of WNT5A protein secretion into media from transient transfections was carried out by western blot before stimulating naïve differentiated cells. Additionally, the time to start the 24 hour media conditioning was optimised to see if there was a difference in protein expression/secretion with the 24 hour period starting either directly after the 5 hour transfection (Day 1) or 24 (Day 2) or 48 hours (Day 3) after the transfection. No appreciable differences were observed between conditioning media for 24 hours starting immediately after the five hour transfection (Day 1) or the following day (Day 2), with perhaps a slight decrease in WNT5A protein by Day 3 (Figure 4.4). Therefore subsequent experiments used media conditioned for 24 hours starting immediately after the five hour transfection, confirming the presence or absence of WNT5A (via anti-FLAG) with each batch of WNT5A or Vector Only conditioned media respectively (data not shown).

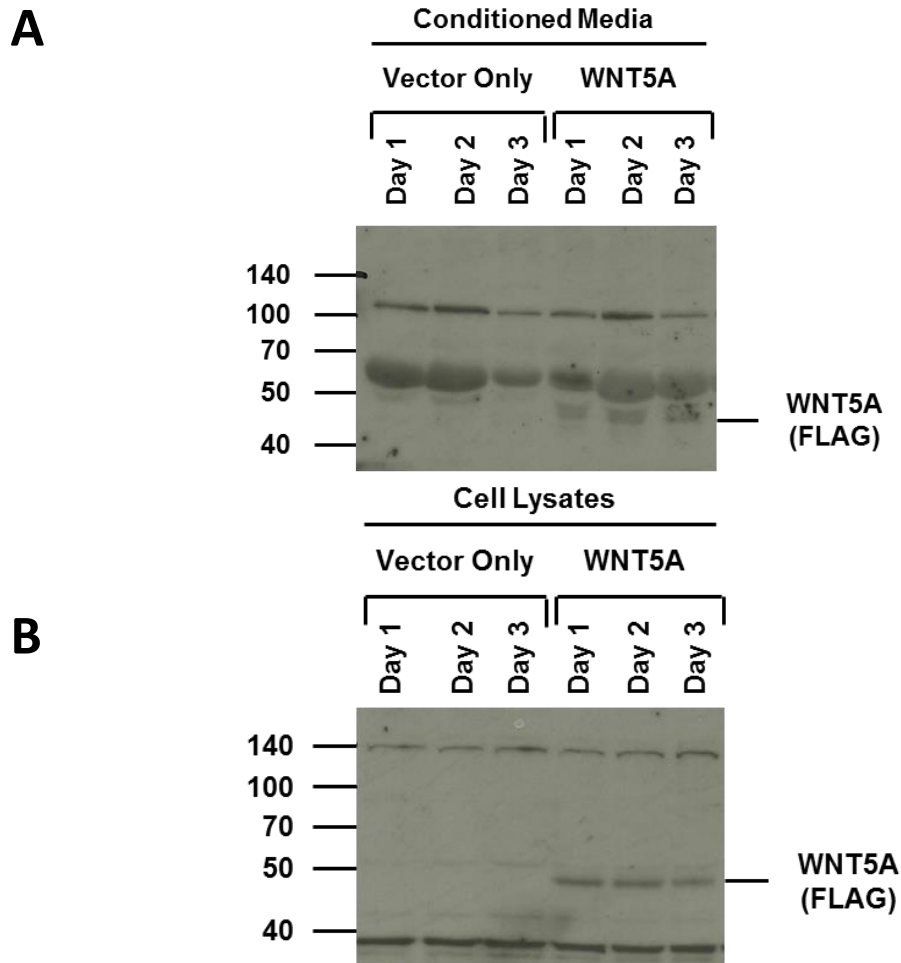


Figure 4.4 – Detection of WNT5A protein from transient transfection timecourse. WNT5A was probed for (via anti-FLAG antibody) in TCA-precipitated conditioned media generated from 7 ml media (A) and cell lysates (B) at indicated time points after transiently transfecting non-induced ATDC5 cells with Vector Only or WNT5A plasmids for 5 h. Predicted M_r WNT5A-FLAG = 44.99 kDa based on amino acid sequence. Day 1 = First 24 h period. Day 2 = Second 24 h period. Day 3 = Third 34 h period. N=1

4.2.5 Gene regulation in conditioned media- and cytokine-stimulated naïve ATDC5 cells

Naïve, 14-day differentiated ATDC5 micromass cultures (as described previously) were stimulated after differentiation for 24 hours with WNT5A conditioned medium and co-stimulated with and without cytokines to investigate the effect of osteoarthritic-like changes on gene regulation and identify whether WNT5A-mediated gene regulation is dependent on, or regulated in, an osteoarthritic-like environment. For a more in-depth description of the stimulation method, please see section 2.6.

In experiment 1, regulation by WNT5A conditioned medium stimulation was seen across a number of candidate genes tested by qRT-PCR analysis, chosen based on their involvement in chondrogenesis, WNT5A signalling or osteoarthritis. Subsequent repeats however, failed to reproduce the results from experiment 1. However, expression of *Ror2*, *Col2a1* and *Adamts4* were consistently not regulated by WNT5A over four experiments (Figure 4.5 A-C). In experiment 1, expression of *Runx2*, *Ddr2*, *Ctgf* and *Nov* were all down-regulated by WNT5A conditioned medium stimulation in the presence of cytokines. No effects were seen by WNT5A stimulation in the absence of cytokines (Figure 4.5 D, E, G, H; left-hand figures). No significant differences in *Runx2*, *Ddr2*, *Ctgf* and *Nov* expression were observed in three subsequent repeats by WNT5A stimulation in the presence or absence of cytokines (Figure 4.5 D, E, G, H; right-hand figures). No regulation of *Cyr61*, *Wisp1*, *Wisp2*, *Frzb* or *Col10a1* by WNT5A stimulation in any experiment by qRT-PCR (Figure 4.5 F, I-L).

Cytokine stimulation caused a trend towards down-regulation of *Ror2* in the presence or absence of WNT5A in three out of four experiments, although this only reached statistical significance in one of the examples shown in the presence of WNT5A by ANOVA + Tukey post-hoc test (Figure 4.5 A). Similarly, cytokine stimulation caused an overall down-regulation of *Col2a1* (Figure 4.5 B). In contrast, as expected, a rise in *Adamts4* expression, an aggrecanase, was seen consistently with cytokine stimulation (Figure 4.5 C). Expression of *Runx2* was down-regulated consistently by cytokine stimulation (Figure 4.5 D). Regulation of *Ddr2* by cytokine stimulation was largely inconsistent, being down-regulated in two out of four experiments in the presence of WNT5A but up-regulated in one experiment in the absence of WNT5A (Figure 4.5 E). No conclusions can therefore be drawn regarding *Ddr2* regulation by cytokine stimulation. Similarly, in two of four experiments, *Ctgf* was down-regulated by cytokine stimulation regardless of WNT5A, but was up-regulated by cytokine stimulation in one experiment in the absence of cytokines (Figure 4.5 G). *Nov*, on the other hand, was also up-regulated in one experiment in the absence of WNT5A by cytokine

stimulation, but no differences were seen in the other three experiments, suggesting that cytokine stimulation does not regulate *Nov* expression (Figure 4.5 H). In contrast, expression levels of *Cyr61*, *Wisp1*, *Wisp2*, *Frzb* and *Col10a1* consistently decreased with cytokine expression (Figure 4.5 F, I-L).

Experiment 1

Representative Experiment

Also analysed by microarray

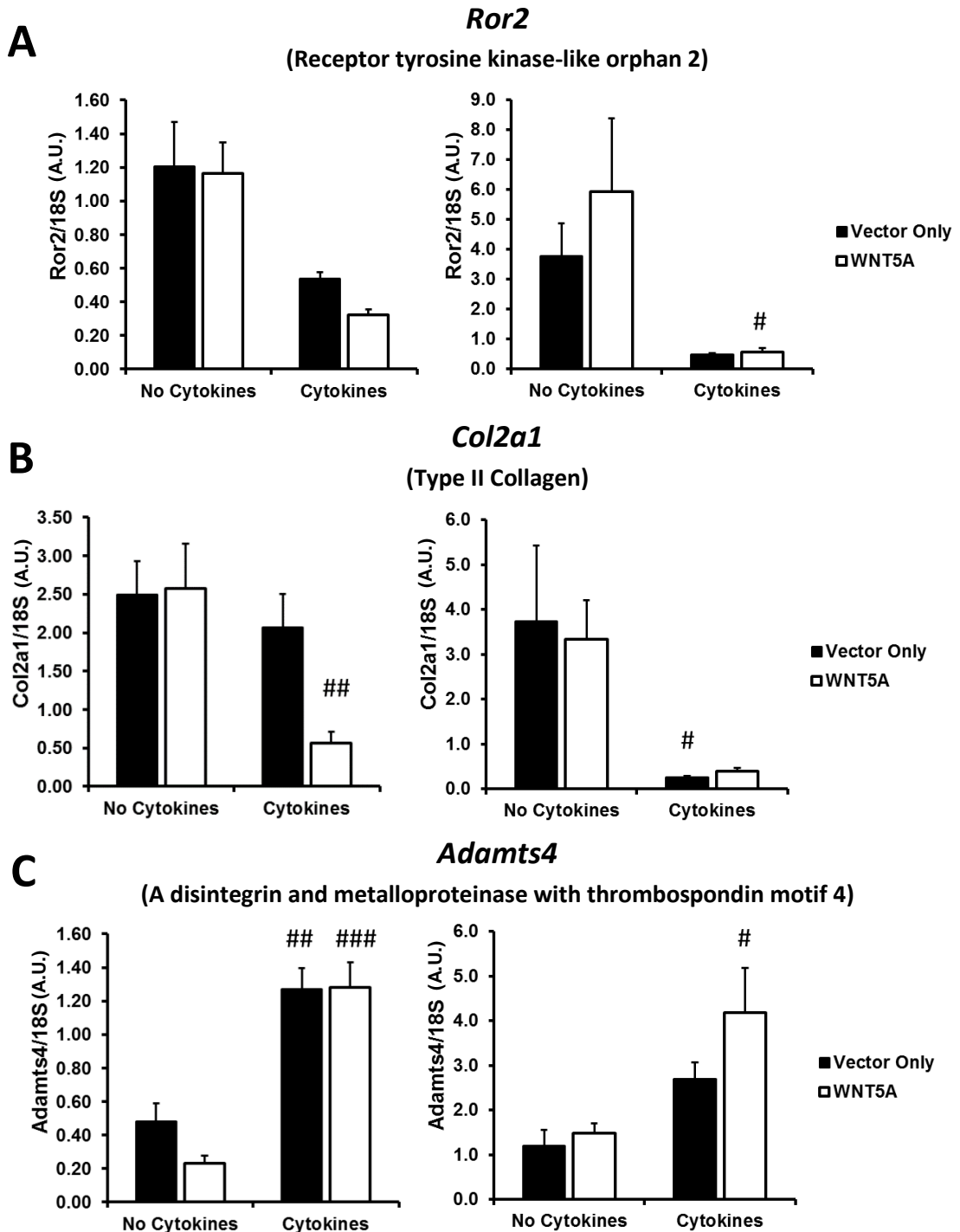


Figure 4.5 A-C – Gene regulation in WNT5A and cytokine stimulated differentiated ATDC5 micromass cultures. Steady-state mRNA expression levels of *Ror2* (A), *Col2a1* (B) and *Adamts4* (C) in micromass cultures stimulated with insulin and ascorbic acid for 14 days then treated with WNT5A conditioned medium (or Vector Only control) with/without IL-1 α and OSM cytokines for 24 h. Experiment performed four times. Left-hand figure from experiment 1. Right-hand figure from representative example from three further repeats, also sent for microarray analysis. C_T values can be found in Appendix, Table S4.2. * = significant compared to Vector Only. # = significant compared to no cytokines.

Experiment 1

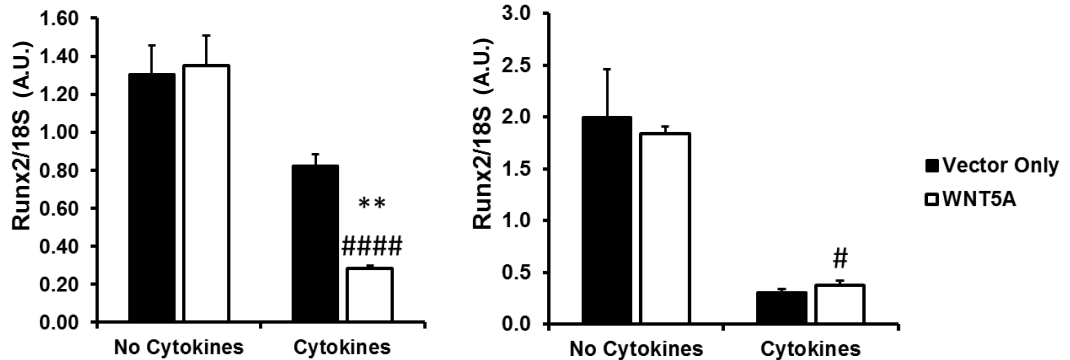
Representative Experiment

Also analysed by microarray

D

Runx2

(Runt-related transcription factor 2)



E

Ddr2

(Discoidin domain receptor 2)

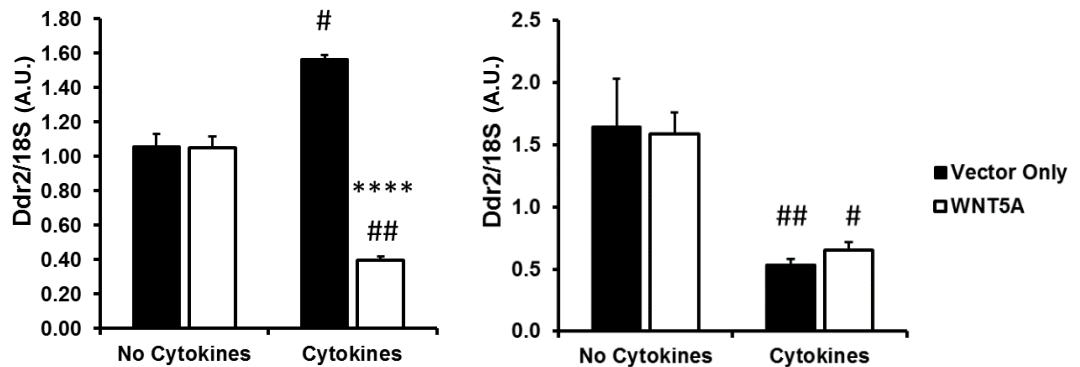


Figure 4.5 D-E – Gene regulation in WNT5A and cytokine stimulated differentiated ATDC5 micromass cultures. Steady-state mRNA expression levels of *Runx2* (D) and *Ddr2* (E) in micromass cultures stimulated with insulin and ascorbic acid for 14 days then treated with WNT5A conditioned medium (or Vector Only control) with/without IL-1 α and OSM cytokines for 24 h. Experiment performed four times. Left-hand figure from experiment 1. Right-hand figure from representative example from three further repeats, also sent for microarray analysis. C_T values can be found in Appendix, Table S4.2. * = significant compared to Vector Only. # = significant compared to no cytokines.

Experiment 1

Representative Experiment

Also analysed by microarray

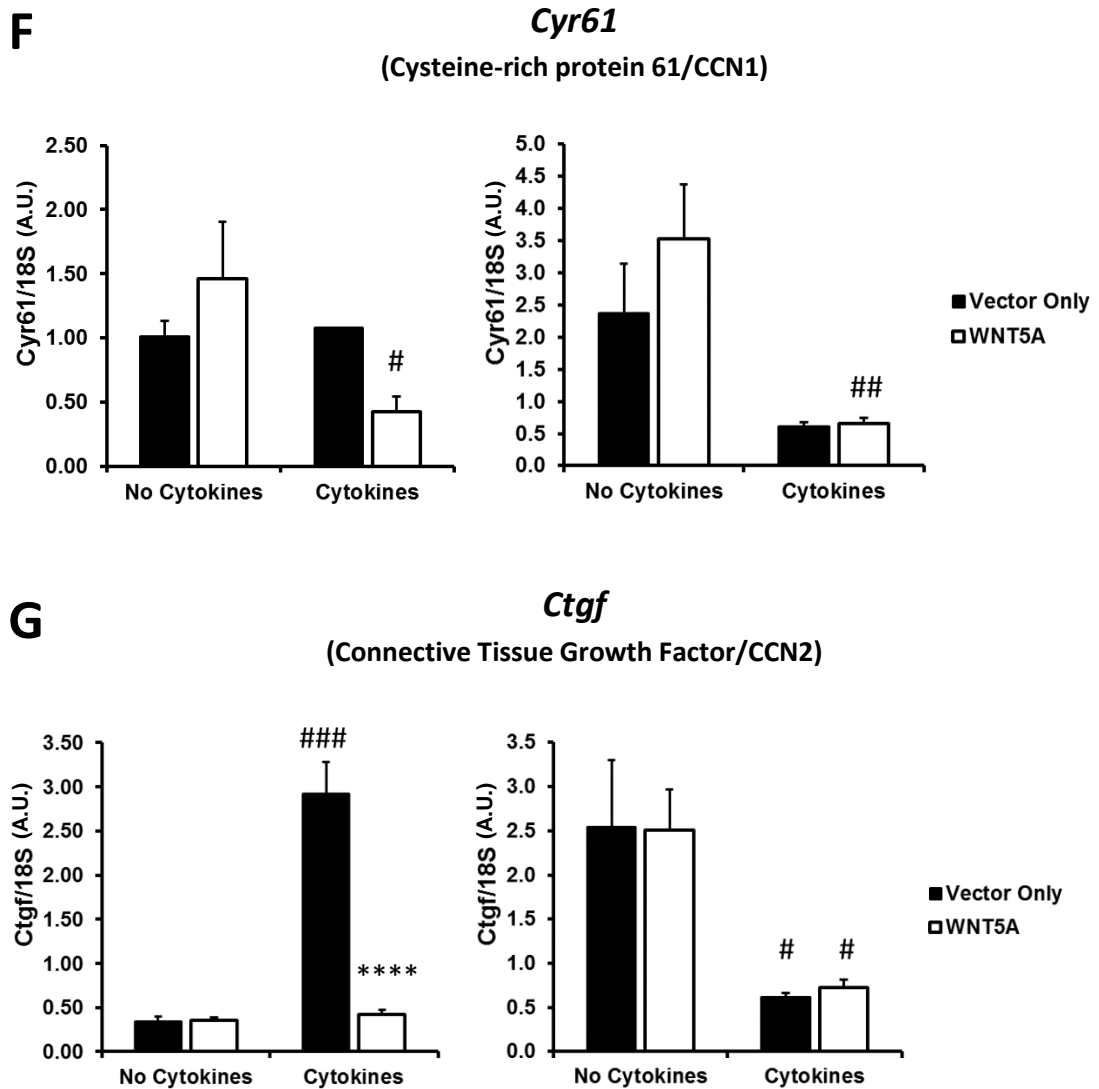


Figure 4.5 F-G – Gene regulation in WNT5A and cytokine stimulated differentiated ATDC5 micromass cultures. Steady-state mRNA expression levels of *Cyr61* (F) and *Ctgf* (G) in micromass cultures stimulated with insulin and ascorbic acid for 14 days then treated with WNT5A conditioned medium (or Vector Only control) with/without IL-1 α and OSM cytokines for 24 h. Experiment performed four times. Left-hand figure from experiment 1. Right-hand figure from representative example from three further repeats, also sent for microarray analysis. C_T values can be found in Appendix, Table S4.2. * = significant compared to Vector Only. # = significant compared to no cytokines.

Experiment 1

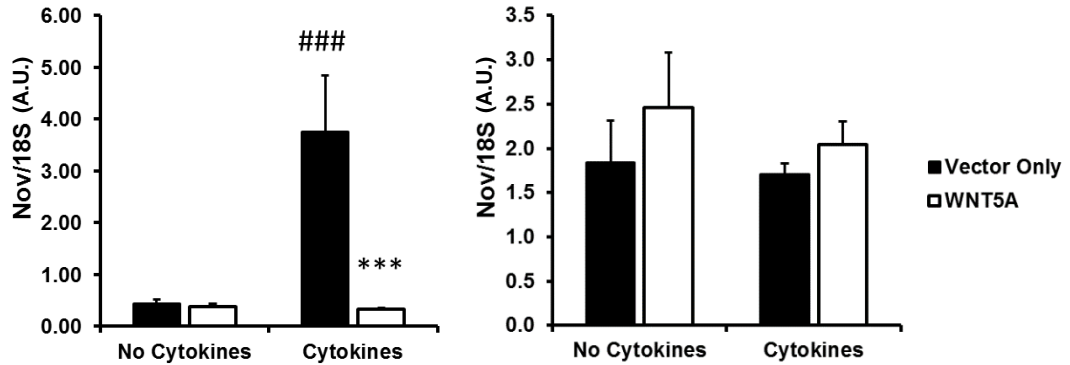
Representative Experiment

Also analysed by microarray

H

Nov

(Nephroblastoma Overexpressed/CCN3)



I

Wisp1

(Wnt-inducible secreted protein 1/CCN4)

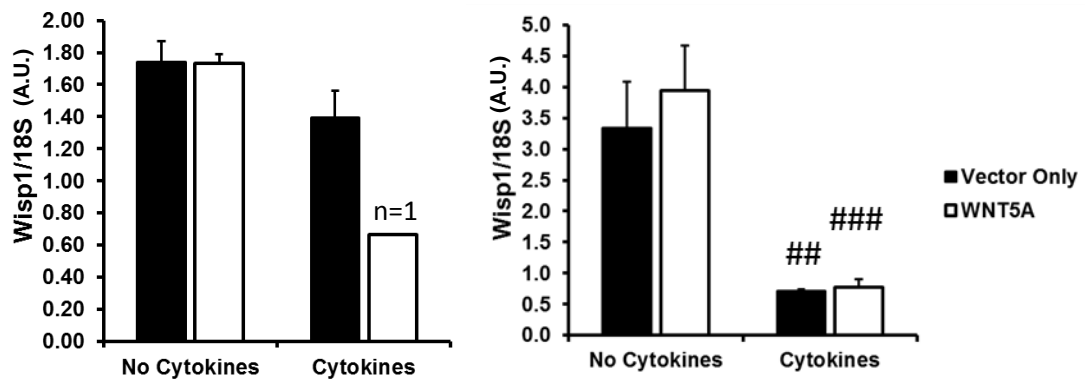


Figure 4.5 H-I – Gene regulation in WNT5A and cytokine stimulated differentiated ATDC5 micromass cultures. Steady-state mRNA expression levels of *Nov* (H) and *Wisp1* (I) in micromass cultures stimulated with insulin and ascorbic acid for 14 days then treated with WNT5A conditioned medium (or Vector Only control) with/without IL-1 α and OSM cytokines for 24 h. Experiment performed four times. Left-hand figure from experiment 1. Right-hand figure from representative example from three further repeats, also sent for microarray analysis. WNT5A+Cytokine condition for *Wisp1* from Experiment 1 (Left-hand figure) consists of one sample only (n=1) as two samples were not detected. C_T values can be found in Appendix, Table S4.2. * = significant compared to Vector Only. # = significant compared to no cytokines.

Experiment 1

Representative Experiment

Also analysed by microarray

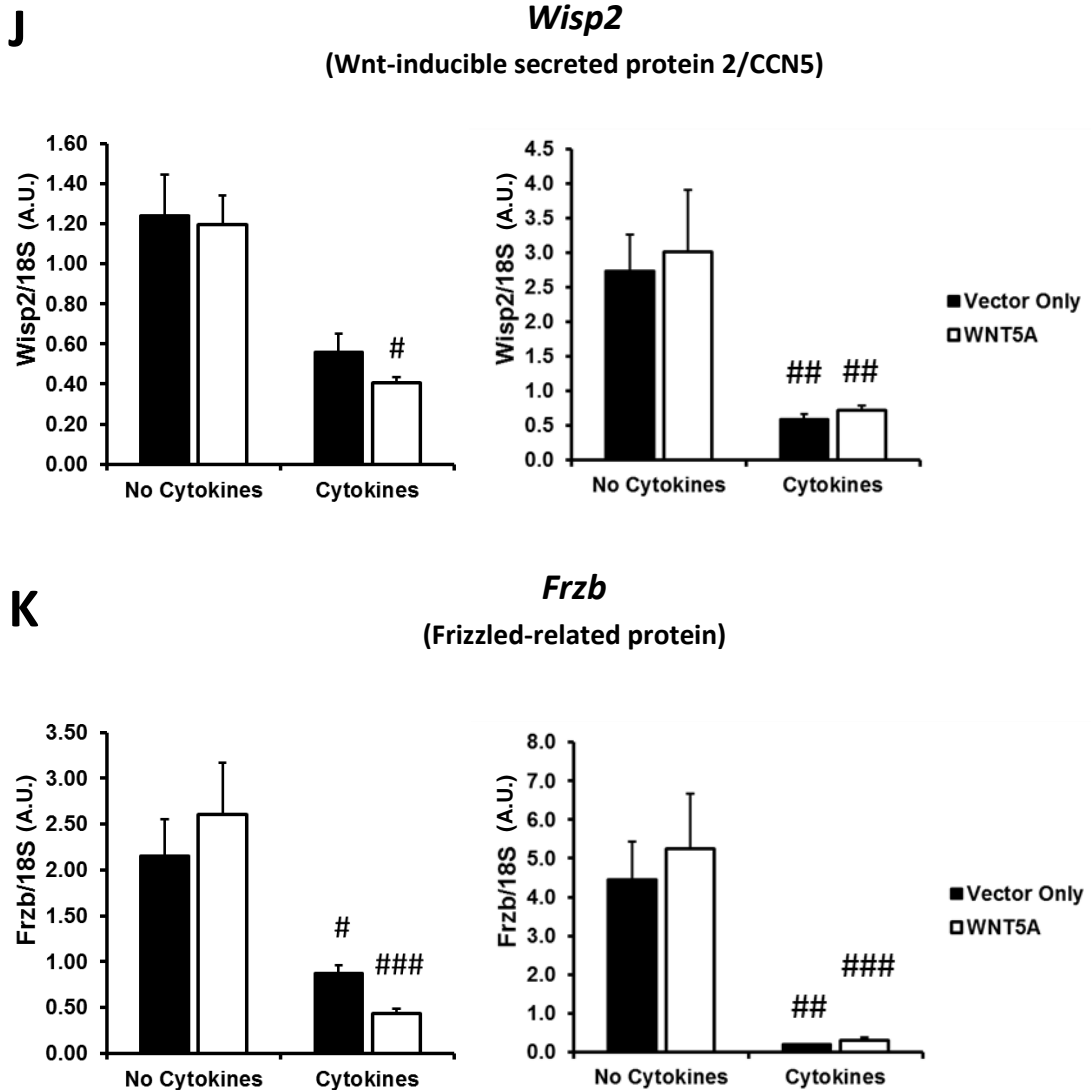


Figure 4.5 J-K – Gene regulation in WNT5A and cytokine stimulated differentiated ATDC5 micromass cultures. Steady-state mRNA expression levels of *Wisp2* (J) and *Nov* (K) in micromass cultures stimulated with insulin and ascorbic acid for 14 days then treated with WNT5A conditioned medium (or Vector Only control) with/without IL-1 α and OSM cytokines for 24 h. Experiment performed four times. Left-hand figure from experiment 1. Right-hand figure from representative example from three further repeats, also sent for microarray analysis. C_T values can be found in Appendix, Table S4.2. * = significant compared to Vector Only. # = significant compared to no cytokines.

Experiment 1

Representative Experiment

Also analysed by microarray

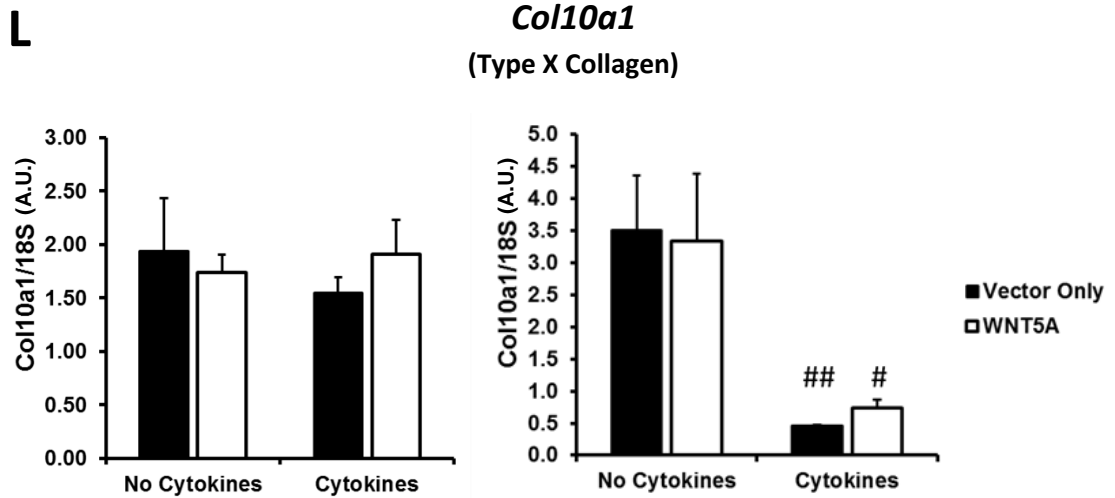


Figure 4.5 L – Gene regulation in WNT5A and cytokine stimulated differentiated ATDC5 micromass cultures. Steady-state mRNA expression levels of *Col10a1* (L) in micromass cultures stimulated with insulin and ascorbic acid for 14 days then treated with WNT5A conditioned medium (or Vector Only control) with/without IL-1 α and OSM cytokines for 24 h. Experiment performed four times. Left-hand figure from experiment 1. Right-hand figure from representative example from three further repeats, also sent for microarray analysis. C_T values can be found in Appendix, Table S4.2. * = significant compared to Vector Only. # = significant compared to no cytokines.

4.2.6 Microarray analysis of WNT5A and cytokine-stimulation in differentiated ATDC5 cells

An unbiased approach was also taken to investigate the effect of WNT5A and cytokine stimulation on differentiated ATDC5 micromass cultures by carrying out microarray analysis of total RNA to identify potentially novel regulation of genes or pathways.

4.2.6.1 Cytokine stimulation strongly regulated gene expression

Principle component analysis (PCA), which highlights similarities or differences in expression patterns across samples based on visual proximity, revealed differences in the expression from the 45,000 probe sets tested across the four conditions. The most striking difference between conditions was revealed to be through the addition of cytokines, regardless of the presence or absence of WNT5A. Samples treated with WNT5A in the presence of cytokines also clustered apart from Vector Only-treated samples, indicating that WNT5A had some regulatory effect on gene expression. Interestingly, this difference was not as apparent in samples without cytokines, suggesting that some WNT5A-mediated regulation may in part be dependent on cytokine signalling (Figure 4.6).

The striking regulation by cytokine stimulation can also be seen by hierarchical clustering in the form of a heat map, highlighting the differences in colour temperature and thus expression, which is more apparent with the addition of cytokines compared to no cytokines (Figure 4.7)

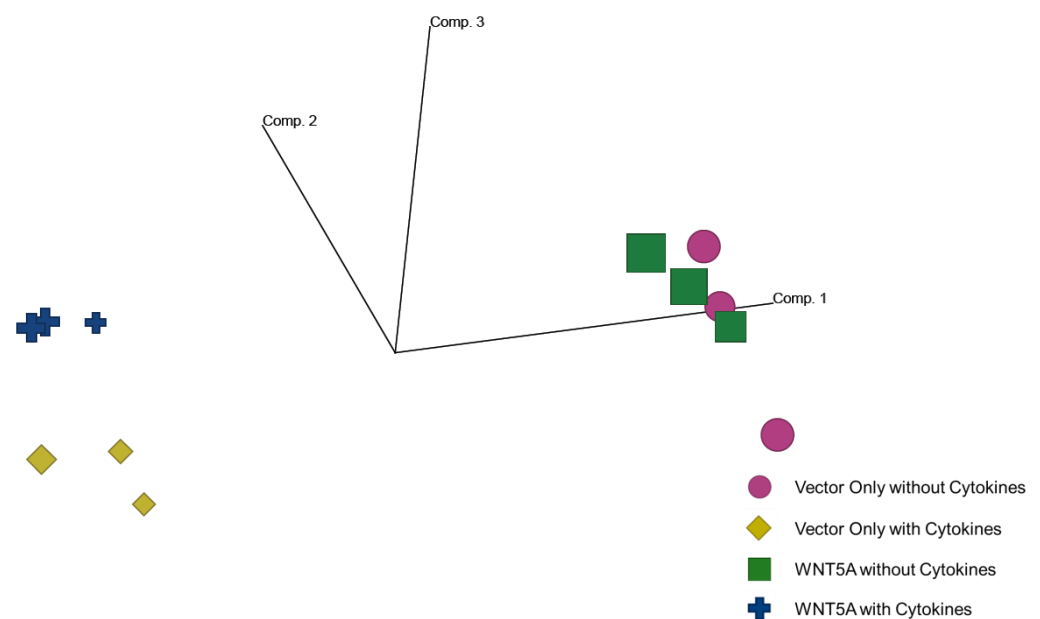
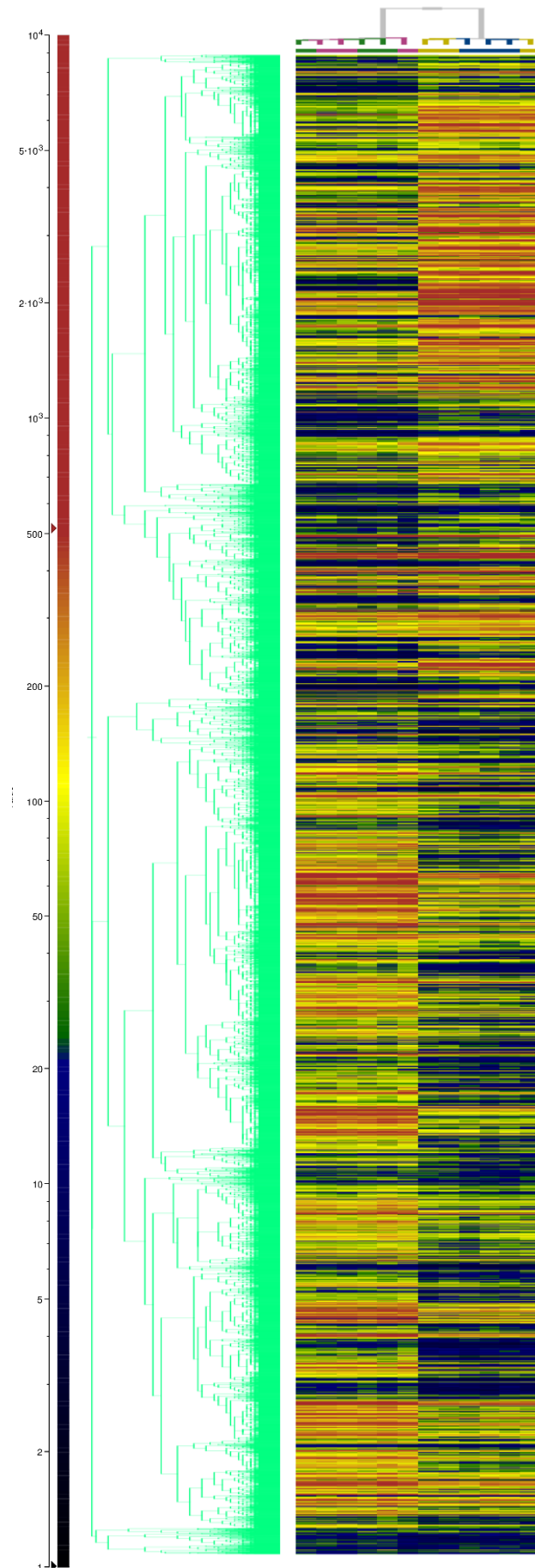


Figure 4.6 – Principle Component Analysis (PCA) of WNT5A and cytokine stimulated micromass cultures from microarray analysis. Clustering of samples indicates similar expression patterns.

Figure 4.7 – Hierarchical clustering of WNT5A and Cytokine-treated micromass cultures by microarray analysis. Expression from all 12 samples (columns) analysed by microarray shown as a heat map based on expression levels of each probe (rows). Red = high expression. Blue = low expression. Clustering based on expression levels and samples.

Column

- Vector Only, No Cytokines
- Vector Only, Oncostatin M + IL-1alpha
- WNT5A, No Cytokines
- WNT5A, Oncostatin M + IL-1alpha



4.2.6.2 Selecting genes for subsequent analysis

Four comparisons were made based on the four conditions to investigate the following questions:

1. What effect does WNT5A stimulation have on gene regulation in the absence of cytokines?
(Vector only, no cytokines vs. WNT5A, no cytokines)
2. What effect does WNT5A stimulation have on gene regulation in the presence of cytokines?
(Vector only with cytokines vs. WNT5A with cytokines)
3. What effect does cytokine stimulation have on gene regulation in the absence of WNT5A?
(Vector only, no cytokines vs. Vector only with cytokines)
4. What effect does cytokine stimulation have on gene regulation in the presence of WNT5A?
(WNT5A, no cytokines vs. WNT5A with cytokines)

Volcano plots were created, plotting fold change regulation based upon the above comparisons against *P*-values determined by pairwise comparisons using student's *t*-test. Probe sets displaying an absolute fold-change (positive or negative) greater than or equal to 1.5x with a *P*-value less than 0.05 were chosen for further analysis, highlighted in red on the volcano plots (Figure 4.8, 4.9). As evidenced by the number of red marks, addition of cytokines significantly regulated more genes above an absolute fold change of 1.5x. Table 4.2 quantifies this difference, revealing around 20-30x the number of *probe sets* significantly regulated by the addition of cytokines in comparison to the number of probe sets significantly regulated by the addition of WNT5A.

Furthermore, the volcano plots reveal that not only were more probe sets significantly regulated more than 1.5-fold by the addition of cytokines, but the effect was much greater, reaching fold changes in the region of 3000x compared to around 3x by the addition of WNT5A (Figure 4.8, 4.9). The top 50 for each comparison, ranked by absolute fold change, can be found in Appendix Table S4.3, S4.4, S4.5 and S4.6.

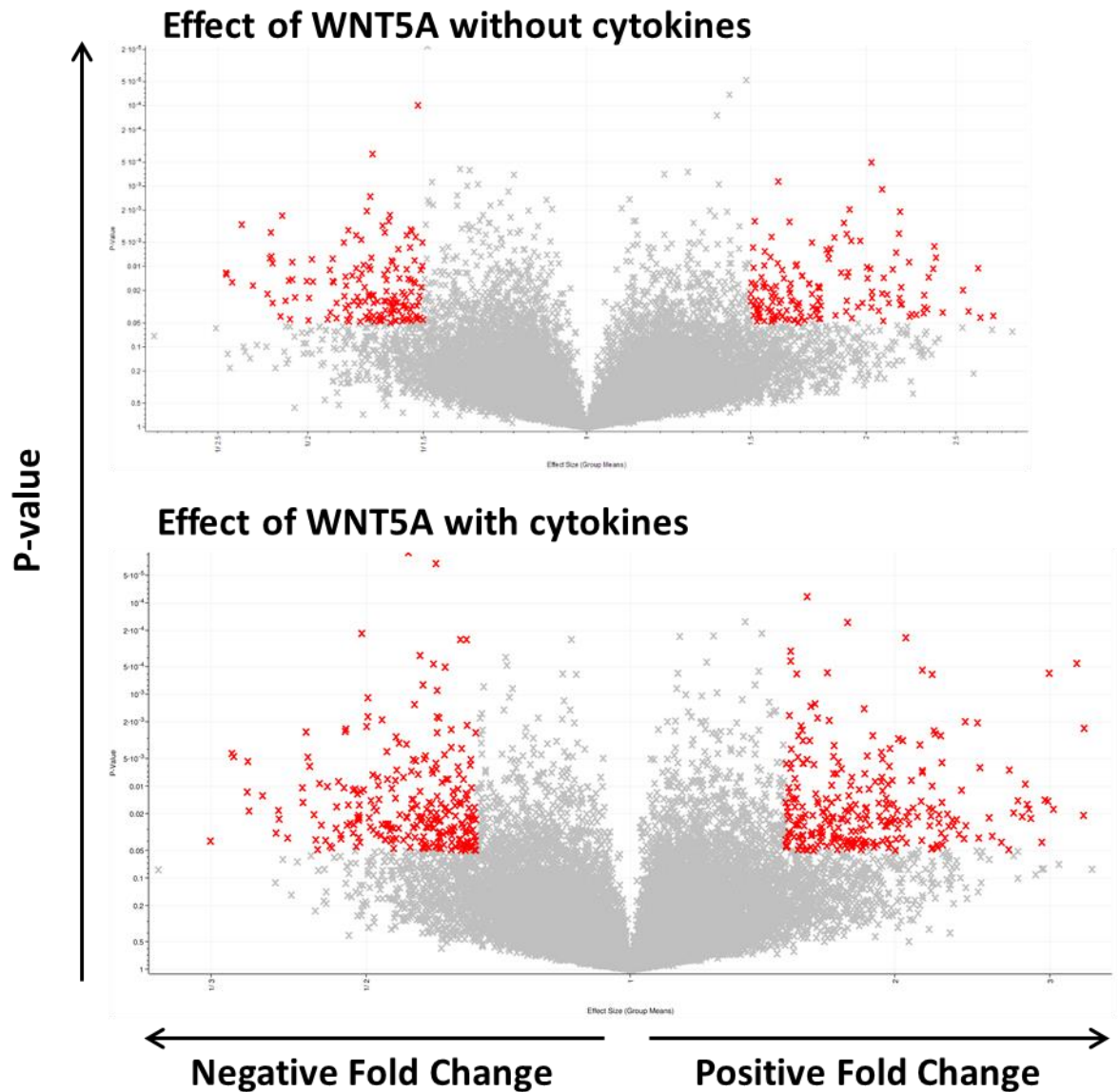


Figure 4.8 – Volcano plot of effect of WNT5A with and without cytokine stimulation on gene regulation in ATDC5 micromass cultures. Probe sets plotted according to fold change regulation (x axis) against *P*-value (y axis). Highlighted probe sets have absolute fold change ≥ 1.5 and *P*-value < 0.05 .

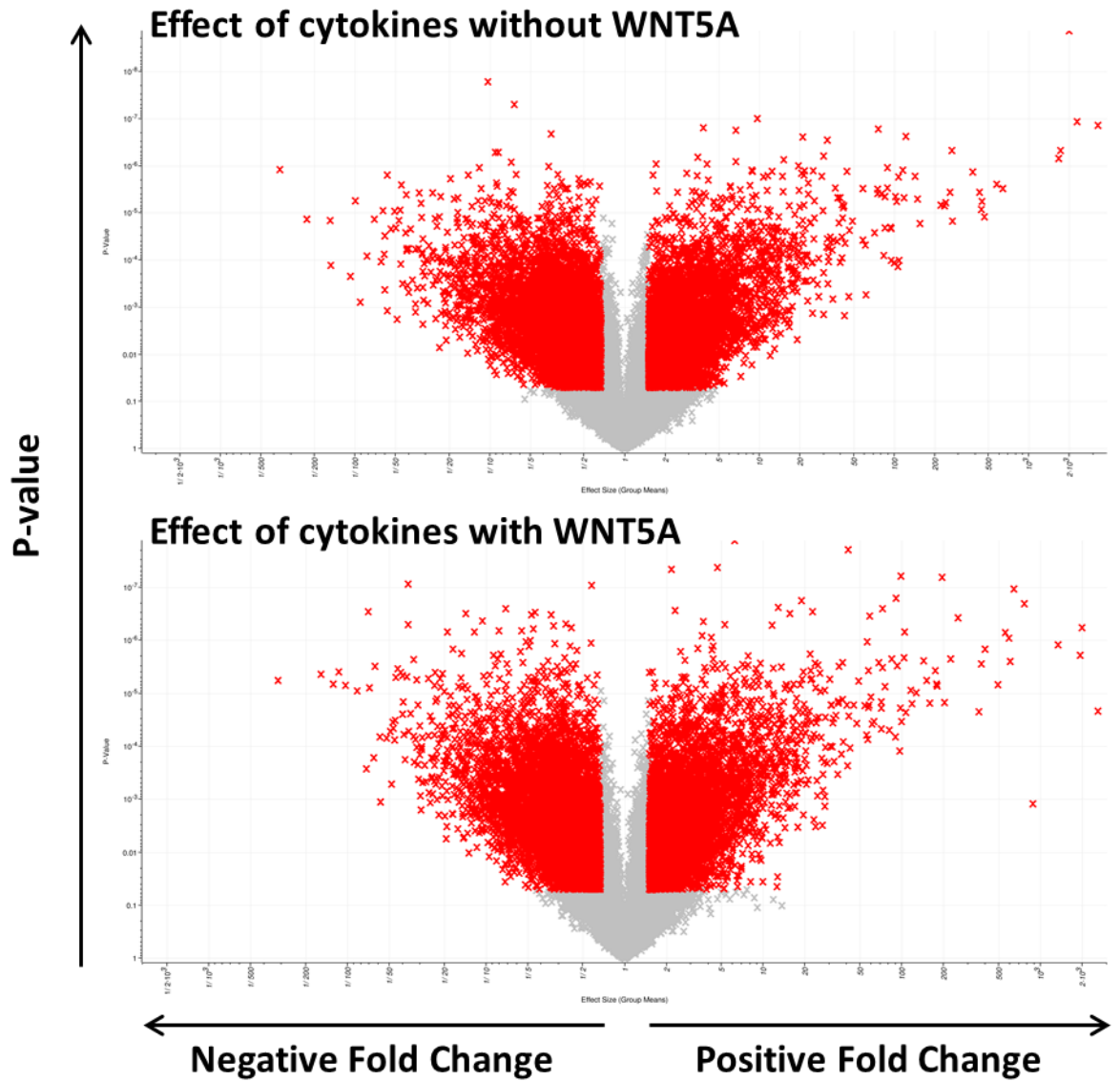


Figure 4.9 – Volcano plot of effect of cytokines with and without WNT5A stimulation on gene regulation in ATDC5 micromass cultures. Probe sets plotted according to fold change regulation (x axis) against *P*-value (y axis). Highlighted probe sets have absolute fold change ≥ 1.5 and *P*-value < 0.05 .

Table 4.2 – Number of significantly regulated probe sets according to P-Value based on absolute fold change greater than or equal to 1.5 and P-Value less than 0.05 by multiple t-tests

	Effect of	Number of probe sets regulated		
		Up-regulated	Down-regulated	Total
1	WNT5A without cytokines	152	156	308
2	WNT5A with cytokines	270	255	525
3	Cytokines without WNT5A	4608	5979	10587
4	Cytokines with WNT5A	4626	6333	10959

However, due to the nature of performing multiple t-tests, it was suspected that a large number of these significant differences were ‘false positives’. To test for this, a more stringent analysis was performed using the Benjamini-Hochberg procedure to calculate Q-values that take into consideration the false discovery rate. Using the more stringent analysis based on using Q-values, no probe sets were significantly regulated by WNT5A (Table 4.3), suggesting that the WNT5A was either not active, or the cells were non-responsive to it. In comparison, only a relatively small number of probe sets were excluded when comparing the effects of cytokines, losing just 12.8 % and 11.2 % of probe sets in the absence and presence of WNT5A respectively compared to the 100 % lost when comparing the effects of WNT5A with/without cytokines (Table 4.3).

Despite no significant differences based on the Q-values for the effect of WNT5A, differences were found in the number of probe sets that were regulated by cytokines depending on the presence or absence of WNT5A. Results revealed that 2356 probe sets were only regulated by cytokines in the presence of WNT5A and 1858 probe sets were only regulated by cytokines in the absence of WNT5A (Figure 4.10), suggesting there may have been some effect after all.

Table 4.3 – Number of significantly regulated probe sets according to Q-Value using Benjamini–Hochberg procedure to take into account false discovery rate

	Effect of	Number of probe sets regulated		
		Up-regulated	Down-regulated	Total
1	WNT5A without cytokines	0	0	0
2	WNT5A with cytokines	0	0	0
3	Cytokines without WNT5A	3971	5262	9233
4	Cytokines with WNT5A	4095	5636	9731

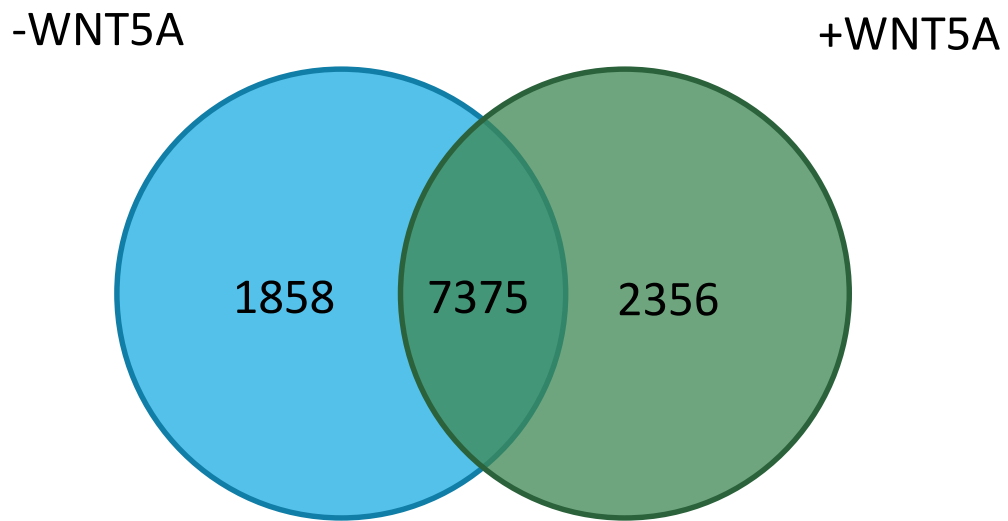


Figure 4.10 – Distribution of cytokine-regulated probe sets with respect to presence or absence of WNT5A based on probe sets deemed to be significantly regulated by cytokines according to Q-values.

Appendix Table S4.7 highlights the top 50 cytokine-regulated genes that were only regulated in the presence of WNT5A. Of these, Kruppel-like factor 9 (*Klf9*) and Protocadherin 7 (*Pcdh7*) were the most up-regulated and down-regulated genes respectively, excluding any hypothesised genes. Interestingly, using the less stringent analysis based on P-Values rather than Q-Values, only *Pcdh7* was regulated by WNT5A in the absence of cytokines, and interestingly was up-regulated as opposed to the down-regulation by cytokines in the presence of WNT5A. However, as stated, this is based on using P-Values, which may therefore have been a false positive. It would therefore be interesting to observe any changes using qRT-PCR to validate the finding.

4.2.6.3 Comparison of candidate genes between qRT-PCR analysis and microarray analysis

The samples used in the right-hand figures in Figure 4.5 were used for the microarray analysis. After calculating which genes were significantly regulated according to the threshold criteria described previously, the data were compared back to the qRT-PCR analysis for confirmation of the same changes in gene expression. Since qRT-PCR was used to validate any findings from the microarray, comparisons against the microarray were based on the less-stringent P-values only to observe any similarities or differences that may have been hidden due to much more stringent parameters. A full comparison for each gene and each condition can be found in Table 4.4.

Table 4.4 reveals that the microarray analysis was largely consistent with the findings seen by qRT-PCR analysis, with only a small number of exceptions. Microarray analysis revealed an increase in *Cyr61* and a decrease in *Col10a1* expression by WNT5A in the absence of cytokines and an increase in *Frzb* expression by WNT5A in the presence of cytokines. However, qRT-PCR analysis of the most representative samples, all from the same experiment which was also analysed by the microarray, showed this was not the case. These are therefore false positives on the microarray. On the other hand, a lack of regulation of *Ror2*, *Col2a1*, *Adamts4*, *Runx2*, *Ddr2*, *Ctgf*, *Nov*, *Wisp1* and *Wisp2* by WNT5A conditioned medium was seen by microarray analysis in agreement with the qRT-PCR analysis.

Similarly, significant down-regulation of *Col2a1*, *Wisp1*, *Wisp2* and *Frzb* by cytokines in Vector Only conditioned medium, seen by the microarray analysis was in agreement with representative data from the qRT-PCR analysis. Similarly, up-regulation of *Adamts4* and down-regulation of *Cyr61*, *Wisp1*, *Wisp2* and *Frzb* by cytokines in the presence of WNT5A seen by microarray analysis was also in agreement with the qRT-PCR analysis. However, results obtained from the microarray did not agree with results for *Ror2*, *Ctgf* and *Nov* by cytokines either in Vector Only or WNT5A conditioned media, or with *Col2a1* and *Col10a1* by cytokines only in the presence of WNT5A.

Together, this shows that the microarray findings were largely consistent with the findings seen by qRT-PCR.

Table 4.4 – Comparison between microarray analysis and qRT-PCR analysis. Candidate genes from Figure 4.5 were analysed by microarray analysis and regulation compared to previous analysis by qRT-PCR in addition to regulation of *Anxa1*, *Matn3* and *Prg4*. Only genes with significant regulation as determined by P-value ($P \leq 0.05$) shown. Regulation that was not deemed significant by Benjamini-Hochberg analysis ($Q > 0.05$) but were by P-Value are marked by †. “-” = No significant regulation. Arrows represent regulation where gene was either strongly induced (up arrows) or strongly repressed (down arrows) – since expression went to (up) or from (down) not being detected, no fold change can be given. NS = non-significant trend. Biggest fold change shown from microarray analysis where more than one probe set was used per gene. **Runx2* and *Ddr2* each had multiple probe sets which were inconsistent with each other and thus no regulation is shown by microarray analysis for these genes

	Effect of WNT5A in the presence of				Effect of Cytokines in the presence of			
	No Cytokines		Cytokines		Vector Only		WNT5A	
	qRT-PCR	Microarray	qRT-PCR	Microarray	qRT-PCR	Microarray	qRT-PCR	Microarray
<i>Ror2</i>	-	-	-	-	-	-2.22	-10.42	-
<i>Col2a1</i>	-	-	-	-	-14.08	-2.71	-	-2.00
<i>Adamts4</i>	-	-	-	-	2.24 (NS)	4.91	2.83	6.93
<i>Runx2*</i>	-	-	-	-	-	-	-4.84	-
<i>Ddr2*</i>	-	-	-	-	-3.06	-	-2.43	-
<i>Cyr61</i>	-	1.83†	-	-	-	-	-5.40	-1.57†
<i>Ctgf</i>	-	-	-	-	-4.12	-	-3.45	-
<i>Nov</i>	-	-	-	-	-	2.67	-	3.28
<i>Wisp1</i>	-	-	-	-	-4.69	-3.53	-5.10	-2.91
<i>Wisp2</i>	-	-	-	-	-4.61	-2.00	-4.21	-1.84
<i>Frzb</i>	-	-	-	1.72†	-21.50	-9.73	-16.98	-4.37
<i>Col10a1</i>	-	-1.5†	-	-	-7.59	-2.83	-4.51	-
<i>Anxa1</i>	-	1.53†	-	-	-	2.95†	-	-
<i>Matn3</i>	-	-2.13†	-	-	↓↓↓	-2.56	↓↓↓	-1.90
<i>Prg4</i>	-	-	-	-	↑↑↑	444.50	↑↑↑	601.27

4.2.6.4 Confirmation of gene regulation proposed by microarray analysis

In addition to the candidate genes previously investigated, microarray analysis revealed significant regulation of a number of interesting genes related to the topics investigated in this thesis. qRT-PCR was used to validate these findings.

Using the less stringent parameters by analysing P-values only, by microarray analysis, expression of *Anxa1*, which encodes the Ca²⁺/phospholipid-binding protein, Annexin 1 (Sheu, *et al.*, 2014) and is involved in cell migration (Cote, *et al.*, 2010), was up-regulated by WNT5A in the absence of cytokines and paradoxically up-regulated by cytokines in the *absence* of WNT5A (Table 4.4). However, no such regulation was seen after Benjamini-Hochberg analysis using Q-values, and expression was unchanged in three experiments by qRT-PCR analysis (Figure 4.11 A; Table 4.4), confirming the results seen using the more stringent parameters.

Matn3, which encodes the cartilage matrix component, matrilin 3, was down-regulated by WNT5A in the absence of cytokines by microarray analysis when observing P-values only (Table 4.4), however, this remained unchanged by qRT-PCR analysis (Figure 4.11 B; Table 4.4). However, microarray analysis revealed a significant down-regulation of *Matn3* by cytokines in both Vector Only and WNT5A conditioned media after Benjamini-Hochberg analysis. qRT-PCR analysis revealed a similar change in expression, with C_T values around 32-34 in the absence of cytokines to C_T values around 35 and higher in the presence of cytokines (Appendix Table S4.8), and was therefore deemed to not be expressed in the presence of cytokines. This suggests that expression of *Matn3* was repressed by cytokine stimulation and validates the findings from the microarray.

Conversely, expression of *Prg4*, which encodes Proteoglycan 4, more commonly known as lubricin, was significantly up-regulated by cytokine stimulation as seen by the microarray analysis after Benjamini-Hochberg analysis (Table 4.4). In agreement, massive up-regulation of *Prg4* was seen by qRT-PCR, with C_T values higher than the limits of detection (35+) in the absence of cytokines to around 27-29 in the presence of cytokines (Appendix Table S4.8). This therefore suggests the *Prg4* was induced by cytokine stimulation.

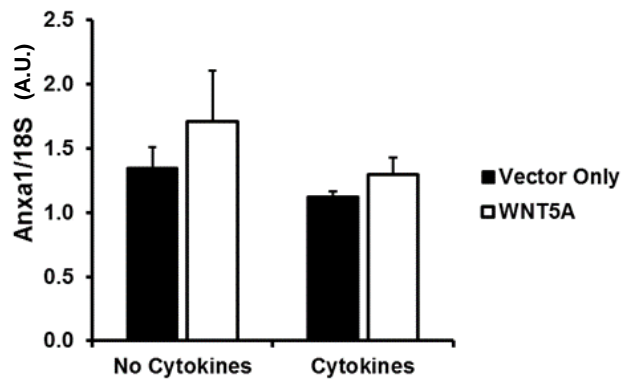
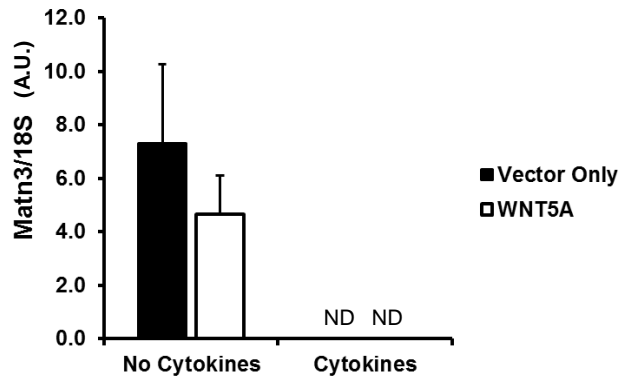
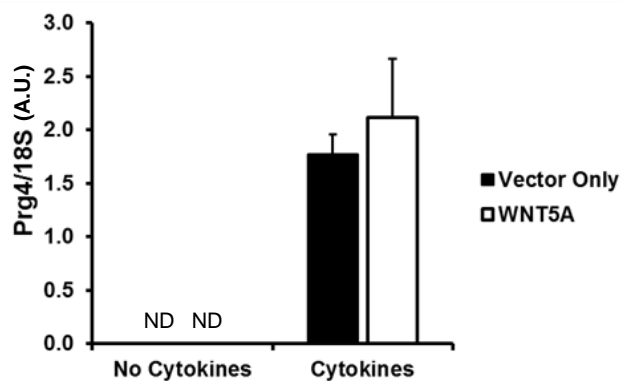
A***Anxa1***
(Annexin A1)**B*****Matn3***
(Matrilin 3)**C*****Prg4***
(Proteoglycan 4/Lubricin)

Figure 4.11 – Confirmation of gene regulation changes seen by microarray analysis by qRT-PCR. Steady-state mRNA expression levels of *Anxa1* (A), *Matn3* (B) and *Prg4* (C) were analysed by qRT-PCR. Data shown from the same samples used for microarray analysis (and right-hand figures in Figure 4.5), which were representative across three experiments. ND = not detected. C_T values can be found in Appendix Table S4.8

4.2.6.5 Pathway Analysis

All significantly regulated probe sets, as determined by Benjamini-Hochberg analysis using Q-values, were subject to pathway analysis using the freely available DAVID software to identify entire pathways that may be regulated by cytokine stimulation, based upon known genes within the pathway. Table 4.5 highlights the top 10 pathways that were significantly regulated in each comparison, ranked by their significance as determined by Benjamini-Hochberg analysis. Since no genes were regulated by WNT5A conditioned media stimulation as determined by the Benjamini-Hochberg analysis, only probe sets identified by the effect of cytokine stimulation were analysed.

Pathway analysis results showed similar pathways were being regulated by cytokines irrespective of the presence or absence of WNT5A (Table 4.5). Interestingly, the results showed that cytokine stimulation of differentiated ATDC5 micromass cultures highly regulated WNT signalling (Table 4.5). Closer inspection of the result revealed that both the canonical and non-canonical pathways were regulated, with all genes listed in the WNT5A pathway being regulated and several genes in the canonical pathway (Figure 4.12). However, due to the limitations of the DAVID software, the results do not determine whether the pathways were up-regulated or down-regulated as DAVID only calculates results based on the gene IDs entered and not any fold changes. Closer inspection of individual genes revealed that *Wnt5a* itself was down-regulated by cytokine stimulation (around 3.5x to 10x down-regulated, depending on probe set). This decrease in *Wnt5a* was also confirmed at the protein level (n=1) in both cell lysates and conditioned media (Figure 4.14). Its main receptor, *Ror2*, was also down-regulated as previously stated (Table 4.4). These results suggest cytokine stimulation of ATDC5 micromass cultures inhibit the WNT5A pathway.

Another interesting pathway that was highly regulated by cytokine stimulation was the focal adhesion pathway (Figure 4.13), with down-regulation of several pathway members including various genes that encode for integrin members, ROCK, JNK and ERK1/2 (fold change data not shown), suggesting inhibition of the pathway. Since focal adhesions are important in migration, this may have ramifications for the data described in Chapter 5, which focuses on adhesion and migration of ATDC5 cells

Table 4.5 – Effect of cytokines on pathway regulation. Top 15 significantly regulated pathways in the absence and presence of WNT5A as determined using DAVID software ranked by Benjamini-Hochberg (BH) Q-Values

Rank	Pathway	P-value	BH Q-value
Effect of cytokines in the <i>absence</i> of WNT5A			
1	Pathways in cancer	1.80E-12	3.40E-10
2	Ubiquitin mediated proteolysis	1.40E-11	1.40E-09
3	Cell cycle	3.20E-09	2.10E-07
4	Wnt signalling pathway	1.90E-07	9.20E-06
5	Colorectal cancer	2.90E-07	1.10E-05
6	Prostate Cancer	1.40E-06	4.10E-05
7	Renal cell carcinoma	1.60E-06	4.40E-05
8	MAPK signalling pathway	1.70E-06	4.60E-05
9	Spliceosome	4.60E-06	9.80E-05
10	Insulin signalling pathway	1.20E-05	2.30E-04
11	Progesterone-mediated oocyte maturation	1.30E-05	2.40E-04
12	Focal adhesion	1.60E-05	2.50E-04
13	Chronic myeloid leukaemia	2.20E-05	3.30E-04
14	Pyrimidine metabolism	4.10E-05	5.60E-04
15	Endocytosis	7.00E-05	9.00E-04
Effect of cytokines in the <i>presence</i> of WNT5A			
1	Pathways in cancer	2.00E-10	3.80E-08
2	Ubiquitin mediated proteolysis	5.20E-10	5.10E-08
3	Wnt signalling pathway	2.20E-09	1.40E-07
4	Renal cell carcinoma	1.50E-07	7.30E-06
5	Insulin signalling pathway	4.60E-07	1.80E-05
6	MAPK signalling pathway	7.40E-07	2.40E-05
7	Chronic myeloid leukaemia	1.10E-06	2.90E-05
8	Prostate cancer	2.60E-06	6.20E-05
9	Neurotrophin signalling pathway	5.60E-06	1.20E-04
10	Adherens junction	9.50E-06	1.80E-04
11	Colorectal cancer	1.00E-05	1.80E-04
12	mTOR signalling pathway	2.30E-05	3.70E-04
13	ErbB signalling pathway	3.90E-05	5.80E-04
14	Focal adhesion	5.50E-05	7.50E-04
15	Glioma	8.30E-05	1.10E-03

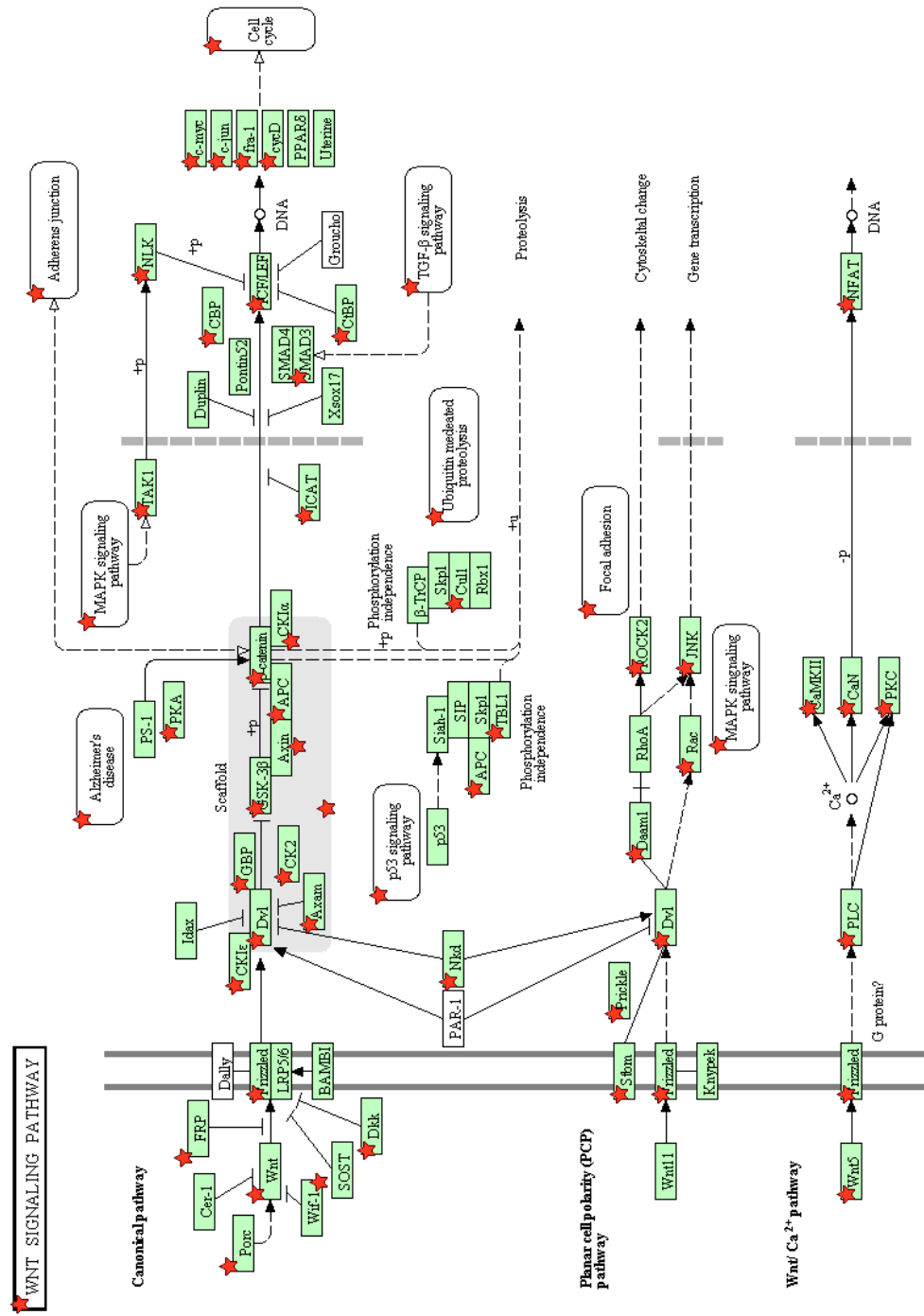


Figure 4.12 – Cytokine stimulation WNT pathways. Pathway map from DAVID based on genes regulated due to the effect of cytokine stimulation in the absence of WNT5A. A similar result was also seen in the presence of WNT5A (data not shown). Red stars = genes regulated.

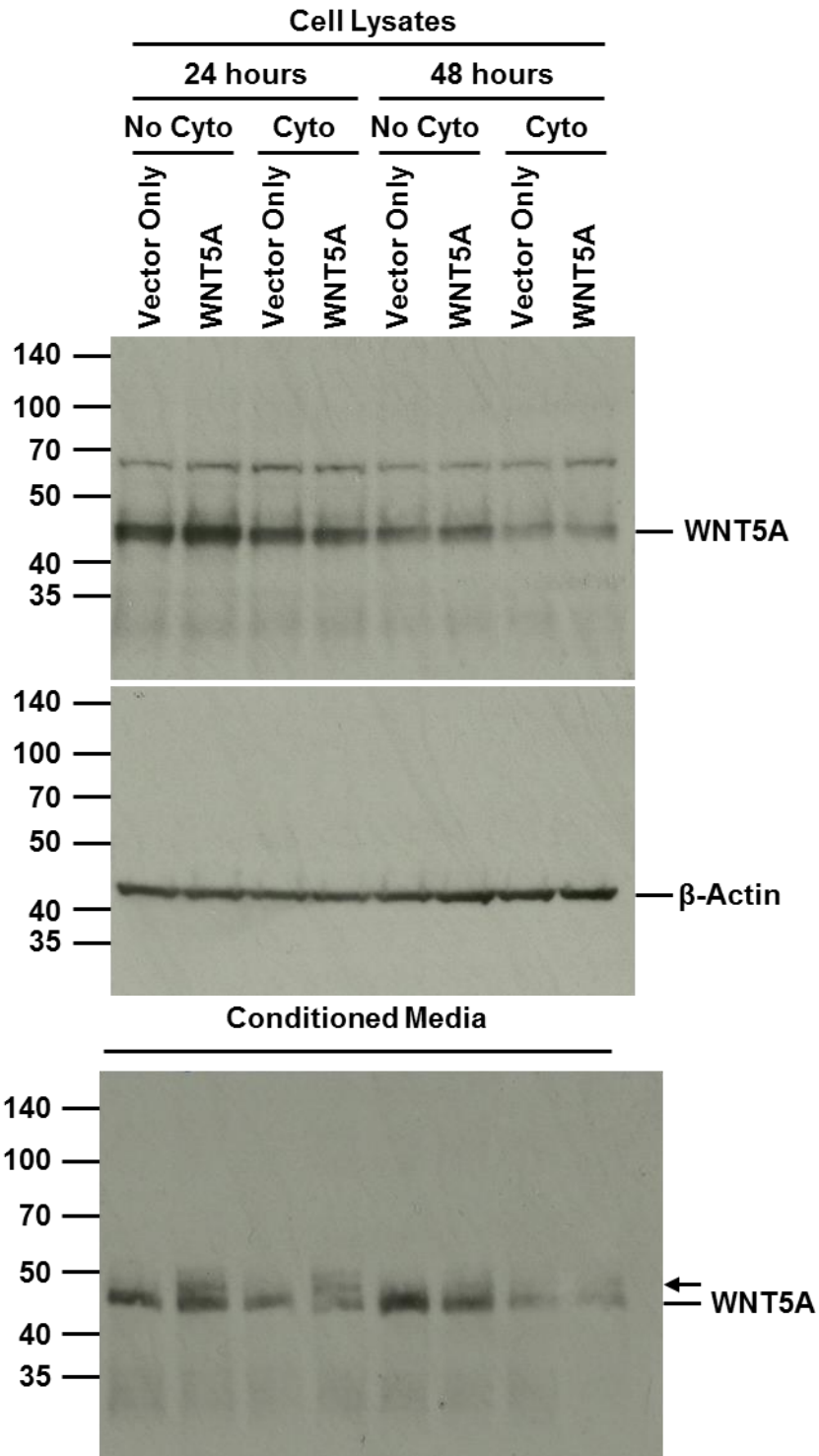


Figure 4.14 – Cytokine stimulation down-regulates WNT5A. Changes in WNT5A expression by microarray were confirmed by western blot in cell lysates and TCA-precipitated conditioned media after 24 hours and 48 hours, probing for WNT5A using a WNT5A-specific antibody. Arrow = possible detection of human WNT5A-FLAG present in conditioned medium used to stimulate cells. Ability for WNT5A antibody to detect WNT5A-FLAG confirmed in Appendix Figure S4.1. Endogenous mouse WNT5A = 42.35 kDa (isoform 1) or 40.89 kDa (isoform 2). Human WNT5A-FLAG = 44.99 kDa. β -Actin used as loading control (41.74 kDa). Molecular weights based on amino acid sequence. Experiment performed once.

4.3 Discussion

Understanding gene regulation in an osteoarthritic-like setting is important to help understand the mechanisms of the disease. This chapter took a number of approaches and described a new model with similarities to an established model of early OA, revealing novel gene regulation.

4.3.1 Gene regulation in non-induced WNT5A-overexpressing clones

4.3.1.1 *Ror2*

Overexpression of WNT5A in non-induced ATDC5 cells revealed interesting results. A slight trend was observed towards increased expression of *Ror2* in WNT5A-overexpressing cells, although this did not reach significance (Figure 4.2 A). WNT5A expression has been shown to positively correlate with ROR2 expression, and can positively regulate ROR2 expression in various cell lines at the RNA and protein levels (O'Connell, *et al.*, 2010; Yuan, *et al.*, 2011). Interestingly, inducible overexpression of WNT5A in a transgenic mouse decreased ROR2 expression at the protein level *in vivo* in embryonic and adult intestinal cells, but had no effect at the RNA level, suggesting ROR2 may undergo endocytosis and lysosomal degradation (Bakker, *et al.*, 2012). Identification of ROR2 protein expression was not carried out in this study, so it remains unknown whether WNT5A may regulate ROR2 expression in a similar manner in this system.

4.3.1.2 *Adamts4* and *Adamts5*

WNT5A also did not regulate *Adamts4* or *Adamts5* expression in non-induced overexpressing clones, although micromass culture did increase expression of *Adamts4* both in Vector Only and WNT5A clones (Figure 4.2 C-D). Exogenous WNT5A has previously been shown to regulate expression of *ADAMTS5* in chick beak mesenchyme micromass cultures, which led to the destruction of the proteoglycan rich matrix (Hosseini-Farahabadi, *et al.*, 2013). To date, no such link between WNT5A and *Adamts4* has been made.

4.3.1.3 *Grem1*

Up-regulation of *Grem1* (gremlin-1) was observed in WNT5A-overexpressing clones (Figure 4.2 G). Gremlin-1 is a secreted BMP antagonist that may indirectly antagonise WNT signalling (Gazzerro, *et al.*, 2007). No direct link has been made between WNT5A signalling and *Grem1* expression. However, WNT5A has been shown to be important in BMP-2-induced osteogenesis, such that inhibition of WNT5A, which is up-regulated in BMP-2-induced osteogenesis, inhibits osteogenesis in the mouse MC3T3-E1 pre-osteoblastic cell line (Nemoto, *et al.*, 2012). BMP-2 is known to increase *Grem1* expression, and Gremlin-1 is known to bind and inhibit BMP-2, creating a negative feedback

loop (Pereira, *et al.*, 2000), although this may be concentration dependent (Nissim, *et al.*, 2006). It would therefore be interesting to identify the state of BMP-2 regulation in this system.

4.3.1.4 *Alpl*, *Runx2* and *Ddr2*

Down-regulation of *Alpl* (alkaline phosphatase) was seen in WNT5A overexpressing cells (Figure 4.2 H), consistent with reports that WNT5A prevents hypertrophy (Hartmann & Tabin, 2000; Church, *et al.*, 2002; Bradley & Drissi, 2010), however, levels of *Runx2* and *Ddr2* were not regulated by WNT5A overexpression (Figure 4.2 E-F), two important factors in hypertrophic differentiation, discussed in Chapter 3. However, it is important to note that overexpressing clones were not induced to undergo differentiation with insulin and did not exhibit increased levels of *Col2a1* (Figure 4.2 B), so any WNT5A-mediated regulation of other hypertrophic factors may depend on the differentiation status of the cell.

4.3.1.5 CCN Growth Factor Family

Of the CCN family of growth factors, WNT5A overexpression increased expression of *Cyr61* (Figure 4.2 I). No direct regulation of *Cyr61* by WNT5A has been reported, although WNT5A and *CYR61* have been reported to be both up-regulated in liver fibrosis at the protein level (Rashid, *et al.*, 2012) and dermal remodelling following CO₂ laser-mediated ablative fractional resurfacing of human skin following abdominoplasty (“tummy tuck”) at both the mRNA and protein levels (Kim, *et al.*, 2013b). Microarray analysis did reveal a significant increase of *Cyr61* with WNT5A conditioned medium stimulation of differentiated cells, although subsequent validation by qRT-PCR analysis revealed this not to be the case (discussed later). A slight decrease in *Wisp1* expression was also seen (Figure 4.2 L), although expression in the individual clones did not seem to differ apart from in one clone. Interestingly, WNT5A has been suggested to increase *WISP1* expression after crush injury of human saphenous vein based on their expression from microarray data, although this was not confirmed by qRT-PCR or further experiments (Price, *et al.*, 2004).

It is important to note however that these data are from a preliminary experiment performed once and so absolute conclusions about the effect of WNT5A-overexpression in non-induced ATDC5 cells cannot be made without further experiments. A summary of the data can be found in Table 4.6.

Table 4.6 – Summary of basal gene regulation in non-induced WNT5A clones compared to Vector Only clones

Gene Association/Family	Up-regulated	Down-regulated	No Regulation
Chondrocytic		<i>Col2a1</i> (micromass) <i>Alpl</i>	<i>Col2a1</i> (monolayer) <i>Runx2</i> <i>Ddr2</i>
WNT Signalling	<i>Grem1</i> (micromass)		<i>Grem1</i> (monolayer) <i>Ror2</i>
CCNs	<i>Cyr61</i>	<i>Wisp1</i> (monolayer) <i>Wisp2</i> (micromass)	<i>Ctgf</i> <i>Nov</i> <i>Wisp1</i> (micromass) <i>Wisp2</i> (monolayer)
Metalloproteinases			<i>Adamts4</i> <i>Adamts5</i>

4.3.2 ATDC5 clones failed to differentiate

Upon identification of gene regulation in non-induced cells, gene regulation was to be investigated in insulin-induced cells to identify potential differential regulation based upon the differentiated state of the cells. Unfortunately, ATDC5 clones failed to differentiate, as noted by low *Col2a1* expression, the lack of cartilage-like nodules and rich matrix observed macroscopically and flatter, larger cells reminiscent of undifferentiated cells (data not shown).

It is possible upon stable integration into the genome that the linearised plasmid interfered with the expression of, or knocked out genes crucial to differentiation. Due to the nature of cloning, it is possible that not all clones generated may have interfered with this pathway, as evidenced by the increased expression of *Col2a1* in Clone 6 (WNT5A-overexpressing clone), which macroscopically did appear to, at least partially, undergo chondrogenesis.

However, due to this uncertainty and the lack of chondrogenesis in even Vector Only clones and interesting results in another model using conditioned media on differentiated cells, the decision was made to pursue results found in the conditioned media model.

4.3.3 WNT5A-mediated gene regulation using conditioned media on differentiated ATDC5 micromass cultures

Since the generated clones tested appeared to fail to undergo chondrogenesis, conditioned medium from ATDC5 cells transiently overexpressing WNT5A was used. This also enabled the observation of the effect of WNT5A in already differentiated cells, and in a disease-like context,

since most studies of WNT5A in cartilage have investigated its effect on chondrogenesis. Experiments were analysed both by qRT-PCR to investigate candidate genes and by microarray for a global investigation.

4.3.3.1 *Cyr61*

Interestingly, microarray analysis revealed 1.8-fold up-regulation of *Cyr61* by WNT5A in the absence of cytokines (Table 4.4), reminiscent of the up-regulation previously found in, albeit non-induced, WNT5A-overexpressing clones (Figure 4.2 I). However, qRT-PCR analysis of four individual experiments revealed no such regulation and this was not deemed to be significant after Benjamini-Hochberg analysis of Q-values. Although a slight increase in *Cyr61* expression by WNT5A in the absence of cytokines was found by qRT-PCR in two experiments, including the samples sent for microarray analysis, this did not reach significance (Figure 4.11 A) and no trend was found in the other two experiments.

4.3.3.2 *Col10a1*

Similarly, *Col10a1* was revealed to be significantly decreased 1.5-fold by microarray analysis by WNT5A (Table 4.4). However, by qRT-PCR analysis, this regulation was only seen in one out of three experiments, and intriguingly not in the samples that were also used for the microarray (Figure 4.11 B), suggesting that this was another false-positive. However, *Col10a1* was decreased by cytokine stimulation, in contrast to the established increase seen in osteoarthritic cartilage (von der Mark, *et al.*, 1995; Girkontaite, *et al.*, 1996). However, in agreement with the cytokine effect confirmed by qRT-PCR, *COL10A1* has previously been shown to be decreased by cytokine stimulation by TNF α in porcine chondrocyte micromass cultures (Schlichting, *et al.*, 2014).

4.3.3.3 *Anxa1* (Annexin A1)

Microarray analysis revealed *Anxa1*, which encodes annexin A1, a lipocortin protein involved in calcium and phospholipid binding (Damazo, *et al.*, 2007), was up-regulated 1.5-fold in response to WNT5A stimulation in the absence of cytokines, however, this was not seen by qRT-PCR analysis of three experiments and was not deemed to be significant after Benjamini-Hochberg analysis of Q-values (Figure 4.11 A; Table 4.4). No direct link between *Anxa1* and WNT5A has previously been made. However, annexin A1 is an important component in the induction of migration and invasion in a number of cell types, including endothelial cells (Cote, *et al.*, 2010), breast carcinoma cells (Kang, *et al.*, 2012) and myoblasts (Bizarro, *et al.*, 2012), as is WNT5A, discussed in Chapter 5. It has also been shown to be important for the normal development of the mouse skull, with knockout mice having a delay in the formation of the sagittal suture system and having a thicker, more mineralised

frontal bone (Damazo, *et al.*, 2007). It would therefore be interesting to see if migration of ATDC5 cells is mediated by Annexin A1, for example, by silencing *Anxa1* expression.

4.3.3.4 *Matn3* (Matrilin 3)

Expression of *Matn3*, which encodes the non-collagenous ECM component matrilin 3, was significantly down-regulated 2.1-fold by WNT5A stimulation in the absence of cytokines, making it the 39th most regulated probe in that comparison, although it was not deemed significant based on Q-values (Appendix Table S4.3). qRT-PCR analysis of three experiments also revealed no such changes in expression (Figure 4.11 B; Table 4.4). No direct link has been made with WNT5A and *Matn3* expression. However, functional *Matn3* knockout mice exhibit an enlarged hypertrophic zone in the growth plate, with increases in type X collagen, indicating that matrilin 3-null chondrocytes prematurely enter hypertrophic differentiation (van der Weyden, *et al.*, 2006). A down-regulation of *Matn3* seen by the microarray would therefore suggest entry into hypertrophic differentiation, in contrast to WNT5A's established role in preventing this (discussed previously). However, a lack of increase in other hypertrophic markers by WNT5A stimulation, such as *Col10a1*, *Runx2* and *Ddr2*, and a lack of regulation seen by qRT-PCR, suggest this is not the case.

4.3.3.5 Variation in WNT5A-mediated gene regulation between experiments

Interesting regulation by WNT5A was found in a number of candidate genes by qRT-PCR in an initial experiment, however, as just described, these were not reproducible. This may highlight a potential problem with using conditioned media from transiently transfecting cells. Although care was taken to ensure each transfection was performed under the same conditions, confirming the presence of WNT5A in each batch of conditioned medium via western blotting, batch to batch variation may still occur, affecting expression levels, potency and activity.

In future, it may therefore be necessary to confirm activity of each batch of generated conditioned media using a reporter assay. One such assay that is used in the literature is the WNT5A-mediated inhibition of β -catenin-dependent WNT signalling via a TCF/Lef reporter, such as TOPFlash (Ekstrom, *et al.*, 2011). An initial attempt was made using the TOPFlash reporter, however, the results were inconclusive as no luminescence could be read for any condition, including a positive control using rHWNT3A stimulation (data not shown). It is not known whether this was due to user error or lack of optimisation of the protocol. Regardless, depending on the receptor context, WNT5A may not inhibit β -catenin-dependent WNT signalling, but enhance it (Mikels & Nusse, 2006). Since WNT5A is known to activate other pathways, such as the JNK/AP-1 pathway, an AP-1 reporter could also be used to confirm WNT5A activity in conditioned media before stimulating experiments (De Cat, 2003; Nishita, *et al.*, 2010).

However, principle component analysis of microarray data did reveal separation of Vector Only and WNT5A-stimulated samples (Figure 4.6), indicating different gene expression patterns between the conditions. Indeed, 308 and 525 probe sets were significantly ($P < 0.05$) regulated at least 1.5-fold due to WNT5A stimulation in the absence or presence of cytokines (Table 4.2) although these may have been false positives as these were not deemed to be significant after Benjamini-Hochberg analysis.

However, it has been reported that FRZB (also known as secreted Frizzled-Related Protein 3/SFRP3) can bind to WNT5A (Yamada, *et al.*, 2013) and inhibit WNT5A signalling and WNT5A-mediated migration and invasion in a human malignant melanoma cell line (Ekstrom, *et al.*, 2011). This thesis has previously shown that insulin-induced, ascorbic acid-stimulated micromass cultures of ATDC5 cells, used in the WNT5A stimulation experiments, express high levels of *Frzb* at the mRNA level (Figure 3.10 B). However, other reports have shown WNT5A may inhibit the activity of FRZB, as shown in mouse cochlear extension, which is inhibited by incubation with FRZB and rescued with WNT5A (Qian, *et al.*, 2007), suggesting that the antagonistic roles of WNT5A and FRZB on each other may be context dependent.

4.3.4 Cytokine-mediated gene regulation by qRT-PCR in differentiated ATDC5 micromass cultures

In comparison to WNT5A, cytokines had a more dramatic effect, with microarray analysis revealing significant regulation of 20-30 fold more genes using the less stringent P-values (Table 4.2), and to a much greater extent (Appendix Table S4.5 and S4.6).

4.3.4.1 *Ror2*

Cytokine stimulation revealed consistent and interesting results. By qRT-PCR, a consistent trend towards down-regulation was observed in *Ror2* expression with cytokine stimulation (Figure 4.5 A). This is an interesting and apparently novel finding. Of interest, an increase in *ROR2* expression was seen in cells differentiating along the osteogenic lineage in response to IL-1 β in human BMSCs (Sonomoto, *et al.*, 2012) or IL-6, of which family OSM is a member of (Richards, 2013), along with soluble IL-6 receptor (sIL-6R) in human ADSCs (Fukuyo, *et al.*, 2014). In keeping with this, the *ROR2* ligand, WNT5A, was also down-regulated by cytokine stimulation, revealing novel regulation, discussed later.

4.3.4.2 *Col2a1*

Expression of *Col2a1* was also decreased with cytokine stimulation (Figure 4.5 B). Stimulation of porcine chondrocyte micromasses with TNF- α to induce osteoarthritic-like changes also revealed

down-regulation of *COL2A1* (Schlichting, *et al.*, 2014). IL-1 β has also been reported to decrease *COL2A1* expression in human OA chondrocytes (Roman-Blas, *et al.*, 2007; Akhtar, *et al.*, 2011) and bovine articular chondrocytes cultured on polyHEMA to preserve the differentiated phenotype, discussed in Chapter 1 (Roman-Blas, *et al.*, 2007). Expression of *Col2a1* was also decreased in a mouse DMM model of OA six hours post-surgery by microarray analysis, validated by qRT-PCR (Burleigh, *et al.*, 2012). This finding is therefore in line with other works reported in literature. Interestingly, WNT5A has previously been shown to enhance IL-1 β -mediated decrease in type II collagen in rabbit articular chondrocytes (Ryu & Chun, 2006).

4.3.4.3 *Runx2* and *Ddr2*

Decreases in *Runx2* and *Ddr2* were also seen with cytokine stimulation (Figure 4.5 D-E). As previously discussed in Chapter 3, RUNX2 and DDR2 are key players in hypertrophic differentiation, both of which have been shown to mediate expression of MMP13 (Xu, *et al.*, 2005; Boumah, *et al.*, 2009; Shimizu, *et al.*, 2010), a major collagen-degrading enzyme in osteoarthritis. However, cytokine stimulation with TNF α or IL-1 β has been shown to decrease expression of *RUNX2* in pre-osteoblastic cells and during osteogenesis (Gilbert, *et al.*, 2002; Ding, *et al.*, 2009). Interestingly in *cho/+* mice, a chondrodysplasia model that uses a frameshift mutation in *Col11a1 a1* to model OA-like changes (Li, *et al.*, 1995), expression of DDR2 mRNA and protein is increased compared to wild-type mice (Xu, *et al.*, 2005). DDR2 has also been found to be increased in cartilage from humans with OA and in mice with surgically-induced OA (Xu, *et al.*, 2007a). Culture of chondrocytes on type II collagen has been reported to lead to a DDR2-mediated increase in *Mmp13* expression, but no *IL-1* transcripts could be detected (Xu, *et al.*, 2005). Similarly, treatment of a human immortalised chondrocyte cell line with IL-1 receptor antagonist (IL-1RA) failed to inhibit the DDR2-mediated increase in *MMP13* expression (Xu, *et al.*, 2007a), indicating IL-1 is not involved in MMP13 regulation by DDR2. The cytokine-mediated down-regulation of *Ddr2* in this present study is therefore an intriguing and novel finding, and would therefore be interesting to see whether DDR2 protein is affected in the same manner.

4.3.4.4 CCN Growth Factor Family

4.3.4.4.1 *Cyr61*

Microarray and qRT-PCR analysis revealed a significant decrease in *Cyr61* expression by cytokine stimulation in the presence of WNT5A, with a definite trend towards down-regulation in three out of four experiments by cytokine stimulation in Vector Only conditioned medium by qRT-PCR analysis. Similarly, a previous study has shown expression of *CYR61* decreased in a human chondrocyte cell line by stimulation with TNF α , another inflammatory cytokine (Moritani, *et al.*,

2005). However, in human osteoblasts and osteoblast-like cells, various cytokines, including IL-1 β , IL-6, OSM and TNF α , increased expression of CYR61/CCN1 protein and mRNA (Schutze, *et al.*, 1998; Wu, *et al.*, 2012). Cytokine-mediated regulation of *Cyr61* may therefore be cell/context dependent. This decrease in expression may therefore potentially reveal novel regulation of *Cyr61* in chondrocytes by IL-1 α and OSM specifically.

4.3.4.4.2 *Ctgf*

Ctgf, which is increased in human osteoarthritic cartilage with worsening severity (Omoto, *et al.*, 2004), was decreased by cytokine stimulation. Basal levels of CTGF and TGF β -induced CTGF have been shown to be decreased by IL-1 α at the mRNA and protein level, and by IL-1 β at the mRNA level in human dermal fibroblasts (Nowinski, *et al.*, 2010). Similarly, CTGF/CCN2 protein expression is decreased by TNF α and IL-1 β in human Nucleus Pulposus cells via NF- κ B signalling (Tran, *et al.*, 2014) and IL-1 β is known to down-regulate *CTGF* expression in human OA chondrocytes (Masuko, *et al.*, 2010). Interestingly, CTGF/CCN2 can also suppress the induction of IL-1 β -regulated genes in Nucleus Pulposus cells, such as *ADAMTS5* and *MMP3* (Tran, *et al.*, 2014), indicating CTGF/CCN2 has anti-catabolic properties. Nevertheless, the down-regulation of *Ctgf* in this thesis is therefore in-line with previously published reports on cytokine signalling.

4.3.4.4.3 *Wisp1*

Regardless of the presence or absence of WNT5A, cytokine stimulation of differentiated ATDC5 micromass cultures significantly down-regulated expression of *Wisp1*, as seen by both microarray and qRT-PCR analysis (Table 4.4). WISP1/CCN4 protein was found to be up-regulated in murine OA knee joints after collagenase-induced OA, as well as in the STR/Ort mouse model of spontaneous OA and also in human OA cartilage (Blom, *et al.*, 2009). Interestingly, injection of *Wisp1* adenovirus into murine knee joints, which resulted in increased expression of *Adamts4* and *Adamts5* in the synovium in wild-type mice, revealed no significant differences in *Adamts4* or *Adamts5* expression, nor changes in cartilage destruction/neo-epitope formation in IL-1 α /IL-1 β -null mice compared to wild-type, suggesting that the effects of WISP1/CCN4 in cartilage-destruction is not dependent on the downstream effects of IL-1 α and IL-1 β (Blom, *et al.*, 2009). The reduction of *Wisp1* as a result of cytokine stimulation in this thesis is therefore an interesting finding.

4.3.4.4.4 *Wisp2*

Similar to *Wisp1*, expression of *Wisp2* also decreased with cytokine stimulation as seen by both microarray and qRT-PCR analysis (Table 4.4). Little is known about the involvement of WISP2/CCN5 and osteoarthritis in comparison to the other CCN members, although it has been shown at the mRNA level to be preferentially detected in the synovium of RA patients compared to OA patients

(Tanaka, *et al.*, 2005). However, shear stress at 0.82 Pa of human OA chondrocytes did reveal a 1.6-fold decrease in *WISP2* expression by microarray analysis (Lee, *et al.*, 2009). However, in a mouse DMM model of OA, microarray analysis revealed a significant up-regulation of *Wisp2* six hours post-surgery, 4.6-fold as validated by qRT-PCR (Burleigh, *et al.*, 2012), and was also up-regulated in a rat medial meniscus tear model 1.6-2.2-fold 3-21 days post-surgery by microarray analysis (Wei, *et al.*, 2010). This decrease in *Wisp2* by IL-1 α and OSM stimulation in this thesis is therefore an interesting and potentially novel finding.

4.3.4.5 *Lcn2* (Lipocalin 2)

The most regulated gene by cytokine stimulation, regardless of the presence or absence of WNT5A, was *Lcn2* (Appendix Table S4.5 and S4.6), which encodes the adipokine lipocalin 2. This has previously been shown to be very strongly up-regulated by IL-1 β stimulation in ATDC5 cells, a human chondrocytic cell line and in primary human chondrocytes at the mRNA and protein levels (Conde, *et al.*, 2011). Lipocalin 2 is also expressed in osteoarthritic cartilage and has been shown to form a complex with MMP9, protecting it from degradation, demonstrating a possible mechanism for lipocalin 2 to contribute to cartilage degradation (Gupta, *et al.*, 2007). It has also been suggested to be a marker of late-phase/hypertrophic differentiation, increasing in expression in differentiating ATDC5 cells when cells switched from *Col2a1* expression to *Col10a1* expression (Conde, *et al.*, 2011). The increase in *Lcn2* in this present study is therefore in agreement with previously published work and highlights the relevance of this model to osteoarthritis and osteoarthritic changes.

4.3.4.6 *Prg4* (Proteoglycan 4/Lubricin)

Also amongst the most highly up-regulated genes by cytokine stimulation regardless of the presence or absence of WNT5A was *Prg4* (Table 4.4; Appendix Table S4.5, S4.6), which encodes the superficial zone marker, proteoglycan 4, more commonly known as lubricin. Lubricin has a well-defined role in protecting cartilage, as the name suggests, by providing lubrication to the joint, protecting the joint from damage (Rhee, *et al.*, 2005; Jay, *et al.*, 2010). Interestingly, IL-1 α stimulation of primary rat mandibular condylar chondrocytes and cartilage explants from bovine stifle joints have previously been shown to decrease expression of *Prg4*/lubricin (Schmidt, *et al.*, 2008; Cheng, *et al.*, 2010), in contradiction to the results seen in this thesis by microarray. A decrease in *PRG4*/lubricin expression was also found in a sheep model of early OA by lateral meniscectomy (Young, *et al.*, 2006). The increase of *Prg4* observed in this thesis by cytokine stimulation may therefore present novel regulation of *Prg4* by IL-1 α and OSM. However, in a bovine articular cartilage explant injury model, levels of *PRG4*/lubricin increased following injury (Jones, *et al.*, 2009), suggesting lubricin may act in response to cartilage damage to help protect the cartilage

from further damage. In agreement with this, mice overexpressing *Prg4* under the control of the *Col2a1* promoter are protected from the development of OA (Ruan, *et al.*, 2013).

4.3.4.7 WNT Pathway

Pathway analysis revealed strong down-regulation of the WNT5A pathway, regardless of the presence or absence of WNT5A in the conditioned media (Table 4.5; Figure 4.12). This was confirmed in one experiment at the protein level in both cell lysates and conditioned medium (Figure 4.14). Not only was *Wnt5a* itself significantly down-regulated, but a number of members in the WNT5A signalling cascade were also down-regulated, including its cognate receptor, *Ror2*, and many members of the frizzled receptors. This is in contrast to previously established regulation of WNT5A which has been shown to be increased in response to IL-1 β stimulation (Ge, *et al.*, 2011; Sonomoto, *et al.*, 2012), revealing novel regulation of WNT5A by cytokine stimulation.

Intriguingly, strong down-regulation of the canonical pathway was also observed by cytokine stimulation, including a down-regulation of *Ctnnb1* (β -catenin) and TCF/LEF (Table 4.5; Figure 4.11; fold change data not shown), suggesting a total overall down-regulation of the WNT pathways. However it should be noted that *Wnt5a*, which can also activate the canonical WNT pathway depending on receptor context, was the only WNT ligand that was significantly regulated by cytokine stimulation (data not shown). Since aberrant WNT signalling is often associated with osteoarthritis, down-regulation of the WNT pathways may suggest an attempt at protecting against damage, in agreement with the very strong up-regulation of *Prg4* also seen.

4.3.4.8 Focal Adhesion Pathway

Pathway analysis revealed strong regulation of the focal adhesion pathway due to cytokine stimulation of ATDC5 micromass cultures. Several members of this pathway were down-regulated, including genes that encode for ROCK, JNK and ERK1/2. It has been shown in adherent fibroblasts that focal adhesions are enriched with IL-1 receptors required for IL-1 signalling (Qwarnstrom, *et al.*, 1988; Dower, *et al.*, 1990), as well as in chondrocytes (Luo, *et al.*, 1997), which can mediate ROCK, JNK and ERK signalling (Wang, *et al.*, 2011; Rafferty, *et al.*, 2012). Down-regulation of a number of these genes may therefore represent a negative feedback loop to protect the cell from the potential harmful effects of the cytokines, as also seen by the large increase in *Prg4*, as previously discussed.

4.3.5 Similarities with an OA model microarray

In addition to the similarities in expression of *Col2a1* and *Adamts4* previously discussed, the microarray analysis revealed a number of other genes with similar expression patterns to a

microarray analysis conducted on a DMM model of OA, six hours post-surgery. Expression of *Saa3* (serum amyloid a3), *Il6*, *Ccl7* (chemokine (C-C motif) ligand 7) and *Mmp3* were amongst the top 15 most highly up-regulated genes in this thesis following cytokine stimulation both in the presence or absence of WNT5A (Appendix Table S4.5, S4.6) and were also amongst the most highly up-regulated six hours post DMM surgery (Burleigh, *et al.*, 2012). These genes, amongst others, were not significantly regulated four weeks post-surgery in the DMM model (Burleigh, *et al.*, 2012). Together, these similarities further suggest cytokine-stimulated ATDC5 micromass cultures may be a good alternative model of experimental osteoarthritis. This enables investigation into the gene regulation changes and signalling events in a model resembling cartilage changes in early osteoarthritis which otherwise may not be possible from cartilage obtained from patients with end-stage OA undergoing joint replacement surgery.

4.4 Summary

Several genes were found to be regulated by WNT5A in differentiated ATDC5 micromass cultures by microarray analysis, revealing potentially novel pathways stimulated by WNT5A, including *Anxa1* (annexin a1), which has been associated with increased migration and invasion in a number of cells, which WNT5A has also been attributed to. However, of three genes chosen for validation by qRT-PCR, no such regulation by WNT5A was revealed, indicating these may have been false positives.

Variation in WNT5A-mediated signalling seen by qRT-PCR between experiments revealed possible batch to batch variation in the potency and activity of WNT5A in conditioned media from transiently transfected ATDC5 cells, highlighting the need for a more consistent approach by testing the activity of WNT5A via various reporter assays, or using a commercially available active source.

Finally, cytokine stimulation, which very strongly regulated several genes, revealed interesting and novel results, down-regulating the WNT5A pathway regardless of the presence or absence of WNT5A in the conditioned media as well as several CCN family members, adding to the previously established link between the cytokine, WNT signalling and CCN signalling pathways in some novel ways.

Investigating ATDC5 migration and invasion and the potential modulation by cytokine and WNT signalling

5.1 Introduction

5.1.1 Migration and invasion in cartilage and chondrogenesis

One of the initial stages of chondrogenesis during the development of cartilage is the migration of chondroprogenitor cells from the developing paraxial mesoderm, lateral plate mesoderm or cranial neural crest via cellular condensation to form aggregates of chondroprogenitor cells, directed by cell-cell and cell-matrix interactions to form the axial, limb and craniofacial skeletons respectively (Olsen, *et al.*, 2000). One such matrix component, fibronectin, is enriched in cellular aggregates during chondrogenesis (Dessau, *et al.*, 1980; Gehris, *et al.*, 1997) and has previously been shown to increase cellular condensation during chondrogenesis via peanut agglutinin (PNA) staining by plating micromass cultures on top of it (White, *et al.*, 2003).

Chondroprogenitor cells are characterised by their enhanced ability to adhere to fibronectin compared to differentiated chondrocytes (Dowthwaite, *et al.*, 2004; Williams, *et al.*, 2010). It is therefore apparent that fibronectin plays an important role in the adhesion and migration of chondroprogenitor cells. Furthermore, chondroprogenitor cells in cartilage have previously been shown to be migratory. This migratory ability can be modulated in response to both cartilage damage and cytokine stimulation (Seol, *et al.*, 2012; Joos, *et al.*, 2013).

5.1.2 WNT5A and migration/invasion

WNT5A has been known to modulate migration and invasion in numerous cell types and tissues, both positively and negatively. For example, overexpression of WNT5A in various pancreatic cancer cell lines have been shown to enhance migration in 2D wound healing scratch assays (Bo, *et al.*, 2013; Wei, *et al.*, 2013), whereas overexpression of WNT5A in a hepatocarcinoma cell line has been shown to decrease migration (Bi, *et al.*, 2014). WNT5A has also been shown to act as a chemoattractant to primary human neutrophils (Jung, *et al.*, 2013) and as a haptotactic agent in the developing palate (He, *et al.*, 2008). Furthermore, WNT5A stimulation promoted invasion of the typically non-invasive breast carcinoma cell line, MCF-7 (Pukrop, *et al.*, 2006), whereas WNT5A overexpression in the highly invasive mouse breast carcinoma cell line, 4T1, inhibited migration in a transwell assay and inhibited lung invasion and colonisation (Jiang, *et al.*, 2013). The role of WNT5A on migration and invasion may therefore be context-dependent.

5.1.3 Aims

Since WNT5A is expressed in osteoarthritic cartilage (Nakamura, *et al.*, 2005), and chondroprogenitor cells have been shown to migrate to sites of cartilage damage (Seol, *et al.*, 2012), it was hypothesised that WNT5A may modulate chondroprogenitor cell migration and invasion.

To test this, non-induced ATDC5 cells were used as a model for chondroprogenitor cells. Migration of non-induced ATDC5 cells was investigated using a range of biologically relevant substrates, as well as tissue culture-treated plastic (hereafter simply referred to as plastic) in combination with 0.2 % FCS, which also contains fibronectin (Hayman & Ruoslahti, 1979).

Potential chemokinetic and chemoattractive abilities of WNT5A was also investigated in both physiological and pathophysiological settings by the use of the inflammatory cytokines, IL-1 α and OSM. This was investigated both in 2D random migration, where cytokines were used in conjunction with WNT5A to stimulate the migrating cells directly, as well as 3D invasion into differentiated micromasses, where cytokines were used to initiate potential breakdown of the matrix before the invasion of non-induced cells took place towards a WNT5A gradient. In some experiments, WNT3A was also used to investigate the difference between the impact of non-canonical and canonical WNT signalling.

5.2 Results

5.2.1 Non-induced ATDC5 cells adhere better to fibronectin than to type II collagen

The ability for non-induced ATDC5 cells to adhere to fibronectin or type II collagen at various concentrations was investigated following 60 min of adhesion. Adhesion was calculated based on the absorbance of staining with methylene blue, which was proportional to the number of adhered cells after non-adhered cells were washed off (for more detailed information on the adhesion assay, please see section 2.7).

After plating for 60 min, significantly more non-induced ATDC5 cells adhered to fibronectin compared to type II collagen above 2 $\mu\text{g/ml}$ (Figure 5.1). Adhesion did not occur at concentrations of 0.4 $\mu\text{g/ml}$ or below on either substrate. Dose response curves were evident, with increased adhesion as a result of increasing concentration of substrate used. Maximal adhesion to fibronectin occurred at lower concentrations than to type II collagen, with adhesion to fibronectin plateauing around 10 $\mu\text{g/ml}$ compared to 50 $\mu\text{g/ml}$ to type II collagen (Figure 5.1). Based on these results, future experiments were conducted using 10 $\mu\text{g/ml}$ fibronectin and 50 $\mu\text{g/ml}$ type II collagen.

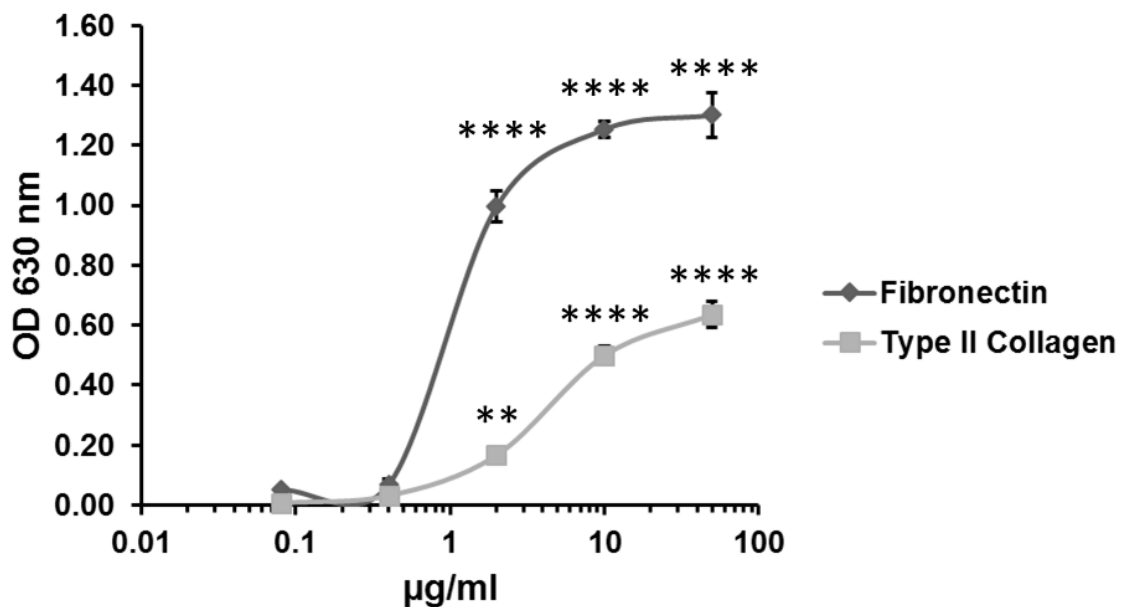


Figure 5.1 – Adhesion of non-induced ATDC5 cells to Fibronectin and Type II Collagen at different concentrations. Non-induced ATDC5 cells were allowed to adhere to either fibronectin or type II collagen for 60 min and non-adhered cells were washed off. Results expressed as average absorbance at OD 630 nm of methylene blue staining, normalised to adhesion to BSA. Significance tested by ANOVA + Dunnett post-hoc test compared to 0.08 $\mu\text{g/ml}$ substrate. N=4

5.2.2 Type II Collagen substrate impedes non-induced ATDC5 random migration

To investigate the ability for non-induced ATDC5 cells to randomly migrate, time-lapse microscopy was used to observe and measure the speed of migration on plastic, fibronectin and on type II collagen in the presence of 0.2 % FCS. This was calculated based on the tracking of 20 individual cells per condition, frame by frame, on different matrix substrates over 17 hours, with images taken every 10 min. For more detailed information, please see section 2.8.

Non-induced ATDC5 cells migrated more slowly on type II collagen than on plastic or fibronectin (Figure 5.2). This result was seen consistently across three experiments comparing plastic to type II collagen and in three out of four experiments comparing fibronectin to type II collagen. The comparison between plastic and fibronectin was only made once as results were not significantly different. Additionally, the use of 0.2 % FCS provided a fibronectin-containing matrix. Together, these data suggest that type II collagen impedes random two-dimensional migration in non-induced cells.

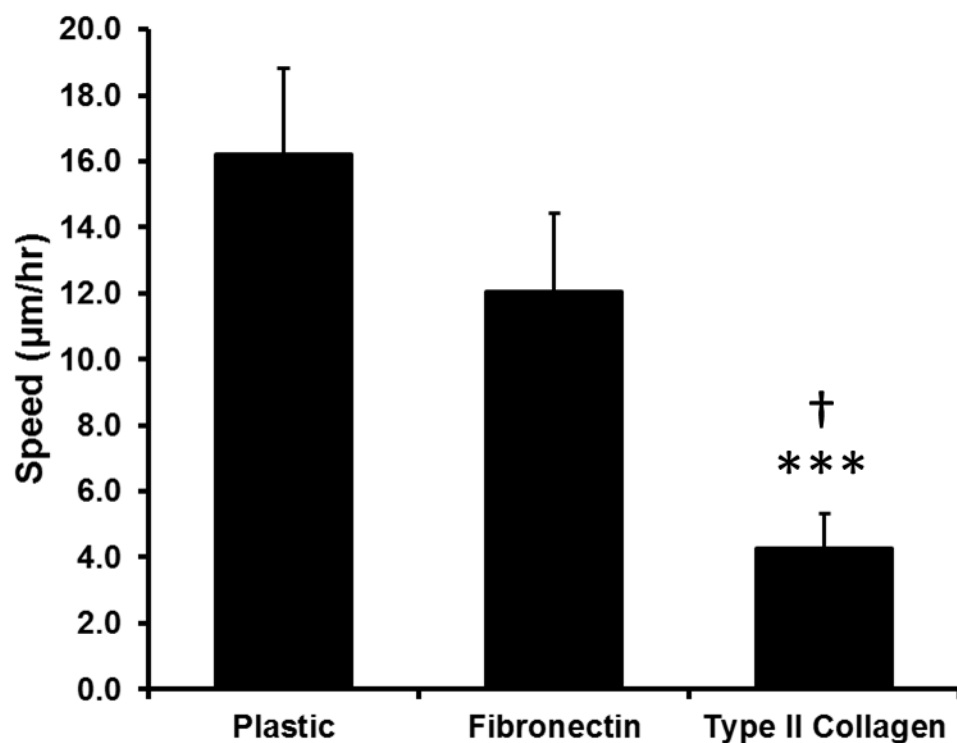


Figure 5.2 – Non-induced ATDC5 random migration. Non-induced ATDC5 cells were plated on either plastic, 10 µg/ml fibronectin or 50 µg/ml type II collagen, all in the presence of 0.2 % FCS for 17 hours. Data expressed as average cell speed over 17 hours, tracking 20 cells across quadruplicate wells. Plastic to fibronectin comparison performed once. Type II Collagen to plastic or fibronectin comparisons performed three and four times respectively.

* = significant compared to Plastic

† = significant compared to Fibronectin

5.2.3 Differentiated ATDC5 cells are less migratory than undifferentiated cells

Cells isolated using trypsin from insulin-induced ATDC5 cells cultured in micromass and stimulated with ascorbic acid were allowed to randomly migrate over 17 hours on plastic or on type II collagen in media containing 0.2 % FCS. Non-induced cells which had been maintained in their undifferentiated state were used as a comparison as described previously. For more detailed information, please see section 2.8.

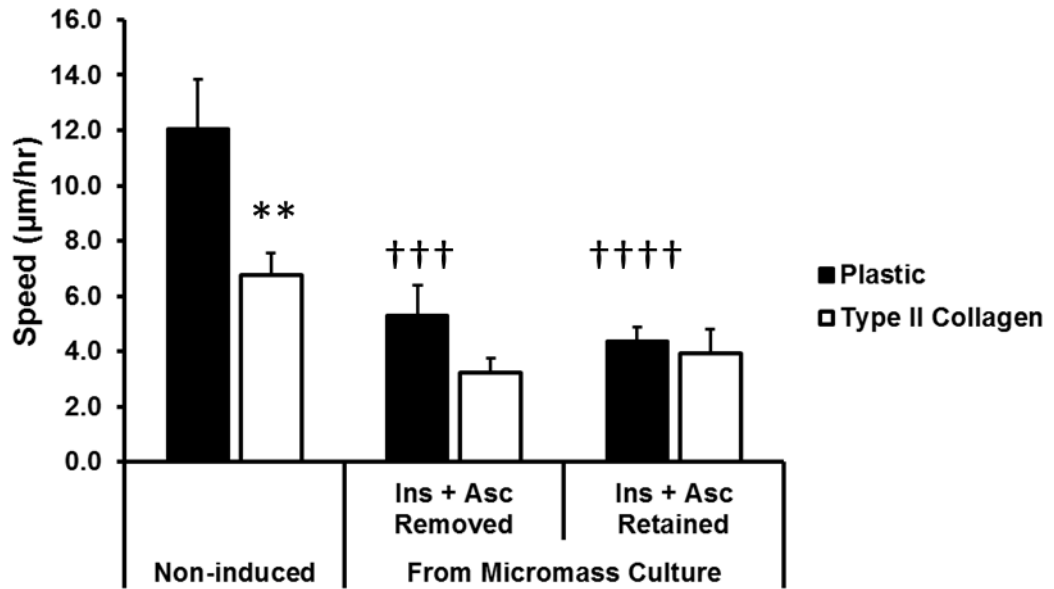
ATDC5 cells isolated from induced micromass cultures were significantly slower than non-induced cells on plastic. No significant reduction in speed was seen in two out of three experiments when micromass-isolated cells were plated on type II collagen compared to non-induced cells. Non-induced cells were also significantly slower when migrating on type II collagen compared to plastic. Removal of insulin and ascorbic acid from differentiated cells had no effect on the average speed (Figure 5.3 A).

At the end of the migration assay, 21 hours after isolating cells from differentiated micromass cultures, cells had retained their differentiated status, as noted by significantly higher levels of *Col2a1* compared to undifferentiated cells. Interestingly, micromass-isolated cells which were kept in differentiating medium (insulin and ascorbic acid) had lower expression of *Col2a1* compared to cells which had insulin and ascorbic acid removed (Figure 5.3 B). However, this change in *Col2a1* expression was only seen once in cells plated on plastic, compared to consistently across three experiments when plated on type II collagen.

On plastic, non-induced cells were flat and spread throughout the time-course (Figure 5.4 A-B). Cells isolated from micromass cultures began with a slightly more round, less spread morphology, which became flatter and more spread with time (Figure 5.4 C-F). On type II collagen, most cells from all conditions started with a round, unspread morphology, with those coming from non-induced cells exhibiting slightly more spread cells (Figure 5.5 A, C, E). With time on type II collagen, some cells from all conditions became flatter and more spread (Figure 5.5 B, D, F).

These results indicate that differentiated ATDC5 cells are less migratory than non-induced, undifferentiated cells.

A



B

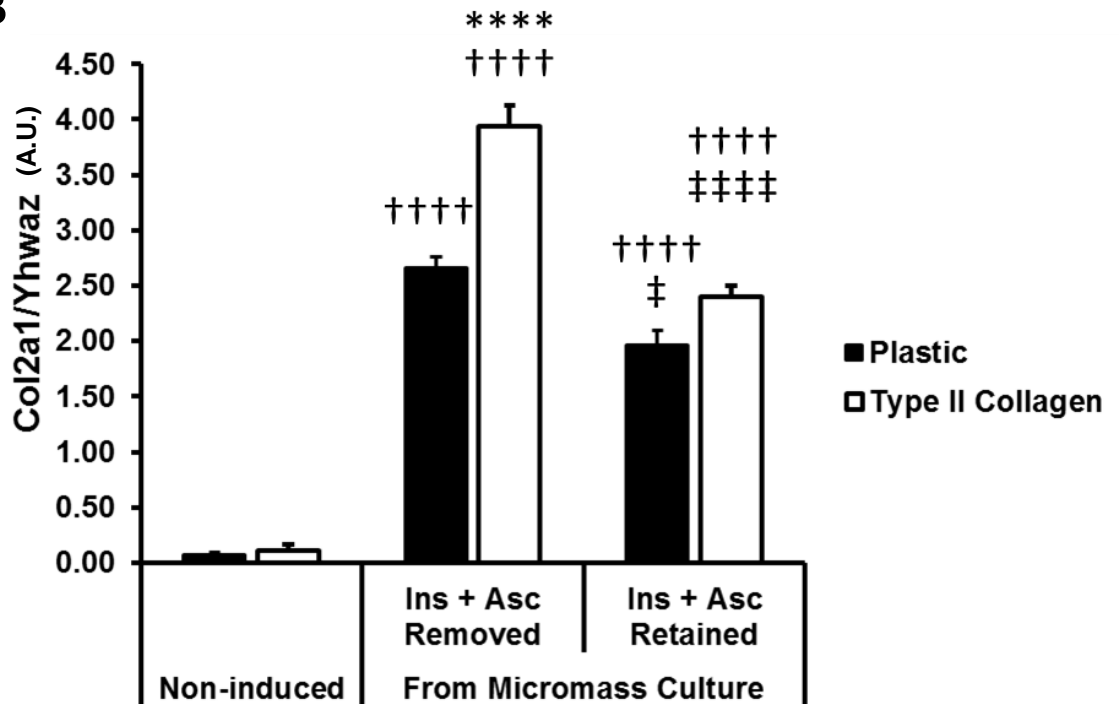


Figure 5.3 – Comparison of speed in randomly migrating undifferentiated and differentiated ATDC5 cells. A) Average speed in $\mu\text{m/hr}$ of ATDC5 cells isolated from 14-day insulin-induced, ascorbic acid-stimulated micromass cultures, with (Ins + Asc Retained) and without (Ins + Asc Removed) insulin and ascorbic acid was compared to non-induced, undifferentiated cells migrating on plastic or type II collagen in media containing 0.2 % FCS over 17 hours, tracking 20 cells across quadruplicate wells. B) Expression of *Col2a1* after tracking migration of cells used in A, normalised to *Yhwaz* expression.

* = significant compared to Plastic

† = significant compared to Non-induced

‡ = significant compared to Ins + Asc Removed

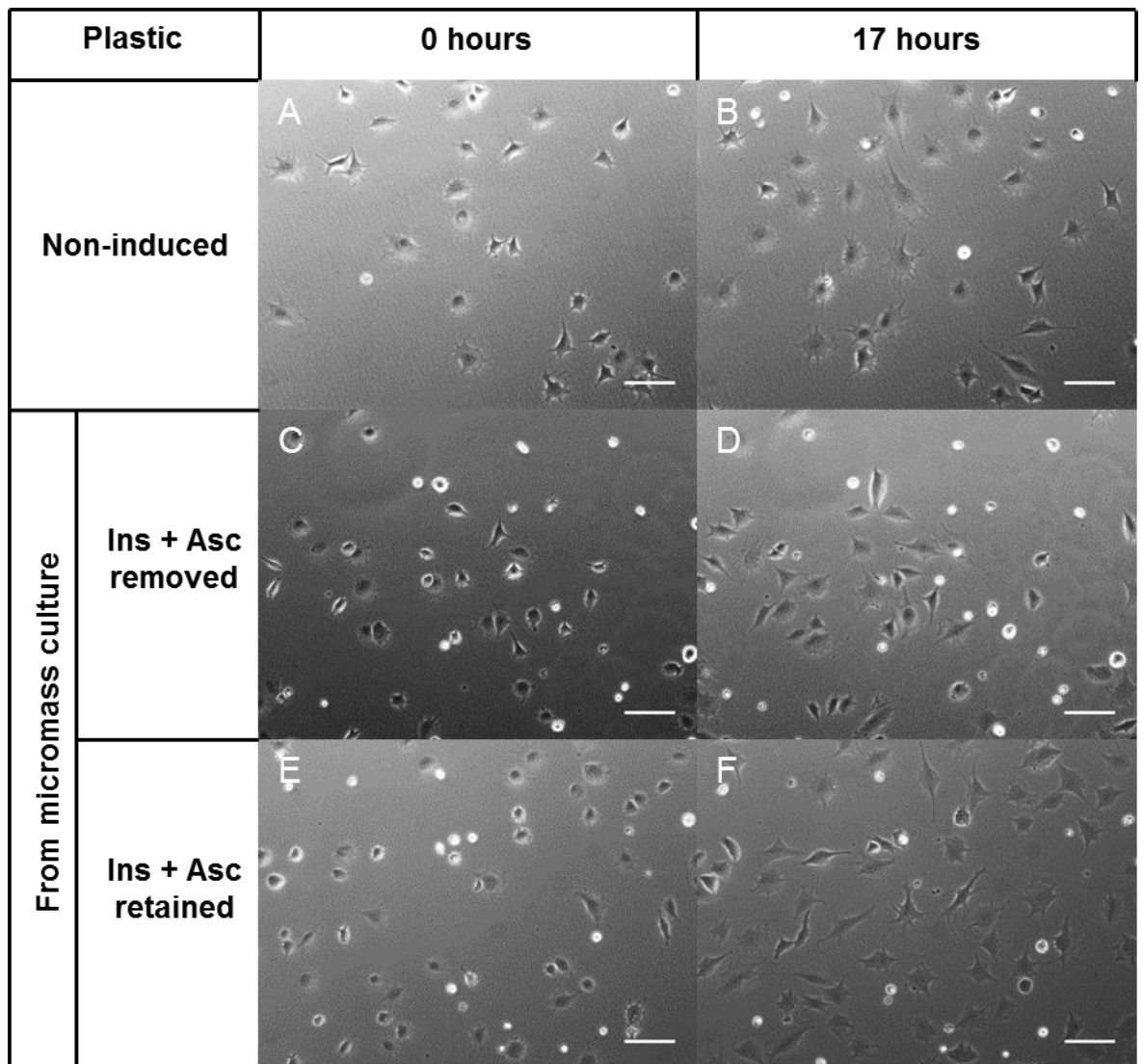


Figure 5.4 – Morphological differences on plastic over time after isolating cells from differentiated micromass cultures. ATDC5 cells were isolated from 14-day insulin-induced micromass cultures stimulated with ascorbic acid and plated onto plastic in the presence of 0.2 % FCS. A-B) Non-induced ATDC5 cells obtained from maintained monolayer cultures. C-D) ATDC5 cells isolated from micromass cultures with removal of insulin and ascorbic acid from medium before plating (Ins + Asc Removed). E-F) ATDC5 cells isolated from micromass cultures retaining insulin and ascorbic acid in the media over the 17 hours (Ins + Asc Retained). Images shown are from 0 hours from time-lapse analysis (4 hours after isolation)(A,C,E), or at 17 hours at the end of the time-lapse analysis (21 hours after isolation) (B,D,F). Scale = 100 μ m

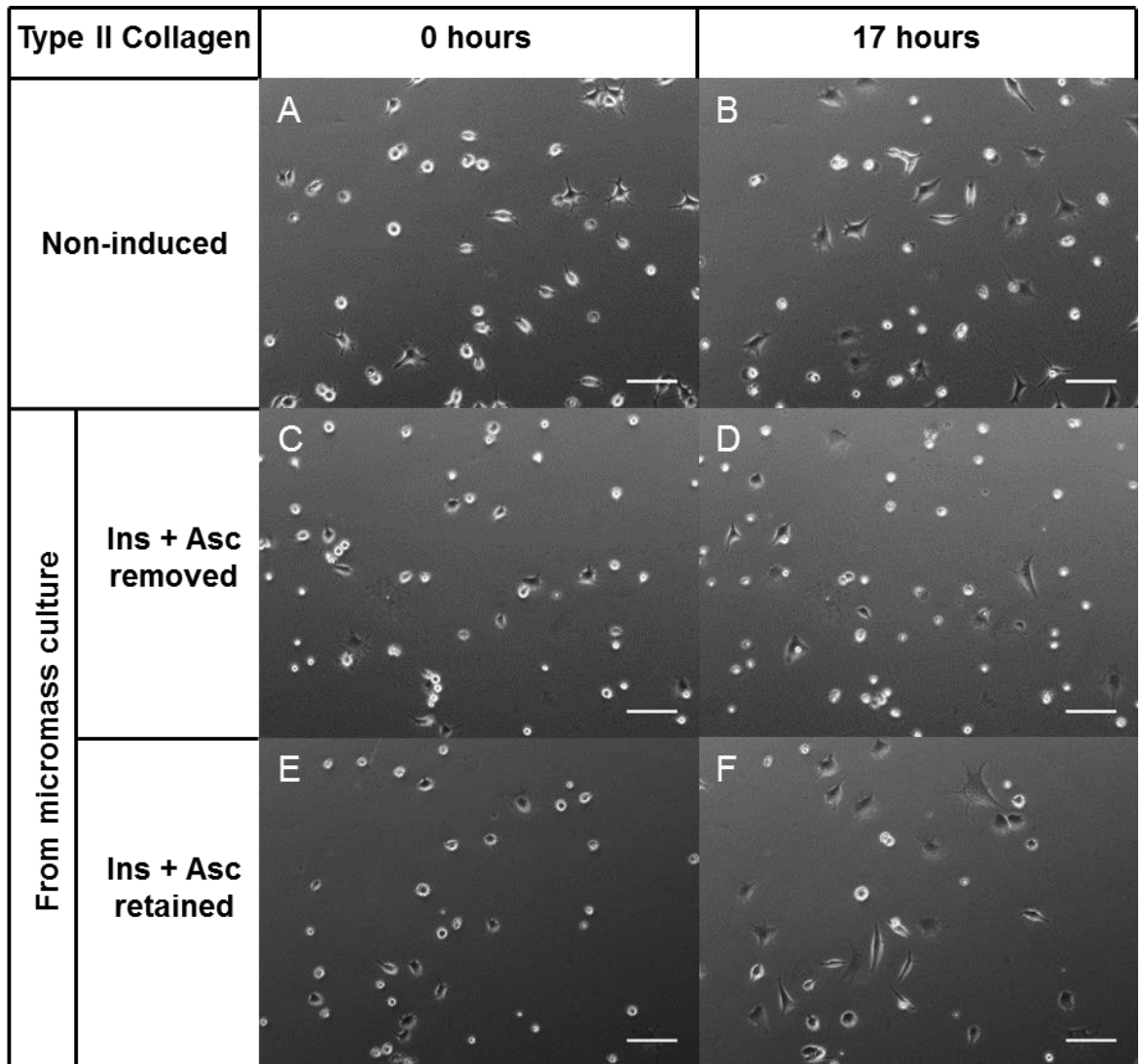


Figure 5.5 – Morphological differences on type II collagen over time after isolating cells from differentiated micromass cultures. ATDC5 cells were isolated from 14-day insulin-induced micromass cultures stimulated with ascorbic acid and plated onto 50 $\mu\text{g/ml}$ type II collagen in the presence of 0.2 % FCS. A-B) Non-induced ATDC5 cells obtained from maintained monolayer cultures. C-D) ATDC5 cells isolated from micromass cultures with removal of insulin and ascorbic acid from medium before plating (Ins + Asc Removed). E-F) ATDC5 cells isolated from micromass cultures retaining insulin and ascorbic acid in the media over the 17 hours (Ins + Asc Retained). Images shown are from 0 hours from time-lapse analysis (4 hours after isolation)(A,C,E), or at 17 hours at the end of the time-lapse analysis (21 hours after isolation) (B,D,F). Scale = 100 μm

5.2.4 Effect of WNT stimulation on non-induced ATDC5 migration

Potential modulation of migration in non-induced ATDC5 cells by WNT stimulation was explored by stimulating ATDC5 cells at the start of the 17 hour migration period with either WNT3A (thought to typically induce canonical wnt signalling), or WNT5A (thought to typically induce non-canonical wnt signalling) conditioned media generated from transiently overexpressing ATDC5 cells, in the presence of 0.2 % FCS. For more information, please see section 2.8.

By pairwise comparison, no modulation of migration was seen by WNT5A stimulation regardless of substrate (Figure 5.6 A). However, a small but significant increase was seen in the speed of migration when cells were stimulated with WNT3A conditioned medium compared to Vector Only medium when plated on type II collagen (Figure 5.6 B).

Comparisons were also made when stimulating the cells with and without cytokines to represent an osteoarthritic-like context. However, data between some conditions were inconsistent when cytokines were present and so are not shown, although WNT5A was seen to decrease the speed of migration compared to WNT3A in the presence of cytokines when plated on type II collagen across two experiments (Appendix Figure S5.1).

However, it should be noted that due to time constrictions, only two experiments were performed, so more experiments are needed to confirm any changes or lack thereof.

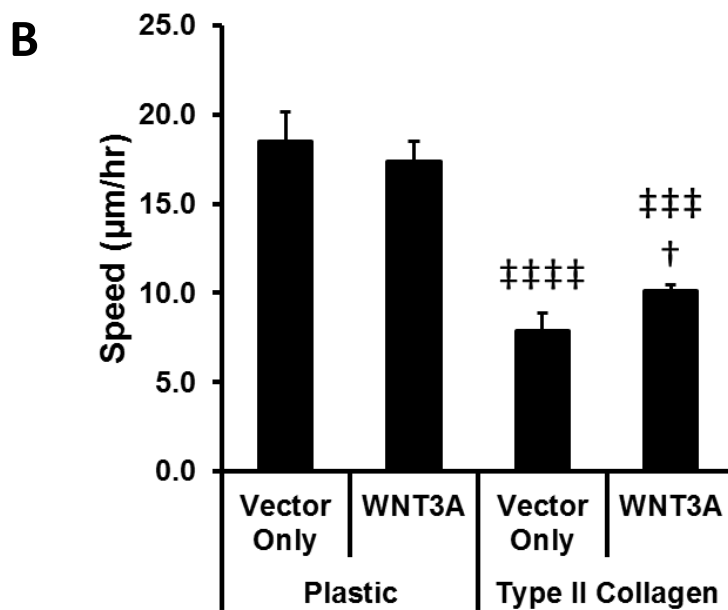
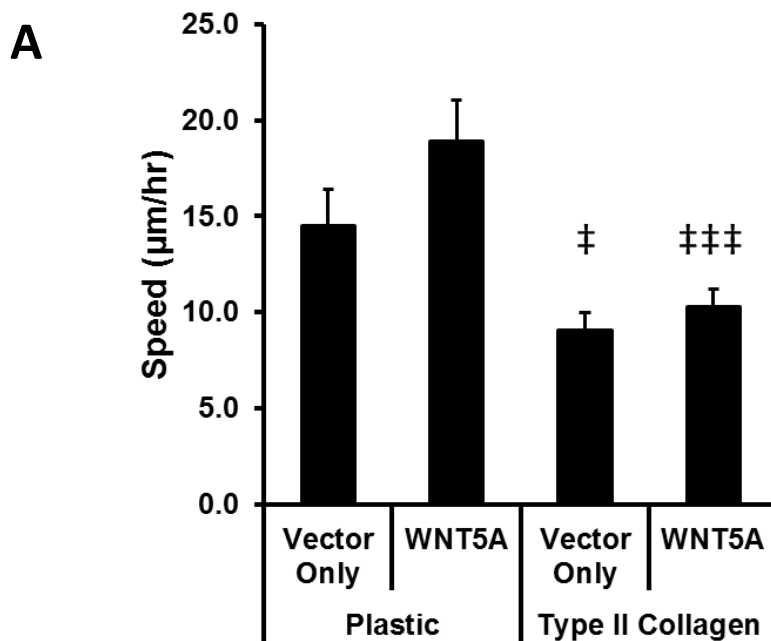


Figure 5.6 – Effect of WNT5A and WNT3A stimulation on non-induced ATDC5 migration. Non-induced ATDC5 cells were plated on either plastic or type II collagen, both in the presence of 0.2 % FCS and stimulated with WNT5A conditioned medium (A), or WNT3A conditioned medium (B) for 17 hours. Data expressed as average cell speed over 17 hours, tracking 20 cells across quadruplicate wells. Experiment performed twice, with one example shown, displaying consistent changes.

† = significant compared to Vector Only

‡ = significant compared to Plastic

5.2.5 Modelling chondroprogenitor cell invasion through cartilage

No effect was observed in random migration assays due to WNT5A stimulation compared to the Vector Only conditioned medium control, indicating that the WNT5A conditioned medium used did not act as a chemokinetic agent. Therefore the potential ability to act as a chemoattractant to non-induced ATDC5 cells was investigated.

To investigate this in a more physiologically-relevant environment, non-induced ATDC5 cells (plated on the underside of a transwell) were allowed to invade towards a gradient of WNT5A conditioned medium through methanol-fixed, insulin-induced and ascorbic acid-stimulated micromasses (in the upper chamber of the transwell) that had been previously stimulated with or without cytokines for 48 hours at the end of the 14-day chondrogenesis induction period to simulate osteoarthritic-like cartilage prior to fixation. For a more in-depth description of this novel assay, please see section 2.9.

All conditions exhibited some invasion, with non-induced cells commonly featuring extended cells processes found in invading cells (Zamora, *et al.*, 1980; Witz, *et al.*, 2003) (Figure 5.7 arrows), indicating that non-induced ATDC5 chondroprogenitor cells are able to invade through a cartilage-like matrix.

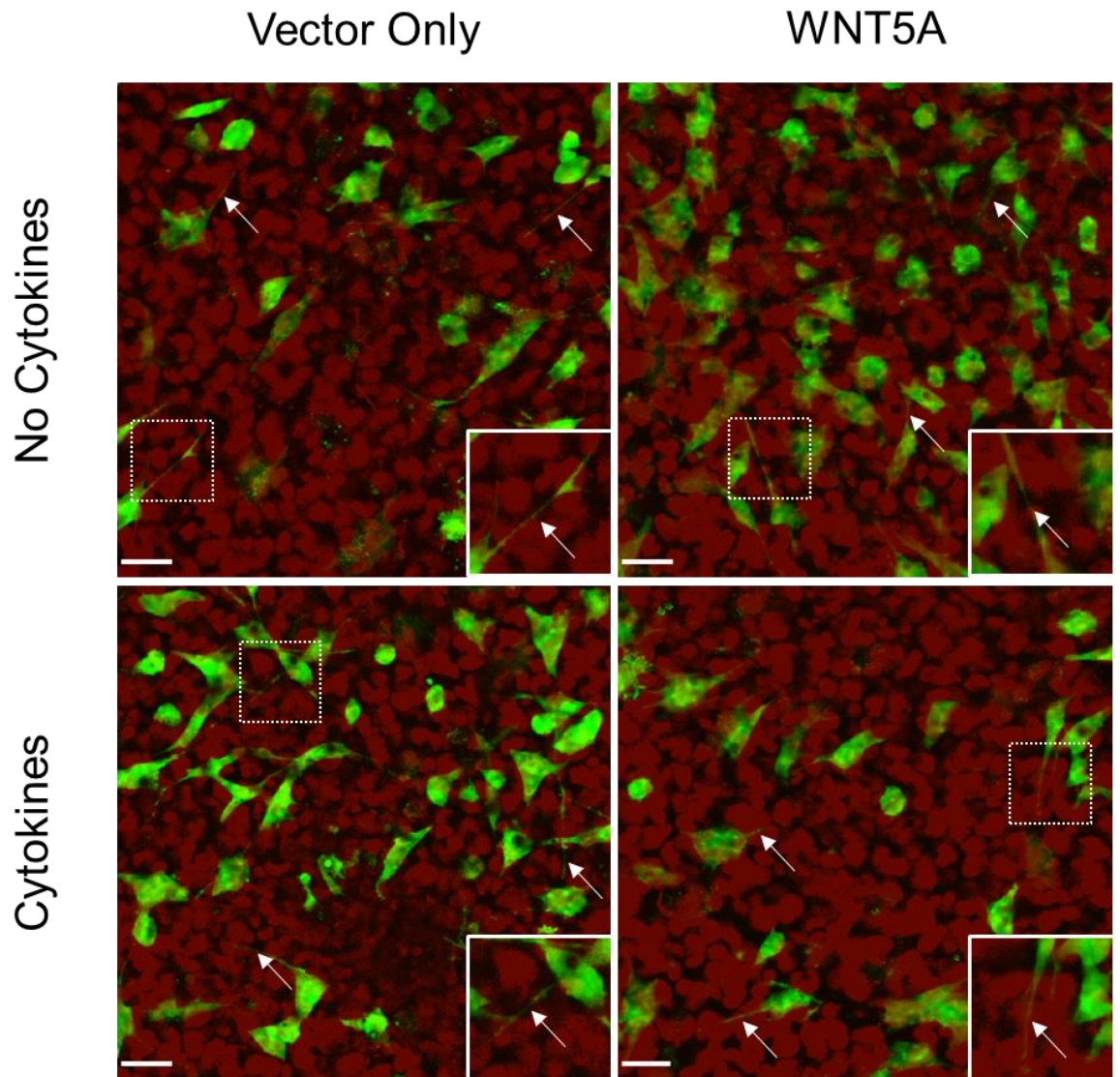


Figure 5.7 – Extended focus comparison of non-induced ATDC5 cells invading towards WNT5A. Non-induced ATDC5 cells were allowed to invade towards WNT5A conditioned medium (or Vector Only control) for 48 hours through methanol-fixed 14-day insulin/ascorbic acid-treated micromass cultures which had previously been stimulated with or without IL-1 α and OSM cytokines for 48 hours. Fixed and dead cells were stained with ethidium homodimer-1 (red) and live cells were stained with calcein-AM (green). Optical sections were taken every 2 μ m and images shown are an extended focus view, compressing all sections into one image with a top-down perspective, with a higher WNT5A concentration above the image and lower concentration through the image). White arrows show extended cell processes. Inserts = magnified image of dotted area highlighting an extended cell process. Scale = 50 μ m

When micromasses had not previously been stimulated with cytokines, a trend towards increased invasion towards WNT5A conditioned medium was observed in two out of three experiments, although this did not reach significance (Figure 5.8). Cytokine pre-stimulation of the micromass cultures before invasion resulted in a decrease of invasion towards WNT5A conditioned medium, but not towards the Vector Only control, likely due to the slight increase in invasion exhibited towards WNT5A in micromass cultures which were not pre-stimulated with cytokines (Figure 5.8). This may suggest that any potential chemoattractive ability of WNT5A on non-induced ATDC5 cells may be dependent on an intact matrix.

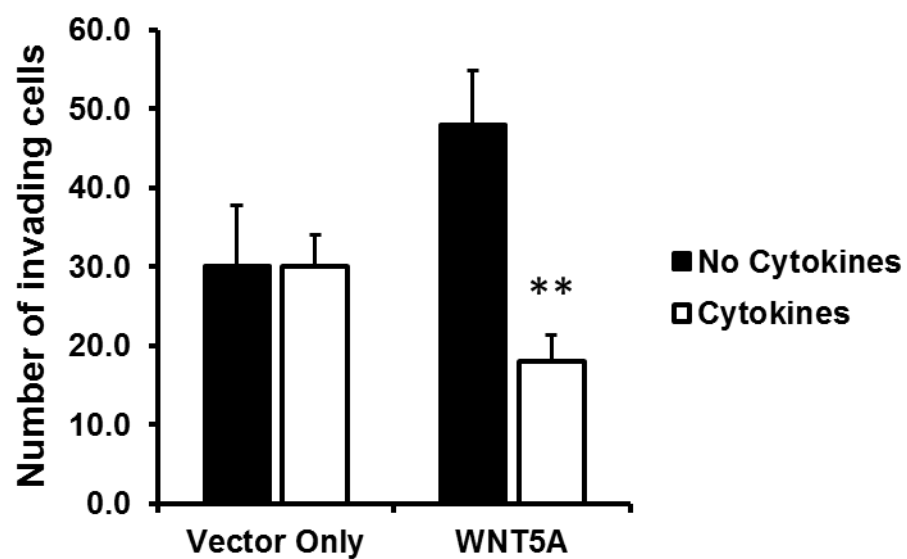


Figure 5.8 – Identifying the potential chemoattractive ability of WNT5A on non-induced ATDC5 cells invading through fixed differentiated micromass cultures. Non-induced ATDC5 cells were allowed to invade for 48 hours through methanol-fixed 14-day, insulin/ascorbic acid stimulated micromass cultures that had previously been stimulated with or without cytokines for 48 hours. Results expressed as number of invading cells above transwell membrane. Experiment performed three times with representative experiment shown. * = significant compared to No Cytokines.

To explore further the trend of increased invasion towards WNT5A, recombinant human (rh)WNT5A was used (a kind gift from Dr. Victoria Sherwood, UEA) instead of WNT5A conditioned medium, using a carrier control (0.1 % BSA stock). In line with results obtained from conditioned media, rhWNT5A led to a slight increase in invasion through micromass cultures that had not been previously stimulated with cytokines, however, this again did not reach significance (Figure 5.9). Interestingly, invasion was significantly increased towards rhWNT5A when micromass cultures were pre-stimulated with cytokines, in contrast to the results seen in Figure 5.8, which reflect interaction of WNT5A with other ATDC5 media constituents in the conditioned medium experiment. However, it should be noted that this experiment was only performed once and further repeats are needed.

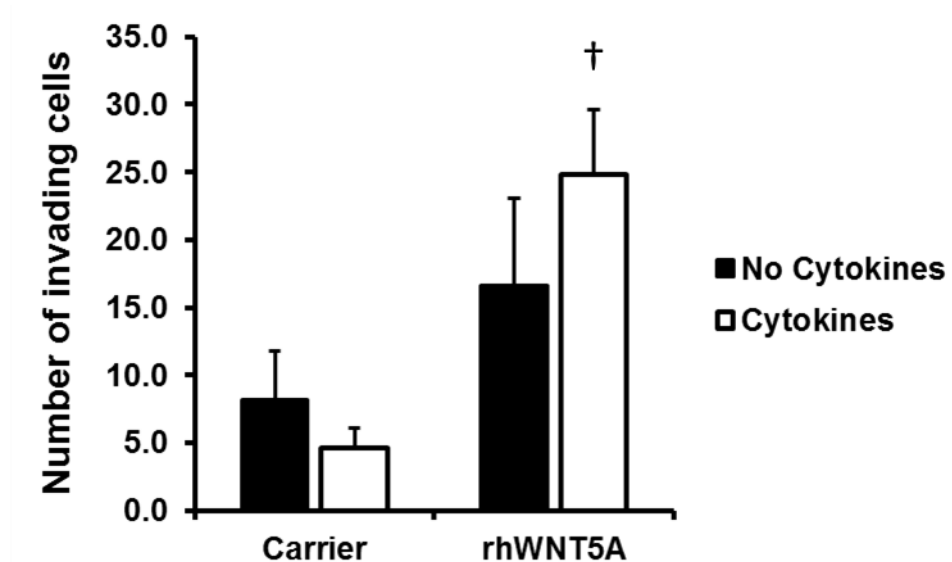


Figure 5.9 – Confirming invasion of non-induced ATDC5 cells through fixed micromass cultures using rhWNT5A. Non-induced ATDC5 cells were allowed to invade for 48 hours through methanol-fixed 14-day, insulin/ascorbic acid stimulated micromass cultures that had previously been stimulated with or without cytokines for 48 hours towards rhWNT5A or Carrier control. Results expressed as number of invading cells above transwell membrane. Experiment performed once. † = significant compared to Carrier.

5.3 Discussion

5.3.1 Non-induced ATDC5 cells adhere better to fibronectin than to type II collagen

In a short-term adhesion assay, more non-induced ATDC5 cells adhered to fibronectin than to type II collagen, with maximal adhesion occurring at a lower concentration of fibronectin compared to type II collagen (Figure 5.1). These data agree with studies where both human and bovine chondroprogenitor cells isolated from the superficial zone of articular cartilage have an enhanced ability to adhere to fibronectin compared to mature chondrocytes and can be selected by this adhesion potential (Dowthwaite, *et al.*, 2004; Williams, *et al.*, 2010).

Little work has been conducted investigating the adhesion of chondroprogenitor cells to type II collagen. In contrast to this thesis, it has previously been reported that chondroprogenitor cells isolated from human osteoarthritic cartilage adhered equally well to both fibronectin and type II collagen (Koelling, *et al.*, 2009) plated at 10 $\mu\text{g}/\text{cm}^2$, which would be the equivalent of a concentration of 36 $\mu\text{g}/\text{ml}$ if used in this study. By interpolation at this concentration, roughly a two-fold difference was seen in this thesis (Figure 5.1). However, it is not known how long the cells were allowed to adhere in the Koelling study, which could allow for increased adhesion if cells were allowed to adhere over a longer time period. Furthermore, as previously noted, these cells were isolated from human osteoarthritic cartilage. It would therefore be interesting to see if the same results were seen in human non-OA chondroprogenitor cells or if a difference would be seen in cytokine-challenged ATDC5 cells. Additionally, the chondroprogenitor cells were isolated from the cartilage based on their ability to migrate away from the explant culture rather than their enhanced ability to adhere to fibronectin.

Similarly in another study, chondrocytes extracted from calf patellae by collagenase II digestion exhibited similar adhesion to both type II collagen and fibronectin (Schmal, *et al.*, 2006). However, upon sequential passaging, which induces de-differentiation of chondrocytes, P2 chondrocytes exhibited increased adhesion to fibronectin and a decreased adhesion to type II collagen compared to P0 chondrocytes cultured for 3 days, resulting in roughly a five-fold increase in adhesion to fibronectin compared to type II collagen in the P2 chondrocytes (Schmal, *et al.*, 2006). This suggests that chondrocyte adhesion to matrix components may depend on the differentiated status of cell. Since the ATDC5 cells used in this thesis were non-induced, the preference for fibronectin compared to type II collagen would correlate with the findings in this study, although adhesion using insulin-induced ATDC5 cells was not tested to see how this might change with differentiation.

5.3.2 Type II Collagen impedes the speed of migration

Non-induced cells migrating on fibronectin showed a similar migratory speed averaged over 17 hours to those migrating on plastic. Migration studies however were performed in the presence of 0.2 % FCS, which is known to contain various ECM components, including fibronectin (Hayman & Ruoslahti, 1979). Cells migrating on type II collagen migrated significantly more slowly compared to those migrating on fibronectin (Figure 5.5). Figure 5.1 showed that non-induced ATDC5 cells adhere significantly more to fibronectin than to type II collagen. This may partly explain the decrease in migration observed on type II collagen in Figure 5.5. It is known that cells require an optimal strength or amount of adhesion to the substratum to promote migration; too strong or too much adhesion and cells may be unable to detach their rear end from the substratum efficiently to move forward, potentially immobilising the cell; too weak or too little adhesion and there may not be enough traction for the cells to pull themselves forward, generating a biphasic dependence on adhesion for migration to occur (DiMilla, *et al.*, 1993; Palecek, *et al.*, 1997; Ware, *et al.*, 1998; Cox, *et al.*, 2001).

5.3.2.1 DDR2

Since a reduction in migration was observed by type II collagen, it is relevant to consider the type II collagen-binding receptor, DDR2. This thesis has shown that at the protein level, DDR2 was down-regulated with increasing chondrogenesis in ATDC5 cells (Figure 3.16). DDR2 is known to bind to both types I and II collagen (Leitinger, *et al.*, 2004; Konitsiotis, *et al.*, 2008). Knockdown of DDR2 in fibroblasts has been shown to decrease migration both in 2D and 3D using a type I collagen matrix (Herrera-Herrera & Quezada-Calvillo, 2012; Ruiz & Jarai, 2012; Kim, *et al.*, 2013a), and antibody-mediated inhibition of DDR2 has been shown to decrease chemotactic migration to IL-8 in neutrophils (Afonso, *et al.*, 2013). Overexpression in HEK293 cells has been shown to increase adhesion to type I collagen and activation of DDR2 can promote $\alpha 1\beta 1$ and $\alpha 2\beta 1$ integrin activation and mediated adhesion (Xu, *et al.*, 2012). Conversely, no significant differences were found in adhesion and migration on type I collagen between *Ddr2*^{+/+} and *Ddr2*^{-/-} smooth muscle cells. However, the importance of DDR2 and adhesion to or migration on type II collagen in chondrocytes remains to be elucidated. It would therefore be interesting to investigate differences in adhesion and migration to type II collagen by modulating DDR2 expression in ATDC5 cells.

5.3.3 The differentiated state of ATDC5 cells affects the migratory potential

This study has shown that non-induced ATDC5 cells have a migratory phenotype. In accordance with this, faster migrating ATDC5 cells were flat and spread, exhibiting extended processes associated with a migratory phenotype (Figure 5.4 A-B). However, ATDC5 cells isolated from

differentiated micromasses migrated more slowly (Figure 5.3 A). Many of these cells were rounded, representative of the chondrocytic phenotype, which became flatter and more spread with time. Although flat spread cells are less reminiscent of the chondrocytic phenotype, qRT-PCR analysis revealed that at the end of the 17 hour migration assay, 21 hours after isolation, these cultures still expressed large amounts of *Col2a1* compared to non-induced cells, indicating these cells were still differentiated (Figure 5.3 B). Whilst it is known that chondrocytes begin to de-differentiate upon isolation and passaging in monolayer culture, this process is still time dependent. Previous studies have shown isolated chondrocytes migrating across a transwell membrane retain their differentiated status (Chang, *et al.*, 2003) and that morphological differences are not enough to distinguish de-differentiation (von der Mark, *et al.*, 1977; Benya, *et al.*, 1988; Chang, *et al.*, 2003).

Chondroprogenitor cells, which are not fully differentiated into chondrocytes (Koelling, *et al.*, 2009; Zhou, *et al.*, 2014), are a subpopulation of cells that reside within cartilage (Dowthwaite, *et al.*, 2004; Koelling, *et al.*, 2009; Seol, *et al.*, 2012; Matta, *et al.*, 2014). These cells, which are enriched in osteoarthritic cartilage (Alsalameh, *et al.*, 2004), can be isolated from osteoarthritic cartilage based on their ability to migrate away from cartilage explant cultures (Koelling, *et al.*, 2009; Joos, *et al.*, 2013; Matta, *et al.*, 2014), as well as their increased adhesion to fibronectin (Dowthwaite, *et al.*, 2004; Seol, *et al.*, 2012). The migratory and adhesive phenotype of non-induced undifferentiated ATDC5 cells in this study is therefore reminiscent of the migratory and adhesive phenotype of primary chondroprogenitors.

Since non-induced ATDC5 cells have a migratory phenotype similar to primary chondroprogenitor cells compared to insulin-induced ATDC5 cells, and that chondroprogenitor cells are enriched in osteoarthritic cartilage and are able to elicit a migratory response to damage signals, only non-induced ATDC5 cells were used in further experiments investigating migration.

5.3.3.1 Aquaporin-1

As previously discussed, adhesion to type II collagen, and subsequently possibly migration, may depend on the differentiated status of the cell, with a negative correlation between the differentiated state of the cell and its ability to adhere to type II collagen previously reported (Schmal, *et al.*, 2006).

A decrease in adhesion to type II collagen has also been reported in aquaporin-1 knockout (*Aqp1*^{-/-}) primary mouse articular chondrocytes (Liang, *et al.*, 2008). Aquaporin-1 is part of the aquaporin family of membrane proteins involved in water transport, and sometimes small solutes such as glycerol, across the cell membrane (Verkman, 2005; Monzani, *et al.*, 2009). Aquaporin-1 has also

been shown to modulate cell migration, such that overexpression increases migration and/or knockdown decreases migration in a number of cell types, including a human melanoma cell line (Monzani, *et al.*, 2009), human and mouse endothelial cells (Saadoun, *et al.*, 2005; Monzani, *et al.*, 2009), a human glioblastoma cell line (McCoy & Sontheimer, 2007), rat BMSCs (Meng, *et al.*, 2014) and mouse articular chondrocytes (Liang, *et al.*, 2008). It has been proposed that aquaporins enhance cell migration due to a local increase in hydrostatic pressure due to water influx which may cause membrane protrusions associated with migration, creating space for actin polymerisation (Verkman, 2005). In rat BMSCs, it was reported that aquaporin-mediated migration was via the focal adhesion kinase (FAK) and β -catenin pathways, which in addition to its role in the canonical WNT signalling pathway, is also important in modulation of the actin cytoskeleton, linking actin at the cell surface via α -catenin (Meng, *et al.*, 2014).

A recent study showed mRNA levels of *AQP1* significantly increased with increasing chondrogenesis in differentiating human MSCs (Ishihara, *et al.*, 2014). In insulin-induced ATDC5 cells, *Aqp1* was significantly up-regulated at the early stages of chondrogenesis, reaching peak expression after 3-4 days of insulin-induction, corresponding with the very early increases in *Col2a1* expression, but decreased in expression from days 4-11 as *Col2a1* expression reached its peak expression (Ishihara, *et al.*, 2014). These results suggest that aquaporin-1-mediated plasma membrane water permeability may play a role in chondrocyte migration and adhesion, and the differences in migration seen between non-induced and induced cells may be due in part to the different levels of aquaporin-1 in differentiating chondrocytes. It would therefore be interesting to compare the levels of *Aqp1* in the isolated ATDC5 chondrocytes from the micromass cultures to the non-induced ATDC5 chondroprogenitor cells to see whether these correlated with the differences in migration.

5.3.4 Modulation of migration and invasion by WNT5A and WNT3A

Stimulation of non-induced ATDC5 cells with WNT5A conditioned medium did not modulate the speed of migration regardless of substratum (Figure 5.6 A). On type II collagen, speed of migration was increased by stimulation with WNT3A conditioned medium (Figure 5.6 B). Additionally, in the presence of cytokines, WNT5A impeded the speed migration compared to WNT3A conditioned medium (Appendix Figure S5.1).

In contrast, a non-significant trend to increase in invasion towards WNT5A conditioned medium was observed when non-induced ATDC5 cells were allowed to invade through differentiated micromass cultures (Figure 5.8). When rhWNT5A was used to validate these findings, a significant increase was seen when micromasses had been pre-stimulated with cytokines along with the similar trend towards increased invasion when micromass cultures had not been pre-stimulated

(Figure 5.9), suggesting a potential ability of WNT5A to act as a chemokinetic agent for chondroprogenitor cells. Given that rhWNT5A promoted invasion in the one experiment performed, it would be interesting to see if rhWNT5A also modulated 2D migration, to confirm whether the lack of significant effects with WNT5A conditioned medium is real or due to a lack of activity of the generated WNT5A. Further experiments are also needed to validate the potential chemokinetic ability of rhWNT5A and whether a higher concentration may further enhance this. Additionally, non-induced ATDC5 cells were not observed to invade far beyond the transwell filter and so longer periods of invasion may result in greater differences between conditions, leading to more significant results.

As previously discussed, WNT5A has been known to both positively and negatively regulate migration in a variety of cells (see section 5.1). Similarly, WNT3A is known to regulate migration in a number of cell types. For example, stimulation with WNT3A promoted migration of trophoblast cells in a transwell assay (Sonderegger, *et al.*, 2010) and inhibition of WNT3A has been shown to decrease migration of glioma stem cells (Kaur, *et al.*, 2013). WNT3A has also been reported to act as a chemoattractant, promoting migration of HUVECs in a transwell assay across a WNT3A gradient (Samarzija, *et al.*, 2009).

Little data has been reported investigating the roles of WNT5A or WNT3A in the migration or invasion of chondrocytes or chondroprogenitor cells. However, there are several reports of migration modulated by WNT5A/WNT3A non-canonical/canonical signalling in MSCs, which are capable of differentiating into chondrocytes and share a similar transcriptomic phenotype with chondroprogenitor cells (Seol, *et al.*, 2012). WNT3A has been shown to increase migration of rat BMSCs in a scratch assay and act as a chemoattractant in a transwell assay (Shang, *et al.*, 2007). Similarly, treatment of mouse BMSCs with WNT3A has been shown to increase migration towards FCS and acute lung injury extracts (Liu, *et al.*, 2013a). However, another paper reported a *decrease* in invasion across a matrigel-coated transwell of mouse BMSCs pre-treated with WNT3A migrating towards mouse serum (Karow, *et al.*, 2009). The differences seen in the modulation of migration and invasion may therefore be due to different experimental approaches despite both groups using mouse BMSCs, suggesting that the use of matrigel or the different types of serum may interact or interfere with the canonical WNT signalling pathway.

Conversely, the same group reporting a decrease in invasion had previously reported an increase in invasion of human MSCs pre-treated with WNT3A invading through human placental ECM towards human serum (Neth, *et al.*, 2006), and suggest the differences seen between mouse and human MSCs may be partially explained by the differential regulation of MT1-MMP, known to

modulate cell migration and invasion (reviewed in Seiki, *et al.* (2003)), which was down-regulated in mouse MSCs but no significant differences were seen in human MSCs when treated with WNT3A.

In comparison to WNT3A, less is known about the effect of WNT5A on MSC migration. However, one group has reported that migration was increased in mouse MSCs overexpressing either *Ror2* (a non-canonical WNT5A receptor) or *Cttnb1* (which encodes β -catenin), and decreased by shRNA inhibition (Cai, *et al.*, 2014).

Taken together, this indicates that both non-canonical and canonical WNT signalling may modulate migration in MSCs, both in a positive and negative manner. This thesis has extended this knowledge to the ATDC5 chondroprogenitor model, observing the ability for WNT5A to act as a potential chemoattractant (Figure 5.8) and WNT3A to act as a potential chemokinetic agent (Figure 5.6 B).

5.4 Summary

This thesis has identified that ATDC5 cells have an adhesive and migratory phenotype reminiscent of primary chondroprogenitor cells and chondrocytes, depending on the state of chondrogenesis. Additionally, it was found that type II collagen impedes the speed of 2D migration, which may have ramifications for the ability of chondroprogenitor cells to migrate *in vivo*.

This thesis also identified that WNT5A and WNT3A may act as potential chemoattractant and chemokinetic agents respectively in ATDC5 cells. Since WNT5A is known to promote early-stage chondrogenesis (Bradley & Drissi, 2010), is known to be expressed in osteoarthritic cartilage (Nakamura, *et al.*, 2005) and that chondroprogenitor cells migrate to sites of cartilage injury (Seol, *et al.*, 2012), it could be hypothesised that chondroprogenitor cells could be recruited to sites of osteoarthritic cartilage by WNT5A in an attempt to repair any damage, enhanced by the chemokinetic abilities of WNT3A, which is also expressed in osteoarthritic cartilage (Nakamura, *et al.*, 2005). However, further experiments are needed to confirm these effects on ATDC5 cells.

Regardless of the effect of WNT signalling, this thesis also described apparently for the first time a quantitative invasion model of chondroprogenitor cells invading through a cartilage-like matrix, by combining and building upon two techniques. Given that chondroprogenitor cells are known to migrate to sites of cartilage injury, this somewhat novel model may therefore be important in understanding the factors modulating chondroprogenitor cell translocation to help us further understand the events that occur during cartilage injury and osteoarthritis. A summary of all the findings from Chapter 5 can be found in Table 5.1.

Table 5.1 – Summary of the effect of various components on adhesion, migration and invasion of ATDC5 cells. Compiled using information from section 5.2. For more details on the individual experiments and conditions used, please refer to the original figures in section 5.2.

Component	Effect On...		
	Adhesion	Migration	Invasion
Fibronectin	↑ with increasing concentration		
Type II Collagen	↑ with increasing concentration	↓ compared to plastic	
Differentiated chondrocytes		↓ compared to undifferentiated cells	
WNT3A CM		↔	
WNT5A CM		↔	↔
Cytokine-treated micromass			↓ towards WNT5A gradient
rhWNT5A			↑

Chapter 6

General Discussion

6.1 General Discussion

Understanding chondrogenic differentiation and gene expression changes which relate to osteoarthritis require robust *in vitro* model systems to test relevant hypotheses to help further understand the mechanisms of the osteoarthritis and how the cartilage might attempt to repair itself.

In this thesis, data have been provided identifying the changes in gene and protein regulation during chondrogenic differentiation of the murine chondroprogenitor cell line, ATDC5. Data showed that this model of chondrogenesis could be further enhanced by combining techniques used for the culture of primary chondrocytes, producing a cartilage-like tissue that had similar expression patterns to articular cartilage previously reported.

These cultures were then used to investigate regulation of molecular pathways in both a physiological and disease-like context by stimulation with by exogenous factors or overexpression of WNT5A, leading to the identification of novel regulation of a number of genes.

Additionally, migration studies revealed that undifferentiated cells and differentiated cells had similar migratory phenotypes to the previously reported migratory phenotypes of primary chondroprogenitor cells and mature chondrocytes respectively. A novel method to model invasion by chondrocytic cells was also developed.

Together, this indicates that the ATDC5 cell line may be a good model for understanding many aspects of articular cartilage biology and pathology.

6.1.1 An enhanced ATDC5 chondrogenesis model

In chapter 3, data revealed that modification of the standard ATDC5 chondrogenesis model by culturing in a three-dimensional micromass culture, in combination with stimulation with ascorbic acid, enhanced chondrogenesis, producing a type II collagen- and proteoglycan-rich cartilage-like tissue in comparison to the heterogeneity observed with standard induction by insulin in monolayer which had large areas of undifferentiated cells surrounding differentiated nodules. An increase in *Col10a1* steady-state mRNA, a marker of chondrocyte hypertrophy, coincided with only small regions of type X collagen protein immunolocalisation within the central micromass cultures, whilst expression of other hypertrophy markers decreased, such as *Tgfb3*, *Ctgf* and DDR2. Furthermore, expression of *Frzb*, which is enriched in articular cartilage (Leijten, *et al.*, 2012), was significantly increased. Together, this suggests that the modified ATDC5 chondrogenesis model is an enhanced model, more reminiscent of articular cartilage compared to growth plate cartilage. This makes the

enhanced ATDC5 chondrogenesis model a suitable and desirable model for investigating osteoarthritis-related changes, a disease characterised by the degradation of articular cartilage and not growth plate cartilage.

Nevertheless, it has been reported that a more growth plate/hypertrophic cartilage-like tissue can also be obtained by adapting the culturing conditions in monolayer, including culturing for longer periods of time, reducing CO₂ levels and switching medium to α -MEM (Shukunami, *et al.*, 1997; Swingler, *et al.*, 2012), indicating the adaptability and usefulness of ATDC5 cells to model different types of cartilage.

It is known that the extracellular microenvironment plays a very important role in modulating the behaviour and actions of a cell. This is especially true in chondrocytes which only sparsely populate mature cartilage and are surrounded by extensive matrix in all three dimensions. The use of high density cultures therefore may be thought of as a peculiar method to enhance chondrogenesis. However, it is thought that this high-density culture recapitulates events during early chondrogenesis whereby progenitor cells condense into aggregates, increasing cell-cell contacts, as discussed previously. Other models exist which also enhance chondrogenesis by increasing the three-dimensional cell-cell contacts, such as the pellet culture described previously in Chapter 1, including in ATDC5 cells (Tare, *et al.*, 2005). However, compared to micromass cultures, pellet cultures are typically grown in 15 ml centrifuge tubes, requiring a larger amount of space in the incubator. Additionally, only one pellet can be placed in one tube, making scaling of experiments difficult. On the other hand, micromass cultures are grown in standard multi-well plates and multiple cultures can be grown in the same well, making the micromass culture system an ideal system for high-throughput screening experiments.

In summary, this thesis appears to be the first time the beneficial effects of the combination of both micromass culture and ascorbic acid stimulation, over their use alone in ATDC5 cells, have been established, and importantly, directly compared to the standard culture of ATDC5 cells in monolayer with insulin-induction alone.

6.1.2 Novel cytokine-mediated regulation of the WNT and CCN molecular signalling pathways

The role of WNT5A during cartilage development has been well established, however, the involvement of WNT5A in cartilage in a pathological setting remained to be elucidated. Furthermore, whilst it is known that cytokines play an important role in the development of osteoarthritis, inducing the up-regulation of a number of metalloproteinases to degrade the cartilage matrix, and knowing that cytokines may modulate the WNT signalling pathways, the mechanisms behind this interaction and how this attributed to the progression of osteoarthritis remained unclear.

Several approaches were taken to address these points, including over-expression of WNT5A and exogenous WNT5A/cytokine stimulation of the enhanced ATDC5 chondrogenesis model described in Chapter 3. Data from this thesis provided interesting results by stimulating differentiated micromass cultures with a combination of WNT5A conditioned medium with the IL-1 α and OSM cytokines. Pathway analysis from data obtained from the microarray revealed strong down-regulation of the WNT5A pathway. qRT-PCR analysis similarly revealed down-regulation of the WNT5A receptor, *Ror2*, and western blotting confirmed the down-regulation of WNT5A itself with cytokine stimulation.

This down-regulation is an apparently novel finding, with several reports describing up-regulation of WNT5A following stimulation from a number of different cytokines, (including IL- α , IL-1 β , IL-6 and TNF α) in a number of cell types, including myofibroblasts, melanomas, keratinocytes, MSCs and chondrocytes (Gudjonsson, *et al.*, 2010; Ge, *et al.*, 2011; Rauner, *et al.*, 2012; Raymond, *et al.*, 2012; Sonomoto, *et al.*, 2012; Briolay, *et al.*, 2013; Linnskog, *et al.*, 2014). Since WNT5A is known to induce metalloproteinases such as ADAMTS5 in chondrocytes to degrade matrix (Hosseini-Farahabadi, *et al.*, 2013), it may be speculated that down-regulation of WNT5A may be an attempt to protect the cartilage from damage. In agreement with this, a strong up-regulation of *Prg4* (lubricin) was also seen, which is known to help protect cartilage from damage (Ruan, *et al.*, 2013). Additionally, cytokine stimulation resulted in the down-regulation of several CCN members, with the down-regulation of *Wisp1* and *Wisp2* being apparently novel findings. Together, these findings further strengthen the interrelationship between cytokine, WNT and CCN signalling in novel ways.

Finally, comparisons made between the cytokine-stimulated model described in this thesis compared to established models of osteoarthritis revealed similarities in the steady-state expression of a number of genes. Taken together, the findings in this thesis suggest that cytokine stimulation of differentiated ATDC5 micromass cultures may provide a good alternative model of

early osteoarthritis, enabling investigations of signalling pathway regulation that may not be possible from cartilage explants obtained from patients with end-stage OA undergoing joint replacement surgery.

6.1.3 ATDC cells can be used to model chondroprogenitor migration and invasion

In addition to chondrocytes, it has been previously reported that chondroprogenitor cells are also resident within articular cartilage. It has also been shown that these chondroprogenitor cells, which can either be isolated based on their affinity to fibronectin or their ability to migrate away from explant cultures, can migrate to sites of cartilage damage (Seol, *et al.*, 2012).

Data from thesis showed that ATDC5 cells have a similar adhesion and migratory phenotype similar to chondroprogenitor cells and chondrocytes, depending on the state of chondrogenesis. Type II collagen was found to have a negative effect on the speed of migration on non-induced ATDC5 cells, which may have ramifications for the ability of chondroprogenitor cells to migrate *in vivo* and may possibly add to the inability for cartilage to adequately repair itself.

By combining and adapting the inverted invasion assay already used in our laboratory for macrophage invasion (Murray, *et al.* (2013) and based on Hennigan, *et al.* (1994)) with the micromass culturing technique, this thesis described a relatively novel way of modelling chondroprogenitor cell invasion through a cartilage-like matrix. Using WNT5A conditioned medium, a positive trend towards increased invasion towards WNT5A was observed. Validation of this finding in one experiment using rhWNT5A similarly resulted in an increased trend towards increased invasion, which was deemed significant when invading through micromass cultures that had been pre-stimulated with cytokines to induce potential osteoarthritic-like degradation of the matrix. These results may suggest that WNT5A, which is over-expressed in osteoarthritic cartilage, may act as a potential chemoattractant for primary chondroprogenitor cells towards sites of cartilage damage. Given that WNT5A is also important in promoting the early stages of chondrogenesis, it may be speculated that WNT5A produced by damaged cartilage may also help induce differentiation of the chondroprogenitor cells to produce more matrix to repair the damage. Further experiments are needed to validate this finding.

In summary, this thesis has revealed that ATDC5 cells may also be a good model for investigating the translocation of cells in cartilage in response to cartilage damage, which may provide useful insights for potential future therapies for osteoarthritis.

6.1.4 Summary of findings

An overall scheme of key findings described in section 6.1 can be found in Figure 6.1.

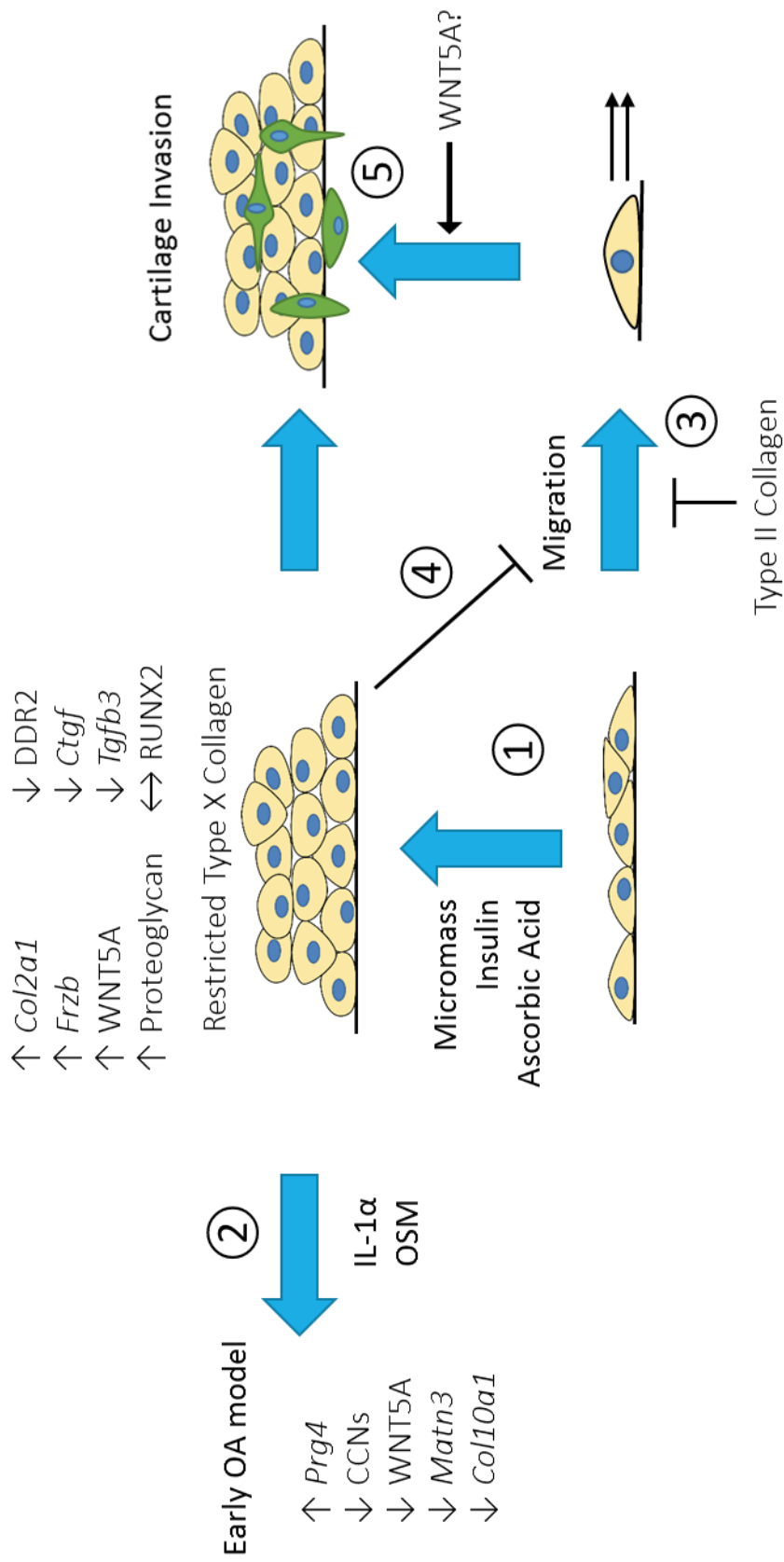


Figure 6.1 – Summary of findings. 1) Micromass, insulin and ascorbic acid enhance ATDC5 chondrogenesis, with a phenotype reminiscent of articular cartilage. 2) Cytokine stimulation of micromass cultures can be used to model early OA changes. 3) Non-induced ATDC5 cells are migratory which can be impeded by type II collagen. 4) Differentiation impedes migration. 5) Non-induced cells can invade through micromass cultures and this may be enhanced by WNT5A.

6.2 Future Work

6.2.1 Transcriptomic analysis and comparison with articular cartilage

Results in Chapter 3 revealed that the enhanced ATDC5 model is more reminiscent of articular cartilage compared to growth plate cartilage, which is important when wanting to investigate changes that occur during osteoarthritis, which results in the degradation of articular cartilage. However, these were not compared directly to primary cultures.

Using transcriptomic analysis, using either microarray or RNA-seq, it would be interesting to directly compare the enhanced ATDC5 culture model, along with the standard monolayer model, to primary articular and growth plate chondrocytes. Using principle component analysis, as seen in Chapter 4, clustering of samples would indicate similarities in the expression of mRNA. Close proximity of enhanced ATDC5 cultures with primary articular chondrocytes would further strengthen the idea that the enhanced ATDC5 cultures described in this thesis are reminiscent of articular cartilage, reinforcing the notion that the enhanced ATDC5 cultures are a good model for investigating osteoarthritis.

In addition to changes in the steady-state levels of mRNA, the use of next generation technologies, such as RNA-seq, would also allow the investigation of alternatively spliced mRNA transcripts and post-transcriptional modifications, as well as investigating other RNA species such as microRNAs (miRNA) (Cullum, *et al.*, 2011; Qian, *et al.*, 2014). Using this next generation technology may therefore reveal other novel markers of articular differentiation in addition to *Frzb*, *Grem1* (gremlin-1) and *Dkk1* (dickkopf 1) previously reported (Leijten, *et al.*, 2012) that may have otherwise been missed by standard microarray analysis, such as isoform switching. Additionally, this might provide insight into the mechanisms of the fate determination of escaping the endochondral process to become articular chondrocytes compared to becoming growth plate chondrocytes during endochondral ossification.

6.2.2 Epigenetic regulation of WNT5A

It has been well-established that epigenetic changes occur during osteoarthritis (reviewed in Barter and Young (2013)).

One form of epigenetic regulation is DNA methylation occurring at CpG islands in the promoter regions of genes. DNA methylation is a mechanism for silencing gene expression and so demethylation of DNA may result in inappropriate gene activation. Studies have shown dysregulation of the methylation of osteoarthritic chondrocytes in the promoter regions of a

number of matrix degrading enzymes, including *MMP3*, *MMP13* and *ADAMTS4* (Roach, *et al.*, 2005; Cheung, *et al.*, 2009). Differences in the methylation status of genes have also been reported between different stages of OA, revealing hypermethylation of *Wnt11* in more severe OA (Moazed-Fuerst, *et al.*, 2014). Interestingly, *Wnt11* is down-regulated by IL-1 β stimulation and exogenous WNT11 can induce type II collagen expression in chondrocytes (Ryu & Chun, 2006).

Expression of WNT5A may also be regulated by DNA methylation and dysregulation of WNT5A methylation has been associated with various diseases such as colorectal cancer (Rawson, *et al.*, 2011; Zhang, *et al.*, 2013), Epstein-Barr virus-associated gastric carcinoma (Liu, *et al.*, 2013b), leukaemia (Deng, *et al.*, 2011) and prostate cancer (Wang, *et al.*, 2007).

It would therefore be interesting to observe the methylated state of the *WNT5A* promoter in osteoarthritic cartilage, as well as in the cytokine-stimulated ATDC5 cells described in this thesis. Since WNT5A was observed to be decreased following cytokine stimulation, it may be hypothesised that the *Wnt5a* promoter was hypermethylated to decrease transcription. Use of a DNA methyltransferase inhibitor to inhibit DNA methylation may reveal whether epigenetic changes are the cause of this novel regulation of WNT5A.

Furthermore, it would be interesting to see whether epigenomic analysis to identify the global state of methylation would correlate with the findings from the microarray, identifying which genes are most regulated by epigenetic changes induced by cytokine stimulation. This may provide insight into the mechanisms behind gene regulation in early osteoarthritis.

In addition to DNA methylation, epigenetic regulation of genes can occur due to the changes in histone acetylation, whereby deacetylation causes chromatin condensation, impeding access of transcription factors to the promoter regions of genes. Interestingly, it has been shown that extended administration of a histone deacetylase (HDAC) inhibitor in mice (which prevents chromatin condensation and thus allows for greater access of transcription factors to promoter regions) decreased type II collagen expression by directly up-regulating the transcription of *Wnt5a* (Huh, *et al.*, 2007). It would therefore also be interesting to see whether the down-regulation of WNT5A observed in this thesis as a result of cytokine stimulation could also be due to histone deacetylation.

6.3.3 Osteoarthritic cartilage secretome

As previously mentioned, chondroprogenitor cells resident with osteoarthritic cartilage are able to migrate to sites of cartilage injury, and it was reported that the alarmin, high mobility group box chromosomal protein 1 (HMGB-1), may be one factor produced by damaged chondrocytes to elicit

the migratory response of chondroprogenitor cells (Seol, *et al.*, 2012). This thesis has proposed that WNT5A and possibly WNT3A may also be potential candidates for the induction of chondroprogenitor migration.

Proteomic analysis to identify the global expression levels of proteins could be used to identify the largest changes in protein expression (both positively and negatively) of the osteoarthritic cartilage secretome compared to non-OA cartilage, which could be generated by conditioning media with cartilage explants. After identifying the most up-regulated and down-regulated proteins, conditioned media could be generated from cells overexpressing these proteins, or alternatively if available, commercial recombinant proteins could be sourced. These media or purified proteins, along with other alarmins such as S100A8 (which was highly up-regulated in the microarray analysis of cytokine-stimulated ATDC5 cells (Appendix Table S4.5, S4.6) and known to induce migration/invasion of other cell types including breast and gastric cancer cells (Kwon, *et al.*, 2013; Yin, *et al.*, 2013)), could then be used in conjunction with the migration assay and cartilage invasion assay described in this thesis to observe whether these proteins modulated translocation of non-induced ATDC5 cells or primary chondroprogenitor cells. This may reveal potentially novel proteins that may either be up-regulated to promote invasion or down-regulated to inhibit proteins that may otherwise impede invasion.

6.3.4 High-throughput screening

Additionally, proteomic analysis of the osteoarthritic secretome could help reveal novel candidates that might mediate the destruction of cartilage by regulating expression of various metalloproteinases. Conditioned media generated by transient overexpression of regulated proteins found via proteomic analysis, or commercially available purified proteins, could be used to stimulate cultures in a high-throughput screening assay. Steady-state gene expression of known cartilage-degrading enzymes could be measured to identify which proteins may induce catabolism. Degradation of cartilage could then be examined by using either the dimethyl methylene blue (DMMB) assay or the hydroxyproline assay, which are colorimetric assays to measure the release of GAGs from proteoglycans or the hydroxyproline content from cleaved collagens respectively into the media.

Potential drug candidates could also be screened in a similar manner to detect changes in enzyme expression and prevent cartilage destruction, mediated by cytokines or potential components of the secretome. The nature of ATDC5 micromass cultures, their ease of culturing in multi-well plates and the ability to easily scale up cultures by plating multiple micromass cultures in the same well, makes ATDC5 micromass cultures an attractive model for high-throughput screening assays to help

identify mediators of osteoarthritis and potential drug candidates to prevent or reverse cartilage damage.

6.3 Summary

In summary, this thesis has shown that ATDC5 cells are a versatile cell type that may be used for several applications. The enhanced ATDC5 chondrogenesis model, by combining micromass culture and ascorbic acid stimulation, produces a cartilage-like tissue reminiscent of articular cartilage, which is important for studying osteoarthritis. Indeed, cytokine stimulation of these cultures revealed similarities in gene expression to early OA models, which is useful for studying events that occur in early OA that may not occur in end-stage OA, which would otherwise be missed when examining cartilage from patients undergoing joint replacement surgery. Furthermore, this thesis showed that ATDC5 cells have a similar migratory phenotype to both chondroprogenitor cells and chondrocytes, depending on the differentiation status, and may be used to model chondroprogenitor invasion through cartilage, an event that occurs *in vivo* in response to cartilage damage.

Therefore this thesis has shown that the ATDC5 cell line is an effective tool in studying several aspects of cartilage biology and pathology.

Appendix

Table S3.1 – TaqMan C_T values for Figure 3.2 with normalised averages and SEM

				Col2a1			
				Minimum Ct	Maximum Ct	Average	SE
Day 7	Monolayer	No Insulin	No Ascorbic Acid	30.81	31.86	0.036	0.003
			Ascorbic Acid	28.90	30.85	0.099	0.065
		Insulin	No Ascorbic Acid	29.82	30.78	0.089	0.010
			Ascorbic Acid	27.58	30.54	0.234	0.081
	Micromass	No Insulin	No Ascorbic Acid	28.22	30.39	0.209	0.058
			Ascorbic Acid	26.64	26.64	0.897	0.236
Insulin		No Ascorbic Acid	25.84	26.65	1.321	0.312	
		Ascorbic Acid	24.25	26.45	4.597	1.282	
Day 14	Monolayer	No Insulin	No Ascorbic Acid	30.27	31.91	0.066	0.022
			Ascorbic Acid	29.35	29.98	0.211	0.037
		Insulin	No Ascorbic Acid	29.75	30.08	0.184	0.037
			Ascorbic Acid	26.56	27.64	2.903	0.847
	Micromass	No Insulin	No Ascorbic Acid	28.81	29.44	0.209	0.021
			Ascorbic Acid	28.18	29.59	0.650	0.159
Insulin		No Ascorbic Acid	25.55	26.55	3.846	0.430	
		Ascorbic Acid	23.53	24.89	20.747	6.804	
Day 21	Monolayer	No Insulin	No Ascorbic Acid	28.80	32.82	0.149	0.075
			Ascorbic Acid	28.79	29.56	0.411	0.052
		Insulin	No Ascorbic Acid	28.60	31.77	0.225	0.067
			Ascorbic Acid				
	Micromass	No Insulin	No Ascorbic Acid	26.41	29.40	0.928	0.364
			Ascorbic Acid	25.52	28.04	2.832	1.097
Insulin		No Ascorbic Acid	21.79	23.80	32.350	12.587	
		Ascorbic Acid	21.48	22.23	52.202	9.479	

				Frzb			
				Minimum Ct	Maximum Ct	Average	SE
Day 7	Monolayer	No Insulin	No Ascorbic Acid	35.60	36.57		
			Ascorbic Acid	33.32	34.38	0.003	0.003
		Insulin	No Ascorbic Acid	32.89	33.36	0.010	0.002
			Ascorbic Acid	29.53	30.34	0.095	0.017
	Micromass	No Insulin	No Ascorbic Acid	32.24	33.04	0.014	0.002
			Ascorbic Acid	31.44	31.44	0.022	0.006
Insulin		No Ascorbic Acid	26.88	27.80	0.576	0.030	
		Ascorbic Acid	26.59	27.79	0.966	0.155	
Day 14	Monolayer	No Insulin	No Ascorbic Acid	34.07	36.74	0.006	
			Ascorbic Acid	32.46	33.29	0.019	0.003
		Insulin	No Ascorbic Acid	30.43	32.28	0.089	0.026
			Ascorbic Acid	27.60	28.30	1.389	0.265
	Micromass	No Insulin	No Ascorbic Acid	33.08	33.42	0.010	0.001
			Ascorbic Acid	31.93	32.96	0.045	0.005
Insulin		No Ascorbic Acid	26.11	26.86	2.749	0.431	
		Ascorbic Acid	25.33	25.68	7.024	1.733	
Day 21	Monolayer	No Insulin	No Ascorbic Acid	33.19	35.18	0.011	0.002
			Ascorbic Acid	30.82	32.27	0.067	0.020
		Insulin	No Ascorbic Acid	29.99	31.23	0.123	0.041
			Ascorbic Acid				
	Micromass	No Insulin	No Ascorbic Acid	31.41	34.26	0.023	0.009
			Ascorbic Acid	29.00	32.42	0.152	0.065
Insulin		No Ascorbic Acid	24.19	25.19	7.529	0.557	
		Ascorbic Acid	23.48	24.08	11.621	1.046	

Table S3.2 – TaqMan C_T values for Figure 3.3 with normalised averages and SEM

				Tgfb1			
				Minimum Ct	Maximum Ct	Average	SE
Day 7	Monolayer	No Insulin	No Ascorbic Acid	28.83	29.34	1.318	0.324
			Ascorbic Acid	28.63	28.78	1.362	0.069
		Insulin	No Ascorbic Acid	29.76	30.08	0.915	0.113
			Ascorbic Acid	28.98	30.91	0.992	0.250
	Micromass	No Insulin	No Ascorbic Acid	28.36	28.92	1.702	0.136
			Ascorbic Acid	28.73	28.73	2.041	0.204
		Insulin	No Ascorbic Acid	28.49	29.01	1.340	0.278
			Ascorbic Acid	28.77	29.27	1.666	0.114
Day 14	Monolayer	No Insulin	No Ascorbic Acid	29.32	29.65	1.621	0.123
			Ascorbic Acid	29.03	29.61	1.791	0.160
		Insulin	No Ascorbic Acid	29.52	29.82	1.608	0.273
			Ascorbic Acid	29.59	29.79	2.741	0.499
	Micromass	No Insulin	No Ascorbic Acid	28.75	29.89	1.346	0.203
			Ascorbic Acid	29.15	29.48	3.275	0.458
		Insulin	No Ascorbic Acid	28.44	29.09	3.020	0.166
			Ascorbic Acid	27.73	28.80	4.671	1.179
Day 21	Monolayer	No Insulin	No Ascorbic Acid	28.77	29.17	2.276	0.191
			Ascorbic Acid	28.87	29.66	2.433	0.090
		Insulin	No Ascorbic Acid	28.78	30.64	1.438	0.287
			Ascorbic Acid				
	Micromass	No Insulin	No Ascorbic Acid	28.60	29.51	2.466	0.259
			Ascorbic Acid	28.14	28.63	3.219	0.322
		Insulin	No Ascorbic Acid	27.07	28.01	4.319	0.345
			Ascorbic Acid	26.46	27.25	5.517	0.342
				Tgfb3			
				Minimum Ct	Maximum Ct	Average	SE
Day 7	Monolayer	No Insulin	No Ascorbic Acid	28.47	28.90	9.275	2.312
			Ascorbic Acid	28.37	28.78	8.750	1.390
		Insulin	No Ascorbic Acid	29.56	29.93	5.887	0.382
			Ascorbic Acid	29.98	30.96	3.080	0.491
	Micromass	No Insulin	No Ascorbic Acid	29.38	29.94	5.207	0.350
			Ascorbic Acid	29.58	29.58	6.926	0.237
		Insulin	No Ascorbic Acid	29.82	30.71	3.205	0.672
			Ascorbic Acid	30.62	31.35	3.163	0.258
Day 14	Monolayer	No Insulin	No Ascorbic Acid	28.91	29.16	11.922	0.841
			Ascorbic Acid	28.85	29.76	10.249	1.140
		Insulin	No Ascorbic Acid	30.11	30.41	6.452	1.039
			Ascorbic Acid	31.30	31.78	5.685	1.064
	Micromass	No Insulin	No Ascorbic Acid	29.47	30.04	6.196	0.994
			Ascorbic Acid	30.12	30.98	9.491	1.054
		Insulin	No Ascorbic Acid	30.82	31.41	5.010	0.550
			Ascorbic Acid	30.87	32.28	4.014	1.020
Day 21	Monolayer	No Insulin	No Ascorbic Acid	28.85	29.47	12.529	1.481
			Ascorbic Acid	29.97	30.50	9.129	0.855
		Insulin	No Ascorbic Acid	29.87	30.73	6.237	1.345
			Ascorbic Acid				
	Micromass	No Insulin	No Ascorbic Acid	29.15	29.65	11.325	1.553
			Ascorbic Acid	29.96	30.29	7.037	0.497
		Insulin	No Ascorbic Acid	30.11	30.97	4.397	0.349
			Ascorbic Acid	29.98	30.91	3.811	0.243

Table S3.3 – TaqMan C_T values for Figure 3.4 with normalised averages and SEM

				Col10a1			
				Minimum Ct	Maximum Ct	Average	SE
Day 7	Monolayer	No Insulin	No Ascorbic Acid	35.87	35.87		
			Ascorbic Acid	36.60	37.76		
		Insulin	No Ascorbic Acid	34.09	37.36	0.027	
			Ascorbic Acid	34.51	37.58		
	Micromass	No Insulin	No Ascorbic Acid	34.72	37.88	0.020	
			Ascorbic Acid	35.61	35.61		
		Insulin	No Ascorbic Acid	34.50	35.43	0.030	
			Ascorbic Acid	33.92	35.53	0.045	0.007
Day 14	Monolayer	No Insulin	No Ascorbic Acid	35.77	37.98		
			Ascorbic Acid	34.14	35.03	0.044	
		Insulin	No Ascorbic Acid	36.19	37.68		
			Ascorbic Acid	32.94	33.64	0.160	0.035
	Micromass	No Insulin	No Ascorbic Acid	33.50	36.15	0.044	
			Ascorbic Acid	36.11	36.62		
		Insulin	No Ascorbic Acid	30.73	31.63	0.367	0.066
			Ascorbic Acid	29.33	29.87	1.162	0.249
Day 21	Monolayer	No Insulin	No Ascorbic Acid	36.22	37.46		
			Ascorbic Acid	34.62	37.49	0.034	
		Insulin	No Ascorbic Acid	32.73	35.38	0.053	0.007
			Ascorbic Acid				
	Micromass	No Insulin	No Ascorbic Acid	34.85	36.54	0.029	
			Ascorbic Acid	33.74	35.73	0.056	0.008
		Insulin	No Ascorbic Acid	28.26	29.28	1.245	0.027
			Ascorbic Acid	27.33	28.36	1.712	0.063

				Apl			
				Minimum	Maximum	Average	SE
Day 7	Monolayer	No Insulin	No Ascorbic Acid	28.23	28.70	1.251	0.229
			Ascorbic Acid	27.24	27.73	2.395	0.439
		Insulin	No Ascorbic Acid	27.98	28.08	1.940	0.170
			Ascorbic Acid	26.97	28.30	2.286	0.463
	Micromass	No Insulin	No Ascorbic Acid	27.91	28.40	1.649	0.101
			Ascorbic Acid	28.19	28.19	1.944	0.167
		Insulin	No Ascorbic Acid	26.80	27.36	2.598	0.472
			Ascorbic Acid	27.09	28.20	2.565	0.171
Day 14	Monolayer	No Insulin	No Ascorbic Acid	28.58	28.79	1.796	0.164
			Ascorbic Acid	27.63	27.91	3.140	0.281
		Insulin	No Ascorbic Acid	27.92	28.72	2.748	0.545
			Ascorbic Acid	27.64	27.73	6.267	0.862
	Micromass	No Insulin	No Ascorbic Acid	28.07	29.10	1.473	0.201
			Ascorbic Acid	28.48	28.94	3.370	0.440
		Insulin	No Ascorbic Acid	26.77	27.40	5.612	0.172
			Ascorbic Acid	27.04	28.44	4.587	1.148
Day 21	Monolayer	No Insulin	No Ascorbic Acid	27.99	28.49	2.539	0.215
			Ascorbic Acid	27.05	27.96	5.353	0.331
		Insulin	No Ascorbic Acid	27.05	28.28	3.126	0.496
			Ascorbic Acid				
	Micromass	No Insulin	No Ascorbic Acid	27.70	28.47	3.196	0.154
			Ascorbic Acid	26.76	27.20	5.546	0.568
		Insulin	No Ascorbic Acid	25.53	26.23	7.834	0.451
			Ascorbic Acid	25.42	26.31	7.286	0.345

Table S3.4 – TaqMan C_T values for Figure 3.5 with normalised averages and SEM

				Runx2			
				Minimum Ct	Maximum Ct	Average	SE
Day 7	Monolayer	No Insulin	No Ascorbic Acid	26.20	26.52	1.253	0.315
			Ascorbic Acid	26.04	26.37	1.485	0.278
		Insulin	No Ascorbic Acid	26.98	27.19	0.991	0.110
			Ascorbic Acid	26.38	27.23	1.000	0.191
	Micromass	No Insulin	No Ascorbic Acid	26.60	27.02	1.007	0.060
			Ascorbic Acid	26.74	26.74	1.332	0.112
		Insulin	No Ascorbic Acid	26.28	26.92	1.007	0.163
			Ascorbic Acid	26.64	27.43	1.047	0.076
Day 14	Monolayer	No Insulin	No Ascorbic Acid	26.83	27.02	1.439	0.093
			Ascorbic Acid	26.58	26.75	1.722	0.126
		Insulin	No Ascorbic Acid	27.20	28.06	1.111	0.223
			Ascorbic Acid	27.40	27.68	2.029	0.391
	Micromass	No Insulin	No Ascorbic Acid	26.52	27.08	1.213	0.178
			Ascorbic Acid	26.97	27.44	2.309	0.332
		Insulin	No Ascorbic Acid	26.46	27.10	1.997	0.141
			Ascorbic Acid	26.76	27.53	1.864	0.428
Day 21	Monolayer	No Insulin	No Ascorbic Acid	26.71	26.96	1.606	0.143
			Ascorbic Acid	26.57	27.28	2.110	0.129
		Insulin	No Ascorbic Acid	26.74	27.84	1.244	0.272
			Ascorbic Acid				
	Micromass	No Insulin	No Ascorbic Acid	26.32	26.93	2.156	0.130
			Ascorbic Acid	25.84	26.37	2.433	0.208
		Insulin	No Ascorbic Acid	26.00	26.54	1.990	0.165
			Ascorbic Acid	25.62	26.36	1.772	0.125

Table S3.5 – TaqMan C_T values for Figure 3.7 with normalised averages and SEM

Col2a1		Ct Range	Average	SE	
Monolayer	No Insulin	No Ascorbic	32.38 - 34.63	1.53	0.19
		Ascorbic	32.26 - 33.27	3.42	0.38
	Insulin	No Ascorbic	31.74 - 33.36	3.16	0.28
		Ascorbic	29.75 - 31.34	5.19	1.27
Micromass	No Insulin	No Ascorbic	32.78 - 33.41	2.17	0.25
		Ascorbic	32.73 - 33.39	4.23	1.71
	Insulin	No Ascorbic	30.28 - 31.67	5.79	0.74
		Ascorbic	28.28 - 30.13	11.18	0.70

Frzb		Ct Range	Average	SE	
Monolayer	No Insulin	No Ascorbic	Undetermined		
		Ascorbic	Undetermined		
	Insulin	No Ascorbic	33.80 - 38.37	2.01	1.01
		Ascorbic	33.84 - 35.39	1.30	0.34
Micromass	No Insulin	No Ascorbic	Undetermined		
		Ascorbic	Undetermined		
	Insulin	No Ascorbic	30.85 - 34.02	5.60	0.97
		Ascorbic	29.45 - 32.34	7.83	1.04

Grem1		Minimum Ct	Maximum Ct	Average	SE	
Monolayer	No Insulin	No Ascorbic Acid	23.37	23.77	5.996	0.224
		Ascorbic Acid	23.49	24.14	5.240	0.534
	Insulin	No Ascorbic Acid	25.32	25.87	2.045	0.393
		Ascorbic Acid	27.28	27.45	1.071	0.166
Micromass	No Insulin	No Ascorbic Acid	24.30	24.94	2.297	0.267
		Ascorbic Acid	24.92	25.65	3.720	0.570
	Insulin	No Ascorbic Acid	25.95	26.36	1.500	0.099
		Ascorbic Acid	26.56	27.41	1.012	0.240

Tgfb1		Min	Max	Normalised	SEM	
Micromass	No Insulin	No Ascorbic Acid	27.37	28.74	1.19	0.08
		Ascorbic Acid	27.23	28.05	1.49	0.11
	Insulin	No Ascorbic Acid	26.84	27.16	1.51	0.22
		Ascorbic Acid	26.96	27.84	2.31	0.28

Table S3.6 – TaqMan C_T values for Figure 3.8 with normalised averages and SEM

Col10a1			Minimum Ct	Maximum Ct	Average	SE
Monolayer	No Insulin	No Ascorbic Acid	35.77	37.98		
		Ascorbic Acid	34.14	35.03	0.044	
	Insulin	No Ascorbic Acid	36.19	37.68		
		Ascorbic Acid	32.94	33.64	0.160	0.035
Micromass	No Insulin	No Ascorbic Acid	33.50	36.15	0.044	
		Ascorbic Acid	36.11	36.62		
	Insulin	No Ascorbic Acid	30.73	31.63	0.367	0.066
		Ascorbic Acid	29.33	29.87	1.162	0.249

DDR2			Ct Range	Average	SE
Monolayer	No Insulin	No Ascorbic	27.23 - 29.03	3.43	0.38
		Ascorbic	26.74 - 29.21	4.78	0.61
	Insulin	No Ascorbic	27.40 - 29.04	2.92	0.82
		Ascorbic	27.88 - 30.64	1.51	0.12
Micromass	No Insulin	No Ascorbic	27.88 - 29.42	2.20	0.16
		Ascorbic	29.25 - 32.05	2.40	0.54
	Insulin	No Ascorbic	28.86 - 32.51	2.06	0.43
		Ascorbic	28.18 - 30.30	1.71	0.15

Runx2			Minimum Ct	Maximum Ct	Average	SE
Monolayer	No Insulin	No Ascorbic Acid	26.83	27.02	1.439	0.093
		Ascorbic Acid	26.58	26.75	1.722	0.126
	Insulin	No Ascorbic Acid	27.20	28.06	1.111	0.223
		Ascorbic Acid	27.40	27.68	2.029	0.391
Micromass	No Insulin	No Ascorbic Acid	26.52	27.08	1.213	0.178
		Ascorbic Acid	26.97	27.44	2.309	0.332
	Insulin	No Ascorbic Acid	26.46	27.10	1.997	0.141
		Ascorbic Acid	26.76	27.53	1.864	0.428

Table S3.6 (cont.) – TaqMan C_T values for Figure 3.8 with normalised averages and SEM

Alpl		Minimum Ct	Maximum Ct	Average	SE	
Monolayer	No Insulin	No Ascorbic Acid	28.58	28.79	1.796	0.164
		Ascorbic Acid	27.63	27.91	3.140	0.281
	Insulin	No Ascorbic Acid	27.92	28.72	2.748	0.545
		Ascorbic Acid	27.64	27.73	6.267	0.862
Micromass	No Insulin	No Ascorbic Acid	28.07	29.10	1.473	0.201
		Ascorbic Acid	28.48	28.94	3.370	0.440
	Insulin	No Ascorbic Acid	26.77	27.40	5.612	0.172
		Ascorbic Acid	27.04	28.44	4.587	1.148

Tgfb3		Ct Range	Average	SE	
Monolayer	No Insulin	No Ascorbic	25.65 - 26.80	2.00	0.20
		Ascorbic	26.38 - 27.82	2.01	0.19
	Insulin	No Ascorbic	27.92 - 29.19	0.81	0.17
		Ascorbic	28.31 - 29.92	0.29	0.05
Micromass	No Insulin	No Ascorbic	26.79 - 28.37	1.01	0.23
		Ascorbic	28.08 - 29.50	0.86	0.16
	Insulin	No Ascorbic	28.67 - 29.75	0.39	0.04
		Ascorbic	28.45 - 30.05	0.31	0.02

Table S3.7 – TaqMan C_T values for Figure 3.9 with normalised averages and SEM

Cyr61			Ct Range	Average	SE
Monolayer	No Insulin	No Ascorbic	28.41 - 30.19	4.29	0.59
		Ascorbic	29.07 - 30.52	4.55	0.15
	Insulin	No Ascorbic	29.23 - 30.72	3.89	0.65
		Ascorbic	29.80 - 31.10	1.60	0.15
Micromass	No Insulin	No Ascorbic	29.32 - 30.84	3.27	0.49
		Ascorbic	29.43 - 31.54	4.10	1.01
	Insulin	No Ascorbic	29.71 - 31.21	2.41	0.18
		Ascorbic	29.74 - 31.26	1.76	0.10

CTGF			Ct Range	Average	SE
Monolayer	No Insulin	No Ascorbic	30.33 - 31.35	12.41	1.91
		Ascorbic	30.24 - 31.54	20.40	0.86
	Insulin	No Ascorbic	31.80 - 35.52	3.38	1.04
		Ascorbic	32.60 - 34.37	1.80	0.46
Micromass	No Insulin	No Ascorbic	32.05 - 33.51	4.57	0.87
		Ascorbic	32.74 - 34.08	4.01	0.80
	Insulin	No Ascorbic	32.62 - 34.02	2.52	0.36
		Ascorbic	31.98 - 35.86	2.28	0.70

Table S4.1 – TaqMan C_T values for Figure 4.1 with normalised averages and SEM

	Ror2		Minimum Ct	Maximum Ct	Normalised	SEM
Vector Only	Clone 1	Monolayer	30.50	30.96	1.33	0.20
		Micromass	31.03	31.51	1.58	0.31
	Clone 2	Monolayer	30.61	31.25	1.03	0.18
		Micromass	30.07	30.54	1.74	0.48
	Clone 3	Monolayer	32.23	36.52	0.16	0.08
		Micromass	32.52	33.99	0.44	0.09
WNT5A	Clone 4	Monolayer	28.93	31.29	2.59	0.42
		Micromass	31.11	31.84	2.46	0.35
	Clone 5	Monolayer	30.56	32.02	1.31	0.25
		Micromass	31.07	32.21	2.11	0.25
	Clone 6	Monolayer	31.49	31.98	1.01	0.12
		Micromass	31.32	31.97	1.19	0.06
	Vector Only	Monolayer	30.50	36.52	0.84	0.19
		Micromass	30.07	33.99	1.25	0.26
	Wnt5a	Monolayer	28.93	32.02	1.64	0.28
		Micromass	31.07	32.21	1.92	0.23

	Col2a1		Minimum Ct	Maximum Ct	Normalised	SEM
Vector Only	Clone 1	Monolayer	31.48	32.98	0.07	0.02
		Micromass	34.14	34.18	0.03	0.00
	Clone 2	Monolayer	33.14	33.82	0.02	0.00
		Micromass	32.81	33.25	0.04	0.01
	Clone 3	Monolayer	34.36	34.85	0.01	0.01
		Micromass	31.63	32.71	0.12	0.02
WNT5A	Clone 4	Monolayer	34.56	34.69	0.01	0.00
		Micromass	38.56	38.56		
	Clone 5	Monolayer	39.12	39.12		
		Micromass	39.93	39.93		
	Clone 6	Monolayer	34.97	38.80	0.01	
		Micromass	37.00	37.73		
	Vector Only	Monolayer	31.48	34.85	0.04	0.01
		Micromass	31.63	34.18	0.07	0.02
	Wnt5a	Monolayer	34.56	39.12	0.01	0.00
		Micromass	37.00	39.93		

Table S4.1 (cont.) – TaqMan C_T values for Figure 4.1 with normalised averages and SEM

Adamts4		Minimum Ct	Maximum Ct	Normalised	SEM	
Vector Only	Clone 1	Monolayer	34.26	35.02	0.43	0.08
		Micromass	34.52	34.89	0.69	0.12
	Clone 2	Monolayer	33.68	34.23	0.56	0.02
		Micromass	32.08	32.46	2.61	0.70
	Clone 3	Monolayer	33.33	35.10	0.47	0.11
		Micromass	32.20	32.78	2.94	0.21
WNT5A	Clone 4	Monolayer	32.99	35.96	0.65	0.22
		Micromass	34.43	35.04	1.13	0.21
	Clone 5	Monolayer	35.02	35.78	0.29	0.04
		Micromass	34.23	34.36	1.59	0.18
	Clone 6	Monolayer	33.56	35.28	0.77	0.15
		Micromass	33.04	33.32	2.12	0.22
	Vector Only	Monolayer	33.33	35.10	0.49	0.05
		Micromass	32.08	34.89	2.08	0.41
	Wnt5a	Monolayer	32.99	35.96	0.57	0.11
		Micromass	33.04	35.04	1.62	0.18

Adamts5		Minimum Ct	Maximum Ct	Normalised	SEM	
Vector Only	Clone 1	Monolayer	33.35	34.05	0.75	
		Micromass	Undetermined	Undetermined		
	Clone 2	Monolayer	31.61	31.98	1.33	0.23
		Micromass	33.83	34.41	0.65	0.07
	Clone 3	Monolayer	31.43	32.40	1.51	0.19
		Micromass	33.13	33.21	1.40	0.14
WNT5A	Clone 4	Monolayer	33.04	33.39	0.83	
		Micromass	Undetermined	Undetermined		
	Clone 5	Monolayer	33.78	34.48	0.95	0.14
		Micromass	Undetermined	Undetermined		
	Clone 6	Monolayer	Undetermined	Undetermined		
		Micromass	Undetermined	Undetermined		
	Vector Only	Monolayer	31.43	34.05	1.25	0.15
		Micromass	33.13	34.41	1.02	0.18
	Wnt5a	Monolayer	33.04	34.48	0.75	0.18
		Micromass	Undetermined	Undetermined		

Table S4.1 (cont.) – TaqMan C_T values for Figure 4.1 with normalised averages and SEM

		Runx2	Minimum Ct	Maximum Ct	Normalised	SEM
Vector Only	Clone 1	Monolayer	29.91	30.12	0.57	0.04
		Micromass	30.08	31.17	0.67	0.08
	Clone 2	Monolayer	28.24	28.95	1.15	0.02
		Micromass	28.49	28.97	1.30	0.35
	Clone 3	Monolayer	28.56	29.40	1.05	0.08
		Micromass	28.18	28.89	2.22	0.17
WNT5A	Clone 4	Monolayer	27.19	29.98	2.08	0.46
		Micromass	29.47	29.90	2.28	0.44
	Clone 5	Monolayer	29.60	30.45	0.88	0.04
		Micromass	29.95	30.67	1.53	0.08
	Clone 6	Monolayer	29.34	30.80	0.85	0.06
		Micromass	29.35	30.50	1.08	0.10
	Vector Only	Monolayer	28.24	30.12	0.92	0.09
		Micromass	28.18	31.17	1.40	0.25
	Wnt5a	Monolayer	27.19	30.80	1.27	0.24
		Micromass	29.35	30.67	1.63	0.22

		Ddr2	Minimum Ct	Maximum Ct	Normalised	SEM
Vector Only	Clone 1	Monolayer	27.98	29.02	1.00	0.18
		Micromass	28.85	29.57	0.98	0.08
	Clone 2	Monolayer	27.66	28.30	1.29	0.04
		Micromass	27.90	28.58	1.39	0.43
	Clone 3	Monolayer	27.73	28.90	1.09	0.06
		Micromass	28.12	28.44	1.72	0.04
WNT5A	Clone 4	Monolayer	27.31	29.67	1.42	0.31
		Micromass	29.60	29.73	1.29	0.19
	Clone 5	Monolayer	29.27	29.97	0.66	0.04
		Micromass	29.35	30.30	1.01	0.12
	Clone 6	Monolayer	28.54	29.70	0.86	0.09
		Micromass	28.48	29.12	1.37	0.08
	Vector Only	Monolayer	27.66	29.02	1.13	0.07
		Micromass	27.90	29.57	1.36	0.17
	Wnt5a	Monolayer	27.31	29.97	0.98	0.15
		Micromass	28.48	30.30	1.22	0.09

Table S4.1 (cont.) – TaqMan C_T values for Figure 4.1 with normalised averages and SEM

Grem1		Minimum Ct	Maximum Ct	Normalised	SEM	
Vector Only	Clone 1	Monolayer	31.29	32.06	0.33	0.03
		Micromass	31.24	32.56	0.54	0.08
	Clone 2	Monolayer	29.94	30.75	0.72	0.02
		Micromass	29.52	30.24	1.34	0.33
	Clone 3	Monolayer	29.75	31.02	0.78	0.03
		Micromass	30.23	30.49	1.32	0.14
WNT5A	Clone 4	Monolayer	27.72	31.31	2.70	0.90
		Micromass	29.86	30.26	3.43	0.64
	Clone 5	Monolayer	30.59	31.05	0.95	0.02
		Micromass	30.62	30.83	2.16	0.26
	Clone 6	Monolayer	29.84	31.40	1.11	0.12
		Micromass	30.42	31.31	1.03	0.05
	Vector Only	Monolayer	29.75	32.06	0.61	0.07
		Micromass	29.52	32.56	1.07	0.17
	Wnt5a	Monolayer	27.72	31.40	1.59	0.38
		Micromass	29.86	31.31	2.20	0.40

Alpl		Minimum Ct	Maximum Ct	Normalised	SEM	
Vector Only	Clone 1	Monolayer	34.37	34.58	0.03	0.00
		Micromass	33.87	34.74	0.05	0.00
	Clone 2	Monolayer	27.02	28.02	1.41	0.09
		Micromass	26.77	27.61	2.00	0.70
	Clone 3	Monolayer	26.57	27.83	1.87	0.12
		Micromass	26.43	27.25	3.72	0.30
WNT5A	Clone 4	Monolayer	30.14	30.48	0.20	0.08
		Micromass	30.92	32.08	0.49	0.17
	Clone 5	Monolayer	33.61	35.11	0.04	0.01
		Micromass	31.52	32.66	0.31	0.03
	Clone 6	Monolayer	33.82	35.94	0.03	
		Micromass	32.45	33.27	0.12	0.03
	Vector Only	Monolayer	26.57	34.58	1.10	0.28
		Micromass	26.43	34.74	1.92	0.57
	Wnt5a	Monolayer	30.14	35.94	0.10	0.04
		Micromass	30.92	33.27	0.31	0.07

Table S4.1 (cont.) – TaqMan C_T values for Figure 4.1 with normalised averages and SEM

Cyr61		Minimum Ct	Maximum Ct	Normalised	SEM	
Vector Only	Clone 1	Monolayer	27.19	27.59	0.85	0.01
		Micromass	28.69	29.00	0.53	0.02
	Clone 2	Monolayer	27.44	27.99	0.56	0.05
		Micromass	28.71	29.02	0.29	0.03
	Clone 3	Monolayer	27.42	28.24	0.59	0.03
		Micromass	28.72	29.35	0.39	0.02
WNT5A	Clone 4	Monolayer	25.74	27.60	2.17	0.45
		Micromass	28.61	28.83	1.02	0.15
	Clone 5	Monolayer	26.80	27.38	1.58	0.03
		Micromass	28.27	28.92	1.09	0.08
	Clone 6	Monolayer	26.72	27.39	1.60	0.08
		Micromass	27.48	28.31	0.97	0.03
	Vector Only	Monolayer	27.19	28.24	0.67	0.05
		Micromass	28.69	29.35	0.40	0.04
	Wnt5a	Monolayer	25.74	27.60	1.78	0.16
		Micromass	27.48	28.92	1.03	0.05

Ctgf		Minimum Ct	Maximum Ct	Normalised	SEM	
Vector Only	Clone 1	Monolayer	26.61	26.88	1.71	0.07
		Micromass	28.26	28.62	1.07	0.05
	Clone 2	Monolayer	27.40	27.98	0.78	0.03
		Micromass	29.96	30.38	0.22	0.04
	Clone 3	Monolayer	27.73	28.56	0.70	0.06
		Micromass	29.66	30.12	0.36	0.00
WNT5A	Clone 4	Monolayer	26.72	28.63	1.28	0.14
		Micromass	29.72	29.91	0.81	0.11
	Clone 5	Monolayer	27.49	28.01	1.36	0.03
		Micromass	29.48	29.84	0.90	0.09
	Clone 6	Monolayer	27.34	28.03	1.43	0.10
		Micromass	28.35	29.04	0.90	0.07
	Vector Only	Monolayer	26.61	28.56	1.07	0.16
		Micromass	28.26	30.38	0.55	0.13
	Wnt5a	Monolayer	26.72	28.63	1.36	0.05
		Micromass	28.35	29.91	0.87	0.05

Table S4.1 (cont.) – TaqMan C_T values for Figure 4.1 with normalised averages and SEM

Nov		Minimum Ct	Maximum Ct	Normalised	SEM	
Vector Only	Clone 1	Monolayer	32.77	33.02	1.05	0.07
		Micromass	31.66	32.61	4.20	1.25
	Clone 2	Monolayer	34.33	36.12	0.19	0.08
		Micromass	33.04	34.84	0.46	0.12
	Clone 3	Monolayer	37.42	37.42		
		Micromass	34.97	36.48	0.19	0.05
WNT5A	Clone 4	Monolayer	32.70	34.70	0.76	0.31
		Micromass	33.78	34.23	1.21	0.12
	Clone 5	Monolayer	33.77	34.92	0.49	0.21
		Micromass	32.93	33.50	2.48	0.68
	Clone 6	Monolayer	32.74	33.07	1.66	0.31
		Micromass	31.27	31.96	5.21	0.17
	Vector Only	Monolayer	32.77	37.42	0.62	0.20
		Micromass	31.66	36.48	1.62	0.74
	Wnt5a	Monolayer	32.70	34.92	0.97	0.22
		Micromass	31.27	34.23	2.97	0.63

Wisp1		Minimum Ct	Maximum Ct	Normalised	SEM	
Vector Only	Clone 1	Monolayer	27.76	28.47	1.38	0.08
		Micromass	28.71	29.35	1.36	0.03
	Clone 2	Monolayer	27.49	27.84	1.57	0.12
		Micromass	28.78	29.13	0.89	0.19
	Clone 3	Monolayer	27.37	28.69	1.41	0.05
		Micromass	29.03	29.06	1.19	0.11
WNT5A	Clone 4	Monolayer	27.68	30.21	1.13	0.20
		Micromass	29.85	30.63	1.11	0.13
	Clone 5	Monolayer	29.47	30.16	0.70	0.04
		Micromass	30.22	30.54	1.07	0.12
	Clone 6	Monolayer	28.32	29.71	1.17	0.08
		Micromass	28.05	29.24	1.82	0.21
	Vector Only	Monolayer	27.37	28.69	1.45	0.05
		Micromass	28.71	29.35	1.15	0.09
	Wnt5a	Monolayer	27.68	30.21	1.00	0.10
		Micromass	28.05	30.63	1.33	0.15

Table S4.1 (cont.) – TaqMan C_T values for Figure 4.1 with normalised averages and SEM

Wisp2		Minimum Ct	Maximum Ct	Normalised	SEM	
Vector Only	Clone 1	Monolayer	27.61	28.10	0.92	0.05
		Micromass	26.75	26.93	3.58	
	Clone 2	Monolayer	26.72	27.45	1.24	0.06
		Micromass	26.89	27.46	1.62	0.39
	Clone 3	Monolayer	26.16	27.28	1.81	0.03
		Micromass	26.87	27.29	2.32	0.13
WNT5A	Clone 4	Monolayer	26.64	29.05	1.26	0.18
		Micromass	29.75	30.49	0.68	0.05
	Clone 5	Monolayer	28.64	29.38	0.69	0.03
		Micromass	29.28	29.80	1.10	0.14
	Clone 6	Monolayer	28.36	30.07	0.73	0.14
		Micromass	28.72	29.57	0.71	0.02
	Vector Only	Monolayer	26.16	28.10	1.32	0.13
		Micromass	26.75	27.46	2.37	0.32
	Wnt5a	Monolayer	26.64	30.07	0.89	0.11
		Micromass	28.72	30.49	0.83	0.08

Table S4.2 – TaqMan C_T values for Figure 4.4 with normalised averages and SEM

Ror2 (Left-hand figure)		Min Ct	Max Ct	Normalised	SEM
Vector Only	No Cytokines	29.58	30.61	1.21	0.26
	Cytokines	30.01	31.13	1.16	0.19
WNT5A	No Cytokines	31.10	31.60	0.54	0.04
	Cytokines	31.76	32.32	0.32	0.03

Ror2 (Right-hand figure)		Min Ct	Max Ct	Normalised	SEM
Vector Only	No Cytokines	30.16	31.29	3.77	1.10
	Cytokines	31.62	32.93	0.47	0.05
WNT5A	No Cytokines	29.04	30.98	5.95	2.44
	Cytokines	31.25	32.73	0.57	0.14

Col2a1 (Left-hand figure)		Min Ct	Max Ct	Normalised	SEM
Vector Only	No Cytokines	27.19	28.02	2.50	0.44
	Cytokines	26.87	28.92	2.58	0.58
WNT5A	No Cytokines	27.17	28.02	2.07	0.43
	Cytokines	28.81	29.93	0.57	0.14

Col2a1 (Right-hand figure)		Min Ct	Max Ct	Normalised	SEM
Vector Only	No Cytokines	23.30	25.26	3.73	1.70
	Cytokines	26.62	27.96	0.27	0.02
WNT5A	No Cytokines	23.48	25.47	3.33	0.88
	Cytokines	25.86	27.34	0.39	0.07

Adamts4 (Left-hand figure)		Min Ct	Max Ct	Average	SEM
Vector Only	No Cytokines	33.11	34.06	0.48	0.11
	Cytokines	33.87	35.23	0.23	0.05
WNT5A	No Cytokines	32.24	32.58	1.27	0.13
	Cytokines	32.24	32.53	1.28	0.15

Adamts4 (Right-hand figure)		Min Ct	Max Ct	Average	SEM
Vector Only	No Cytokines	33.26	34.34	1.20	0.36
	Cytokines	30.98	32.66	2.70	0.38
WNT5A	No Cytokines	32.91	33.99	1.48	0.23
	Cytokines	30.24	31.93	4.19	0.99

Table S4.2 (cont.) – TaqMan C_T values for Figure 4.4 with normalised averages and SEM

Ddr2 (Left-hand figure)		Min Ct	Max Ct	Normalised	SEM
Vector Only	No Cytokines	27.62	27.99	1.06	0.07
	Cytokines	27.52	28.66	1.05	0.07
WNT5A	No Cytokines	27.12	27.19	1.57	0.02
	Cytokines	29.19	29.36	0.40	0.02

Ddr2 (Right-hand figure)		Min Ct	Max Ct	Normalised	SEM
Vector Only	No Cytokines	25.95	27.31	1.64	0.39
	Cytokines	26.63	28.25	0.54	0.05
WNT5A	No Cytokines	26.39	26.96	1.59	0.18
	Cytokines	26.71	27.73	0.65	0.07

Runx2 (Left-hand figure)		Min Ct	Max Ct	Normalised	SEM
Vector Only	No Cytokines	28.31	28.99	1.30	0.15
	Cytokines	28.38	29.30	1.35	0.16
WNT5A	No Cytokines	29.03	29.50	0.82	0.06
	Cytokines	30.57	30.94	0.28	0.01

Runx2 (Right-hand Figure)		Min Ct	Max Ct	Normalised	SEM
Vector Only	No Cytokines	26.37	27.67	2.00	0.46
	Cytokines	27.84	29.59	0.31	0.03
WNT5A	No Cytokines	26.82	27.07	1.84	0.07
	Cytokines	27.93	28.86	0.38	0.04

Cyr61 (Left-hand figure)		Min Ct	Max Ct	Normalised	SEM
Vector Only	No Cytokines	28.35	29.01	1.01	0.12
	Cytokines	28.23	29.32	1.46	0.45
WNT5A	No Cytokines	28.50	28.59	1.08	0.01
	Cytokines	29.43	30.51	0.43	0.12

Cyr61 (Right-hand figure)		Min Ct	Max Ct	Normalised	SEM
Vector Only	No Cytokines	28.48	30.96	2.37	0.78
	Cytokines	29.35	30.83	0.61	0.06
WNT5A	No Cytokines	27.70	29.27	3.52	0.86
	Cytokines	29.53	30.62	0.65	0.10

Table S4.2 (cont.) – TaqMan CT values for Figure 4.4 with normalised averages and SEM

Ctgf (Left-hand figure)		Min Ct	Max Ct	Normalised	SEM
Vector Only	No Cytokines	30.03	30.84	0.34	0.05
	Cytokines	29.97	31.37	0.36	0.04
WNT5A	No Cytokines	26.82	27.48	2.92	0.35
	Cytokines	29.96	30.50	0.42	0.05

Ctgf (Right-hand figure)		Min Ct	Max Ct	Normalised	SEM
Vector Only	No Cytokines	27.62	28.75	2.55	0.76
	Cytokines	28.99	30.24	0.62	0.04
WNT5A	No Cytokines	27.52	29.14	2.51	0.46
	Cytokines	28.57	29.74	0.73	0.09

Nov (Left-hand figure)		Min Ct	Max Ct	Average	SEM
Vector Only	No Cytokines	32.69	33.88	0.43	0.09
	Cytokines	33.21	33.78	0.39	0.05
WNT5A	No Cytokines	29.30	30.77	3.76	1.09
	Cytokines	33.21	33.71	0.33	0.02

Nov (Right-hand figure)		Min Ct	Max Ct	Average	SEM
Vector Only	No Cytokines	31.83	33.91	1.84	0.47
	Cytokines	31.29	32.86	1.71	0.12
WNT5A	No Cytokines	31.75	33.62	2.46	0.62
	Cytokines	30.97	31.91	2.05	0.26

Wisp1 (Left-hand figure)		Min Ct	Max Ct	Average	SEM
Vector Only	No Cytokines	28.56	29.01	1.74	0.13
	Cytokines	28.61	29.87	1.73	0.06
WNT5A	No Cytokines	28.68	29.36	1.40	0.16
	Cytokines	30.52	Undetermined	0.67	

Wisp1 (Right-hand figure)		Min Ct	Max Ct	Average	SEM
Vector Only	No Cytokines	30.38	31.81	3.35	0.74
	Cytokines	32.26	33.15	0.71	0.03
WNT5A	No Cytokines	29.91	31.39	3.94	0.73
	Cytokines	31.73	33.94	0.77	0.13

Table S4.2 (cont.) – TaqMan CT values for Figure 4.4 with normalised averages and SEM

Wisp2 (Left-hand figure)		Min Ct	Max Ct	Average	SEM
Vector Only	No Cytokines	27.31	28.60	1.24	0.21
	Cytokines	27.90	29.24	1.20	0.14
WNT5A	No Cytokines	29.21	30.56	0.56	0.09
	Cytokines	30.25	30.98	0.41	0.03

Wisp2 (Right-hand figure)		Min Ct	Max Ct	Average	SEM
Vector Only	No Cytokines	26.79	28.03	2.74	0.52
	Cytokines	28.46	29.48	0.59	0.07
WNT5A	No Cytokines	26.51	29.11	3.01	0.90
	Cytokines	28.31	28.99	0.72	0.07

Frzb (Left-hand figure)		Min Ct	Max Ct	Average	SEM
Vector Only	No Cytokines	28.14	29.07	2.15	0.40
	Cytokines	27.59	29.89	2.60	0.57
WNT5A	No Cytokines	29.57	30.16	0.87	0.09
	Cytokines	30.82	31.39	0.43	0.05

Frzb (Right-hand figure)		Min Ct	Max Ct	Average	SEM
Vector Only	No Cytokines	25.86	27.12	4.46	0.98
	Cytokines	29.76	30.80	0.21	0.01
WNT5A	No Cytokines	25.51	27.54	5.26	1.41
	Cytokines	28.86	30.42	0.31	0.06

Col10a1 (Left-hand figure)		Min Ct	Max Ct	Average	SEM
Vector Only	No Cytokines	30.91	32.40	1.94	0.50
	Cytokines	31.25	32.96	1.74	0.16
WNT5A	No Cytokines	31.54	32.13	1.55	0.14
	Cytokines	31.13	31.81	1.91	0.32

Col10a1 (Right-hand figure)		Min Ct	Max Ct	Average	SEM
Vector Only	No Cytokines	26.35	27.62	3.50	0.86
	Cytokines	28.53	29.28	0.46	0.02
WNT5A	No Cytokines	26.30	28.99	3.33	1.05
	Cytokines	27.66	28.85	0.74	0.13

Table S4.3 – Effect of WNT5A in the absence of cytokines. Top 50 significantly regulated probes are ranked by absolute fold change. Positive and negative fold changes are highlighted in blue and orange respectively. Statistically significant ($Q \leq 0.05$) and non-significant Benjamin-Hochberg Q-Values are highlighted in green and red respectively.

Rank	Row	Gene Symbol	Gene Name	+/- FC	Absolute FC	P-Value	BH Q-Value
1	1429900_at	5330406M23Rik	RIKEN cDNA 5330406M23 gene	2.7406	2.7406	0.0410	0.9370
2	1442494_at	C79242	expressed sequence C79242	2.6546	2.6546	0.0431	0.9370
3	1460096_at			2.6393	2.6393	0.0106	0.9370
4	1448018_at			2.5769	2.5769	0.0361	0.9370
5	1447381_at			2.5409	2.5409	0.0198	0.9370
6	1429804_at	Slc22a16	solute carrier family 22 (organic cation transporter), member 16	-2.4470	2.4470	0.0120	0.9370
7	1449434_at	Car3	carbonic anhydrase 3	-2.4444	2.4444	0.0125	0.9370
8	1456914_at	Slc16a4	Solute carrier family 16 (monocarboxylic acid transporters), member 4 (Slc16a4), mRNA	2.4160	2.4160	0.0377	0.9370
9	1423396_at	Agt	angiotensinogen (serpin peptidase inhibitor, clade A, member 8)	-2.4111	2.4111	0.0158	0.9370
10	1437066_at	Zbtb20	zinc finger and BTB domain containing 20	2.3780	2.3780	0.0078	0.9370
11	1438009_at	Hist1h2ad	histone cluster 1, H2ad	2.3680	2.3680	0.0057	0.9370
12	1458452_at	Ankrd11	Ankyrin repeat domain 11, mRNA (cDNA clone MGC:198846 IMAGE:9054811)	2.3609	2.3609	0.0108	0.9370
13	1417507_at	Cyb561	cytochrome b-561	-2.3536	2.3536	0.0030	0.9370
14	1457888_at			2.3355	2.3355	0.0137	0.9370
15	1442418_at	B930096F20Rik	RIKEN cDNA B930096F20 gene	2.3259	2.3259	0.0342	0.9370
16	1440120_at	Gnb211	Guanine nucleotide binding protein (G protein), beta polypeptide 2 like 1 (Gnb211), mRNA	2.3088	2.3088	0.0229	0.9370
17	1438299_at	9230108I15Rik	RIKEN cDNA 9230108I15 gene	2.3080	2.3080	0.0322	0.9370
18	1448054_at			2.3043	2.3043	0.0378	0.9370
19	1418486_at	Vnn1	vanin 1	-2.2889	2.2889	0.0174	0.9370
20	1447509_at			2.2649	2.2649	0.0397	0.9370
21	1449168_a_at	Akap2	A kinase (PRKA) anchor protein 2	2.2399	2.2399	0.0390	0.9370
22	1456821_at			2.2255	2.2255	0.0419	0.9370
23	1458684_at			2.2244	2.2244	0.0088	0.9370
24	1439260_a_at	Enpp3	ectonucleotide pyrophosphatase/phosphodiesterase 3	-2.2076	2.2076	0.0221	0.9370
25	1436905_x_at	Laptm5	lysosomal-associated protein transmembrane 5	-2.1958	2.1958	0.0080	0.9370
26	1449419_at	Dock8	dedicator of cytokinesis 8	-2.1894	2.1894	0.0038	0.9370
27	1417426_at	Srgn	serglycin	-2.1879	2.1879	0.0075	0.9370
28	1444764_at	A130022J21Rik	RIKEN cDNA A130022J21 gene	2.1837	2.1837	0.0296	0.9370
29	1446331_at	Ptgrf	prostaglandin F receptor	-2.1814	2.1814	0.0287	0.9370
30	1444611_at			-2.1799	2.1799	0.0092	0.9370
31	1441253_at			2.1793	2.1793	0.0181	0.9370
32	1420935_a_at	Srrm1	serine/arginine repetitive matrix 1	2.1790	2.1790	0.0298	0.9370
33	1437775_at	Dlst	dihydrolypoamide S-succinyltransferase (E2 component of 2-oxo-glutarate complex)	2.1737	2.1737	0.0021	0.9370
34	1460574_at	Fat4	FAT tumor suppressor homolog 4 (Drosophila)	2.1723	2.1723	0.0247	0.9370
35	1443547_at			2.1674	2.1674	0.0039	0.9370
36	1456933_at			2.1526	2.1526	0.0067	0.9370
37	1426316_at	6330416G13Rik	RIKEN cDNA 6330416G13 gene	-2.1372	2.1372	0.0416	0.9370
38	1427285_s_at	Malat1	metastasis associated lung adenocarcinoma transcript 1 (non-coding RNA)	2.1351	2.1351	0.0109	0.9370
39	1455948_x_at	Matn3	matrilin 3	-2.1284	2.1284	0.0023	0.9370
40	1456262_at	Rbm5	RNA binding motif protein 5	2.1153	2.1153	0.0285	0.9370
41	1421257_at	Pigb	phosphatidylinositol glycan anchor biosynthesis, class B	-2.1131	2.1131	0.0266	0.9370
42	1422865_at	Runx1	runt related transcription factor 1	2.1055	2.1055	0.0226	0.9370
43	1455139_at	A1851716	expressed sequence A1851716	-2.0937	2.0937	0.0149	0.9370
44	1457815_at			2.0886	2.0886	0.0139	0.9370
45	1434325_x_at	Prkar1b	protein kinase, cAMP dependent regulatory, type I beta	-2.0879	2.0879	0.0454	0.9370
46	1458507_at	Rnf216	Ring finger protein 216, mRNA (cDNA clone IMAGE:6822422)	2.0846	2.0846	0.0478	0.9370
47	1459687_x_at			2.0798	2.0798	0.0218	0.9370
48	1457653_at			2.0795	2.0795	0.0011	0.9370
49	1451767_at	Ncf1	neutrophil cytosolic factor 1	-2.0768	2.0768	0.0089	0.9370
50	1437979_at	Zcchc2	Zinc finger, CCHC domain containing 2, mRNA (cDNA clone IMAGE:5365587)	-2.0758	2.0758	0.0146	0.9370

Table S4.4 – Effect of WNT5A in the presence of cytokines. Top 50 significantly regulated probes are ranked by absolute fold change. Positive and negative fold changes are highlighted in blue and orange respectively. Statistically significant ($Q \leq 0.05$) and non-significant Benjamin-Hochberg Q-Values are highlighted in green and red respectively.

Rank	Row	Gene Symbol	Gene Name	+/- FC	Absolute FC	P-Value	BH Q-Value
1	1457508_at	C430003N24Rik	RIKEN cDNA C430003N24 gene	3.2743	3.2743	0.0023	0.6064
2	1458110_at	D430030G11Rik	RIKEN cDNA D430030G11 gene	3.2695	3.2695	0.0210	0.7138
3	1446736_at			3.2135	3.2135	0.0005	0.4401
4	1437806_x_at	Mtch2	mitochondrial carrier homolog 2 (C. elegans)	3.0219	3.0219	0.0178	0.7107
5	1417301_at	Fzd6	frizzled homolog 6 (Drosophila)	-3.0033	3.0033	0.0397	0.7351
6	1433369_at	8430401P03Rik	RIKEN cDNA 8430401P03 gene	2.9924	2.9924	0.0006	0.4401
7	1439036_a_at	Atp1b1	ATPase, Na ⁺ /K ⁺ transporting, beta 1 polypeptide	2.9785	2.9785	0.0146	0.7107
8	1439929_at			2.9548	2.9548	0.0141	0.7107
9	1447723_at			2.9317	2.9317	0.0407	0.7351
10	1440314_at			2.8488	2.8488	0.0225	0.7138
11	1422962_a_at	Psmb8	proteasome (prosome, macropain) subunit, beta type 8 (large multifunctional peptidase 7)	-2.8430	2.8430	0.0044	0.6698
12	1458916_at			2.8372	2.8372	0.0178	0.7107
13	1449623_at	Txnrd3	thioredoxin reductase 3	-2.8284	2.8284	0.0048	0.6698
14	1432114_at	1110035E04Rik	RIKEN cDNA 1110035E04 gene	2.8240	2.8240	0.0157	0.7107
15	1445898_at	Ggcx	gamma-glutamyl carboxylase	2.8111	2.8111	0.0095	0.6948
16	1441816_at	2900056M20Rik	RIKEN cDNA 2900056M20 gene	2.7881	2.7881	0.0216	0.7138
17	1438331_at			2.7573	2.7573	0.0143	0.7107
18	1440809_at			-2.7288	2.7288	0.0117	0.7107
19	1441516_a_at	C130050O18Rik	RIKEN cDNA C130050O18 gene	-2.7255	2.7255	0.0054	0.6776
20	1420288_at			2.7248	2.7248	0.0197	0.7138
21	1430708_a_at	Usp45	ubiquitin specific petidase 45	-2.7155	2.7155	0.0186	0.7138
22	1444992_at	A1120166	expressed sequence A1120166	2.6930	2.6930	0.0067	0.6948
23	1459005_at			2.6888	2.6888	0.0494	0.7351
24	1439928_at			2.6395	2.6395	0.0412	0.7351
25	1440231_at	Mtap9	microtubule-associated protein 9	-2.6210	2.6210	0.0128	0.7107
26	1460092_at			2.5760	2.5760	0.0350	0.7351
27	1446798_at	Map4k3	Mitogen-activated protein kinase kinase kinase 3, mRNA (cDNA clone IMAGE:3603090)	2.5539	2.5539	0.0222	0.7138
28	1415923_at	Ndn	necdin	-2.5316	2.5316	0.0325	0.7328
29	1447055_at	Dnajc11	Dnaj (Hsp40) homolog, subfamily C, member 11	-2.5157	2.5157	0.0184	0.7138
30	1425747_at	Dock5	dedicator of cytokinesis 5	-2.5120	2.5120	0.0228	0.7138
31	1459961_a_at	Stat3	Signal transducer and activator of transcription 3, mRNA (cDNA clone IMAGE:3665873)	2.4956	2.4956	0.0062	0.6948
32	1425555_at	Crks	CDC2-related kinase, arginine/serine-rich	2.4868	2.4868	0.0369	0.7351
33	1445695_at			2.4802	2.4802	0.0021	0.6059
34	1452319_at	Zfp82	zinc finger protein 82	-2.4557	2.4557	0.0367	0.7351
35	1458578_at			2.4049	2.4049	0.0271	0.7203
36	1447706_at			2.3986	2.3986	0.0020	0.6059
37	1439109_at	Ccdc68	coiled-coil domain containing 68	2.3911	2.3911	0.0375	0.7351
38	1440892_at			2.3762	2.3762	0.0111	0.7078
39	1457930_at	Kdm5c	lysine (K)-specific demethylase 5C	2.3636	2.3636	0.0333	0.7328
40	1451418_a_at	Spsb4	splA/ryanodine receptor domain and SOCS box containing 4	-2.3620	2.3620	0.0104	0.6948
41	1446457_at	Ddx58	DEAD (Asp-Glu-Ala-Asp) box polypeptide 58	-2.3572	2.3572	0.0151	0.7107
42	1459641_at			2.3485	2.3485	0.0232	0.7138
43	1450611_at	Orm3	orosomucoid 3	-2.3385	2.3385	0.0026	0.6064
44	1445068_at	Malt1	mucosa associated lymphoid tissue lymphoma translocation gene 1	2.3292	2.3292	0.0269	0.7203
45	1440946_at			-2.3275	2.3275	0.0048	0.6698
46	1429951_at	Ssbp2	single-stranded DNA binding protein 2	2.3217	2.3217	0.0235	0.7138
47	1435575_at	Kntc1	kinetochore associated 1	-2.3182	2.3182	0.0061	0.6948
48	1421989_s_at	Papss2	3'-phosphoadenosine 5'-phosphosulfate synthase 2	2.3004	2.3004	0.0273	0.7203
49	1424775_at	Oas1a	2'-5' oligoadenylate synthetase 1A	-2.2924	2.2924	0.0205	0.7138
50	1444378_at			2.2921	2.2921	0.0201	0.7138

Table S4.5 – Effect of cytokines in the absence of WNT5A. Top 50 significantly regulated probes are ranked by absolute fold change. Positive and negative fold changes are highlighted in blue and orange respectively. Statistically significant ($Q \leq 0.05$) and non-significant Benjamin-Hochberg Q-Values are highlighted in green and red respectively.

Rank	Row	Gene Symbol	Gene Name	+/- FC	Absolute FC	P-Value	BH Q-Value
1	1427747_a_at	Lcn2	lipocalin 2	3211.3040	3211.3040	1.41E-07	4.46E-04
2	1419075_s_at	Saa1	serum amyloid A 1	2256.2703	2256.2703	1.17E-07	4.46E-04
3	1450826_a_at	Saa3	serum amyloid A 3	1963.1525	1963.1525	1.38E-09	3.08E-05
4	1450788_at	Saa1	serum amyloid A 1	1694.9266	1694.9266	4.69E-07	6.84E-04
5	1436530_at	OTTMUSG00000000971	predicted gene, OTTMUSG00000000971	1642.8577	1642.8577	7.02E-07	7.32E-04
6	1449326_x_at	Saa2	serum amyloid A 2	638.6769	638.6769	3.01E-06	8.49E-04
7	1419561_at	Ccl3	chemokine (C-C motif) ligand 3	569.8519	569.8519	2.48E-06	8.49E-04
8	1421228_at	Ccl7	chemokine (C-C motif) ligand 7	463.5318	463.5318	1.20E-05	0.00127659
9	1449824_at	Prg4	proteoglycan 4 (megakaryocyte stimulating factor, articular superficial zone protein)	444.4955	444.4955	5.64E-06	9.35E-04
10	1450297_at	Il6	interleukin 6	441.2112	441.2112	8.44E-06	0.00104345
11	1448881_at	Hp	haptoglobin	428.0871	428.0871	3.67E-06	8.72E-04
12	1423954_at	C3	complement component 3	382.0203	382.0203	1.37E-06	7.32E-04
13	1451344_at	Tmem119	transmembrane protein 119	-359.6308	359.6308	1.19E-06	7.32E-04
14	1418945_at	Mmp3	matrix metalloproteinase 3	268.9582	268.9582	1.51E-05	0.00131501
15	1428815_at	Gstt4	glutathione S-transferase, theta 4	267.4842	267.4842	4.80E-07	6.84E-04
16	1451054_at	Orm1	orosomuroid 1	257.2303	257.2303	3.66E-06	8.72E-04
17	1420380_at	Ccl2	chemokine (C-C motif) ligand 2	239.3932	239.3932	5.98E-06	9.54E-04
18	1451537_at	Chi3l1	chitinase 3-like 1	233.8305	233.8305	7.11E-06	9.89E-04
19	1438665_at	Smpd3	sphingomyelin phosphodiesterase 3, neutral	-228.3422	228.3422	1.37E-05	0.00128759
20	1434484_at	1100001G20Rik	RIKEN cDNA 1100001G20 gene	219.7001	219.7001	6.87E-06	9.89E-04
21	1419530_at	Il12b	interleukin 12b	155.2335	155.2335	1.69E-05	0.00134199
22	1433924_at			-152.1493	152.1493	1.45E-05	0.00130956
23	1455717_s_at	Daam2	dishevelled associated activator of morphogenesis 2	-150.8834	150.8834	1.28E-04	0.00275011
24	1449984_at	Cxcl2	chemokine (C-X-C motif) ligand 2	147.6220	147.6220	5.01E-06	9.09E-04
25	1420438_at	Orm2	orosomuroid 2	142.0294	142.0294	1.66E-06	7.32E-04
26	1449591_at	Casp4	caspase 4, apoptosis-related cysteine peptidase	121.0935	121.0935	2.41E-07	4.59E-04
27	1442726_s_at	A1845619	expressed sequence A1845619	117.7428	117.7428	4.78E-06	8.83E-04
28	1441855_x_at	Cxcl1	chemokine (C-X-C motif) ligand 1	115.5795	115.5795	1.26E-06	7.32E-04
29	1443745_s_at	Dmp1	dentin matrix protein 1	-108.1294	108.1294	2.19E-04	0.00335869
30	1431182_at	EG666031 : Hspa8 : LOC624853 : LOC641192	predicted gene, EG666031 : heat shock protein 8 : hypothetical LOC624853 : similar to heat shock protein 8	108.0675	108.0675	1.02E-04	0.00246132
31	1417314_at	Cfb	complement factor B	106.8491	106.8491	1.72E-06	7.32E-04
32	1457644_s_at	Cxcl1	chemokine (C-X-C motif) ligand 1	105.5933	105.5933	1.35E-04	0.00278365
33	1432523_at	Hipk2	homeodomain interacting protein kinase 2	104.0568	104.0568	5.77E-06	9.35E-04
34	1419684_at	Ccl8	chemokine (C-C motif) ligand 8	101.7400	101.7400	4.48E-06	8.83E-04
35	1436698_x_at	Tmem204	transmembrane protein 204	-99.6293	99.6293	5.62E-06	9.35E-04
36	1438148_at	Cxcl3	chemokine (C-X-C motif) ligand 3	99.4725	99.4725	1.13E-04	0.00257189
37	1419394_s_at	S100a8	S100 calcium binding protein A8 (calgranulin A)	94.8861	94.8861	2.13E-05	0.00144375
38	1423719_at	LOC632073 : U46068	similar to long palate, lung and nasal epithelium carcinoma associated 1 isoform 2 : cDNA sequence U46068	94.3277	94.3277	1.01E-04	0.00245357
39	1417936_at	Ccl9	chemokine (C-C motif) ligand 9	93.3756	93.3756	2.04E-05	0.00143277
40	1443746_x_at	Dmp1	dentin matrix protein 1	-91.7840	91.7840	7.72E-04	0.00603247
41	1418126_at	Ccl5	chemokine (C-C motif) ligand 5	88.8513	88.8513	2.95E-06	8.49E-04
42	1439423_x_at	U46068	cDNA sequence U46068	88.3544	88.3544	1.09E-06	7.32E-04
43	1449153_at	Mmp12	matrix metalloproteinase 12	85.1682	85.1682	2.06E-05	0.00143454
44	1425649_at	Slc39a14	solute carrier family 39 (zinc transporter), member 14	84.6762	84.6762	4.47E-06	8.83E-04
45	1429947_a_at	Zbp1	Z-DNA binding protein 1	82.8222	82.8222	7.94E-05	0.00227951
46	1455993_at	Odz4	odd Oz/ten-m homolog 4 (Drosophila)	-81.2267	81.2267	8.31E-05	0.00231782
47	1417160_s_at	Expi	extracellular proteinase inhibitor	79.9065	79.9065	4.02E-06	8.83E-04
48	1426008_a_at	Slc7a2	solute carrier family 7 (cationic amino acid transporter, y+ system), member 2	75.6727	75.6727	1.65E-07	4.46E-04
49	1456893_at			74.9601	74.9601	3.17E-06	8.52E-04
50	1451922_at	Lman1l	lectin, mannose-binding 1 like	74.6722	74.6722	3.90E-06	8.83E-04

Table S4.6 – Effect of cytokines in the presence of WNT5A. Top 50 significantly regulated probes are ranked by absolute fold change. Positive and negative fold changes are highlighted in blue and orange respectively. Statistically significant ($Q \leq 0.05$) and non-significant Benjamin-Hochberg Q-Values are highlighted in green and red respectively.

Rank	Row	Gene Symbol	Gene Name	+/- FC	Absolute FC	P-Value	BH Q-Value
1	1427747_a_at	Lcn2	lipocalin 2	2563.3347	2563.3347	2.15E-05	0.00116383
2	1419075_s_at	Saa1	serum amyloid A 1	1982.0406	1982.0406	5.71E-07	3.84E-04
3	1450788_at	Saa1	serum amyloid A 1	1911.3606	1911.3606	1.90E-06	6.54E-04
4	1436530_at	OTTMUSG00000000971	predicted gene, OTTMUSG00000000971	1322.0448	1322.0448	1.22E-06	5.41E-04
5	1450826_a_at	Saa3	serum amyloid A 3	878.7861	878.7861	0.00121606	0.00682299
6	1449326_x_at	Saa2	serum amyloid A 2	760.6014	760.6014	2.07E-07	3.22E-04
7	1419561_at	Ccl3	chemokine (C-C motif) ligand 3	638.6044	638.6044	1.08E-07	2.69E-04
8	1449824_at	Prg4	proteoglycan 4 (megakaryocyte stimulating factor, articular superficial zone protein)	601.2683	601.2683	2.48E-06	7.11E-04
9	1448881_at	Hp	haptoglobin	589.7481	589.7481	9.13E-07	4.64E-04
10	1450297_at	Il6	interleukin 6	552.9445	552.9445	7.22E-07	3.94E-04
11	1423954_at	C3	complement component 3	487.5731	487.5731	6.82E-06	8.16E-04
12	1418945_at	Mmp3	matrix metalloproteinase 3	396.9287	396.9287	1.48E-06	5.90E-04
13	1421228_at	Ccl7	chemokine (C-C motif) ligand 7	370.7286	370.7286	2.82E-06	7.11E-04
14	1451537_at	Chi3l1	chitinase 3-like 1	356.2876	356.2876	2.23E-05	0.00118104
15	1451344_at	Tmem119	transmembrane protein 119	-315.3444	315.3444	5.76E-06	7.89E-04
16	1428815_at	Gstt4	glutathione S-transferase, theta 4	251.7484	251.7484	3.81E-07	3.41E-04
17	1420438_at	Orm2	orosomucoid 2	222.2727	222.2727	2.28E-06	7.09E-04
18	1451054_at	Orm1	orosomucoid 1	202.6931	202.6931	1.48E-05	0.00105608
19	1417314_at	Cfb	complement factor B	193.5781	193.5781	6.58E-08	2.45E-04
20	1419530_at	Il12b	interleukin 12b	178.5912	178.5912	7.36E-06	8.16E-04
21	1420380_at	Ccl2	chemokine (C-C motif) ligand 2	176.9120	176.9120	6.74E-06	8.16E-04
22	1449984_at	Cxcl2	chemokine (C-X-C motif) ligand 2	173.0926	173.0926	3.78E-06	7.26E-04
23	1434484_at	1100001G20Rik	RIKEN cDNA 1100001G20 gene	157.7251	157.7251	1.52E-05	0.00106395
24	1460465_at	A930038C07Rik	RIKEN cDNA A930038C07 gene	-155.4903	155.4903	4.41E-06	7.59E-04
25	1423719_at	LOC632073 : U46068	similar to long palate, lung and nasal epithelium carcinoma associated 1 isoform 2 : cDNA sequence U46068	150.8190	150.8190	5.73E-06	7.89E-04
26	1425649_at	Slc39a14	solute carrier family 39 (zinc transporter), member 14	142.0118	142.0118	2.47E-06	7.11E-04
27	1426008_a_at	Slc7a2	solute carrier family 7 (cationic amino acid transporter, y+ system), member 2	126.5383	126.5383	9.74E-06	9.00E-04
28	1455717_s_at	Daam2	dishevelled associated activator of morphogenesis 2	-126.3871	126.3871	6.70E-06	8.16E-04
29	1417936_at	Ccl9	chemokine (C-C motif) ligand 9	117.9082	117.9082	1.57E-05	0.00106395
30	1455993_at	Odz4	odd Oz/ten-m homolog 4 (Drosophila)	-115.5581	115.5581	3.95E-06	7.26E-04
31	1418126_at	Ccl5	chemokine (C-C motif) ligand 5	115.0684	115.0684	8.79E-06	8.50E-04
32	1419394_s_at	S100a8	S100 calcium binding protein A8 (calgranulin A)	106.2597	106.2597	2.27E-05	0.00118982
33	1448550_at	Lbp	lipopolysaccharide binding protein	104.4957	104.4957	7.05E-07	3.94E-04
34	1449591_at	Casp4	caspase 4, apoptosis-related cysteine peptidase	103.1238	103.1238	2.16E-06	7.09E-04
35	1438665_at	Smpd3	sphingomyelin phosphodiesterase 3, neutral	-102.4950	102.4950	7.16E-06	8.16E-04
36	1439423_x_at	U46068	cDNA sequence U46068	99.2122	99.2122	3.42E-05	0.00140771
37	1430998_at	Sqrdl	sulfide quinone reductase-like (yeast)	97.3844	97.3844	6.12E-08	2.45E-04
38	1425197_at	Ptpn2	protein tyrosine phosphatase, non-receptor type 2	97.1053	97.1053	1.88E-05	0.00110395
39	1441855_x_at	Cxcl1	chemokine (C-X-C motif) ligand 1	95.7483	95.7483	1.22E-04	0.00224954
40	1451922_at	Lman1l	lectin, mannose-binding 1 like	91.6415	91.6415	3.05E-06	7.11E-04
41	1435477_s_at	Fcgr2b	Fc receptor, IgG, low affinity IIb	90.4095	90.4095	1.62E-07	3.22E-04
42	1438148_at	Cxcl3	chemokine (C-X-C motif) ligand 3	89.0340	89.0340	6.60E-05	0.00175383
43	1441516_a_at	C130050O18Rik	RIKEN cDNA C130050O18 gene	-85.0116	85.0116	8.98E-06	8.52E-04
44	1457644_s_at	Cxcl1	chemokine (C-X-C motif) ligand 1	84.3500	84.3500	2.28E-06	7.09E-04
45	1417160_s_at	Expi	extracellular proteinase inhibitor	80.9290	80.9290	4.93E-05	0.00159284
46	1419209_at	Cxcl1	chemokine (C-X-C motif) ligand 1	74.9025	74.9025	7.38E-06	8.16E-04
47	1443746_x_at	Dmp1	dentin matrix protein 1	-73.1457	73.1457	2.66E-04	0.00317814
48	1449153_at	Mmp12	matrix metalloproteinase 12	72.0990	72.0990	2.53E-07	3.22E-04
49	1442726_s_at	A1845619	expressed sequence A1845619	71.8896	71.8896	3.24E-06	7.11E-04
50	1433691_at	Ppp1r3c	protein phosphatase 1, regulatory (inhibitor) subunit 3C	-70.8717	70.8717	2.92E-07	3.22E-04

Table S4.7 – Top 50 genes significantly regulated by cytokines only in presence of WNT5A based on significant Q-Value and ranked by absolute fold change. Positive and negative fold changes are highlighted in blue and orange respectively

Rank	Row	Gene Symbol	Gene Name	+/- FC	Absolute FC	P-Value	BH Q-Value
1	1439799_at			-16.0050	16.0050	0.00088745	0.00571949
2	1442335_at			-10.4927	10.4927	0.00017424	0.00265872
3	1437442_at	Pcdh7	Protocadherin 7 (Pcdh7), transcript variant 2, mRNA	-9.8019	9.8019	9.5848E-05	0.00204591
4	1430893_at	2610016E04Rik	RIKEN cDNA 2610016E04 gene	9.6412	9.6412	0.01394941	0.03263388
5	1435787_at	Ppm1l	protein phosphatase 1 (formerly 2C)-like	-8.9455	8.9455	0.00314168	0.01197396
6	1422264_s_at	Klf9	Kruppel-like factor 9	8.6721	8.6721	0.00425507	0.01458118
7	1455377_at	Ttll7	tubulin tyrosine ligase-like family, member 7	-8.2681	8.2681	0.00131814	0.00715582
8	1452398_at	Plce1	phospholipase C, epsilon 1	-8.2459	8.2459	0.00032901	0.00353004
9	1450037_at	Usp9x	ubiquitin specific peptidase 9, X chromosome	-7.8583	7.8583	0.00767457	0.02164671
10	1430834_at	Gprn3	GPRIN family member 3	-7.7692	7.7692	0.00869807	0.02346549
11	1429236_at	Galntl2	UDP-N-acetyl-alpha-D-galactosamine:polypeptide N-acetylgalactosaminyltransferase-like 2	-7.4364	7.4364	0.00101328	0.00614103
12	1440797_at	Dlx6os2	Dlx6 opposite strand transcript 2	-7.1202	7.1202	4.55E-05	0.00152586
13	1445492_at			7.0539	7.0539	0.01055106	0.02674227
14	1421477_at	Cplx2	complexin 2	-6.9635	6.9635	2.436E-05	0.00121824
15	1443257_at	9630050E16Rik	RIKEN cDNA 9630050E16 gene	6.8821	6.8821	0.00291568	0.0114629
16	1447313_at			-6.8778	6.8778	0.0089739	0.02395537
17	1427363_at			6.8657	6.8657	0.00332228	0.01243841
18	1447854_s_at	Hist2h2be	histone cluster 2, H2be	-6.4702	6.4702	0.00028808	0.00328966
19	1426546_at	Tesk2	testis-specific kinase 2	-6.3263	6.3263	0.00725669	0.02087606
20	1420178_at			6.1460	6.1460	1.0654E-05	0.00094634
21	1439077_at	Zxda	zinc finger, X-linked, duplicated A	-6.1398	6.1398	0.00080325	0.00544791
22	1438352_at			6.1270	6.1270	0.00202856	0.00918042
23	1430581_at	Bclaf1	BCL2-associated transcription factor 1	6.0971	6.0971	0.00018969	0.00275892
24	1425220_x_at	LOC100038935	hypothetical protein LOC100038935	-6.0751	6.0751	0.01909001	0.04095949
25	1458586_at			5.9533	5.9533	0.011252	0.02797992
26	1444069_at			-5.9239	5.9239	0.00153559	0.00778232
27	1458592_at			-5.9132	5.9132	0.00043945	0.00405213
28	1458282_at			5.8215	5.8215	0.01253779	0.0302884
29	1440833_at	Cdc2l5	cell division cycle 2-like 5 (cholinesterase-related cell division controller)	5.7823	5.7823	0.00544289	0.01716588
30	1457529_x_at			5.7786	5.7786	0.020961	0.04407347
31	1439929_at			5.7167	5.7167	0.0012802	0.00703638
32	1435398_at	Stxbp5	syntaxin binding protein 5 (tomosyn)	-5.7156	5.7156	0.00033593	0.00355812
33	1440934_at	6230409E13Rik	RIKEN cDNA 6230409E13 gene	-5.6813	5.6813	0.00121665	0.00682461
34	1441187_at	E330037M01Rik	RIKEN cDNA E330037M01 gene	5.6509	5.6509	0.00751738	0.02135015
35	1433819_s_at	Agpat3	1-acylglycerol-3-phosphate O-acyltransferase 3	-5.6200	5.6200	0.00174765	0.00840934
36	1440560_at			5.5874	5.5874	0.00096323	0.0059842
37	1449651_x_at	EG668525	PREDICTED: Mus musculus predicted gene, EG668525 (EG668525), mRNA	5.5680	5.5680	0.00615021	0.01862967
38	1427265_at	Bcr	breakpoint cluster region	-5.5646	5.5646	0.00248726	0.01035933
39	1440417_at	D19Ertd409e	DNA segment, Chr 19, ERATO Doi 409, expressed	5.4770	5.4770	0.0012998	0.00709878
40	1416893_at	Fam107b	family with sequence similarity 107, member B	5.4738	5.4738	0.00272887	0.01099781
41	1453361_at	Hells	helicase, lymphoid specific	5.4031	5.4031	0.00051353	0.00435873
42	1437127_at	A630033E08Rik	RIKEN cDNA A630033E08 gene (A630033E08Rik), transcript variant 1, mRNA	-5.3335	5.3335	0.01602933	0.03607262
43	1421222_at	Fip1l1	FIP1 like 1 (S. cerevisiae)	5.2150	5.2150	0.00079221	0.00540936
44	1440769_at	2010305A19Rik	RIKEN cDNA 2010305A19 gene, mRNA (cDNA clone MGC:8003 IMAGE:3585966)	-5.1741	5.1741	0.01461774	0.03374952
45	1433600_at	Adra2a	adrenergic receptor, alpha 2a	-5.1643	5.1643	0.00669055	0.01973726
46	1449006_at	Gla	galactosidase, alpha	5.0932	5.0932	0.01245876	0.03014507
47	1438331_at			5.0190	5.0190	0.00355731	0.01297982
48	1442332_at			4.9912	4.9912	0.00029235	0.00330176
49	1443354_at			-4.9863	4.9863	0.00596998	0.01825335
50	1421851_at	Mtap1b	microtubule-associated protein 1B	-4.9762	4.9762	0.01007685	0.02595078

Table S4.8 – TaqMan C_T values for Figure 4.11 with normalised averages and SEM

Anxa1		Min Ct	Max Ct	Average	SEM
Vector Only	No Cytokines	23.88	25.26	1.35	0.16
	Cytokines	23.71	24.62	1.12	0.04
WNT5A	No Cytokines	23.72	25.50	1.71	0.40
	Cytokines	23.51	24.47	1.30	0.14

Matn3		Min Ct	Max Ct	Average	SEM
Vector Only	No Cytokines	32.28	34.33	7.30	2.95
	Cytokines	36.17	36.17		
WNT5A	No Cytokines	32.82	34.89	4.65	1.46
	Cytokines	34.96	38.04	0.67	

Prg4		Min Ct	Max Ct	Average	SEM
Vector Only	No Cytokines	35.51	39.28		
	Cytokines	27.61	29.23	1.77	0.18
WNT5A	No Cytokines	35.78	39.41		
	Cytokines	27.09	29.01	2.12	0.54

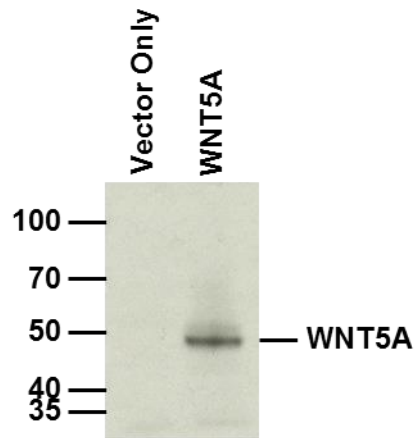


Figure S4.1 – Detection of human WNT5A-FLAG with specific WNT5A antibody. ATDC5 cells were transiently transfected with human WNT5A-FLAG and cell lysates were probed using an antibody specific for WNT5A via western blot. Human WNT5A-FLAG = 44.99 kDa. Endogenous mouse WNT5A = 42.35 kDa (isoform 1) or 40.89 kDa (isoform 2). Predicted molecular weights based on amino acid sequence.

Table S5.1 – TaqMan C_T values for Figure 5.4 B

Col2a1		Min	Max	Normalised	SEM	
Plastic	Non-induced	28.26	29.78	0.08	0.02	
	From Micromass Culture	Ins + Asc Removed	22.48	24.39	2.66	0.09
		Ins + Asc Retained	22.91	23.93	1.97	0.13
Type II Collagen	Non-induced	27.42	29.96	0.11	0.05	
	From Micromass Culture	Ins + Asc Removed	22.77	23.37	3.94	0.19
		Ins + Asc Retained	23.28	24.56	2.40	0.11

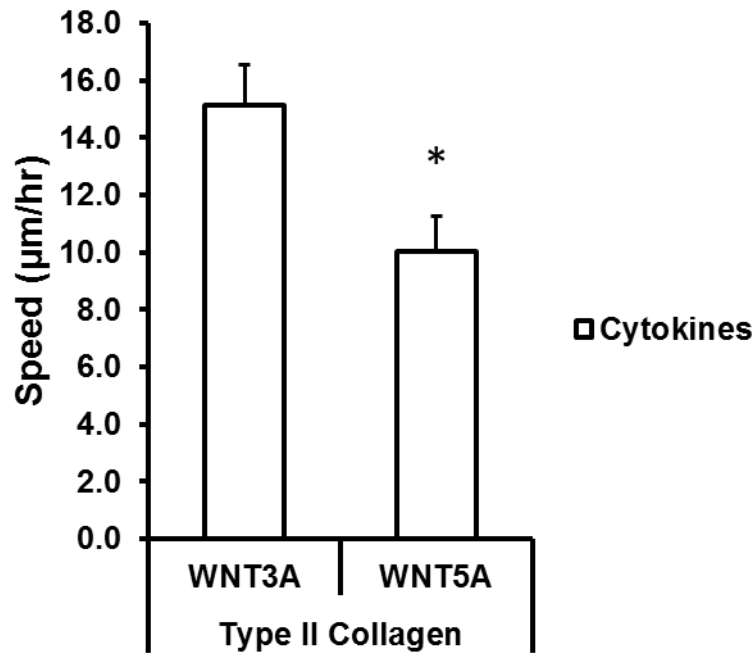


Figure S5.1 – WNT5A decreases speed of migration in cytokine-stimulated ATDC5 cells on type II collagen compared to WNT3A. Experiment performed twice and significance observed in both experiments

References

- Adams, C., and Horton Jr, W. (1998). Chondrocyte Apoptosis Increases With Age in the Articular Cartilage of Adult Animals. *The Anatomical Record*. 250, 418-425.
- Afonso, P. V., McCann, C. P., Kapnick, S. M., and Parent, C. A. (2013). Discoidin domain receptor 2 regulates neutrophil chemotaxis in 3D collagen matrices. *Blood*. 121(9), 1644-1650.
- Ahrens, P. B., Solursh, M., and Reiter, R. S. (1977). Stage-related capacity for limb chondrogenesis in cell culture. *Developmental biology*. 60(1), 69-82.
- Aigner, T., and Dudhia, J. (1997). Phenotypic modulation of chondrocytes as a potential therapeutic target in osteoarthritis: a hypothesis. *Annals of the rheumatic diseases*. 56, 287-291.
- Akgun, I., Unlu, M. C., Erdal, O. A., Ogut, T., Erturk, M., Ovali, E., Kantarci, F., Caliskan, G., and Akgun, Y. (2015). Matrix-induced autologous mesenchymal stem cell implantation versus matrix-induced autologous chondrocyte implantation in the treatment of chondral defects of the knee: a 2-year randomized study. *Archives of orthopaedic and trauma surgery*. 135(2), 251-263.
- Akhtar, N., Miller, M. J., and Haqqi, T. M. (2011). Effect of a Herbal-Leucine mix on the IL-1beta-induced cartilage degradation and inflammatory gene expression in human chondrocytes. *BMC Complement Altern Med*. 11, 66.
- Alsalamah, S., Amin, R., Gemba, T., and Lotz, M. (2004). Identification of mesenchymal progenitor cells in normal and osteoarthritic human articular cartilage. *Arthritis Rheum*. 50(5), 1522-1532.
- Altaf, F. M., Hering, T. M., Kazmi, N. H., Yoo, J. U., and Johnstone, B. (2006). Ascorbate-enhanced chondrogenesis of ATDC5 cells. *Eur Cell Mater*. 12, 64-69; discussion 69-70.
- Archer, C., and Francis-West, P. (2003). The Chondrocyte. *Int J Biochem Cell Bio*. 35, 401-404.
- Arthritis Research UK (2011). Osteoarthritis, *Arthritis Research UK*
<http://www.arthritisresearchuk.org/Files/2025-Osteoarthritis.pdf>, Accessed 23rd May 2011
- Atsumi, T., Miwa, Y., Kimata, K., and Ikawa, Y. (1990). A chondrogenic cell line derived from a differentiating culture of AT805 teratocarcinoma cells. *Cell Differ Dev*. 30(2), 109-116.
- Bader, B. L., Rayburn, H., Crowley, D., and Hynes, R. O. (1998). Extensive vasculogenesis, angiogenesis, and organogenesis precede lethality in mice lacking all alpha v integrins. *Cell*. 95(4), 507-519.
- Baker, N., Sharpe, P., Culley, K., Otero, M., Bevan, D., Newham, P., Barker, W., Clements, K. M., Langham, C. J., Goldring, M. B., and Gavrilovic, J. (2012). Dual regulation of metalloproteinase expression in chondrocytes by Wnt-1-inducible signaling pathway protein 3/CCN6. *Arthritis Rheum*. 64(7), 2289-2299.
- Bakker, E. R., Raghoebir, L., Franken, P. F., Helvensteijn, W., van Gurp, L., Meijlink, F., van der Valk, M. A., Rottier, R. J., Kuipers, E. J., van Veelen, W., and Smits, R. (2012). Induced Wnt5a expression perturbs embryonic outgrowth and intestinal elongation, but is well-tolerated in adult mice. *Developmental biology*. 369(1), 91-100.
- Ballock, R. T., Heydemann, A., Wakefield, L. M., Flanders, K. C., Roberts, A. B., and Sporn, M. B. (1993). TGF-beta 1 prevents hypertrophy of epiphyseal chondrocytes: regulation of gene expression for cartilage matrix proteins and metalloproteases. *Developmental biology*. 158(2), 414-429.

- Banu, N., and Tsuchiya, T. (2007). Markedly different effects of hyaluronic acid and chondroitin sulfate-A on the differentiation of human articular chondrocytes in micromass and 3-D honeycomb rotation cultures. *J Biomed Mater Res A*. 80(2), 257-267.
- Barbolina, M. V., Adley, B. P., Kelly, D. L., Shepard, J., Fought, A. J., Scholtens, D., Penzes, P., Shea, L. D., and Stack, M. S. (2009). Downregulation of connective tissue growth factor by three-dimensional matrix enhances ovarian carcinoma cell invasion. *Int J Cancer*. 125(4), 816-825.
- Barter, M. J., and Young, D. A. (2013). Epigenetic mechanisms and non-coding RNAs in osteoarthritis. *Current rheumatology reports*. 15(9), 353.
- Bau, B., Gebhard, P., Haag, J., Knorr, T., Bartnik, E., and Aigner, T. (2002). Relative messenger RNA expression profiling of collagenases and aggrecanases in human articular chondrocytes in vivo and in vitro. *Arthritis & Rheumatism*. 46(10), 2648-2657.
- Beiraghi, S., Leon-Salazar, V., Larson, B. E., John, M. T., Cunningham, M. L., Petryk, A., and Lohr, J. L. (2011). Craniofacial and intraoral phenotype of Robinow syndrome forms. *Clinical genetics*. 80(1), 15-24.
- Benya, P. D., Brown, P. D., and Padilla, S. R. (1988). Microfilament modification by dihydrocytochalasin B causes retinoic acid-modulated chondrocytes to reexpress the differentiated collagen phenotype without a change in shape. *The Journal of cell biology*. 106(1), 161-170.
- Bernstein, P., Dong, M., Corbeil, D., Gelinsky, M., Günther, K., and Fickert, S. (2009). Pellet Culture Elicits Superior Chondrogenic Redifferentiation than Alginate-Based Systems. *Biotechnol Prog*. 25(4).
- Bi, L., Liu, X., Wang, C., Cao, Y., Mao, R., Li, P., and Geng, M. (2014). Wnt5a involved in regulation of the biological behavior of hepatocellular carcinoma. *International journal of clinical and experimental pathology*. 7(3), 987-995.
- Billinghurst, R., Dahlberg, L., Ionescu, M., Reiner, A., Bourne, R., Rorabeck, C., Mitchell, P., Hambor, J., Diekmann, O., Tschesche, H., Chen, J., Van Wart, H., and Poole, A. (1997). Enhanced cleavage of type II collagen by collagenases in osteoarthritic articular cartilage. *The Journal of clinical investigation*. 99(7), 1534-1545.
- Bizzarro, V., Belvedere, R., Dal Piaz, F., Parente, L., and Petrella, A. (2012). Annexin A1 induces skeletal muscle cell migration acting through formyl peptide receptors. *PLoS One*. 7(10), e48246.
- Blanco, F., Ochs, R., Schwarz, H., and Lotz, M. (1995). Chondrocyte Apoptosis Induced by Nitric Oxide. *Am J Path*. 146(1), 75-85.
- Blom, A., Brockbank, S., van Lent, P., van Beuningen, H., Geurts, J., Takahashi, N., van der Kraan, P., van de Loo, F., Schreurs, W., Clements, K., Newham, P., and van den Berg, W. (2009). Involvement of the Wnt Signaling Pathway in Experimental and Human Osteoarthritis. *Arthritis & Rheumatism*. 60(2), 501-512.
- Bo, H., Zhang, S., Gao, L., Chen, Y., Zhang, J., Chang, X., and Zhu, M. (2013). Upregulation of Wnt5a promotes epithelial-to-mesenchymal transition and metastasis of pancreatic cancer cells. *BMC cancer*. 13, 496.

- Bobick, B. E., and Cobb, J. (2012). Shox2 regulates progression through chondrogenesis in the mouse proximal limb. *J Cell Sci.* 125(Pt 24), 6071-6083.
- Bonaventure, J., Kadhom, N., Cohen-Solal, L., Ng, K., Bourguignon, J., Lasselin, C., and Freisinger, P. (1994). Reexpression of Cartilage-Specific Genes by Dedifferentiated Human Articular Chondrocytes Cultured in Alginate Beads. *Exp Cell Res.* 212, 97-104.
- Boos, N., Nerlich, A. G., Wiest, I., von der Mark, K., and Aebi, M. (1997). Immunolocalization of type X collagen in human lumbar intervertebral discs during ageing and degeneration. *Histochemistry and cell biology.* 108(6), 471-480.
- Boot-Handford, R., and Tuckwell, D. (2003). Fibrillar collagen: the key to vertebrate evolution? A tale of molecular incest. *BioEssays.* 25(2), 142-151.
- Boumah, C. E., Lee, M., Selvamurugan, N., Shimizu, E., and Partridge, N. C. (2009). Runx2 recruits p300 to mediate parathyroid hormone's effects on histone acetylation and transcriptional activation of the matrix metalloproteinase-13 gene. *Molecular endocrinology.* 23(8), 1255-1263.
- Bradley, E. W., and Drissi, M. H. (2010). WNT5A regulates chondrocyte differentiation through differential use of the CaN/NFAT and IKK/NF-kappaB pathways. *Molecular endocrinology.* 24(8), 1581-1593.
- Brigstock, D., Goldschmeding, R., Katsube, K., Lam, S., Lau, L., Lyons, K., Naus, C., Perbal, B., Riser, B., Takigawa, M., and Yeger, H. (2003). Proposal for a unified CCN nomenclature. *J Clin Pathol: Mol Pathol.* 56, 127-128.
- Briolay, A., Lencel, P., Bessueille, L., Caverzasio, J., Buchet, R., and Magne, D. (2013). Autocrine stimulation of osteoblast activity by Wnt5a in response to TNF-alpha in human mesenchymal stem cells. *Biochem Biophys Res Commun.* 430(3), 1072-1077.
- Brunetti-Pierri, N., Del Gaudio, D., Peters, H., Justino, H., Ott, C. E., Mundlos, S., and Bacino, C. A. (2008). Robinow syndrome: phenotypic variability in a family with a novel intragenic ROR2 mutation. *American journal of medical genetics Part A.* 146A(21), 2804-2809.
- Buckwalter, J., and Mankin, H. (1997). Articular Cartilage. Part I: Tissue Design and Cartilage-Matrix Interactions. *JBJS.* 79-A(4), 600-611.
- Buda, R., Vannini, F., Castagnini, F., Cavallo, M., Ruffilli, A., Ramponi, L., Pagliuzzi, G., and Giannini, S. (2015). Regenerative treatment in osteochondral lesions of the talus: autologous chondrocyte implantation versus one-step bone marrow derived cells transplantation. *International orthopaedics.*
- Burleigh, A., Chanalaris, A., Gardiner, M. D., Driscoll, C., Boruc, O., Saklatvala, J., and Vincent, T. L. (2012). Joint immobilization prevents murine osteoarthritis and reveals the highly mechanosensitive nature of protease expression in vivo. *Arthritis Rheum.* 64(7), 2278-2288.
- Burrage, P., Mix, K., and Brinckerhoff, C. (2006). Matrix Metalloproteinases: Role In Arthritis. *Frontiers in Bioscience.* 11, 529-543.
- Cai, S. X., Liu, A. R., He, H. L., Chen, Q. H., Yang, Y., Guo, F. M., Huang, Y. Z., Liu, L., and Qiu, H. B. (2014). Stable genetic alterations of beta-catenin and ROR2 regulate the Wnt pathway, affect the fate of MSCs. *J Cell Physiol.* 229(6), 791-800.

- Caldwell, G. M., Jones, C., Gensberg, K., Jan, S., Hardy, R. G., Byrd, P., Chughtai, S., Wallis, Y., Matthews, G. M., and Morton, D. G. (2004). The Wnt antagonist sFRP1 in colorectal tumorigenesis. *Cancer Res.* 64(3), 883-888.
- Cals, F. L., Hellingman, C. A., Koevoet, W., Baatenburg de Jong, R. J., and van Osch, G. J. (2012). Effects of transforming growth factor-beta subtypes on in vitro cartilage production and mineralization of human bone marrow stromal-derived mesenchymal stem cells. *J Tissue Eng Regen Med.* 6(1), 68-76.
- Caron, M. M., Emans, P. J., Cremers, A., Surtel, D. A., Coolen, M. M., van Rhijn, L. W., and Welting, T. J. (2013). Hypertrophic differentiation during chondrogenic differentiation of progenitor cells is stimulated by BMP-2 but suppressed by BMP-7. *Osteoarthritis Cartilage.* 21(4), 604-613.
- Carter, D., Beaupré, G., Wong, M., Smith, L., Andriacchi, T., and Schurman, D. (2004). The Mechanobiology of Articular Cartilage Development and Degeneration. *Clin Ortho Rel Res.* 427, S69-S77.
- CDC (2010). Osteoarthritis, *Centers for Disease Control and Prevention*
<http://www.cdc.gov/arthritis/basics/osteoarthritis.htm>, Accessed 3rd November 2010
- Cha, B. H., Kim, J. H., Kang, S. W., Do, H. J., Jang, J. W., Choi, Y. R., Park, H., Kim, B. S., and Lee, S. H. (2013). Cartilage tissue formation from dedifferentiated chondrocytes by codelivery of BMP-2 and SOX-9 genes encoding bicistronic vector. *Cell Transplant.* 22(9), 1519-1528.
- Chang, C., Lauffenburger, D. A., and Morales, T. I. (2003). Motile chondrocytes from newborn calf: migration properties and synthesis of collagen II. *Osteoarthritis Cartilage.* 11(8), 603-612.
- Chen, C. C., and Lau, L. F. (2009). Functions and mechanisms of action of CCN matricellular proteins. *Int J Biochem Cell Biol.* 41(4), 771-783.
- Chen, L., Fink, T., Ebbesen, P., and Zachar, V. (2006). Temporal transcriptome of mouse ATDC5 chondroprogenitors differentiating under hypoxic conditions. *Exp Cell Res.* 312(10), 1727-1744.
- Chen, L., Fink, T., Zhang, X. Y., Ebbesen, P., and Zachar, V. (2005). Quantitative transcriptional profiling of ATDC5 mouse progenitor cells during chondrogenesis. *Differentiation.* 73(7), 350-363.
- Cheng, J., Wang, Y., Wang, Z., Yang, M., and Wu, Y. (2010). Differential regulation of proteoglycan-4 expression by IL-1alpha and TGF-beta1 in rat condylar chondrocytes. *The Tohoku journal of experimental medicine.* 222(3), 211-218.
- Cheung, K. S., Hashimoto, K., Yamada, N., and Roach, H. I. (2009). Expression of ADAMTS-4 by chondrocytes in the surface zone of human osteoarthritic cartilage is regulated by epigenetic DNA de-methylation. *Rheumatology international.* 29(5), 525-534.
- Cheung, W., Chow, K., Lee, K., and Leung, K. (2008). Chondrocyte Pellet Culture for Cartilage Repair Research. In *A Practical Manual for Musculoskeletal Research*, (World Scientific), pp. 165-175.
- Cho, Y. D., Yoon, W. J., Kim, W. J., Woo, K. M., Baek, J. H., Lee, G., Ku, Y., van Wijnen, A. J., and Ryoo, H. M. (2014). Epigenetic Modifications and Canonical WNT Signaling enable Trans-differentiation of non-osteogenic cells into osteoblasts. *J Biol Chem.*

- Chowdhury, A., Bezuidenhout, L. W., Mulet-Sierra, A., Jomha, N. M., and Adesida, A. B. (2013). Effect of interleukin-1beta treatment on co-cultures of human meniscus cells and bone marrow mesenchymal stromal cells. *BMC musculoskeletal disorders*. 14, 216.
- Church, V., Nohno, T., Linker, C., Marcelle, C., and Francis-West, P. (2002). Wnt regulation of chondrocyte differentiation. *J Cell Sci*. 115(Pt 24), 4809-4818.
- Cigan, A. D., Nims, R. J., Albro, M. B., Esau, J. D., Dreyer, M. P., Vunjak-Novakovic, G., Hung, C. T., and Ateshian, G. A. (2013). Insulin, ascorbate, and glucose have a much greater influence than transferrin and selenous acid on the in vitro growth of engineered cartilage in chondrogenic media. *Tissue Eng Part A*. 19(17-18), 1941-1948.
- Clark, C. E., Nourse, C. C., and Cooper, H. M. (2012). The tangled web of non-canonical Wnt signalling in neural migration. *Neuro-Signals*. 20(3), 202-220.
- Clutterbuck, A. L., Allaway, D., Harris, P., and Mobasheri, A. (2013). Curcumin reduces prostaglandin E2, matrix metalloproteinase-3 and proteoglycan release in the secretome of interleukin 1beta-treated articular cartilage. *F1000Res*. 2, 147.
- Conde, J., Gomez, R., Bianco, G., Scotece, M., Lear, P., Dieguez, C., Gomez-Reino, J., Lago, F., and Gualillo, O. (2011). Expanding the adipokine network in cartilage: identification and regulation of novel factors in human and murine chondrocytes. *Annals of the rheumatic diseases*. 70(3), 551-559.
- Corps, A. N., Robinson, A. H., Movin, T., Costa, M. L., Hazleman, B. L., and Riley, G. P. (2006). Increased expression of aggrecan and biglycan mRNA in Achilles tendinopathy. *Rheumatology*. 45(3), 291-294.
- Cote, M. C., Lavoie, J. R., Houle, F., Poirier, A., Rousseau, S., and Huot, J. (2010). Regulation of vascular endothelial growth factor-induced endothelial cell migration by LIM kinase 1-mediated phosphorylation of annexin 1. *J Biol Chem*. 285(11), 8013-8021.
- Cox, E. A., Sastry, S. K., and Huttenlocher, A. (2001). Integrin-mediated adhesion regulates cell polarity and membrane protrusion through the Rho family of GTPases. *Mol Biol Cell*. 12(2), 265-277.
- Cremer, M., Rosloniec, E., and Kang, A. (1998). The cartilage collagens: a review of their structure, organization, and role in the pathogenesis of experimental arthritis in animals and in human rheumatic disease. *J Mol Med*. 76, 275-288.
- Cullum, R., Alder, O., and Hoodless, P. A. (2011). The next generation: using new sequencing technologies to analyse gene regulation. *Respirology*. 16(2), 210-222.
- Damazo, A. S., Moradi-Bidhendi, N., Oliani, S. M., and Flower, R. J. (2007). Role of annexin 1 gene expression in mouse craniofacial bone development. *Birth defects research Part A, Clinical and molecular teratology*. 79(7), 524-532.
- Davidson, R., Waters, J., Kevorkian, L., Darrah, C., Cooper, A., Donell, S., and Clark, I. (2006). Expression profiling of metalloproteinases and their inhibitors in synovium and cartilage. *Arthritis Res Ther*. 8(4).

De Cat, B. (2003). Processing by proprotein convertases is required for glypican-3 modulation of cell survival, Wnt signaling, and gastrulation movements. *The Journal of cell biology*. 163(3), 625-635.

Dean, D., Martel-Pelletier, J., Pelletier, J., Howell, D., and Woessner Jr, J. (1989). Evidence for metalloproteinase and metalloproteinase inhibitor imbalance in human osteoarthritic cartilage. *The Journal of clinical investigation*. 84(2), 678-685.

Demoor, M., Ollitrault, D., Gomez-Leduc, T., Bouyoucef, M., Hervieu, M., Fabre, H., Lafont, J., Denoix, J. M., Audigie, F., Mallein-Gerin, F., Legendre, F., and Galera, P. (2014). Cartilage tissue engineering: Molecular control of chondrocyte differentiation for proper cartilage matrix reconstruction. *Biochim Biophys Acta*.

Deng, G., Li, Z. Q., Zhao, C., Yuan, Y., Niu, C. C., Zhao, C., Pan, J., and Si, W. K. (2011). WNT5A expression is regulated by the status of its promoter methylation in leukaemia and can inhibit leukemic cell malignant proliferation. *Oncology reports*. 25(2), 367-376.

Denker, A. E., Haas, A. R., Nicoll, S. B., and Tuan, R. S. (1999). Chondrogenic differentiation of murine C3H10T1/2 multipotential mesenchymal cells: I. Stimulation by bone morphogenetic protein-2 in high-density micromass cultures. *Differentiation*. 64(2), 67-76.

Dessau, W., von der Mark, H., von der Mark, K., and Fischer, S. (1980). Changes in the patterns of collagens and fibronectin during limb-bud chondrogenesis. *Journal of embryology and experimental morphology*. 57, 51-60.

Dhar, A., and Ray, A. (2010). The CCN family proteins in carcinogenesis. *Experimental oncology*. 32(1), 2-9.

Diaz-Mendoza, M. J., Lorda-Diez, C. I., Montero, J. A., Garcia-Porrero, J. A., and Hurle, J. M. (2014). Reelin/DAB-1 Signaling in the Embryonic Limb Regulates the Chondrogenic Differentiation of Digit Mesodermal Progenitors. *J Cell Physiol*.

DiMilla, P. A., Stone, J. A., Quinn, J. A., Albelda, S. M., and Lauffenburger, D. A. (1993). Maximal migration of human smooth muscle cells on fibronectin and type IV collagen occurs at an intermediate attachment strength. *The Journal of cell biology*. 122(3), 729-737.

Ding, J., Ghali, O., Lencel, P., Broux, O., Chauveau, C., Devedjian, J. C., Hardouin, P., and Magne, D. (2009). TNF-alpha and IL-1beta inhibit RUNX2 and collagen expression but increase alkaline phosphatase activity and mineralization in human mesenchymal stem cells. *Life sciences*. 84(15-16), 499-504.

Dorsky, R. I., Moon, R. T., and Raible, D. W. (1998). Control of neural crest cell fate by the Wnt signalling pathway. *Nature*. 396(6709), 370-373.

Dower, S. K., Qwarnstrom, E. E., Page, R. C., Blanton, R. A., Kupper, T. S., Raines, E., Ross, R., and Sims, J. E. (1990). Biology of the interleukin-1 receptor. *J Invest Dermatol*. 94(6 Suppl), 68S-73S.

Dowthwaite, G. P., Bishop, J. C., Redman, S. N., Khan, I. M., Rooney, P., Evans, D. J., Houghton, L., Bayram, Z., Boyer, S., Thomson, B., Wolfe, M. S., and Archer, C. W. (2004). The surface of articular cartilage contains a progenitor cell population. *J Cell Sci*. 117(Pt 6), 889-897.

- Dozin, B., Quarto, R., Campanile, G., and Cancedda, R. (1992). In vitro differentiation of mouse embryo chondrocytes: requirement for ascorbic acid. *European journal of cell biology*. 58(2), 390-394.
- Dudhia, J. (2005). Aggrecan, aging and assembly in articular cartilage. *Cell Mol Life Sci*. 62, 2241-2256.
- Egli, R. J., Bastian, J. D., Ganz, R., Hofstetter, W., and Leunig, M. (2008). Hypoxic expansion promotes the chondrogenic potential of articular chondrocytes. *J Orthop Res*. 26(7), 977-985.
- Ekstrom, E. J., Sherwood, V., and Andersson, T. (2011). Methylation and loss of Secreted Frizzled-Related Protein 3 enhances melanoma cell migration and invasion. *PLoS One*. 6(4), e18674.
- Eyre, D., and Wu, J. (1983). Collagen of fibrocartilage: A distinctive molecular phenotype in bovine meniscus. *FEBS*. 158(2), 265-270.
- Faith, S. A., Smith, L. P., Swatland, A. S., and Reed, D. S. (2012). Growth conditions and environmental factors impact aerosolization but not virulence of *Francisella tularensis* infection in mice. *Frontiers in cellular and infection microbiology*. 2, 126.
- Farrell, E., Both, S. K., Odorfer, K. I., Koevoet, W., Kops, N., O'Brien, F. J., Baatenburg de Jong, R. J., Verhaar, J. A., Cuijpers, V., Jansen, J., Erben, R. G., and van Osch, G. J. (2011). In-vivo generation of bone via endochondral ossification by in-vitro chondrogenic priming of adult human and rat mesenchymal stem cells. *BMC musculoskeletal disorders*. 12, 31.
- Fischer, J., Dickhut, A., Rickert, M., and Richter, W. (2010). Human articular chondrocytes secrete parathyroid hormone-related protein and inhibit hypertrophy of mesenchymal stem cells in coculture during chondrogenesis. *Arthritis Rheum*. 62(9), 2696-2706.
- Fischer, L., Boland, G., and Tuan, R. (2002a). Wnt signaling during BMP-2 stimulation of mesenchymal chondrogenesis. *J Cell Bio*. 84(4), 816-831.
- Fischer, L., Boland, G., and Tuan, R. (2002b). Wnt-3A Enhances Bone Morphogenetic Protein-2-mediated Chondrogenesis of Murine C3H10T1/2 Mesenchymal Cells. *J Bio Chem*. 277(34), 30870-30878.
- Folgueras, A. R., Fueyo, A., Garcia-Suarez, O., Cox, J., Astudillo, A., Tortorella, P., Campestre, C., Gutierrez-Fernandez, A., Fanjul-Fernandez, M., Pennington, C. J., Edwards, D. R., Overall, C. M., and Lopez-Otin, C. (2008). Collagenase-2 deficiency or inhibition impairs experimental autoimmune encephalomyelitis in mice. *J Biol Chem*. 283(14), 9465-9474.
- Fong, Y. C., Lin, C. Y., Su, Y. C., Chen, W. C., Tsai, F. J., Tsai, C. H., Huang, C. Y., and Tang, C. H. (2011). CCN6 enhances ICAM-1 expression and cell motility in human chondrosarcoma cells. *J Cell Physiol*.
- Fosang, A., Last, K., Knäuper, V., Neame, P., Murphy, G., Hardingham, T., Tschesche, T., and Hamilton, J. (1993). Fibroblast and neutrophil collagenases cleave at two sites in the cartilage aggrecan interglobular domain. *The Biochemical journal*. 295(1), 273-276.
- Francioli, S., Candrian, C., Martin, K., Heberer, M., Martin, I., and Barbero, A. (2010). Effect of three-dimensional expansion and cell seeding density on the cartilage-forming capacity of human articular chondrocytes in type II collagen sponges. *J Biomed Mat Res A*. 95A(3), 924-931.

- Frazier, S. B., Roodhouse, K. A., Hourcade, D. E., and Zhang, L. (2008). The Quantification of Glycosaminoglycans: A Comparison of HPLC, Carbazole, and Alcian Blue Methods. *Open glycoscience*. 1, 31-39.
- Fujisawa, T., Hattori, T., Ono, M., Uehara, J., Kubota, S., Kuboki, T., and Takigawa, M. (2008). CCN family 2/connective tissue growth factor (CCN2/CTGF) stimulates proliferation and differentiation of auricular chondrocytes. *Osteoarthritis and Cartilage*. 16(7), 787-795.
- Fukuyo, S., Yamaoka, K., Sonomoto, K., Oshita, K., Okada, Y., Saito, K., Yoshida, Y., Kanazawa, T., Minami, Y., and Tanaka, Y. (2014). IL-6-accelerated calcification by induction of ROR2 in human adipose tissue-derived mesenchymal stem cells is STAT3 dependent. *Rheumatology*. 53(7), 1282-1290.
- Gagne, T., Chappell-Afonso, K., Johnson, J., McPherson, J., Oldham, C., Tubo, R., Vaccaro, C., and Vasios, G. (2000). Enhanced proliferation and differentiation of human articular chondrocytes when seeded at low cell densities in alginate in vitro. *J Orthopaedic Res*. 18(6), 882-890.
- Gatcliffe, T. A., Monk, B. J., Planutis, K., and Holcombe, R. F. (2008). Wnt signaling in ovarian tumorigenesis. *International journal of gynecological cancer : official journal of the International Gynecological Cancer Society*. 18(5), 954-962.
- Gawronska-Kozak, B. (2014). Preparation and differentiation of mesenchymal stem cells from ears of adult mice. *Methods Enzymol*. 538, 1-13.
- Gazzerro, E., Smerdel-Ramoya, A., Zanotti, S., Stadmeier, L., Durant, D., Economides, A. N., and Canalis, E. (2007). Conditional deletion of gremlin causes a transient increase in bone formation and bone mass. *J Biol Chem*. 282(43), 31549-31557.
- Ge, X. P., Gan, Y. H., Zhang, C. G., Zhou, C. Y., Ma, K. T., Meng, J. H., and Ma, X. C. (2011). Requirement of the NF-kappaB pathway for induction of Wnt-5A by interleukin-1beta in condylar chondrocytes of the temporomandibular joint: functional crosstalk between the Wnt-5A and NF-kappaB signaling pathways. *Osteoarthritis Cartilage*. 19(1), 111-117.
- Gehris, A. L., Stringa, E., Spina, J., Desmond, M. E., Tuan, R. S., and Bennett, V. D. (1997). The region encoded by the alternatively spliced exon IIIA in mesenchymal fibronectin appears essential for chondrogenesis at the level of cellular condensation. *Developmental biology*. 190(2), 191-205.
- Gelse, K., Ekici, A. B., Cipa, F., Swoboda, B., Carl, H. D., Olk, A., Hennig, F. F., and Klinger, P. (2012). Molecular differentiation between osteophytic and articular cartilage--clues for a transient and permanent chondrocyte phenotype. *Osteoarthritis Cartilage*. 20(2), 162-171.
- Gendron, C., Kashiwagi, M., Han Lim, L., Enghild, J., Thøgersen, I., Hughes, C., Caterson, B., and Nagase, H. (2007). Proteolytic Activities of Human ADAMTS-5. Comparative studies with ADAMTS-4. *J Biol Chem*. 282(25), 18294-18306.
- Giannini, S., Buda, R., Cavallo, M., Ruffilli, A., Cenacchi, A., Cavallo, C., and Vannini, F. (2010). Cartilage repair evolution in post-traumatic osteochondral lesions of the talus: from open field autologous chondrocyte to bone-marrow-derived cells transplantation. *Injury*. 41(11), 1196-1203.
- Gilbert, L., He, X., Farmer, P., Rubin, J., Drissi, H., van Wijnen, A. J., Lian, J. B., Stein, G. S., and Nanes, M. S. (2002). Expression of the osteoblast differentiation factor RUNX2

- (Cbfa1/AML3/Pebp2alpha A) is inhibited by tumor necrosis factor-alpha. *J Biol Chem.* 277(4), 2695-2701.
- Girkontaite, I., Frischholz, S., Lammi, P., Wagner, K., Swoboda, B., Aigner, T., and Von der Mark, K. (1996). Immunolocalization of type X collagen in normal fetal and adult osteoarthritic cartilage with monoclonal antibodies. *Matrix biology : journal of the International Society for Matrix Biology.* 15(4), 231-238.
- Glasson, S. S., Askew, R., Sheppard, B., Carito, B., Blanchet, T., Ma, H. L., Flannery, C. R., Peluso, D., Kanki, K., Yang, Z., Majumdar, M. K., and Morris, E. A. (2005). Deletion of active ADAMTS5 prevents cartilage degradation in a murine model of osteoarthritis. *Nature.* 434(7033), 644-648.
- Goekoop, R., Kloppenburg, K., H, Frölich, H., T, Westendorp, R., and Gussekloo, J. (2010). Low innate production of interleukin-1 β and interleukin-6 is associated with the absence of osteoarthritis in old age. *Osteoarthritis and Cartilage.* 18(7), 942-947.
- Greco, K. V., Iqbal, A. J., Rattazzi, L., Nalesso, G., Moradi-Bidhendi, N., Moore, A. R., Goldring, M. B., Dell'Accio, F., and Perretti, M. (2011). High density micromass cultures of a human chondrocyte cell line: a reliable assay system to reveal the modulatory functions of pharmacological agents. *Biochemical pharmacology.* 82(12), 1919-1929.
- Grimmer, C., Balbus, N., Lang, U., Aigner, T., Cramer, T., Müller, L., Swoboda, B., and Pfander, D. (2006). Regulation of Type II Collagen Synthesis during Osteoarthritis by Prolyl-4-Hydroxylases. Possible Influence of Low Oxygen Levels. *Am J Pathol.* 169(2), 491-502.
- Grimshaw, M., and Mason, R. (2000). Bovine articular chondrocyte function in vitro depends upon oxygen tension. *Osteoarthritis and Cartilage.* 8(5), 386-392.
- Gudjonsson, J. E., Johnston, A., Stoll, S. W., Riblett, M. B., Xing, X., Kochkodan, J. J., Ding, J., Nair, R. P., Aphale, A., Voorhees, J. J., and Elder, J. T. (2010). Evidence for altered Wnt signaling in psoriatic skin. *J Invest Dermatol.* 130(7), 1849-1859.
- Gupta, K., Shukla, M., Cowland, J. B., Malemud, C. J., and Haqqi, T. M. (2007). Neutrophil gelatinase-associated lipocalin is expressed in osteoarthritis and forms a complex with matrix metalloproteinase 9. *Arthritis Rheum.* 56(10), 3326-3335.
- Hadjiargyrou, M., Ahrens, W., and Rubin, C. (2000). Temporal Expression of the Chondrogenic and Angiogenic Growth Factor Cyr61 During Fracture Repair. *JBMR.* 15(6), 1014-1023.
- Hajek, A. S., and Solursh, M. (1977). The effect of ascorbic acid on growth and synthesis of matrix components by cultured chick embryo chondrocytes. *The Journal of experimental zoology.* 200(3), 377-388.
- Han, M. S., Kim, J. E., Shin, H. I., and Kim, I. S. (2008). Expression patterns of betaig-h3 in chondrocyte differentiation during endochondral ossification. *Experimental & molecular medicine.* 40(4), 453-460.
- Hartmann, C., and Tabin, C. J. (2000). Dual roles of Wnt signaling during chondrogenesis in the chicken limb. *Development.* 127(14), 3141-3159.
- Haug, K., and Wu, L. (2008). Aggrecanase and Aggrecan Degradation in Osteoarthritis: a Review. *J Int Med Res.* 36(6), 1149-1160.

- Hayman, E. G., and Ruoslahti, E. (1979). Distribution of fetal bovine serum fibronectin and endogenous rat cell fibronectin in extracellular matrix. *The Journal of cell biology*. 83(1), 255-259.
- He, F., Xiong, W., Yu, X., Espinoza-Lewis, R., Liu, C., Gu, S., Nishita, M., Suzuki, K., Yamada, G., Minami, Y., and Chen, Y. (2008). Wnt5a regulates directional cell migration and cell proliferation via Ror2-mediated noncanonical pathway in mammalian palate development. *Development*. 135(23), 3871-3879.
- Hendren, L., and Beeson, P. (2009). A review of the differences between normal and osteoarthritis articular cartilage in human knee and ankle joints. *The Foot*. 19(3), 171-176.
- Hennigan, R. F., Hawker, K. L., and Ozanne, B. W. (1994). Fos-transformation activates genes associated with invasion. *Oncogene*. 9(12), 3591-3600.
- Hering, T. M., Kollar, J., Huynh, T. D., Varelas, J. B., and Sandell, L. J. (1994). Modulation of extracellular matrix gene expression in bovine high-density chondrocyte cultures by ascorbic acid and enzymatic resuspension. *Arch Biochem Biophys*. 314(1), 90-98.
- Hermansson, M., Sawaji, Y., Bolton, M., Alexander, S., Wallace, A., Begum, S., Wait, R., and Saklatvala, J. (2004). Proteomic analysis of articular cartilage shows increased type II collagen synthesis in osteoarthritis and expression of inhibin betaA (activin A), a regulatory molecule for chondrocytes. *J Biol Chem*. 279(42), 43514-43521.
- Herrera-Herrera, M. L., and Quezada-Calvillo, R. (2012). DDR2 plays a role in fibroblast migration independent of adhesion ligand and collagen activated DDR2 tyrosine kinase. *Biochem Biophys Res Commun*. 429(1-2), 39-44.
- Higashikawa, A., Saito, T., Ikeda, T., Kamekura, S., Kawamura, N., Kan, A., Oshima, Y., Ohba, S., Ogata, N., Takeshita, K., Nakamura, K., Chung, U. I., and Kawaguchi, H. (2009). Identification of the core element responsive to runt-related transcription factor 2 in the promoter of human type X collagen gene. *Arthritis Rheum*. 60(1), 166-178.
- Hill, M. (2009). Collagen Synthesis, *Faculty of Medicine, University of New South Wales* <http://php.med.unsw.edu.au/cellbiology/images/7/70/Collagen-synthesis.jpg>, Accessed 24th May 2011
- Honsawek, S., Tanavalee, A., Yuktanandana, P., Ngarmukos, S., Saetan, N., and Tantavisut, S. (2010). Dickkopf-1 (Dkk-1) in plasma and synovial fluid is inversely correlated with radiographic severity of knee osteoarthritis patients. *BMC musculoskeletal disorders*. 11, 257.
- Horkay, F., Basser, P., Hecht, A., and Geissler, E. (2008). Gel-like behavior in aggrecan assemblies. *J Chem Phys*. 128(13), 135103.
- Horton Jr, W., Bennion, P., and Yang, L. (2006). Cellular, molecular, and matrix changes in cartilage during aging and osteoarthritis. *Journal of musculoskeletal & neuronal interactions*. 6(4), 379-381.
- Horton, W. (1993). Morphology of Connective Tissue: Cartilage. In *Connective Tissue and Its Heritable Disorders: Molecular, Genetic and Medical Aspects*, (New York: Wiley-Liss, Inc.), pp. 73-84.
- Hosseini-Farahabadi, S., Geetha-Loganathan, P., Fu, K., Nimmagadda, S., Yang, H. J., and Richman, J. M. (2013). Dual functions for WNT5A during cartilage development and in disease. *Matrix biology : journal of the International Society for Matrix Biology*. 32(5), 252-264.

- Huang, B. L., Brugger, S. M., and Lyons, K. M. (2010). Stage-specific control of connective tissue growth factor (CTGF/CCN2) expression in chondrocytes by Sox9 and beta-catenin. *J Biol Chem.* 285(36), 27702-27712.
- Huang, K., and Wu, L. (2008). Aggrecanase and Aggrecan Degradation in Osteoarthritis: a Review. *J Int Med Res.* 36, 1149-1160.
- Huh, Y. H., Ryu, J. H., and Chun, J. S. (2007). Regulation of type II collagen expression by histone deacetylase in articular chondrocytes. *J Biol Chem.* 282(23), 17123-17131.
- Hui, W., Rowan, A. D., and Cawston, T. (2001). Insulin-like growth factor 1 blocks collagen release and down regulates matrix metalloproteinase-1, -3, -8, and -13 mRNA expression in bovine nasal cartilage stimulated with oncostatin M in combination with interleukin 1alpha. *Annals of the rheumatic diseases.* 60(3), 254-261.
- Hurvitz, J., Suwairi, D., Van Hul, W., El-Shanti, H., Superti-Furga, A., Roudier, J., Holderbaum, D., Pauli, R., Herd, K., Van Hul, E., Rezai-Delui, H., Legius, E., Le Merrer, M., Al-Alami, J., Bahabri, S., and Warman, M. (1999). Mutations in the CCN gene family member WISP3 cause progressive pseudorheumatoid dysplasia. *Nature Genetics.* 23, 94-98.
- Hwang, S. G., Yu, S. S., Lee, S. W., and Chun, J. S. (2005). Wnt-3a regulates chondrocyte differentiation via c-Jun/AP-1 pathway. *FEBS letters.* 579(21), 4837-4842.
- Ishihara, T., Kakiya, K., Takahashi, K., Miwa, H., Rokushima, M., Yoshinaga, T., Tanaka, Y., Ito, T., Togame, H., Takemoto, H., Amano, M., Iwasaki, N., Minami, A., and Nishimura, S. (2014). Discovery of novel differentiation markers in the early stage of chondrogenesis by glycoform-focused reverse proteomics and genomics. *Biochim Biophys Acta.* 1840(1), 645-655.
- Ivkovic, S., Yoon, B. S., Popoff, S. N., Safadi, F. F., Libuda, D. E., Stephenson, R. C., Daluiski, A., and Lyons, K. M. (2003). Connective tissue growth factor coordinates chondrogenesis and angiogenesis during skeletal development. *Development.* 130(12), 2779-2791.
- Jay, G. D., Fleming, B. C., Watkins, B. A., McHugh, K. A., Anderson, S. C., Zhang, L. X., Teeple, E., Waller, K. A., and Elsaid, K. A. (2010). Prevention of cartilage degeneration and restoration of chondroprotection by lubricin tribosupplementation in the rat following anterior cruciate ligament transection. *Arthritis Rheum.* 62(8), 2382-2391.
- Jiang, W., Crossman, D. K., Mitchell, E. H., Sohn, P., Crowley, M. R., and Serra, R. (2013). WNT5A inhibits metastasis and alters splicing of Cd44 in breast cancer cells. *PLoS One.* 8(3), e58329.
- Jones, A. R., Chen, S., Chai, D. H., Stevens, A. L., Gleghorn, J. P., Bonassar, L. J., Grodzinsky, A. J., and Flannery, C. R. (2009). Modulation of lubricin biosynthesis and tissue surface properties following cartilage mechanical injury. *Arthritis Rheum.* 60(1), 133-142.
- Jones, S., and Jomary, C. (2002). Secreted Frizzled-related proteins: searching for relationships and patterns. *BioEssays.* 24(9), 811-820.
- Joos, H., Wildner, A., Hogrefe, C., Reichel, H., and Brenner, R. E. (2013). Interleukin-1 beta and tumor necrosis factor alpha inhibit migration activity of chondrogenic progenitor cells from non-fibrillated osteoarthritic cartilage. *Arthritis Res Ther.* 15(5), R119.
- Juhász, T., Matta, C., Somogyi, C., Katona, E., Takacs, R., Soha, R. F., Szabo, I. A., Cserhati, C., Szody, R., Karacsonyi, Z., Bako, E., Gergely, P., and Zakany, R. (2014). Mechanical loading

stimulates chondrogenesis via the PKA/CREB-Sox9 and PP2A pathways in chicken micromass cultures. *Cell Signal*. 26(3), 468-482.

Jung, Y. S., Lee, H. Y., Kim, S. D., Park, J. S., Kim, J. K., Suh, P. G., and Bae, Y. S. (2013). Wnt5a stimulates chemotactic migration and chemokine production in human neutrophils. *Experimental & molecular medicine*. 45, e27.

Kang, H., Ko, J., and Jang, S. W. (2012). The role of annexin A1 in expression of matrix metalloproteinase-9 and invasion of breast cancer cells. *Biochem Biophys Res Commun*. 423(1), 188-194.

Karlsson, C., Dehne, T., Lindahl, A., Brittberg, M., Pruss, A., Sittlinger, M., and Ringe, J. (2010). Genome-wide expression profiling reveals new candidate genes associated with osteoarthritis. *Osteoarthritis Cartilage*. 18(4), 581-592.

Karow, M., Popp, T., Egea, V., Ries, C., Jochum, M., and Neth, P. (2009). Wnt signalling in mouse mesenchymal stem cells: impact on proliferation, invasion and MMP expression. *J Cell Mol Med*. 13(8B), 2506-2520.

Kaur, N., Chettiar, S., Rathod, S., Rath, P., Muzumdar, D., Shaikh, M. L., and Shiras, A. (2013). Wnt3a mediated activation of Wnt/beta-catenin signaling promotes tumor progression in glioblastoma. *Molecular and cellular neurosciences*. 54, 44-57.

Kawai, I., Hisaki, T., Sugiura, K., Naito, K., and Kano, K. (2012). Discoidin domain receptor 2 (DDR2) regulates proliferation of endochondral cells in mice. *Biochem Biophys Res Commun*. 427(3), 611-617.

Kawaki, H., Kubota, S., Suzuki, A., Lazar, N., Yamada, T., Matsumura, T., Ohgawara, T., Maeda, T., Perbal, B., Lyons, K. M., and Takigawa, M. (2008). Cooperative regulation of chondrocyte differentiation by CCN2 and CCN3 shown by a comprehensive analysis of the CCN family proteins in cartilage. *J Bone Miner Res*. 23(11), 1751-1764.

Kengaku, M., Capdevila, J., Rodriguez-Esteban, C., De La Peña, J., Johnson, R., Belmonte, J., and Tabin, C. (1998). Distinct WNT Pathways Regulating AER Formation and Dorsoroventral Polarity in the Chick Limb Bud. *Science*. 280, 1274-1277.

Kim, D., You, E., Min, N. Y., Lee, K. H., Kim, H. K., and Rhee, S. (2013a). Discoidin domain receptor 2 regulates the adhesion of fibroblasts to 3D collagen matrices. *Int J Mol Med*. 31(5), 1113-1118.

Kim, J. E., Won, C. H., Bak, H., Kositratna, G., Manstein, D., Dotto, G. P., and Chang, S. E. (2013b). Gene profiling analysis of the early effects of ablative fractional carbon dioxide laser treatment on human skin. *Dermatologic surgery : official publication for American Society for Dermatologic Surgery [et al]*. 39(7), 1033-1043.

Kim, W., Kim, M., and Jho, E. H. (2013c). Wnt/beta-catenin signalling: from plasma membrane to nucleus. *The Biochemical journal*. 450(1), 9-21.

Kipnes, J., Carlberg, A. L., Loredó, G. A., Lawler, J., Tuan, R. S., and Hall, D. J. (2003). Effect of cartilage oligomeric matrix protein on mesenchymal chondrogenesis in vitro. *Osteoarthritis Cartilage*. 11(6), 442-454.

- Kobayashi, H., Hirata, M., Saito, T., Itoh, S., Chung, U. I., and Kawaguchi, H. (2013). Transcriptional induction of ADAMTS5 protein by nuclear factor-kappaB (NF-kappaB) family member RelA/p65 in chondrocytes during osteoarthritis development. *J Biol Chem.* 288(40), 28620-28629.
- Koelling, S., Kruegel, J., Irmer, M., Path, J. R., Sadowski, B., Miro, X., and Miosge, N. (2009). Migratory chondrogenic progenitor cells from repair tissue during the later stages of human osteoarthritis. *Cell stem cell.* 4(4), 324-335.
- Konitsiotis, A. D., Raynal, N., Bihan, D., Hohenester, E., Farndale, R. W., and Leitinger, B. (2008). Characterization of high affinity binding motifs for the discoidin domain receptor DDR2 in collagen. *J Biol Chem.* 283(11), 6861-6868.
- Koshy, P. J., Lundy, C. J., Rowan, A. D., Porter, S., Edwards, D. R., Hogan, A., Clark, I. M., and Cawston, T. E. (2002). The modulation of matrix metalloproteinase and ADAM gene expression in human chondrocytes by interleukin-1 and oncostatin M: a time-course study using real-time quantitative reverse transcription-polymerase chain reaction. *Arthritis Rheum.* 46(4), 961-967.
- Kumar, S., Hand, A., Connor, J., Dodds, R., Ryan, P., Trill, J., Fisher, S., Nuttall, M., Lipshutz, D., Zou, C., Hwang, S., Votta, B., James, I., Rieman, D., Gowen, M., and Lee, J. (1999). Identification and Cloning of a Connective Tissue Growth Factor-like cDNA from Human Osteoblasts Encoding a Novel Regulator of Osteoblast Functions. *J Biol Chem.* 272(24), 17123-17131.
- Kwon, C. H., Moon, H. J., Park, H. J., Choi, J. H., and Park do, Y. (2013). S100A8 and S100A9 promotes invasion and migration through p38 mitogen-activated protein kinase-dependent NF-kappaB activation in gastric cancer cells. *Molecules and cells.* 35(3), 226-234.
- Lafont, J., Jacques, C., Le Drea, G., Calhabeu, F., Thibout, H., Dubois, C., Berenbaum, F., Laurent, M., and Martinerie, C. (2005a). New Target Genes for NOV/CCN3 in Chondrocytes: TGF- β 2 and Type X Collagen. *JBMR.* 20(12), 2213-2223.
- Lafont, J., Jacques, C., Le Dreau, G., Calhabeu, F., Thibout, H., Dubois, C., Berenbaum, F., Laurent, M., and Martinerie, C. (2005b). New target genes for NOV/CCN3 in chondrocytes: TGF-beta2 and type X collagen. *J Bone Miner Res.* 20(12), 2213-2223.
- Lafont, J. E., Talma, S., and Murphy, C. L. (2007). Hypoxia-inducible factor 2alpha is essential for hypoxic induction of the human articular chondrocyte phenotype. *Arthritis Rheum.* 56(10), 3297-3306.
- Lane, N. E., Lian, K., Nevitt, M. C., Zmuda, J. M., Lui, L., Li, J., Wang, J., Fontecha, M., Umblas, N., Rosenbach, M., de Leon, P., and Corr, M. (2006). Frizzled-related protein variants are risk factors for hip osteoarthritis. *Arthritis Rheum.* 54(4), 1246-1254.
- Lee, M. S., Sun, M. T., Pang, S. T., Ueng, S. W., Chen, S. C., Hwang, T. L., and Wang, T. H. (2009). Evaluation of differentially expressed genes by shear stress in human osteoarthritic chondrocytes in vitro. *Chang Gung medical journal.* 32(1), 42-50.
- Leijten, J. C., Emons, J., Sticht, C., van Gool, S., Decker, E., Uitterlinden, A., Rappold, G., Hofman, A., Rivadeneira, F., Scherjon, S., Wit, J. M., van Meurs, J., van Blitterswijk, C. A., and Karperien, M. (2012). Gremlin 1, frizzled-related protein, and Dkk-1 are key regulators of human articular cartilage homeostasis. *Arthritis Rheum.* 64(10), 3302-3312.

- Leitinger, B., Steplewski, A., and Fertala, A. (2004). The D2 period of collagen II contains a specific binding site for the human discoidin domain receptor, DDR2. *Journal of molecular biology*. 344(4), 993-1003.
- Lettry, V., Hosoya, K., Takagi, S., and Okumura, M. (2010). Coculture of equine mesenchymal stem cells and mature equine articular chondrocytes results in improved chondrogenic differentiation of the stem cells. *Jpn J Vet Res*. 58(1), 5-15.
- Li, Y., Lacerda, D. A., Warman, M. L., Beier, D. R., Yoshioka, H., Ninomiya, Y., Oxford, J. T., Morris, N. P., Andrikopoulos, K., Ramirez, F., and et al. (1995). A fibrillar collagen gene, Col11a1, is essential for skeletal morphogenesis. *Cell*. 80(3), 423-430.
- Liacini, A., Sylvester, J., Qing Li, W., Huang, W., Dehnade, F., Ahmad, M., and Zafarullah, M. (2003). Induction of matrix metalloproteinase-13 gene expression by TNF- α is mediated by MAP kinases, AP-1, and NF- κ B transcription factors in articular chondrocytes. *Exp Cell Res*. 288(1), 208-217.
- Liang, H. T., Feng, X. C., and Ma, T. H. (2008). Water channel activity of plasma membrane affects chondrocyte migration and adhesion. *Clinical and experimental pharmacology & physiology*. 35(1), 7-10.
- Linnskog, R., Jonsson, G., Axelsson, L., Prasad, C. P., and Andersson, T. (2014). Interleukin-6 drives melanoma cell motility through p38alpha-MAPK-dependent up-regulation of WNT5A expression. *Molecular oncology*.
- Little, C. B., Barai, A., Burkhardt, D., Smith, S. M., Fosang, A. J., Werb, Z., Shah, M., and Thompson, E. W. (2009). Matrix metalloproteinase 13-deficient mice are resistant to osteoarthritic cartilage erosion but not chondrocyte hypertrophy or osteophyte development. *Arthritis and rheumatism*. 60(12), 3723-3733.
- Liu, A. R., Liu, L., Chen, S., Yang, Y., Zhao, H. J., Liu, L., Guo, F. M., Lu, X. M., and Qiu, H. B. (2013a). Activation of canonical wnt pathway promotes differentiation of mouse bone marrow-derived MSCs into type II alveolar epithelial cells, confers resistance to oxidative stress, and promotes their migration to injured lung tissue in vitro. *J Cell Physiol*. 228(6), 1270-1283.
- Liu, P., Wakamiya, M., Shea, M. J., Albrecht, U., Behringer, R. R., and Bradley, A. (1999). Requirement for Wnt3 in vertebrate axis formation. *Nat Genet*. 22(4), 361-365.
- Liu, X., Sun, H., Yan, D., Zhang, L., Lv, X., Liu, T., Zhang, W., Liu, W., Cao, Y., and Zhou, G. (2010). In vivo ectopic chondrogenesis of BMSCs directed by mature chondrocytes. *Biomaterials*. 31, 9406-9414.
- Liu, X., Wang, Y., Wang, X., Sun, Z., Li, L., Tao, Q., and Luo, B. (2013b). Epigenetic silencing of WNT5A in Epstein-Barr virus-associated gastric carcinoma. *Arch Virol*. 158(1), 123-132.
- Lodewyckx, L., Cailotto, F., Thysen, S., Luyten, F. P., and Lories, R. J. (2012). Tight regulation of wntless-type signaling in the articular cartilage - subchondral bone biomechanical unit: transcriptomics in Frzb-knockout mice. *Arthritis Res Ther*. 14(1), R16.
- Lohmander, S., Ionescu, M., Jugessur, H., and Poole, R. (1999). Changes in joint cartilage aggrecan after knee injury and in osteoarthritis. *Arthritis & Rheumatism*. 42(3), 534-544.

Lories, R., Peeters, J., Bakker, A., Tylzanowski, P., Derese, I., Schrooten, J., Thomas, T., and Luyten, F. (2007). Articular cartilage and biomechanical properties of the long bones in Frzb-knockout mice. *Arthritis & Rheumatism*. 56(12), 4095-4103.

Loughlin, J., Dowling, B., Chapman, K., Marcelline, L., Mustafa, Z., Southam, L., Ferreira, A., Ciesielski, C., Carson, D., and Corr, M. (2004). Functional variants within the secreted frizzled-related protein 3 gene are associated with hip osteoarthritis in females. *PNAS*. 101(26), 9757-9762.

Luo, L., Cruz, T., and McCulloch, C. (1997). Interleukin 1-induced calcium signalling in chondrocytes requires focal adhesions. *The Biochemical journal*. 324 (Pt 2), 653-658.

MacDonald, B., Tamai, K., and He, X. (2009). Wnt/ β -Catenin Signaling: Components, Mechanisms and Diseases. *Developmental cell*. 17, 9-26.

Maen, K. H. (2010). Joint, *Wikimedia*

<http://upload.wikimedia.org/wikipedia/commons/1/19/Joint.png>, Accessed 24th May 2011

Malfait, A., Liu, R., Ijiri, K., Komiya, S., and Tortorella, M. (2002). Inhibition of ADAM-TS4 and ADAM-TS5 Prevents Aggrecan Degradation in Osteoarthritic Cartilage. *J Biol Chem*. 277(25), 22201-22208.

Malladi, P., Xu, Y., Chiou, M., Giaccia, A. J., and Longaker, M. T. (2006). Effect of reduced oxygen tension on chondrogenesis and osteogenesis in adipose-derived mesenchymal cells. *Am J Physiol Cell Physiol*. 290(4), C1139-1146.

Mampaey, S., Vanhoenacker, F., Boven, K., Van Hul, W., and De Schepper, A. (2000). Progressive Pseudorheumatoid Dysplasia. *Eur Radiol*. 10, 1832-1835.

Markway, B. D., Tan, G. K., Brooke, G., Hudson, J. E., Cooper-White, J. J., and Doran, M. R. (2010). Enhanced chondrogenic differentiation of human bone marrow-derived mesenchymal stem cells in low oxygen environment micropellet cultures. *Cell Transplant*. 19(1), 29-42.

Marrakchi, R., Khadimallah, I., Ouerhani, S., Gamoudi, A., Khomsi, F., Bouzaine, H., Benamor, M., Bougatef, K., Mnif, S., Zitoun, R., Benna, F., Boussen, H., Rahal, K., and Elgaaied, A. (2010). Expression of WISP3 and RhoC Genes at mRNA and Protein Levels in Inflammatory and Noninflammatory Breast Cancer in Tunisian Patients. *Cancer Invest*. 28(4), 399-407.

Masuko, K., Murata, M., Yudoh, K., Shimizu, H., Beppu, M., Nakamura, H., and Kato, T. (2010). Prostaglandin E2 regulates the expression of connective tissue growth factor (CTGF/CCN2) in human osteoarthritic chondrocytes via the EP4 receptor. *BMC research notes*. 3, 5.

Matta, C., Fodor, J., Miosge, N., Takacs, R., Juhasz, T., Rybaltovszki, H., Toth, A., Csernoch, L., and Zakany, R. (2014). Purinergic signalling is required for calcium oscillations in migratory chondrogenic progenitor cells. *Pflugers Archiv : European journal of physiology*.

Matta, C., Juhasz, T., Szigyarto, Z., Kolozsvari, B., Somogyi, C., Nagy, G., Gergely, P., and Zakany, R. (2011). PKCdelta is a positive regulator of chondrogenesis in chicken high density micromass cell cultures. *Biochimie*. 93(2), 149-159.

McCoy, E., and Sontheimer, H. (2007). Expression and function of water channels (aquaporins) in migrating malignant astrocytes. *Glia*. 55(10), 1034-1043.

- Melchiorri, C., Meliconi, R., Frizziero, L., Silvestri, T., Pulsatelli, L., Mazzetti, I., Borzi, R. M., Ugucioni, M., and Facchini, A. (1998). Enhanced and coordinated in vivo expression of inflammatory cytokines and nitric oxide synthase by chondrocytes from patients with osteoarthritis. *Arthritis Rheum.* 41(12), 2165-2174.
- Meng, F., Rui, Y., Xu, L., Wan, C., Jiang, X., and Li, G. (2014). Aqp1 enhances migration of bone marrow mesenchymal stem cells through regulation of FAK and beta-catenin. *Stem cells and development.* 23(1), 66-75.
- Merino, R., Rodriguez-Leon, J., Macias, D., Ganan, Y., Economides, A. N., and Hurler, J. M. (1999). The BMP antagonist Gremlin regulates outgrowth, chondrogenesis and programmed cell death in the developing limb. *Development.* 126(23), 5515-5522.
- Messent, A. J., Tuckwell, D. S., Knauper, V., Humphries, M. J., Murphy, G., and Gavrilovic, J. (1998). Effects of collagenase-cleavage of type I collagen on alpha2beta1 integrin-mediated cell adhesion. *J Cell Sci.* 111 (Pt 8), 1127-1135.
- Mikels, A. J., and Nusse, R. (2006). Purified Wnt5a protein activates or inhibits beta-catenin-TCF signaling depending on receptor context. *PLoS biology.* 4(4), e115.
- Milner, J. M., Rowan, A. D., Elliott, S. F., and Cawston, T. E. (2003). Inhibition of furin-like enzymes blocks interleukin-1alpha/oncostatin M-stimulated cartilage degradation. *Arthritis Rheum.* 48(4), 1057-1066.
- Miron, R. J., Gruber, R., Hedbom, E., Saulacic, N., Zhang, Y., Sculean, A., Bosshardt, D. D., and Buser, D. (2013). Impact of bone harvesting techniques on cell viability and the release of growth factors of autografts. *Clinical implant dentistry and related research.* 15(4), 481-489.
- Mitani, K., Haruyama, N., Hatakeyama, J., and Igarashi, K. (2013). Amelogenin splice isoforms stimulate chondrogenic differentiation of ATDC5 cells. *Oral diseases.* 19(2), 169-179.
- Mo, F. E., Muntean, A. G., Chen, C. C., Stolz, D. B., Watkins, S. C., and Lau, L. F. (2002). CYR61 (CCN1) is essential for placental development and vascular integrity. *Mol Cell Biol.* 22(24), 8709-8720.
- Moazedi-Fuerst, F. C., Hofner, M., Gruber, G., Weinhaeusel, A., Stradner, M. H., Lohberger, B., Glehr, M., Leithner, A., Sonntagbauer, M., and Graninger, W. B. (2014). Epigenetic differences in human cartilage between mild and severe OA. *J Orthop Res.*
- Monzani, E., Bazzotti, R., Perego, C., and La Porta, C. A. (2009). AQP1 is not only a water channel: it contributes to cell migration through Lin7/beta-catenin. *PLoS One.* 4(7), e6167.
- Mörgelin, M., Paulsson, M., Hardingham, T., Heinegård, D., and Engel, J. (1988). Cartilage proteoglycans. Assembly with hyaluronate and link protein as studied by electron microscopy. *The Biochemical journal.* 253(1), 175-185.
- Morimoto, R., and Obinata, A. (2011). Overexpression of hematopoietically expressed homeoprotein induces nonapoptotic cell death in mouse prechondrogenic ATDC5 cells. *Biological & pharmaceutical bulletin.* 34(10), 1589-1595.
- Moritani, N. H., Kubota, S., Eguchi, T., Fukunaga, T., Yamashiro, T., Takano-Yamamoto, T., Tahara, H., Ohyama, K., Sugahara, T., and Takigawa, M. (2003). Interaction of AP-1 and the ctgf gene: a

- possible driver of chondrocyte hypertrophy in growth cartilage. *Journal of bone and mineral metabolism*. 21(4), 205-210.
- Moritani, N. H., Kubota, S., Sugahara, T., and Takigawa, M. (2005). Comparable response of *ccn1* with *ccn2* genes upon arthritis: An in vitro evaluation with a human chondrocytic cell line stimulated by a set of cytokines. *Cell Commun Signal*. 3(1), 6.
- Morrison, E. H., Ferguson, M. W., Bayliss, M. T., and Archer, C. W. (1996). The development of articular cartilage: I. The spatial and temporal patterns of collagen types. *Journal of anatomy*. 189 (Pt 1), 9-22.
- Murad, S., Grove, D., Lindberg, K. A., Reynolds, G., Sivarajah, A., and Pinnell, S. R. (1981). Regulation of collagen synthesis by ascorbic acid. *Proc Natl Acad Sci U S A*. 78(5), 2879-2882.
- Murphy, C., and Polak, J. (2004). Control of human articular chondrocyte differentiation by reduced oxygen tension. *J Cell Physiol*. 199(3), 451-459.
- Murphy, C. L., Thoms, B. L., Vaghjiani, R. J., and Lafont, J. E. (2009). Hypoxia. HIF-mediated articular chondrocyte function: prospects for cartilage repair. *Arthritis Res Ther*. 11(1), 213.
- Murphy, G., Knäuper, V., Atkinson, S., Butler, G., English, W., Hutton, M., Stracke, J., and Clark, I. (2002). Matrix metalloproteinases in arthritic disease. *Arthritis research*. 4(suppl 3), S39-S49.
- Murray, M. Y., Birkland, T. P., Howe, J. D., Rowan, A. D., Fidock, M., Parks, W. C., and Gavrilovic, J. (2013). Macrophage migration and invasion is regulated by MMP10 expression. *PLoS One*. 8(5), e63555.
- Mushtaq, T., Farquharson, C., Seawright, E., and Ahmed, S. F. (2002). Glucocorticoid effects on chondrogenesis, differentiation and apoptosis in the murine ATDC5 chondrocyte cell line. *The Journal of endocrinology*. 175(3), 705-713.
- Nakamura, Y., Nawata, M., and Wakitani, S. (2005). Expression profiles and functional analyses of Wnt-related genes in human joint disorders. *Am J Pathol*. 167(1), 97-105.
- Nakanishi, T., Nishida, T., Shimo, T., Kobayashi, K., Kubo, T., Tamatani, T., Tezuka, K., and Takigawa, M. (2000). Effects of CTGF/Hcs24, a Product of a Hypertrophic Chondrocyte-Specific Gene, on the Proliferation and Differentiation of Chondrocytes in Culture. *Endocrinology*. 141(1), 264-273.
- Nakatani, S., Mano, H., Im, R., Shimizu, J., and Wada, M. (2007). Glucosamine regulates differentiation of a chondrogenic cell line, ATDC5. *Biological & pharmaceutical bulletin*. 30(3), 433-438.
- Nam, J., Johnson, J., Lannutti, J. J., and Agarwal, S. (2010). Modulation of Embryonic Mesenchymal Progenitor Cell Differentiation via Control over Pure Mechanical Modulus in Electrospun Nanofibers. *Acta biomaterialia*.
- Nelson, F., Dahlberg, L., Laverty, S., Reiner, A., Pidoux, I., Ionescu, M., Fraser, G., Brooks, E., Tanzer, M., Rosenberg, L., Dieppe, P., and Poole, R. (1998). Evidence for Altered Synthesis of Type II Collagen in Patients with Osteoarthritis. *The Journal of clinical investigation*. 102(12), 2115-2125.

- Nemoto, E., Ebe, Y., Kanaya, S., Tsuchiya, M., Nakamura, T., Tamura, M., and Shimauchi, H. (2012). Wnt5a signaling is a substantial constituent in bone morphogenetic protein-2-mediated osteoblastogenesis. *Biochem Biophys Res Commun.* 422(4), 627-632.
- Neth, P., Ciccarella, M., Egea, V., Hoelters, J., Jochum, M., and Ries, C. (2006). Wnt signaling regulates the invasion capacity of human mesenchymal stem cells. *Stem Cells.* 24(8), 1892-1903.
- Ngoka, L. C. (2008). Sample prep for proteomics of breast cancer: proteomics and gene ontology reveal dramatic differences in protein solubilization preferences of radioimmunoprecipitation assay and urea lysis buffers. *Proteome science.* 6, 30.
- Niehrs, C. (2012). The complex world of WNT receptor signalling. *Nature reviews Molecular cell biology.* 13(12), 767-779.
- Nishida, T., Kubota, S., Nakanishi, T., Kuboki, T., Yosimichi, G., Kondo, S., and Takigawa, M. (2002). CTGF/Hcs24, a hypertrophic chondrocyte-specific gene product, stimulates proliferation and differentiation, but not hypertrophy of cultured articular chondrocytes. *J Cell Physiol.* 192(1), 55-63.
- Nishita, M., Itsukushima, S., Nomachi, A., Endo, M., Wang, Z., Inaba, D., Qiao, S., Takada, S., Kikuchi, A., and Minami, Y. (2010). Ror2/Frizzled complex mediates Wnt5a-induced AP-1 activation by regulating Dishevelled polymerization. *Mol Cell Biol.* 30(14), 3610-3619.
- Nissim, S., Hasso, S. M., Fallon, J. F., and Tabin, C. J. (2006). Regulation of Gremlin expression in the posterior limb bud. *Developmental biology.* 299(1), 12-21.
- Nowinski, D., Koskela, A., Kiwanuka, E., Bostrom, M., Gerdin, B., and Ivarsson, M. (2010). Inhibition of connective tissue growth factor/CCN2 expression in human dermal fibroblasts by interleukin-1alpha and beta. *J Cell Biochem.* 110(5), 1226-1233.
- Nusse, R. (2005). Wnt signaling in disease and in development. *Cell Research.* 15(1), 28-32.
- O'Connell, M. P., Fiori, J. L., Xu, M., Carter, A. D., Frank, B. P., Camilli, T. C., French, A. D., Dissanayake, S. K., Indig, F. E., Bernier, M., Taub, D. D., Hewitt, S. M., and Weeraratna, A. T. (2010). The orphan tyrosine kinase receptor, ROR2, mediates Wnt5A signaling in metastatic melanoma. *Oncogene.* 29(1), 34-44.
- Oberlender, S., and Tuan, R. (1994). Expression and functional involvement of N-cadherin in embryonic limb chondrogenesis. *Development.* 120(1), 177-187.
- Oh, H., Chun, C. H., and Chun, J. S. (2012). Dkk-1 expression in chondrocytes inhibits experimental osteoarthritic cartilage destruction in mice. *Arthritis Rheum.* 64(8), 2568-2578.
- Oishi, I., Suzuki, H., Onishi, N., Takada, R., Kani, S., Ohkawara, B., Koshida, I., Suzuki, K., Yamada, G., Schwabe, G. C., Mundlos, S., Shibuya, H., Takada, S., and Minami, Y. (2003). The receptor tyrosine kinase Ror2 is involved in non-canonical Wnt5a/JNK signalling pathway. *Genes to cells : devoted to molecular & cellular mechanisms.* 8(7), 645-654.
- Olsen, B. R., Reginato, A. M., and Wang, W. (2000). Bone development. *Annual review of cell and developmental biology.* 16, 191-220.

- Omoto, S., Nishida, K., Yamaai, Y., Shibahara, M., Nishida, T., Doi, T., Asahara, H., Nakanishi, T., Inoue, H., and Takigawa, M. (2004). Expression and localization of connective tissue growth factor (CTGF/Hcs24/CCN2) in osteoarthritic cartilage. *Osteoarthritis Cartilage*. 12(10), 771-778.
- Palecek, S. P., Loftus, J. C., Ginsberg, M. H., Lauffenburger, D. A., and Horwitz, A. F. (1997). Integrin-ligand binding properties govern cell migration speed through cell-substratum adhesiveness. *Nature*. 385(6616), 537-540.
- Peach, M., Marsh, N., and Macphee, D. J. (2012). Protein solubilization: attend to the choice of lysis buffer. *Methods Mol Biol*. 869, 37-47.
- Pelttari, K., Winter, A., Steck, E., Goetzke, K., Hennig, T., Ochs, B. G., Aigner, T., and Richter, W. (2006). Premature induction of hypertrophy during in vitro chondrogenesis of human mesenchymal stem cells correlates with calcification and vascular invasion after ectopic transplantation in SCID mice. *Arthritis Rheum*. 54(10), 3254-3266.
- Peng, J., Nemeč, M., Brolese, E., Bosshardt, D. D., Schaller, B., Buser, D., and Gruber, R. (2014). Bone-Conditioned Medium Inhibits Osteogenic and Adipogenic Differentiation of Mesenchymal Cells In Vitro. *Clinical implant dentistry and related research*.
- Pereira, R. C., Economides, A. N., and Canalis, E. (2000). Bone morphogenetic proteins induce gremlin, a protein that limits their activity in osteoblasts. *Endocrinology*. 141(12), 4558-4563.
- Person, A. D., Beiraghi, S., Sieben, C. M., Hermanson, S., Neumann, A. N., Robu, M. E., Schleiffarth, J. R., Billington, C. J., Jr., van Bokhoven, H., Hoogeboom, J. M., Mazzeu, J. F., Petryk, A., Schimmenti, L. A., Brunner, H. G., Ekker, S. C., and Lohr, J. L. (2010). WNT5A mutations in patients with autosomal dominant Robinow syndrome. *Developmental dynamics : an official publication of the American Association of Anatomists*. 239(1), 327-337.
- Pinnell, S. R. (1985). Regulation of collagen biosynthesis by ascorbic acid: a review. *Yale J Biol Med*. 58(6), 553-559.
- Poole, A. (1997). Articular cartilage chondrons: form, function and failure. *Journal of anatomy*. 191, 1-13.
- Poole, A., Kobayashi, M., Yasuda, T., Lavery, S., Mwale, F., Kojima, T., Sakai, T., Wahl, C., El-Maadawy, S., Webb, G., Tchetina, E., and Wu, W. (2002). Type II collagen degradation and its regulation in articular cartilage in osteoarthritis. *Annals of the rheumatic diseases*. 61(Suppl 2), ii78-ii81.
- Poole, R. (1999). An introduction to the pathophysiology of osteoarthritis. *Frontiers in Bioscience*. 4, d662-670.
- Porter, S., Clark, I., Kevorkian, L., and Edwards, D. (2005). The ADAMTS metalloproteinases. *The Biochemical journal*. 386, 15-27.
- Price, R. M., Tulsyan, N., Dermody, J. J., Schwalb, M., Soteropoulos, P., and Castronuovo, J. J., Jr. (2004). Gene expression after crush injury of human saphenous vein: using microarrays to define the transcriptional profile. *Journal of the American College of Surgeons*. 199(3), 411-418.
- Priddy, N. H., 2nd, Cook, J. L., Kreeger, J. M., Tomlinson, J. L., and Steffen, D. J. (2001). Effect of ascorbate and two different media on canine chondrocytes in three-dimensional culture. *Veterinary therapeutics : research in applied veterinary medicine*. 2(1), 70-77.

- Pukrop, T., Klemm, F., Hagemann, T., Gradl, D., Schulz, M., Siemes, S., Trumper, L., and Binder, C. (2006). Wnt 5a signaling is critical for macrophage-induced invasion of breast cancer cell lines. *Proc Natl Acad Sci U S A.* 103(14), 5454-5459.
- Pulsatelli, L., Addimanda, O., Brusi, V., Pavloska, B., and Meliconi, R. (2013). New findings in osteoarthritis pathogenesis: therapeutic implications. *Therapeutic advances in chronic disease.* 4(1), 23-43.
- Qian, D., Jones, C., Rzadzinska, A., Mark, S., Zhang, X., Steel, K. P., Dai, X., and Chen, P. (2007). Wnt5a functions in planar cell polarity regulation in mice. *Developmental biology.* 306(1), 121-133.
- Qian, X., Ba, Y., Zhuang, Q., and Zhong, G. (2014). RNA-Seq technology and its application in fish transcriptomics. *Omics : a journal of integrative biology.* 18(2), 98-110.
- Qwarnstrom, E. E., Page, R. C., Gillis, S., and Dower, S. K. (1988). Binding, internalization, and intracellular localization of interleukin-1 beta in human diploid fibroblasts. *J Biol Chem.* 263(17), 8261-8269.
- Rafferty, B. J., Unger, B. L., Perey, A. C., Tammariello, S. P., Pavlides, S., and McGee, D. W. (2012). A novel role for the Rho-associated kinase, ROCK, in IL-1-stimulated intestinal epithelial cell responses. *Cellular immunology.* 280(2), 148-155.
- Ramachandran, G. (1956). Structure of Collagen. *Nature.* 177, 710-711.
- Rashid, S. T., Humphries, J. D., Byron, A., Dhar, A., Askari, J. A., Selley, J. N., Knight, D., Goldin, R. D., Thursz, M., and Humphries, M. J. (2012). Proteomic analysis of extracellular matrix from the hepatic stellate cell line LX-2 identifies CYR61 and Wnt-5a as novel constituents of fibrotic liver. *Journal of proteome research.* 11(8), 4052-4064.
- Rauner, M., Stein, N., Winzer, M., Goettsch, C., Zwerina, J., Schett, G., Distler, J. H., Albers, J., Schulze, J., Schinke, T., Bornhauser, M., Platzbecker, U., and Hofbauer, L. C. (2012). WNT5A is induced by inflammatory mediators in bone marrow stromal cells and regulates cytokine and chemokine production. *J Bone Miner Res.* 27(3), 575-585.
- Rawson, J. B., Mrkonjic, M., Daftary, D., Dicks, E., Buchanan, D. D., Youngusband, H. B., Parfrey, P. S., Young, J. P., Pollett, A., Green, R. C., Gallinger, S., McLaughlin, J. R., Knight, J. A., and Bapat, B. (2011). Promoter methylation of Wnt5a is associated with microsatellite instability and BRAF V600E mutation in two large populations of colorectal cancer patients. *Br J Cancer.* 104(12), 1906-1912.
- Raymond, M., Marchbank, T., Moyer, M. P., Playford, R. J., Sanderson, I. R., and Kruidenier, L. (2012). IL-1beta stimulation of CCD-18co myofibroblasts enhances repair of epithelial monolayers through Wnt-5a. *American journal of physiology Gastrointestinal and liver physiology.* 303(11), G1270-1278.
- Rhee, D. K., Marcelino, J., Baker, M., Gong, Y., Smits, P., Lefebvre, V., Jay, G. D., Stewart, M., Wang, H., Warman, M. L., and Carpten, J. D. (2005). The secreted glycoprotein lubricin protects cartilage surfaces and inhibits synovial cell overgrowth. *The Journal of clinical investigation.* 115(3), 622-631.

- Richards, C. D. (2013). The enigmatic cytokine oncostatin m and roles in disease. *ISRN inflammation*. 2013, 512103.
- Roach, H. I., Yamada, N., Cheung, K. S., Tilley, S., Clarke, N. M., Oreffo, R. O., Kokubun, S., and Bronner, F. (2005). Association between the abnormal expression of matrix-degrading enzymes by human osteoarthritic chondrocytes and demethylation of specific CpG sites in the promoter regions. *Arthritis Rheum*. 52(10), 3110-3124.
- Roche Applied Science (2009). RealTime ready - Universal ProbeLibrary: Redefining and revolutionizing real-time qPCR assays. In, (Penzberg, Germany: Roche Diagnostics GmbH).
- Roifman, M., Marcelis, C. L., Paton, T., Marshall, C., Silver, R., Lohr, J. L., Yntema, H. G., Venselaar, H., Kayserili, H., van Bon, B., Seaward, G., Consortium, F. C., Brunner, H. G., and Chitayat, D. (2014). De novo WNT5A-associated autosomal dominant Robinow syndrome suggests specificity of genotype and phenotype. *Clinical genetics*.
- Roman-Blas, J. A., Stokes, D. G., and Jimenez, S. A. (2007). Modulation of TGF-beta signaling by proinflammatory cytokines in articular chondrocytes. *Osteoarthritis Cartilage*. 15(12), 1367-1377.
- Ronziere, M. C., Roche, S., Gouttenoire, J., Demarteau, O., Herbage, D., and Freyria, A. M. (2003). Ascorbate modulation of bovine chondrocyte growth, matrix protein gene expression and synthesis in three-dimensional collagen sponges. *Biomaterials*. 24(5), 851-861.
- Roughley, P. (2001). Articular cartilage and changes in arthritis Noncollagenous proteins and proteoglycans in the extracellular matrix of cartilage. *Arthritis research*. 3(6), 342-347.
- Roughley, P. (2006). The Structure and Function of Cartilage Proteoglycans. *Eur Cell Mater*. 12, 92-101.
- Ruan, M. Z., Erez, A., Guse, K., Dawson, B., Bertin, T., Chen, Y., Jiang, M. M., Yustein, J., Gannon, F., and Lee, B. H. (2013). Proteoglycan 4 expression protects against the development of osteoarthritis. *Science translational medicine*. 5(176), 176ra134.
- Rudnicki, J., and Brown, A. (1997). Inhibition of Chondrogenesis by Wnt Gene Expression in Vivo and in Vitro. *Dev Bio*. 185, 104-118.
- Ruiz, P. A., and Jarai, G. (2012). Discoidin domain receptors regulate the migration of primary human lung fibroblasts through collagen matrices. *Fibrogenesis & tissue repair*. 5, 3.
- Ryu, J. H., and Chun, J. S. (2006). Opposing roles of WNT-5A and WNT-11 in interleukin-1beta regulation of type II collagen expression in articular chondrocytes. *J Biol Chem*. 281(31), 22039-22047.
- Ryu, J. H., Yang, S., Shin, Y., Rhee, J., Chun, C. H., and Chun, J. S. (2011). Interleukin-6 plays an essential role in hypoxia-inducible factor 2alpha-induced experimental osteoarthritic cartilage destruction in mice. *Arthritis Rheum*. 63(9), 2732-2743.
- Saadoun, S., Papadopoulos, M. C., Hara-Chikuma, M., and Verkman, A. S. (2005). Impairment of angiogenesis and cell migration by targeted aquaporin-1 gene disruption. *Nature*. 434(7034), 786-792.

- Samarzija, I., Sini, P., Schlange, T., Macdonald, G., and Hynes, N. E. (2009). Wnt3a regulates proliferation and migration of HUVEC via canonical and non-canonical Wnt signaling pathways. *Biochem Biophys Res Commun.* 386(3), 449-454.
- Sandell, L., and Aigner, T. (2001). Articular cartilage and changes in arthritis. An introduction: Cell biology of osteoarthritis. *Arthritis research.* 3, 107-113.
- Schlichting, N., Dehne, T., Mans, K., Endres, M., Stuhlmuller, B., Sittinger, M., Kaps, C., and Ringe, J. (2014). Suitability of porcine chondrocyte micromass culture to model osteoarthritis in vitro. *Mol Pharm.* 11(7), 2092-2105.
- Schmal, H., Mehlhorn, A. T., Fehrenbach, M., Muller, C. A., Finkenzeller, G., and Sudkamp, N. P. (2006). Regulative mechanisms of chondrocyte adhesion. *Tissue Eng.* 12(4), 741-750.
- Schmidt, T. A., Gastelum, N. S., Han, E. H., Nugent-Derfus, G. E., Schumacher, B. L., and Sah, R. L. (2008). Differential regulation of proteoglycan 4 metabolism in cartilage by IL-1alpha, IGF-I, and TGF-beta1. *Osteoarthritis Cartilage.* 16(1), 90-97.
- Schulze-Tanzil, G., de Souza, P., Villegas Castrejon, H., John, T., Merker, H. J., Scheid, A., and Shakibaei, M. (2002). Redifferentiation of dedifferentiated human chondrocytes in high-density cultures. *Cell Tissue Res.* 308(3), 371-379.
- Schutze, N., Lechner, A., Groll, C., Siggelkow, H., Hufner, M., Kohrle, J., and Jakob, F. (1998). The human analog of murine cystein rich protein 61 [correction of 16] is a 1alpha,25-dihydroxyvitamin D3 responsive immediate early gene in human fetal osteoblasts: regulation by cytokines, growth factors, and serum. *Endocrinology.* 139(4), 1761-1770.
- Schütze, N., Noth, U., Schneidereit, J., Hendrich, C., and Jakob, F. (2005). Differential expression of CCN-family members in primary human bone marrow-derived mesenchymal stem cells during osteogenic, chondrogenic and adipogenic differentiation. *Cell Commun Signal.* 3(5).
- Schütze, N., Schenk, R., Fiedler, J., Mattes, T., Jakob, F., and Brenner, R. E. (2007). CYR61/CCN1 and WISP3/CCN6 are chemoattractive ligands for human multipotent mesenchymal stroma cells. *BMC Cell Biol.* 8, 45.
- Schwabe, G. C., Trepczik, B., Suring, K., Brieske, N., Tucker, A. S., Sharpe, P. T., Minami, Y., and Mundlos, S. (2004). Ror2 knockout mouse as a model for the developmental pathology of autosomal recessive Robinow syndrome. *Developmental dynamics : an official publication of the American Association of Anatomists.* 229(2), 400-410.
- Scott, D., Wolfe, F., and Huizinga, T. (2010). Rheumatoid arthritis. *The Lancet.* 376(9746), 1094-1108.
- Seed, S., Dunican, K., and Lynch, A. (2009). Osteoarthritis: A review of treatment options. *Geriatrics.* 64(10), 20-29.
- Seiki, M., Mori, H., Kajita, M., Uekita, T., and Itoh, Y. (2003). Membrane-type 1 matrix metalloproteinase and cell migration. *Biochemical Society symposium.* (70), 253-262.
- Sen, M., Cheng, Y., Goldring, M., Lotz, M., and Carson, D. (2004). WISP3-Dependent Regulation of Type II Collagen and Aggrecan Production in Chondrocytes. *Arthritis & Rheumatism.* 50(2), 488-497.

- Seol, D., McCabe, D. J., Choe, H., Zheng, H., Yu, Y., Jang, K., Walter, M. W., Lehman, A. D., Ding, L., Buckwalter, J. A., and Martin, J. A. (2012). Chondrogenic progenitor cells respond to cartilage injury. *Arthritis Rheum.* 64(11), 3626-3637.
- Seriwatanachai, D., Krishnamra, N., and Charoenphandhu, N. (2012). Chondroregulatory action of prolactin on proliferation and differentiation of mouse chondrogenic ATDC5 cells in 3-dimensional micromass cultures. *Biochem Biophys Res Commun.* 420(1), 108-113.
- Sethi, J., and Videl-Puig, A. (2010). Wnt signalling and the control of cellular metabolism. *The Biochemical journal.* 427, 1-17.
- Shang, Y. C., Wang, S. H., Xiong, F., Zhao, C. P., Peng, F. N., Feng, S. W., Li, M. S., Li, Y., and Zhang, C. (2007). Wnt3a signaling promotes proliferation, myogenic differentiation, and migration of rat bone marrow mesenchymal stem cells. *Acta pharmacologica Sinica.* 28(11), 1761-1774.
- Sheu, M. J., Li, C. F., Lin, C. Y., Lee, S. W., Lin, L. C., Chen, T. J., and Ma, L. J. (2014). Overexpression of ANXA1 confers independent negative prognostic impact in rectal cancers receiving concurrent chemoradiotherapy. *Tumour biology : the journal of the International Society for Oncodevelopmental Biology and Medicine.* 35(8), 7755-7763.
- Shibuya, I., Yoshimura, K., Miyamoto, Y., Yamada, A., Takami, M., Suzawa, T., Suzuki, D., Ikumi, N., Hiura, F., Anada, T., Suzuki, O., and Kamijo, R. (2013). Octacalcium phosphate suppresses chondrogenic differentiation of ATDC5 cells. *Cell Tissue Res.* 352(2), 401-412.
- Shimizu, E., Selvamurugan, N., Westendorf, J. J., Olson, E. N., and Partridge, N. C. (2010). HDAC4 represses matrix metalloproteinase-13 transcription in osteoblastic cells, and parathyroid hormone controls this repression. *J Biol Chem.* 285(13), 9616-9626.
- Shoulders, M., and Raines, R. (2009). Collagen Structure and Stability. *Annu Rev Biochem.* 78, 929-958.
- Shukunami, C., Ishizeki, K., Atsumi, T., Ohta, Y., Suzuki, F., and Hiraki, Y. (1997). Cellular hypertrophy and calcification of embryonal carcinoma-derived chondrogenic cell line ATDC5 in vitro. *J Bone Miner Res.* 12(8), 1174-1188.
- Shukunami, C., Ohta, Y., Sakuda, M., and Hiraki, Y. (1998). Sequential progression of the differentiation program by bone morphogenetic protein-2 in chondrogenic cell line ATDC5. *Exp Cell Res.* 241(1), 1-11.
- Si, W., Kang, Q., Luu, H., Park, J., Luo, Q., Song, W., Jiang, W., Luo, X., Li, X., Yin, H., Montag, A., Haydon, R., and He, T. (2006). CCN1/Cyr61 Is Regulated by the Canonical Wnt Signal and Plays an Important Role in Wnt3A-Induced Osteoblast Differentiation of Mesenchymal Stem Cells. *Mol Cell Bio.* 26(8), 2955-2964.
- Sonderegger, S., Haslinger, P., Sabri, A., Leisser, C., Otten, J. V., Fiala, C., and Knofler, M. (2010). Wntless (Wnt)-3A induces trophoblast migration and matrix metalloproteinase-2 secretion through canonical Wnt signaling and protein kinase B/AKT activation. *Endocrinology.* 151(1), 211-220.
- Song, J., Lee, M., Kim, D., Han, J., Chun, C. H., and Jin, E. J. (2013). MicroRNA-181b regulates articular chondrocytes differentiation and cartilage integrity. *Biochem Biophys Res Commun.* 431(2), 210-214.

- Song, J. J., Aswad, R., Kanaan, R. A., Rico, M. C., Owen, T. A., Barbe, M. F., Safadi, F. F., and Popoff, S. N. (2007a). Connective tissue growth factor (CTGF) acts as a downstream mediator of TGF-beta1 to induce mesenchymal cell condensation. *J Cell Physiol.* 210(2), 398-410.
- Song, R., Tortorella, M., Malfait, A., Alston, J., Yang, Z., Arner, E., and Griggs, D. (2007b). Aggrecan Degradation in Human Articular Cartilage Explants Is Mediated by Both ADAMTS-4 and ADAMTS-5. *Arthritis & Rheumatism.* 56(2), 575-585.
- Sonomoto, K., Yamaoka, K., Oshita, K., Fukuyo, S., Zhang, X., Nakano, K., Okada, Y., and Tanaka, Y. (2012). Interleukin-1beta induces differentiation of human mesenchymal stem cells into osteoblasts via the Wnt-5a/receptor tyrosine kinase-like orphan receptor 2 pathway. *Arthritis Rheum.* 64(10), 3355-3363.
- Spagnoli, A., Longobardi, L., and O'Rear, L. (2005). Cartilage disorders: potential therapeutic use of mesenchymal stem cells. *Endocr Dev.* 9, 17-30.
- Staines, K. A., Macrae, V. E., and Farquharson, C. (2012). Cartilage development and degeneration: a Wnt Wnt situation. *Cell biochemistry and function.* 30(8), 633-642.
- Stanton, H., Rogerson, F. M., East, C. J., Golub, S. B., Lawlor, K. E., Meeker, C. T., Little, C. B., Last, K., Farmer, P. J., Campbell, I. K., Fourie, A. M., and Fosang, A. J. (2005). ADAMTS5 is the major aggrecanase in mouse cartilage in vivo and in vitro. *Nature.* 434(7033), 648-652.
- Stokes, D., Lui, G., Dharmavaram, R., Hawkins, D., Piera-Velazquez, S., and Jimenez, S. (2001). Regulation of type-II collagen gene expression during human chondrocyte de-differentiation and recovery of chondrocyte-specific phenotype in culture involves Sry-type high-mobility-group box (SOX) transcription factors. *The Biochemical journal.* 360(2), 461-470.
- Ströbel, S., Loparic, M., Wendt, D., Schenk, A., Candrian, C., Lindberg, R., Moldovan, F., Barbero, A., and Martin, I. (2010). Anabolic and catabolic responses of human articular chondrocytes to varying oxygen percentages. *Arthritis Res & Therapy.* 12(2).
- Studer, D., Millan, C., Ozturk, E., Maniura-Weber, K., and Zenobi-Wong, M. (2012). Molecular and biophysical mechanisms regulating hypertrophic differentiation in chondrocytes and mesenchymal stem cells. *Eur Cell Mater.* 24, 118-135; discussion 135.
- Sun, M. M., and Beier, F. (2014). Liver X Receptor activation delays chondrocyte hypertrophy during endochondral bone growth. *Osteoarthritis Cartilage.*
- Surmann-Schmitt, C., Widmann, N., Dietz, U., Saeger, B., Eitzinger, N., Nakamura, Y., Rattel, M., Latham, R., Hartmann, C., von der Mark, H., Schett, G., von der Mark, K., and Stock, M. (2009). Wif-1 is expressed at cartilage-mesenchyme interfaces and impedes Wnt3a-mediated inhibition of chondrogenesis. *J Cell Sci.* 122(Pt 20), 3627-3637.
- Swingler, T. E., Wheeler, G., Carmont, V., Elliott, H. R., Barter, M. J., Abu-Elmagd, M., Donell, S. T., Boot-Handford, R. P., Hajihosseini, M. K., Munsterberg, A., Dalmay, T., Young, D. A., and Clark, I. M. (2012). The expression and function of microRNAs in chondrogenesis and osteoarthritis. *Arthritis Rheum.* 64(6), 1909-1919.
- Taipaleenmaki, H., Suomi, S., Hentunen, T., Laitala-Leinonen, T., and Saamanen, A. M. (2008). Impact of stromal cell composition on BMP-induced chondrogenic differentiation of mouse bone marrow derived mesenchymal cells. *Exp Cell Res.* 314(13), 2400-2410.

- Takeda, S., Bonnamy, J. P., Owen, M. J., Ducey, P., and Karsenty, G. (2001). Continuous expression of Cbfa1 in nonhypertrophic chondrocytes uncovers its ability to induce hypertrophic chondrocyte differentiation and partially rescues Cbfa1-deficient mice. *Genes & development*. 15(4), 467-481.
- Takigawa, M., Tajima, K., Pan, H. O., Enomoto, M., Kinoshita, A., Suzuki, F., Takano, Y., and Mori, Y. (1989). Establishment of a clonal human chondrosarcoma cell line with cartilage phenotypes. *Cancer Res*. 49(14), 3996-4002.
- Tamai, K., Semenov, M., Kato, Y., Spokony, R., Liu, C., Katsuyama, Y., Hess, F., Saint-Jeannet, J., and He, X. (2000). LDL-receptor-related proteins in Wnt signal transduction. *Nature*. 407, 530-535.
- Tamhankar, P. M., Vasudevan, L., Kondurkar, S., Yashaswini, K., Agarwalla, S. K., Nair, M., Ramkumar, T. V., Chaubal, N., and Chennuri, V. S. (2014). Identification of novel ROR2 gene mutations in Indian children with Robinow syndrome. *Journal of clinical research in pediatric endocrinology*. 6(2), 79-83.
- Tanaka, H., Murphy, C. L., Murphy, C., Kimura, M., Kawai, S., and Polak, J. M. (2004). Chondrogenic differentiation of murine embryonic stem cells: effects of culture conditions and dexamethasone. *J Cell Biochem*. 93(3), 454-462.
- Tanaka, I., Morikawa, M., Okuse, T., Shirakawa, M., and Imai, K. (2005). Expression and regulation of WISP2 in rheumatoid arthritic synovium. *Biochem Biophys Res Commun*. 334(4), 973-978.
- Tare, R. S., Howard, D., Pound, J. C., Roach, H. I., and Oreffo, R. O. (2005). Tissue engineering strategies for cartilage generation--micromass and three dimensional cultures using human chondrocytes and a continuous cell line. *Biochem Biophys Res Commun*. 333(2), 609-621.
- Tare, R. S. H., D.; Pound, J. C.; Roach, H. I.; Oreffo, R. O. C. (2005). ATDC5: an Ideal Cell Line for Development of Tissue Engineering Strategies Aimed at Cartilage Generation. *European Cells and Materials*. 10(Supplement 2), 22.
- Tay, L. X., Lim, C. K., Mansor, A., and Kamarul, T. (2014). Differential protein expression between chondrogenic differentiated MSCs, undifferentiated MSCs and adult Chondrocytes derived from oryctolagus cuniculus in vitro. *International journal of medical sciences*. 11(1), 24-33.
- Temu, T. M., Wu, K. Y., Gruppuso, P. A., and Phornphutkul, C. (2010). The mechanism of ascorbic acid-induced differentiation of ATDC5 chondrogenic cells. *Am J Physiol Endocrinol Metab*. 299(2), E325-334.
- Thorfve, A., Dehne, T., Lindahl, A., Brittberg, M., Pruss, A., Ringe, J., Sitterling, M., and Karlsson, C. (2011). Characteristic Markers of the WNT Signaling Pathways Are Differentially Expressed in Osteoarthritic Cartilage. *Cartilage*. 3(1), 43-57.
- Tran, C. M., Schoepflin, Z. R., Markova, D. Z., Kepler, C. K., Anderson, D. G., Shapiro, I. M., and Risbud, M. V. (2014). CCN2 suppresses catabolic effects of interleukin-1beta through alpha5beta1 and alphaVbeta3 integrins in nucleus pulposus cells: implications in intervertebral disc degeneration. *J Biol Chem*. 289(11), 7374-7387.
- Tropel, P., Noel, D., Platet, N., Legrand, P., Benabid, A. L., and Berger, F. (2004). Isolation and characterisation of mesenchymal stem cells from adult mouse bone marrow. *Exp Cell Res*. 295(2), 395-406.

- van der Weyden, L., Wei, L., Luo, J., Yang, X., Birk, D. E., Adams, D. J., Bradley, A., and Chen, Q. (2006). Functional knockout of the matrilin-3 gene causes premature chondrocyte maturation to hypertrophy and increases bone mineral density and osteoarthritis. *Am J Pathol.* 169(2), 515-527.
- Vandesompele, J., De Preter, K., Pattyn, F., Poppe, B., Van Roy, N., De Paepe, A., and Speleman, F. (2002). Accurate normalization of real-time quantitative RT-PCR data by geometric averaging of multiple internal control genes. *Genome Biol.* 3(7), RESEARCH0034.
- Velasco, J., Zarrabeitia, M. T., Prieto, J. R., Perez-Castrillon, J. L., Perez-Aguilar, M. D., Perez-Nunez, M. I., Sanudo, C., Hernandez-Elena, J., Calvo, I., Ortiz, F., Gonzalez-Macias, J., and Riancho, J. A. (2010). Wnt pathway genes in osteoporosis and osteoarthritis: differential expression and genetic association study. *Osteoporosis international : a journal established as result of cooperation between the European Foundation for Osteoporosis and the National Osteoporosis Foundation of the USA.* 21(1), 109-118.
- Verkman, A. S. (2005). More than just water channels: unexpected cellular roles of aquaporins. *J Cell Sci.* 118(Pt 15), 3225-3232.
- von der Mark, K., Frischholz, S., Aigner, T., Beier, F., Belke, J., Erdmann, S., and Burkhardt, H. (1995). Upregulation of type X collagen expression in osteoarthritic cartilage. *Acta orthopaedica Scandinavica Supplementum.* 266, 125-129.
- von der Mark, K., Gauss, V., von der Mark, H., and Muller, P. (1977). Relationship between cell shape and type of collagen synthesised as chondrocytes lose their cartilage phenotype in culture. *Nature.* 267(5611), 531-532.
- Wang, G., Woods, A., Sabari, S., Pagnotta, L., Stanton, L. A., and Beier, F. (2004). RhoA/ROCK signaling suppresses hypertrophic chondrocyte differentiation. *J Biol Chem.* 279(13), 13205-13214.
- Wang, Q., Downey, G. P., and McCulloch, C. A. (2011). Focal adhesions and Ras are functionally and spatially integrated to mediate IL-1 activation of ERK. *FASEB J.* 25(10), 3448-3464.
- Wang, Q., Williamson, M., Bott, S., Brookman-Amis, N., Freeman, A., Nariculam, J., Hubank, M. J., Ahmed, A., and Masters, J. R. (2007). Hypomethylation of WNT5A, CRIP1 and S100P in prostate cancer. *Oncogene.* 26(45), 6560-6565.
- Wang, Y., Kim, U., Blasioli, D., Kim, H., and Kaplan, D. (2005). In vitro cartilage tissue engineering with 3D porous aqueous-derived silk scaffolds and mesenchymal stem cells. *Biomaterials.* 26(34), 7082-7094.
- Ware, M. F., Wells, A., and Lauffenburger, D. A. (1998). Epidermal growth factor alters fibroblast migration speed and directional persistence reciprocally and in a matrix-dependent manner. *J Cell Sci.* 111 (Pt 16), 2423-2432.
- Wei, L., Mckee, F., Russo, J., Lemire, J., and Castellot, J. (2009). Domain- and species-specific monoclonal antibodies recognize the Von Willebrand Factor-C domain of CCN5. *J Cell Commun Signal.* 3(1), 65-77.
- Wei, T., Kulkarni, N. H., Zeng, Q. Q., Helvering, L. M., Lin, X., Lawrence, F., Hale, L., Chambers, M. G., Lin, C., Harvey, A., Ma, Y. L., Cain, R. L., Oskins, J., Carozza, M. A., Edmondson, D. D., Hu, T., Miles, R. R., Ryan, T. P., Onyia, J. E., and Mitchell, P. G. (2010). Analysis of early changes in the

articular cartilage transcriptome in the rat meniscal tear model of osteoarthritis: pathway comparisons with the rat anterior cruciate transection model and with human osteoarthritic cartilage. *Osteoarthritis Cartilage*. 18(7), 992-1000.

Wei, W., Li, H., Li, N., Sun, H., Li, Q., and Shen, X. (2013). WNT5A/JNK signaling regulates pancreatic cancer cells migration by Phosphorylating Paxillin. *Pancreatology : official journal of the International Association of Pancreatology*. 13(4), 384-392.

Weiss, S., Hennig, T., Bock, R., Steck, E., and Richter, W. (2010). Impact of growth factors and PTHrP on early and late chondrogenic differentiation of human mesenchymal stem cells. *J Cell Physiol*. 223(1), 84-93.

Weng, L., Wang, C., Ko, J., Sun, Y., Su, Y., and Wang, F. (2009). Inflammation induction of Dickkopf-1 mediates chondrocyte apoptosis in osteoarthritic joint. *Osteoarthritis and Cartilage*. 17(7), 933-943.

White, D. G., Hershey, H. P., Moss, J. J., Daniels, H., Tuan, R. S., and Bennett, V. D. (2003). Functional analysis of fibronectin isoforms in chondrogenesis: Full-length recombinant mesenchymal fibronectin reduces spreading and promotes condensation and chondrogenesis of limb mesenchymal cells. *Differentiation*. 71(4-5), 251-261.

Wigner, N. A., Song do, Y., Einhorn, T. A., Drissi, H., and Gerstenfeld, L. C. (2013). Functional role of Runx3 in the regulation of aggrecan expression during cartilage development. *J Cell Physiol*. 228(11), 2232-2242.

Williams, R., Khan, I. M., Richardson, K., Nelson, L., McCarthy, H. E., Anabalsi, T., Singhrao, S. K., Dowthwaite, G. P., Jones, R. E., Baird, D. M., Lewis, H., Roberts, S., Shaw, H. M., Dudhia, J., Fairclough, J., Briggs, T., and Archer, C. W. (2010). Identification and clonal characterisation of a progenitor cell sub-population in normal human articular cartilage. *PLoS One*. 5(10), e13246.

Witz, C. A., Cho, S., Centonze, V. E., Montoya-Rodriguez, I. A., and Schenken, R. S. (2003). Time series analysis of transmesothelial invasion by endometrial stromal and epithelial cells using three-dimensional confocal microscopy. *Fertility and sterility*. 79 Suppl 1, 770-778.

Wong, M., Kireeva, M., Kolesnikova, T., and Lau, L. (1997). Cyr61, Product of a Growth Factor-Inducible Immediate-Early Gene, Regulates Chondrogenesis in Mouse Limb Bud Mesenchymal Cells. *Dev Bio*. 192, 492-508.

Worster, A., Brower-Toland, B., Fortier, L., Bent, S., Williams, J., and Nixon, A. (2001). Chondrocytic differentiation of mesenchymal stem cells sequentially exposed to transforming growth factor- β 1 in monolayer and insulin-like growth factor-I in a three-dimensional matrix. *J Orthopaedic Res*. 19, 738-749.

Wu, P. H., Lin, S. K., Lee, B. S., Kok, S. H., Wang, J. H., Hou, K. L., Yang, H., Lai, E. H., Wang, J. S., and Hong, C. Y. (2012). Epigallocatechin-3-gallate diminishes cytokine-stimulated Cyr61 expression in human osteoblastic cells: a therapeutic potential for arthritis. *Rheumatology*. 51(11), 1953-1965.

Wu, Q., Zhu, M., Rosier, R., Zuscik, M., O'Keefe, R., and Chen, D. (2010). β -catenin, cartilage, and osteoarthritis. *Annals of the New York Academy of Sciences*. 1192(1), 344-350.

- Wynne-Davies, R., Hall, C., and Ansell, B. (1982). Spondylo-epiphyseal dysplasia tarda with progressive arthropathy. A "new" disorder of autosomal recessive inheritance. *JBS*. 64-B(4), 442-445.
- Xu, H., Bihan, D., Chang, F., Huang, P. H., Farndale, R. W., and Leiting, B. (2012). Discoidin domain receptors promote alpha1beta1- and alpha2beta1-integrin mediated cell adhesion to collagen by enhancing integrin activation. *PLoS One*. 7(12), e52209.
- Xu, L., Peng, H., Glasson, S., Lee, P. L., Hu, K., Ijiri, K., Olsen, B. R., Goldring, M. B., and Li, Y. (2007a). Increased expression of the collagen receptor discoidin domain receptor 2 in articular cartilage as a key event in the pathogenesis of osteoarthritis. *Arthritis Rheum*. 56(8), 2663-2673.
- Xu, L., Peng, H., Wu, D., Hu, K., Goldring, M. B., Olsen, B. R., and Li, Y. (2005). Activation of the discoidin domain receptor 2 induces expression of matrix metalloproteinase 13 associated with osteoarthritis in mice. *J Biol Chem*. 280(1), 548-555.
- Xu, L., Polur, I., Servais, J. M., Hsieh, S., Lee, P. L., Goldring, M. B., and Li, Y. (2011). Intact pericellular matrix of articular cartilage is required for unactivated discoidin domain receptor 2 in the mouse model. *Am J Pathol*. 179(3), 1338-1346.
- Xu, Y., Balooch, G., Chiou, M., Bekerman, E., Ritchie, R. O., and Longaker, M. T. (2007b). Analysis of the material properties of early chondrogenic differentiated adipose-derived stromal cells (ASC) using an in vitro three-dimensional micromass culture system. *Biochem Biophys Res Commun*. 359(2), 311-316.
- Yamada, A., Iwata, T., Yamato, M., Okano, T., and Izumi, Y. (2013). Diverse functions of secreted frizzled-related proteins in the osteoblastogenesis of human multipotent mesenchymal stromal cells. *Biomaterials*. 34(13), 3270-3278.
- Yamaguchi, T. P., Bradley, A., McMahon, A. P., and Jones, S. (1999). A Wnt5a pathway underlies outgrowth of multiple structures in the vertebrate embryo. *Development*. 126(6), 1211-1223.
- Yanagita, T., Kubota, S., Kawaki, H., Kawata, K., Kondo, S., Takano-Yamamoto, T., Tanaka, S., and Takigawa, M. (2007). Expression and physiological role of CCN4/Wnt-induced secreted protein 1 mRNA splicing variants in chondrocytes. *FEBS J*. 274(7), 1655-1665.
- Yang, B., Kang, X., Xing, Y., Dou, C., Kang, F., Li, J., Quan, Y., and Dong, S. (2014). Effect of microRNA-145 on IL-1beta-induced cartilage degradation in human chondrocytes. *FEBS letters*. 588(14), 2344-2352.
- Yang, Y., and Liao, E. (2007). Mutant WISP3 triggers the phenotype shift of articular chondrocytes by promoting sensitivity to IGF-1 hypothesis of spondyloepiphyseal dysplasia tarda with progressive arthropathy (SEDT-PA). *Med Hyp*. 68(6), 1406-1410.
- Yang, Y., Topol, L., Lee, H., and Wu, J. (2003). Wnt5a and Wnt5b exhibit distinct activities in coordinating chondrocyte proliferation and differentiation. *Development*. 130(5), 1003-1015.
- Ye, J., Zhang, H., Wang, T., Cao, L., Qui, J., Han, L., Zhang, Y., and Gu, X. (2010). Clinical diagnosis and WISP3 gene mutation analysis for progressive pseudorheumatoid dysplasia. *Zhonghua Er Ke Za Zhi*. 48(3), 194-198.
- Yin, C., Li, H., Zhang, B., Liu, Y., Lu, G., Lu, S., Sun, L., Qi, Y., Li, X., and Chen, W. (2013). RAGE-binding S100A8/A9 promotes the migration and invasion of human breast cancer cells through

actin polymerization and epithelial-mesenchymal transition. *Breast cancer research and treatment*. 142(2), 297-309.

Yoon, Y. M., Oh, C. D., Kim, D. Y., Lee, Y. S., Park, J. W., Huh, T. L., Kang, S. S., and Chun, J. S. (2000). Epidermal growth factor negatively regulates chondrogenesis of mesenchymal cells by modulating the protein kinase C-alpha, Erk-1, and p38 MAPK signaling pathways. *J Biol Chem*. 275(16), 12353-12359.

Young, A. A., McLennan, S., Smith, M. M., Smith, S. M., Cake, M. A., Read, R. A., Melrose, J., Sonnabend, D. H., Flannery, C. R., and Little, C. B. (2006). Proteoglycan 4 downregulation in a sheep meniscectomy model of early osteoarthritis. *Arthritis Res Ther*. 8(2), R41.

Yu, C., Le, A., Yeager, H., Perbal, B., and Alman, B. (2003). NOV (CCN3) regulation in the growth plate and CCN family member expression in cartilage neoplasia. *J Pathol*. 201(4), 609-615.

Yuan, Y., Niu, C. C., Deng, G., Li, Z. Q., Pan, J., Zhao, C., Yang, Z. L., and Si, W. K. (2011). The Wnt5a/Ror2 noncanonical signaling pathway inhibits canonical Wnt signaling in K562 cells. *Int J Mol Med*. 27(1), 63-69.

Yuasa, T., Otani, T., Koike, T., Iwamoto, M., and Enomoto-Iwamoto, M. (2008). Wnt/ β -catenin signaling stimulates matrix catabolic genes and activity in articular chondrocytes: its possible role in joint degeneration. *Lab Inv*. 88, 264-274.

Zamora, P. O., Danielson, K. G., and Hosick, H. L. (1980). Invasion of endothelial cell monolayers on collagen gels by cells from mammary tumor spheroids. *Cancer Res*. 40(12), 4631-4639.

Zeng, L., Fagotto, F., Zhang, T., Hsu, W., Vasicek, T. J., Perry, W. L., 3rd, Lee, J. J., Tilghman, S. M., Gumbiner, B. M., and Costantini, F. (1997). The mouse Fused locus encodes Axin, an inhibitor of the Wnt signaling pathway that regulates embryonic axis formation. *Cell*. 90(1), 181-192.

Zeng, X., Tamai, K., Doble, B., Li, S., Huang, H., Habas, R., Okamura, H., Woodgett, J., and He, X. (2005). A dual-kinase mechanism for Wnt co-receptor phosphorylation and activation. *Nature*. 438, 873-877.

Zhai, Z., Yao, Y., and Wang, Y. (2013). Importance of suitable reference gene selection for quantitative RT-PCR during ATDC5 cells chondrocyte differentiation. *PLoS One*. 8(5), e64786.

Zhang, L., Su, P., Xu, C., Yang, J., Yu, W., and Huang, D. (2010). Chondrogenic differentiation of human mesenchymal stem cells: a comparison between micromass and pellet culture systems. *Biotechnol Lett*. 32(9), 1339-1346.

Zhang, X., Xu, X., Xu, T., and Qin, S. (2014). beta-Ecdysterone suppresses interleukin-1beta-induced apoptosis and inflammation in rat chondrocytes via inhibition of NF-kappaB signaling pathway. *Drug Dev Res*. 75(3), 195-201.

Zhang, Y., Li, Q., and Chen, H. (2013). DNA methylation and histone modifications of Wnt genes by genistein during colon cancer development. *Carcinogenesis*. 34(8), 1756-1763.

Zhang, Y., Su, J., Yu, J., Bu, X., Ren, T., Liu, X., and Yao, L. (2011). An essential role of discoidin domain receptor 2 (DDR2) in osteoblast differentiation and chondrocyte maturation via modulation of Runx2 activation. *J Bone Miner Res*. 26(3), 604-617.

Zhang, Z., McCaffery, M., Spencer, R., and Francomano, C. (2004). Hyaline cartilage engineered by chondrocytes in pellet culture: histological, immunohistochemical and ultrastructural analysis in comparison with cartilage explants. *Journal of anatomy*. 205(3), 229-237.

Zhou, C., Zheng, H., Seol, D., Yu, Y., and Martin, J. A. (2014). Gene expression profiles reveal that chondrogenic progenitor cells and synovial cells are closely related. *J Orthop Res*. 32(8), 981-988.

Zhou, H., Bu, Y., Peng, Y., Xie, H., Wang, M., Yuan, L., Jiang, Y., Li, D., Wei, Q., He, Y., Xiao, T., Ni, J., and Liao, E. (2007). Cellular and molecular responses in progressive pseudorheumatoid dysplasia articular cartilage associated with compound heterozygous WISP3 gene mutation. *J Mol Med*. 85, 985-996.

Zuo, G., Kohls, C., He, B., Chen, L., Zhang, W., Shi, Q., Zhang, B., Kang, Q., Luo, J., Luo, X., Wagner, E., Kim, S., Restegar, F., Haydon, R., Deng, Z., Luu, H., He, T., and Luo, Q. (2010). The CCN proteins: important signaling mediators in stem cell differentiation and tumorigenesis. *Histol Histopathol*. 25, 795-806.

Zuscik, M., Hilton, M., Zhang, X., Chen, D., and O'Keefe, R. (2008). Regulation of chondrogenesis and chondrocyte differentiation by stress. *J Clin Inv*. 118(2), 429-428.